

**BOOK OF ABSTRACTS**

**XIVth  
International  
Conference  
on  
Gas  
Geochemistry**

**Wrocław – Świeradów Zdrój**

**24–28.09.2017**





*International Conference on Gas Geochemistry 2017*  
*Wrocław-Świeradów, Poland, 24-28 September 2017*

# **XIVth International Conference on Gas Geochemistry**

## **Book of Abstracts**

**Institute of Geological Sciences,  
University of Wrocław  
Faculty of Geoengineering, Mining and Geology  
Wrocław University of Science and Technology**

**Wrocław 2017**

**Editor:**

**Tadeusz A. PRZYLIBSKI**

**Technical Editor:**

**Marek BATTEK**

**Editorial Staff:**

**Agata KOWALSKA**

**Elżbieta DOMIN**

Front cover designed by A. Solecki on the background of archival photograph of Borysław Tustanowice oil gusher (late XIXth) century from the photo album "Dawno temu w Karpatach. Rzecz o polskiej nafcie" (published originally by Poszukiwania Nafty i Gazu, Kraków Sp. z o.o.) due to courtesy of EXALO GRUPA PGNiG (present successor of the publisher).

© Copyright by Wydział Geoinżynierii, Górnictwa i Geologii  
Politechniki Wrocławskiej  
(Faculty of Geoen지니어ing, Mining and Geology  
Wrocław University of Science and Technology)

Wszelkie prawa zastrzeżone. Żadna część niniejszej książki,  
zarówno w całości, jak i we fragmentach, nie może być reprodukowana  
w sposób elektroniczny, fotograficzny i inny bez zgody wydawcy.

**ISBN 978-83-946706-3-4**

Wydział Geoinżynierii, Górnictwa i Geologii  
Wybrzeże Wyspiańskiego 27, 50-370 Wrocław, Polska



*International Conference on Gas Geochemistry 2017*  
Wrocław-Świeradów, Poland, 24-28 September 2017

## **XIVth International Conference on Gas Geochemistry Organizers**

**Institute of Geological Sciences,  
University of Wrocław  
pl. Maksa Born'a 9, 50-204 Wrocław**

**Faculty of Geoengineering,  
Mining and Geology,  
Wrocław University of Science  
and Technology  
ul. Na Grobli 15, 50-421 Wrocław**

### **International Scientific Committee**

Baciu, C. (Romania)  
Chałupnik, S. (Poland)  
**Chyi, L.L. (USA)**  
Etiopie, G. (Italy)  
Fu, C.C. (Taiwan)  
Heinicke, J. (Germany)  
Hilton, D.R. (USA)  
Italiano, F. (Italy)  
Kies, A. (Luxembourg)  
Martinelli, G. (Italy)

Marty, B. (France)  
Papatheodorou G. (Greece)  
Pérez, N.M. (Spain)  
Singh, S. (India)  
Solecki, A.T. (Poland)  
Tamura, Hajimu (Japan)  
Taran, Y. (Mexico)  
Wang, Y.P. (China)  
Woith, H. (Germany)  
Yüce, G. (Turkey)

### **Local Organizing Committee**

#### **Chairman:**

prof. dr hab. Andrzej Solecki, UWr

#### **Co-chairman:**

dr hab. Małgorzata Wysocka, prof. GIG,  
dr hab. Tadeusz A. Przylibski, prof. PWr,

#### **Secretary:**

dr Dagmara Tchorz-Trzeciakiewicz, UWr

#### **Vice Secretary:**

dr Piotr Wojtulek, UWr

#### **Members:**

dr inż. Elżbieta Bilkiewicz, AGH  
mgr inż. Mariusz Borek, GIG  
mgr inż. Elżbieta Domin, PWr  
dr inż. Lidia Fijałkowska-Lichwa, PWr  
mgr inż. Małgorzata Grabowska, GIG  
dr inż. Agata Kowalska, PWr  
dr hab. Antoni Muszer, UWr

### **Local Academic Committee**

#### **Chairman:**

prof. dr hab. inż. Maciej Kotarba

#### **Vice chairman:**

prof. dr hab. inż. Kazimierz Różański

#### **Members:**

dr hab. inż. Stanisław Chałupnik  
prof. dr hab. Wojciech Ciężkowski  
dr hab. inż. Eugeniusz Krause  
dr Jerzy Olszewski  
prof. dr. hab. Anna Pazdur

The organizers gratefully acknowledge the financial support of:



WYDZIAŁ NAUK O ZIEMI I KSZTAŁTOWANIA ŚRODOWISKA

Wydział Geoinżynierii,  
Górnictwa i Geologii





*International Conference on Gas Geochemistry 2017*  
Wrocław-Świeradów, Poland, 24-28 September 2017

Two years ago, the International Scientific Committee of the International Conference on Gas Geochemistry entrusted me with the task of organizing the fourteenth conference, and I would like to thank sincerely for their confidence. I would also like to thank the Colleagues who have agreed to be the members of the Local Academic Committee and the Organizing Committee. It is my honor to thank, on behalf of the organizers, the Authorities of the University of Wrocław and the Wrocław University of Science and Technology, who have supported our activities.

We would also like to thank Individuals and Institutions that have accepted the patronage of our activities: Secretary of State Chief National Geologist, prof. dr. M. O. Jędrysek, Provincial and Municipal Authorities and the Authorities of KGHM. We would also like to thank EXALO Group of the PGNiG for their approval to use photos from their album commemorating the pioneering years of petroleum industry and donating copies of this publication.

We would also like to thank all Delegates who have decided to take part in our Conference and wish them a great stay in Poland.

Andrzej Solecki  
Chairman of the Local Organizing Committee



# **1. Radon in environment**





## **Mineralogical and structural aspects of the radioactive therme formation on the hydrogeological structure Geschieber in Jáchymov, Czech Republic**

Michal Čurda<sup>#</sup>, Viktor Goliáš, Jiří Zachariáš

Institute of Geochemistry, Mineralogy and Mineral Resource, Charles University in Prague,  
Faculty of Science, Albertov 6, 128 43 Prague 2, Czech Republic,  
<sup>#</sup> michalcurda@centrum.cz

**Key words:** *Jáchymov, radioactive springs, structural, tectonic, mineralogy*

### **Introduction**

Jáchymov springs are a world-unique phenomenon in mineralogy (Ondruš et al. 2003) and economic geology. They also are a source of radioactive thermal mineral water. These curative sources were collected by several underground wells in the Svornost mine. In 1962, an exploration drilling HG-1 on the 12th level was localised in the vein structure Geschieber. A spring was captured here, later called after academician František Běhounek. This source with a flow rate of 5 L/s and activity 10 kBq/L <sup>222</sup>Rn is the most important source of the Jáchymov spa (Laboutka and Pačes 1966).

### **Mineralogical character and structural-tectonic situation of the Geschieber vein structure**

The research is focused on the mineralogical character and structural-tectonic situation of the Geschieber vein structure and their relation to the radioactive water sources. This contribution summarizes the results of the structural-geological measurements performed on the 10th and 12th level of the Svornost mine. The results show monotonous orientation of metamorphic foliation in mica schists of the E-W direction dipping approx. 35° N (orientation of the dip direction: 356/36). The fracture system has two dominant directions: W-E and more often NNW-SSE, which is more or less perpendicular to the foliation direction. Fractures dip is mostly steep. Direction of the Geschieber vein structure (NW-SE) differs by approx. 20–30° from the NNW-SSE oriented fractures. This can be caused by different ages of the fractures and hydrothermal veins related with the change of the strain field.

Mineral association of the „clay“ filling in open fractures in the cross cut leading to the HG-1 well (12th level) was studied by X-ray diffraction analysis. The main minerals

are kaolinite, smectite group minerals (montmorillonite), quartz, gypsum, micas and feldspars. Secondary Co-Ni arsenates appear in the fractures close to the Geschieber fault zone. Some differences between the fault zone and fractures in compact granite (in the direction to the HG-1 well) can be observed. Kaolinite is the dominant clay mineral in the fault zone. Its amount decreases in cracks in granite. On the contrary, the proportion of quartz, micas and feldspars increases in the direction from the fault zone. Total amount of fractures also decreases in this direction.

### References

- ONDRUŠ P., VESELOVSKÝ F., GABAŠOVÁ A., HLOUŠEK J. & ŠREJN V. 2003. *Geology and hydrothermal vein system of the Jáchymov (Joachimsthal) ore district*, Journal of the Czech Geological Society 48, 3-18.
- LABOUTKA M. & PAČES T. 1966. *Radioactivity of Czechoslovakian mineral waters*. Sborník geologických věd 4, 59–112. (in Czech)



## Radon risk in underground tourist routes: the Książ Castle case study

Lidia FIJAŁKOWSKA-LICHWA<sup>1</sup>, Tadeusz A. PRZYLIBSKI<sup>2</sup>

<sup>1</sup> Wrocław University of Science and Technology, Faculty of Civil Engineering, Department of Geotechnics, Hydrotechnics, Underground and Water Construction; Wybrzeże S. Wyspiańskiego 27, 50-370 Wrocław, POLAND; e-mail: Lidia.Fijalkowska-Lichwa@pwr.edu.pl

<sup>2</sup> Wrocław University of Science and Technology, Faculty of Geoengineering, Mining and Geology, Division of Geology and Mineral Waters; Wybrzeże S. Wyspiańskiego 27, 50-370 Wrocław, POLAND; e-mail: Tadeusz.Przylibski@pwr.edu.pl

**Keywords:** radon, natural hazard, underground tourist route, ionizing radiation, effective dose

Underground tourist routes enjoy a large and ever-growing popularity. In Poland there are currently about 200 such objects, where about 1500 people work (Olszewski et al., 2015). One of the most important aspects of their business is the safety of the tourists visiting them and the safety of the staff serving the tourist traffic. Very important problem is the exposure of both workers and tourists to ionizing radiation inside such objects. The source of ionizing radiation in underground tourist facilities is primarily radon (<sup>222</sup>Rn) and its decay products (i.e. Przylibski, 2010).

In order to ensure effective radiological protection it is necessary to recognize the activity concentration of <sup>222</sup>Rn in each of the underground facilities available to tourists. Due to the natural or forced ventilation conditions and the geological structure of the underground tourist route, it is also necessary to determine the magnitude of changes in <sup>222</sup>Rn activity concentration in space and time, both in the short-term (diurnal) and seasonal (annual) (Przylibski, 2010; Fijałkowska-Lichwa and Przylibski, 2011; Fijałkowska-Lichwa, 2015; Olszewski et al., 2015). By obtaining information about daily and seasonal fluctuations in <sup>222</sup>Rn activity concentration, it is possible to more accurately determine the effective dose of ionizing radiation received by employees of underground tourist routes based on environmental measurements without the need for individual dose registrations (Fijałkowska-Lichwa, 2014, 2015).

Recommended by international organizations admissible annual average concentration values of <sup>222</sup>Rn for underground workplaces are in the range of 500 to 1500 Bq/m<sup>3</sup> (ICRP, 1993; IAEA, 1996, 2003). On the other hand, the latest EU Council Directive (2013) requires Member States, including Poland, to regulate the maximum permissible annual average concentration of radon in the workplace. No later than February 6, 2018, a legally defined maximum limit value of the average annual activity

concentration of  $^{222}\text{Rn}$  in work places in Poland has to be established. The annual average value specified in the law can't be more than  $300 \text{ Bq/m}^3$  (Council Directive, 2013).

Unlike environmental studies (i.e. Przylibski, 1999), it is most preferable for a dosimetric study to select a place of measurement in an underground tourist object so, that the concentration of  $^{222}\text{Rn}$  activity is as large as possible. As a rule, this is a place far removed from the exit and entrance to the tourist route and / or located within the rocks of the highest uranium (radium) content, close to the ore crusting zones and / or tectonic brittle deformation zones and / or weathering zones. This kind of detector location allows to obtain the most harmful ionizing radiation doses. As a result, estimates of the effective dose based on measurements of the activity concentration of  $^{222}\text{Rn}$  in such a location will certainly not be underestimated (Przylibski, 2010; Fijałkowska-Lichwa, 2014, 2015).

The authors undertook research before launching an underground tourist route under one of the largest castles in Poland – Książ Castle. The castle is located in Wałbrzych city, in the middle part of the Sudetes – a Variscan mountain range building SW part of Poland and the adjacent areas of the Czech Republic and Germany. Radon concentration was measured before and during the preparation and sharing of the tourist route to visitors. On the base of the results of conducted measurements, it was possible to formulating guidelines on the necessity of applying ventilation solutions for the tourist route. At the same time shortly after the tourist route completion, according to the plan in the autumn of 2017, the owner will have annual record of the  $^{222}\text{Rn}$  activity concentration and its changes on a diurnal and seasonal scale. This will ensure appropriate radiation safety conditions for the staff and tourist shortly after the start of the route.

Measurements have been carrying out using SRDN-3 radon probe with a semiconductor detector (Przylibski et al., 2010), which is located in a small hall in the middle of the designed tourist route. The hall is within similar proximity of the entrance and exit of the route. Underground tourist route under the Książ Castle is connected with underground geodynamic laboratory the Polish Academy of Sciences Space Research Centre, in which the authors have been monitoring the activity concentration of  $^{222}\text{Rn}$  for several years (Fijałkowska-Lichwa and Przylibski, 2016).

The measurements conducted so far indicate that in the winter period, i.e. from November to March, the lowest values of  $^{222}\text{Rn}$  activity concentration occur. On the other hand, the greatest values were recorded in summer – in June (Table 1).

The authors did not find significant diurnal fluctuations in activity concentration of  $^{222}\text{Rn}$ . In no month, even in winter, the average monthly activity concentration of  $^{222}\text{Rn}$  was not less than the permissible mean annual value of  $300 \text{ Bq/m}^3$ . It is therefore necessary to use intensive mechanical ventilation of the tourist route even in winter.

Mean ionizing radiation effective dose in the Książ Castle underground tourist route changes from 0.004 to 0.007 mSv/h between November 2016 and June 2017. The maximum value was noted in June 2017 and reaches 0.012 mSv/h. The calculated values of the effective dose allow us to say that even without applying the mechanical

Table 1. Mean, minimum and maximum  $^{222}\text{Rn}$  activity concentration [ $\text{Bq}/\text{m}^3$ ] in the Książ Castle underground tourist route between November 2016 and June 2017

Month	Mean	Minimum	Maximum
November	1191	489	2096
December	1105	489	2171
January	608	130	1145
February	662	169	1379
March	704	247	1340
April	1243	489	2395
May	1584	639	2844
June	1878	826	3180

ventilation, the activity concentration of  $^{222}\text{Rn}$  is not dangerous for tourists. They will spend in the underground route only about 1 hour. However, for tour guides and staff working underground, the effective dose may exceed 1 mSv after approximately 100 hours of work. This confirms the need to use appropriate mechanical devices to ventilate the tourist route under the Książ Castle. Similar problems can be expected in a large number of almost 200 underground tourist routes operating in Poland.

The measured activity concentrations of  $^{222}\text{Rn}$  in underground excavations to become part of the underground tourist route are comparable to the values measured in the air of another part of the same excavation sites as the geodynamic laboratory the Polish Academy of Sciences Space Research Centre in Książ Castle (Fijałkowska-Lichwa i Przylibski, 2016).

## References

- Council Directive 2013/59/EURATOM of 5 December 2013 laying down basic safety standards for protection against the dangers arising from exposure to ionizing radiation, and repealing Directives 89/618/Euratom, 90/641/Euratom, 96/29/Euratom, 97/43/Euratom and 2003/122/Euratom. Official Journal of the European Union, 17.1.2014., L13/1-L13/73.
- Fijałkowska-Lichwa, L., 2014 – *Short-term radon activity concentration changes along the underground educational tourist route in the old uranium mine in Kletno (Sudety Mts., SW Poland)*. Journal of Environmental Radioactivity, Vol. 135, pp. 25-35.
- Fijałkowska-Lichwa, L., 2015 – *Estimation of radon risk exposure in selected underground workplaces in the Sudetes (southern Poland)*. Journal of Radiation Research and Applied Sciences, Vol. 8, No. 3, pp. 334-353.
- Fijałkowska-Lichwa L., Przylibski T.A., 2011 – *Short-term  $^{222}\text{Rn}$  activity concentration changes in underground spaces with limited air exchange with the atmosphere*. Natural Hazards and Earth System Sciences, Vol. 11, pp. 1179-1188.
- Fijałkowska-Lichwa L., Przylibski T.A., 2016 – *First radon measurements and occupational exposure assessments in underground geodynamic laboratory the Polish Academy of Sciences Space Research Centre in Książ Castle (SW Poland)*. Journal of Environmental Radioactivity, Vol. 165, pp. 253-269.
- IAEA, 1996 – International Basic Safety Standards for Protection against Ionizing Radiation and for the Safety of Radiation Sources, Safety Series No. 115, International Atomic Energy Agency, Vienna.

IAEA, 2003 – Radiation Protection against Radon in Workplaces other than Mines. Safety Reports Series No. 33, International Atomic Energy Agency, Vienna.

ICRP, 1993 – Protection against Radon-222 at home and at work. International Commission on Radiation Protection, Publication No. 65, Pergamon Press, Oxford.

Olszewski J., Zmyślony M., Wrzesień M., Walczak K., 2015 – *Occurrence of radon in the Polish underground tourist routes*. *Medycyna Pracy*, Vol. 66 (4), pp. 557-563.

Przylibski T. A., 1999 – *Radon concentration changes in the air of two caves in Poland*. *Journal of Environmental Radioactivity*, Vol. 45, No. 1, pp. 81-94.

Przylibski T.A., 2010 – *Radon and ionizing radiation in underground objects during their exploration, documentation and making accessible*. [in:] Zagożdżon P.P., Madziarz M. (eds.): *History of mining – an element of the European cultural heritage*, Vol. 3, pp. 369-379, Oficyna Wydawnicza Politechniki Wrocławskiej, Wrocław. (in Polish).

Przylibski T.A., Bartak J., Kochowska E., Fijałkowska-Lichwa L., Kozak K., Mazur J., 2010 – *New SRDN-3 probes with a semi-conductor detector for measuring radon activity concentration in underground spaces*. *Journal of Radioanalytical and Nuclear Chemistry*, Vol. 285, No. 3, pp. 599-609.



## **Comprehensive indoor radon study in Romanian urban agglomerations within SMART\_RAD\_EN European Project**

B. Papp<sup>1#</sup>, A. Cucuș<sup>1</sup>, T. Dicu<sup>1</sup>, B. Burghele<sup>1</sup>, M. Moldovan<sup>1</sup>,  
A. Țenter<sup>1</sup>, K. Szacsvai<sup>1</sup>, S. Beldean<sup>1</sup>, C. Sainz<sup>1,2</sup>

<sup>1</sup> Babes-Bolyai University, Faculty of Environmental Science and Engineering, Cluj-Napoca, Romania, papp.botond@ubbcluj.ro

<sup>2</sup> University of Cantabria, Faculty of Medicine, Department of Medical Physics, Santander, Spain

The carcinogenic impact of radon and its decay products has been proven in cohort studies of miners and case-control studies on exposure to residential radon. Current research shows that about 8 to 15% of all lung cancer cases in Europe may be attributable to radon in homes, aspect that makes it the main environmental factor causing lung cancer (George, 2015). Thus, the importance of monitoring radon level and other carcinogenic chemical pollutants inside the new modern houses has been discussed in detail in several papers (Gräser et al., 2010; Jiranek et al., 2014; Cucuș et al., 2015; Pressyanov et al., 2015). Efficiently insulating buildings and modern architectural solutions can lead to the accumulation of high levels of radon indoors. The results clearly prove that in classical conventional homes which were thermally rehabilitated, additional risk of lung cancer increased compared to the previous situation (Jiranek et al., 2014).

Among the factors controlling indoor radon levels the most important are the characteristics of the house, construction technologies used and the behaviour of residents. The migration and transport of radon from the ground or from building materials to the air inside the house depend on a number of factors, such as porosity and type of material, humidity, air pressure differences between indoor and outdoor air, as well as meteorological factors such as wind speed, drafts, etc. The fact that most people spend up to 90% of their time indoors (homes, offices, theatres, etc.) partially protects them from cosmic and terrestrial (soil) radiation, but exposes them to radon and other carcinogenic pollutants that accumulate in unventilated sealed rooms.

Our ongoing project SMART\_RAD\_EN aim to increase the safety and health of the population by improving the indoor environmental quality of housing through the development of integrated intelligent systems to monitor, control and reduce the exposure to indoor radon and other household pollutants in five urban agglomerations in Romania (Bucharest, Cluj-Napoca, Iași, Sibiu and Timișoara).

At present, an extensive campaign by passive monitoring of indoor radon concentration is being carried out in 1,000 energy efficient houses in order to obtain a detailed picture of indoor air quality in studied urban areas.

The selection of houses was based on existing results (Cosma et al., 2013). According to our data, in the municipality of Cluj-Napoca, 227 indoor radon measurements have been carried out. The annual mean of residential radon concentration was 124 Bq/m<sup>3</sup>, the limits ranging between 20 and 1050 Bq/m<sup>3</sup>. For 8% of the total monitored homes in Cluj-Napoca the radon concentration was higher than 300 Bq/m<sup>3</sup>.

In the case of Timișoara metropolitan area, the existing database in 54 houses indicates relatively excessive indoor radon levels, with 46% of measured values higher than 300 Bq/m<sup>3</sup>. The indoor radon concentrations vary from 47 and 1238 Bq/m<sup>3</sup> with the annual mean of 299 Bq/m<sup>3</sup>.

In contrast to the situation of the two cities mentioned above, our previously results for Sibiu report moderate indoor radon exposure, with the annual average of 81 Bq/m<sup>3</sup>. Bucharest and Iași cities have not yet been investigated, thereby representing a challenge their inclusion in the study, in the context of high population density.

In these cities, we consider that further investigations are needed on the factors influencing the accumulation of radon in high concentrations in indoor air, such as soil type and geology, ventilation, or constructive and architectural features of typical houses. Therefore the results of this work are considered to be important for indoor radon management in Romania.

**Acknowledgement:** The research is supported by the project ID P\_37\_229, Contract No. 22/01.09.2016, with the title „Smart Systems for Public Safety through Control and Mitigation of Residential Radon linked with Energy Efficiency Optimization of Buildings in Romanian Major Urban Agglomerations SMART-RAD-EN” of the POC Programme.

## References

- Cosma C., Cucuș (Dinu) A., Dicu T. (2013). *Preliminary results regarding the first map of residential radon in some regions in Romania*, Radiation Protection Dosimetry 155, 343-350.
- Cucuș (Dinu) A., Dicu T., Cosma C., (2015). *Indoor radon exposure in energy-efficient houses from Romania*, Romanian Journal of Physics 60 (9-10), 1574–1580.
- George A.C. (2015). *The history, development and the present status of the radon measurement programme in the United States of America*, Radiation Protection Dosimetry, doi:10.1093/rpd/ncv213.
- Gräser J., Grimm C., Kaineder H., Körner S., et al. (2010). *Radon – The Effect of Retrofitting Thermal Insulation*, Published jointly by the Radon Offices in Austria, Switzerland, southern Germany, South Tyrol.
- Jiranek M., Kacmarikova V. (2014). *Dealing with the increased radon concentration in thermally retrofitted buildings*, Radiation Protection Dosimetry 160, 43-47.
- Pressyanov D., Dimitar D., Ivelina D. (2015). *Energy-efficient reconstructions and indoor radon: the impact assessed by CDs/DVDs*, Journal of Environmental Radioactivity 143, 76-79.



## **Indoor radon concentration in Wrocław (SW Poland)**

Dagmara Tchorz-Trzeciakiewicz<sup>#</sup>, Sławomir Olszewski

Institute of Geological Sciences, University of Wrocław, Pl. M. Borna 9, 50-204 Wrocław

<sup>#</sup> Corresponding author: dagmara.tchorz-trzeciakiewicz@uwr.edu.pl

We performed survey of indoor radon concentrations in Wrocław in order to: (i) evaluate average indoor radon concentration taking into account seasonal variations of radon concentrations, (ii) analyse the relation between indoor radon concentration and the type of soil and bedrock on which buildings were erected (iii) examine vertical changes of indoor radon concentrations from ground floor to six floor

Wrocław is the largest city in south-western part of Poland. It is located on the banks River Oder in the Silesian Lowlands between Trzebnickie Hills and the Sudetes. The population of Wrocław in 2016 was above 630000 making it the fourth-largest city in Poland. Wrocław has a humid continental climate. It is one of the warmest cities in Poland (the mean annual temperature is 9.8 °C). The coldest month is January (average temperature -0.5 °C and the warmest in July (average temperature 19.9 °C). Wrocław is located on the border of two large geological structures: Fore-Sudetic Monokline and Fore-Sudetic Block. The Silesian Lowlands were in the range of Riss glaciation so post-glacial sediments cover the southern part of Wrocław.

The measurements of indoor radon concentration were carried out in four types of buildings: tenement houses, newly build block of flats, detached houses and pre-fabricated concrete blocks using SSNTD LR-115. The survey lasted one year and was divided on four three months periods correlated with seasons. The detectors were placed in the middle of living rooms and after exposition etched in hot NaOH solution and analysed using Digimizer software in Laboratory of Institute of Geological Sciences University of Wrocław. The procedure of etching and analysing of detectors was described by Tchorz-Trzeciakiewicz, (2012).

The indoor radon concentration varied from 28 to 123 Bq m<sup>-3</sup>. We observed seasonal variations of radon concentration with the highest values registered in winter and the lowest in spring–summer seasons. The analyse of influence of soil and bedrock on indoor radon concentration revealed that indoor radon concentration measured on ground and first floors in all type of buildings located on clay deposits were higher than in building located on fluvio-glacial sands and gravels.

We noticed decrease of indoor radon concentration from ground floor till 3th floor in all type of buildings. From 3-th till 6-th floor we observed stabilisation in radon concentration. We put the statement that from 3-th floor mainly building materials have influence on indoor radon concentration.

### References

Tchorz-Trzeciakiewicz, D.E., 2015. *Low-priced, time-saving, reliable and stable LR-115 counting system*. J. Environ. Radioact. 144, 162–167.



## Preliminary results of blood tests in people with elevated radon concentrations in dwellings

Katarzyna Walczak<sup>1#</sup>, Jerzy Olszewski<sup>1</sup>, Marek Zmyślony<sup>1</sup>, Maciej Stępnik<sup>2</sup>

<sup>1</sup> Nofer Institute of Occupational Medicine in Łódź, ul. Św. Teresy od Dzieciątka Jezus 8, 91-348 Łódź, Poland, Department of Radiological Protection

<sup>2</sup> Nofer Institute of Occupational Medicine in Łódź, ul. Św. Teresy od Dzieciątka Jezus 8, 91-348 Łódź, Poland, Department of Toxicology and Carcinogenesis

# corresponding author: Katarzyna.Walczak@imp.lodz.pl

**Keywords:** Radon, dwellings, p53, environmental exposure

### Introduction

Radon, <sup>222</sup>Rn is the second, after tobacco smoking, cause of lung cancer incidence. It contributes to arising the radioactive aerosols. This aerosols emit high energy particles, which cause bombarding the walls of lung tissue, transmitting the energy and causing damage. Examples of such damage are changes the sequence and / or structure of the DNA strand, revealing, for example in mutations of the p53 protein. The main role of the wild type of p53 protein is to protect the cells from changes in the genome, resulting from the broadly understood DNA damage and mainly includes retention of the cell cycle, apoptosis induction and aging cells [1]. Under normal conditions, the p53 protein is kept on the low level in the cell and is inactive. In case of cellular stress lifespan of p53 protein in the cell is greatly increased, and there is a large accumulation of this protein in the cell. Because of it as well as because of the longer half-life of the mutated form of p53 protein in compared to wild one, in the blood the presence of antibodies against p53 protein are observed (which can be regarded as a specific biomarker of cancer process) [2]. Prolonged exposure to higher radon concentration in the air of dwellings may pose a risk of increase an incidence of lung cancer.

### Method

The aim of the project was to study the induction of mutagenic effects in humans after long-term exposure to high concentrations of radon in homes. The level of environmental exposure was monitored by antibodies against p53 protein concentration in biological material (blood) sampled from the individuals.

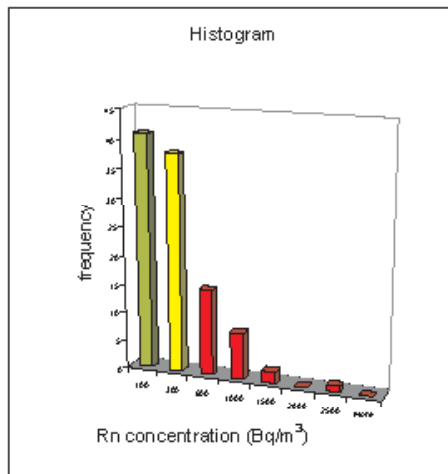
We selected residents of Kowary, city of Poland, which rocks are marked by increased mean  $^{226}\text{Ra}$  contents (potential radon-prone areas) and where naturally occur high concentrations of radon in homes. Quarterly radon concentrations in homes were measured in years 2015-2016 using Cr-39 dosimeters.

We analyzed 105 individuals from city of Kowary. Depending on the level of radon concentration in their dwellings we divided them into groups: exposed to radon concentrations comprised between 0-100 Bq / m<sup>3</sup> (41 people), and 2 groups of compartments of: 100 - 300 Bq / m<sup>3</sup> and 300 and more Bq / m<sup>3</sup> (38 and 26 people respectively). We decided to treat the group with radon concentration in homes less than 100 Bq/m<sup>3</sup> as a control group. In effect we have the same living conditions for control group differing with the study group only with the radon concentration.

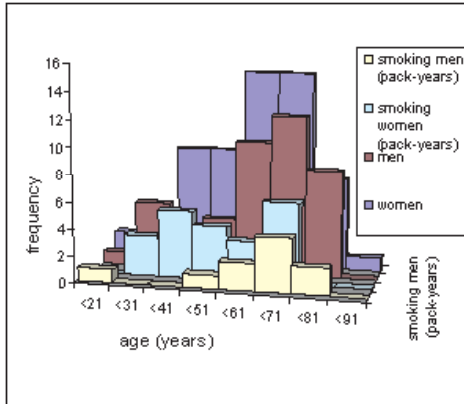
## Results

Arithmetic mean of all measuring points from dwellings in Kowary, excluding basements, varied around 400 Bq/m<sup>3</sup>. This level of radon concentration is higher than the level of significant increase of the risk of inducing cancer according to the Council Directive 2013/59 Euratom [3]. Radon concentration distribution is presented in the graph 1.

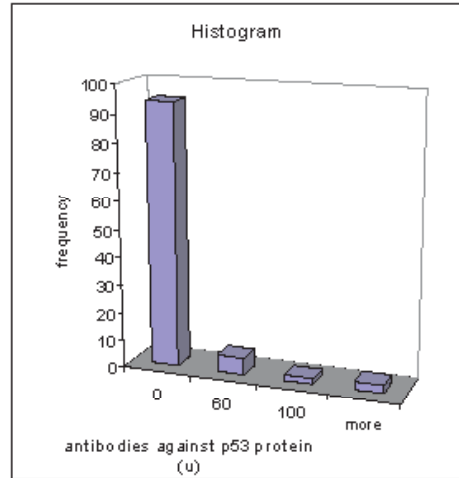
Out of the 11 people with elevated level of antibodies against p53 protein (>31 u), at 5 person the level of antibodies exceeded the reference values determined for that kind of antibodies (>60 u). Distribution of parameters such as age, sex, smoking pack-years, are presented in graphs 2.



Graph 1. Distribution of radon concentration in dwellings (Colors show the degree of threat to radon according to Council Directive 2013/59 / Euratom - green-safe, yellow - may pose the risk, red - dangerous)



Graph 2. Distribution of parameters such as age, sex, smoking pack-years



Graph 3. Distribution of antibodies against p53 protein

The research were conducted under UMO-2015/17/N/NZ7/01128 grant. Completion of the theme is scheduled for the 2018 year. Multivariate statistical analysis is under development, as well as other biomarker and conclusions.

### References

- [1] Sznarkowska A., Olszewski R., Zawacka-Pankau J. 2010. *Pharmacological activation of tumor suppressor, wild-type p53 as a promising strategy to fight cancer*. Postępy Higieny i Medycyny Doświadczalnej (online) 64, 396 – 407
- [2] Lutz W. & Nowakowska-Świrta E. 2002. *Gene p53 mutations, protein p53, and anti-p53 antibodies as biomarkers of cancer process*. International Journal of Occupational Medicine and Environmental Health 3, 209 – 218 (polish)
- [3] COUNCIL DIRECTIVE 2013/59/EURATOM of 5 December 2013 laying down basic safety standards for protection against the dangers arising from exposure to ionising radiation, and repealing Directives 89/618/Euratom, 90/641/Euratom, 96/29/Euratom, 97/43/Euratom and 2003/122/Euratom



## Variability of the Radon Potential of Granitoids and Gneisses of the Polish Part of the Sudetes and Fore-sudetic Block

Stanisław Wołkowicz

Polish Geological Institute – National Research Institute, 4. Rakowiecka Str. 00-975 Warsaw  
e-mail: stanislaw.wolkowicz@pgi.gov.pl

**Keywords:** *radon potential, granites, gneisses, Sudetes, Fore-Sudetic Block, Poland*

### Introduction

Granitoids and gneisses have a large share in the construction of the surface of the Polish part of the Sudetes and the Fore-Sudetic Block. These rocks are characterized by a great diversity of radon potential. A large number of measurements of radon concentration in soil gas on outcrops of these rock allows to identify the reasons of this variation.

### Scope and methods of research

Investigations of radon potential were conducted by measurements of radon concentration in soil gas. In order to obtain reliable information about the radon potential of a given lithological unit, a statistically significant number of measurements were grouped in the so-called testing sites. As a rule, 15 to 35 measurements were made per site. The points were usually set in two profiles at which the measurement step was 10 meters. The testing sites were located in representative areas for selected lithological unit.

The depth of soil gas sampling was fixed to 80 centimetres. The measurements of radon concentration in soil gas were made using two types of emanometers: Canadian RDA 200 device produced by Scintrex Company and Czech LUK-3 and LUK 3A devices produced by eng. J. Plch. All devices operate on the basis of Lucas cells.

In total, 992 measurement points were made on outcrops of granitoids and 967 on gneisses.

### Results and discussion

The obtained results are illustrated using the frame graphs, increasing in rank relative to the median values. Three granitoids groups can be distinguished (Fig. 1).

The first group includes Strzelin granites. It is characterized by a very low and very poorly diversified radon potential. The second group consists of Zawidów granodiorites, Rumburk granites, Kudowa granites and Kłodzko-Złoty Stok granites. They are characterized by an average radon potential, sometimes quite diverse, which is caused by the presence of fault zones. The third group consists of granitoids of Karkonosze and Strzegom Massifs. This group of granitoids is characterized by a very diverse but generally high radon potential. They occur in structural units, where there are numerous uranium deposits and occurrences (Karkonosze-Izera Block, Kaczawa Structure).

The diversity of the radon potential of the Sudetic granitoid massifs depends on their origin, the occurrence and the intensity of the postmagmatic and hydrothermal processes accompanying the intrusion. The first group constitute a series of small, shallow intrusions of the Strzelin granites, probably non-linked with deep-seated magmatic source that could be a source of uranium. The surrounding gneisses have very similar, low, radon potential. It should be emphasized that they originated from granitoidic rocks, for which greywackes were protolites. The second group comprises massifs petrologically represented not only by typical granites, but also by tonalites and quartz diorites. Their intrusions was not accompanied by well-developed hydrothermal and post-magmatic activity. Except the Kłodzko-Zoty Stok granitoids, there is no fault tectonics within them, leading to the creation of preferential pathways of radon migration. The third group contains large, multi-phase plutons, petrographically composed mainly of granites and granodiorites, with larger or smaller admixture of tonalites. Multiphase development has resulted in long-term post-magmatic and hydrothermal activities that resulted in the redistribution of uranium. As a result, a significant part of it is not found in rock-forming and accessory minerals, but is located on the surfaces of crystals, cracks and interstices, generating intense radon emissions to the environment. Small granitoidic bodies occurring locally among Izera gneisses are good example of that how multi-phases melting process can lead to redistribution and enrichment of uranium in rocks.

The analysis of rocks petrographically defined as gneisses (Fig. 2) allows to distinguished three groups within them. The first includes all gneisses of the Fore-Sudetic Block, gneisses of Sowie Mts. and the gneiss-schist-amphibolite formation of Eastern cover of Karkonosze Mts. (Leszczyniec Formation). These rocks are characterized by generally low and poorly differentiated radon potential. There are no occurrences of uranium mineralization or, as is the case of few occurrences in the Sowie Mountains, where U mineralization is genetically related to the Permo-Carboniferous rhyolitic veins cutting gneisses. All these gneisses are paragneisses derived from sedimentary formations with minor contributions of igneous rocks, usually of basic composition. The second group consists gneisses of Bystrzyckie Mts., Kowary and Śnieżnik gneisses, characterized by a relatively high and differentiated (except gneisses of Bystrzyckie Mts.) radon potential. With these rocks are associated uranium mineralization. These are the orthogneisses created by the process of migmatization of granitic intrusion.

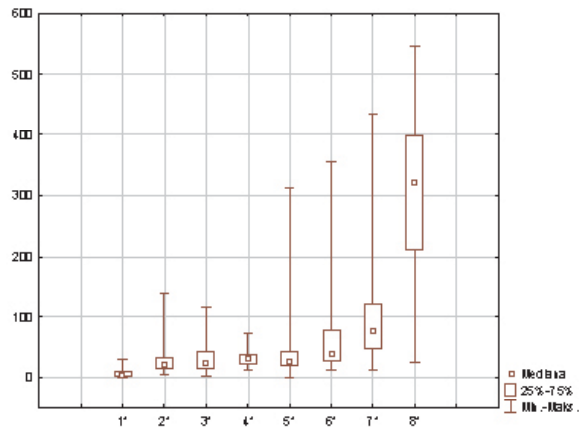


Fig. 1. Comparison of the radon potential of granites from the Sudety Mts. and Fore-Sudetic Block. Explanations: 1\* - granites of Strzelin Massif; 2\* - Zawidów granodiorites; 3\* - Rumburk granites; 4\* - Kudowa granites; 5\* - Kłodzko-Złoty Stok granites; 6\* - Strzegom granites; 7\* - Karkonosze granites; 8\* - Izera Mts. Precambrian granites

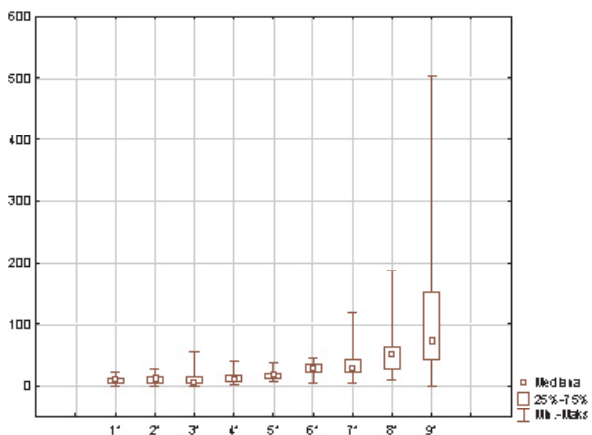


Fig. 2. Comparison of the radon potential of gneisses from the Sudety Mts. and Fore-Sudetic Block. Explanations: 1\* - migmatites and gneisses of down thrown part of Sowie Mts. Block; 2\* - gneisses of Strzelin Massif Border; 3\* - gneisses, amphibolites, chloritic schists of East Karkonosze granite Cover; 4\* - Sowie Mts. gneisses; 5\* - Wądroże Wielkie gneisses; 6\* - Bystrzyca Mts. gneisses; 7\* - Kowary gneisses; 8\* - Śnieżnik gneisses; 9\* - Izera gneisses

Separate group creates the Izera gneisses characterized by high and differentiated radon potential, which are also orthogneisses, forming as a result of mylonitic deformation of old granitic intrusions. There are numerous occurrences of uranium mineralization related to these gneisses. They are distinguished from the second group of gneisses by stronger tectonic engagement and the presence of more advanced metamorphic processes that locally led to the re-melting and formation of granitic bodies.

## **2. Gases in Volcanoes and Geothermal Systems**





## Geochemical survey of soil Rn and CO<sub>2</sub> gas emissions at Salina Island (Aeolian arc, Italy): correlation to structural vs volcanic origin

Caruso C<sup>1</sup>#, Italiano F<sup>1</sup>., Lopez M.<sup>1</sup>, Bonfanti P.<sup>2</sup>

<sup>1</sup> INGV Sezione di Palermo, Via Ugo La Malfa 153, Palermo, Italy.

<sup>2</sup> INGV Sezione di Catania, Piazza Roma 2, Catania, Italy.

# Corresponding author: marinehazard@ingv.it

**Keywords:** *Geochemistry, Radon, carbon dioxide gas, active faults, Aeolian Island.*

Soil gas (<sup>222</sup>Radon and CO<sub>2</sub> flux measurements) were performed over Salina Island, the second largest island among the seven Aeolian Islands. The volcanic Aeolian Archipelago is located in southern Tyrrhenian Sea, off the northeastern coasts of Sicily (Italy), in a complex geodynamic setting characterized by the subduction of the Ionian plate beneath the Calabrian arc (Pasquale et al., 1999). Based on recent geological mapping and stratigraphic reconstruction, the subaerial part of Salina Island developed in 6 different periods, under the control of the main structural trends: NE-SW and NNW-SSE (Lucchi et al., 2013). In general, the oldest rocks show a 0.5 my age (Barberi et al., 1974), cropping out between Capo, Rivi and Corvo volcanoes, while the youngest one are at the northwestern rim: Punta del Perciato (30-15 ky) and Pollara tuff ring, originated by two sub-Plinian explosive eruptions (Lower Pollara, Calanchi et al., 1993; Upper Pollara, Sulpizio et al., 2008). In this work, a total of 38 measurements of CO<sub>2</sub> flux and Radon concentration measurements were carried out. The active method (Gurrieri and Valenza, 1988), measures the CO<sub>2</sub> concentration in a gas mixture driven by a constant flow-rate pumping to a spectrometer. The gas is pumped through a pipe of a section of 2.5 cm<sup>2</sup> inserted at a depth of about 50 cm in the soil. The right CO<sub>2</sub> concentration value of the analyzed gas mixture (soil CO<sub>2</sub> and air) is taken when it reaches the steady state (constant value). The concentration is related to the CO<sub>2</sub> flux by the relationship:

$$\Phi_t = FC_D$$

where  $\Phi_t$  is the CO<sub>2</sub> flux,  $C_D$  is the measured CO<sub>2</sub> concentration and  $F$  is the flow rate of the pump. Although a factor, mainly depending on the soil permeability should be adopted, our approach was aimed to look for the presence of a positive CO<sub>2</sub> flux towards the atmosphere. As such, only the flow rate of the pump and the CO<sub>2</sub>

concentration were taken into consideration. Radon measurements were performed by the AlphaGUARD PQ 2000 PRO Radon Monitor respectively, with the aim to observe any possible correlation between soil gas anomalies and tectonic structures, due to the main faults of this area. The results demonstrate that the soil gas emissions are related to the main structural units. The recorded data highlight Radon values from 0.1 to 21.45 Bq/m<sup>3</sup>, while CO<sub>2</sub> values ranging from 1.100 to 16.900 ppm, only three points in the Pollara zone show the highest values ranging from 25.800 to 29.500ppm. The Pollara area coincides with the last eruptive activity of the Island, ended with the explosion that created the actual shape of the area. The measurements carried out at the site of Rinella revealed the highest CO<sub>2</sub> values up to 186.000 ppm, confirming a residual degassing due to submarine hydrothermal emissions in the past. Actually, the released gas are CO<sub>2</sub>-dominated, characterized by a helium isotopic ratio in the range of 5.5-6 Ra, typical of the magmatic origin (Italiano et al., 2011). High values of the gas emissions are evident in the central part of this island, called Valdichiesa (290m) and in the eastern part too, between Lingua and S. Maria di Salina. Among this area, two huge stratovolcanoes with vertical slopes, are present: Monte dei Porri and Monte Fossa delle Felci, respectively 860 m and 962 m high. For these hard morphological characteristic, many measurements were not possible. The gas emission data of this survey allowed us to outline some particular sector, the central and the southern part of the island, corresponding to the Tindari-Letojanni Fault System (or simply called the Tindari Fault System) and probably another fault system in direction NE-SW on the northern part, between Malfa and Capo Faro. The Tindari Fault System is a regional zone of fragile deformation located at the transition between current contractional and extensional

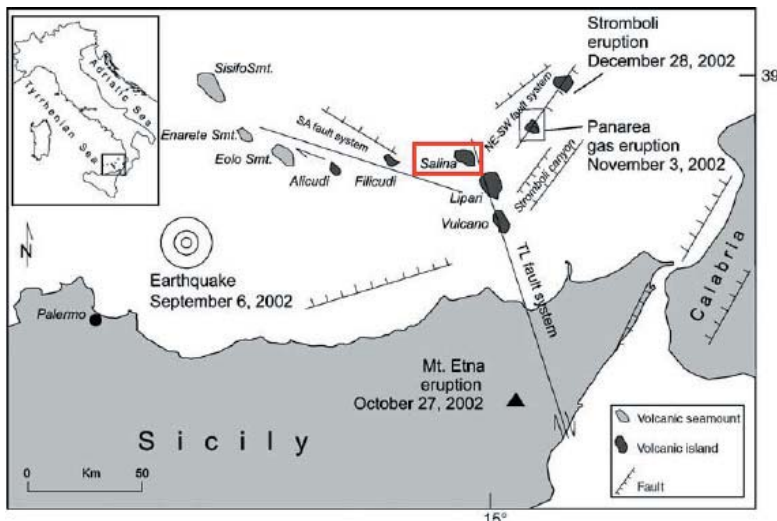


Fig. 1. Location of Salina Island and structural map of the Southern Tyrrhenian Sea and Aeolian arc, showing its main structural domains



Fig. 2-Sampling sites relative to soil emissions of Radon concentrations and CO<sub>2</sub> flux in Salina Island

crustal compartments and lying above the western edge of a narrow subducting slab (Billi et al., 2006). It consists of a NNW striking set of faults previously documented in the northeastern Sicily between Mt. Etna and the Aeolian Islands (Atzori et al., 1978, Ghisetti, 1992; Tortorici et al., 1995). In general, the geochemical monitoring along three profiles (A, B and C), allowed us to observe a correlation between the soil gas emissions (Rn and CO<sub>2</sub>) and the structural-geological context, in accordance with a significant tectonic stresses. High values of these gases occur preferentially along linear zones, in fact, these zones are elongated mainly according to the local fracture trends (NNW-SSE) and subordinately to the fracture trends NE-SW. The first tectonic trend is evident in profile A, between Rinella and Malfa: S9, S11, S13, S14, S15 for CO<sub>2</sub> flux, especially the site S10; while for Radon emissions, the anomalous sites are: S14, S15, S24, S25, S30, in particular S8. In the profile B, showing the same tectonic trend, high values of these gases are present among these sites: S2, S36, S37, S41, S42 and S43. Finally, the profile C, characterized by a trend in direction NE-SW between Capo Faro and Malfa, is marked by S3, S4 and S6. It is evident the trend of the gas emissions are correlated to structural units and their volcanic origin, especially in the maps (Fig. 3) realized by Surfer software: in red color (S8) the peak of Radon gas outlines the tectonic trend, while in blue color (S10) the peak of CO<sub>2</sub> gas emission is in relation with the presence of submarine hydrothermal manifestations, possibly a residual degassing of the past volcanic activity. On the whole, the geochemical features of the fluids are important investigation tools to outline the tectonic structures and active faults. In conclusion, the recorded Rn-CO<sub>2</sub> degassing support a correlation with the tectonic settings of the area, probably related to the Tindari Faults System. The results gained by Italiano and Caruso (2011) indicate that a release of thermal energy is still detectable in the fluids

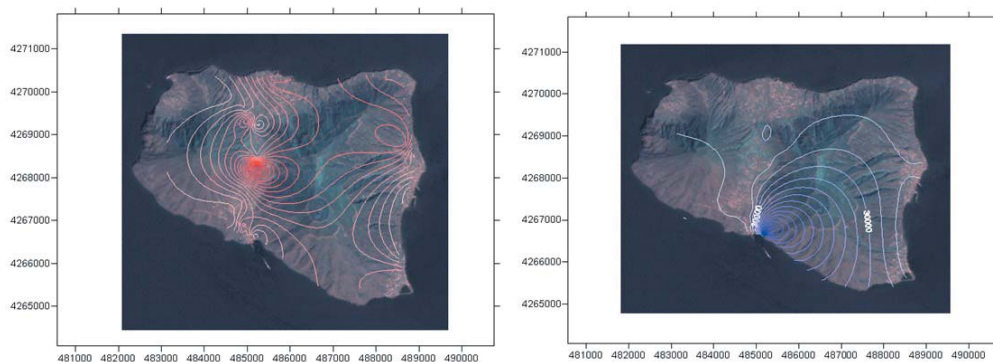


Fig. 3. Rn concentration anomalies map in red color and CO<sub>2</sub> flow anomalies map in blue color by Surfer software

vented over Salina Island. The degassing is thus driven by the local tectonic system superimposed to the release of volcanic fluids from cooling volcanic rocks.

### References

- ATZORI P., GHISSETTI F., PEZZINO A. & VEZZANI L. 1978. Strutture ed evoluzione geodinamica recente dell'area Peloritana (Sicilia Nord-Orientale), *Boll. Soc. Geol. Ital.*, 97, 31-56.
- BARBERI F. & INNOCENTI F. 1974. Evolution of Aeolian Arc Volcanism (Southern Tyrrhenian Sea). *Earth and Planetary Science Letters*, 21, 269-276.
- BILLI A., BARBERI G., FACCENNA C., NERI G., PEPE F. & SULLI A. 2006. Tectonics and seismicity of the Tindari Fault System, southern Italy: Crustal deformations at the transition between ongoing contractional and extensional domains located above the edge of a subducting slab. *Tectonics*, Vol 25.
- CALANCHI N., DE ROSA R., MAZZUOLI R., ROSSI P.L., SANTACROCE R. & VENTURA G. 1993. Silicic magma entering a basaltic magma chamber: eruptive dynamics and magma mixing-an example from Salina (Aeolian Islands, southern Tyrrhenian Sea). *Bull. Volcanol.* 55, 504-522.
- GHISSETTI F. 1992. Fault parameters in the Messina Strait (southern Italy). *Tectonophysics*, 210, 117-133.
- GURRIERI S. & VALENZA M. 1988. Gas transport in natural porous mediums: a method for measuring CO<sub>2</sub> flows from the ground in volcanic and geothermal areas, *Rend. Soc. It. Min. Petrogr.*, 43, 1151-1158.
- ITALIANO F. & CARUSO C. 2011. Detection of fresh and thermal waters over an island with extinct volcanism: the island of Salina (Aeolian arc, Italy). *Procedia Earth and Planetary Science* 4, 39-49.
- LUCCHI F., KELLER J. & TRANNE C.A. 2013. Regional stratigraphic correlations across the Aeolian archipelago (southern Italy). In: LUCCHI F., PECCERILLO A., KELLER J., TRANNE C.A. & ROSSI P.L. (Eds). *The Aeolian Islands Volcanoes*. *Geol. Soc. London, Memories* 37,55 - 81.
- PASQUALE V., VERDOVA M. & CHIOZZI P. 1999. Thermal state and deep earthquakes in the Southern Tyrrhenian. *Tectonophysics* 306, 435 - 448.
- SULPIZIO R., DE ROSA R. & DONATO P. 2008. The influence of variable topography on the depositional behavior of pyroclastic density currents: the examples of the Upper Pollara eruption (Salina Island, southern Italy). *J. Volcanol. Geotherm. Res.* 175, 367-385.
- TORTORICI L., MONACO C., TANSI C. & COCINA O. (1995). Recent and active tectonics in the Calabrian arc (Southern Italy). *Tectonophysics*, 243, 37-55.



## Hydrothermal Fluids and Sea-water Interactions: Geochemical and Mineralogical Characterization of Iron-oids from the Submarine Hydrothermal Area off Panarea Island (Aeolian Arc, Italy)

Caruso Cinzia<sup>1</sup>, Corbo Andrea<sup>1</sup>, Di Bella Marcella<sup>1,2</sup>, Lazzaro Gianluca<sup>1</sup>, Nigrelli  
Alessandra<sup>1</sup>, Romano Davide<sup>1</sup>, Sabatino Giuseppe<sup>2</sup> and Francesco Italiano<sup>1#</sup>

<sup>1</sup> National Institute of Geophysics and Volcanology, Via Ugo La Malfa, Palermo, Italy;

<sup>2</sup> Department of Mathematics and Computer Science, Physics and Earth Sciences, University of Messina, Italy

# Corresponding author: francesco.italiano@ingv.it

**Keywords:** *hydrothermal field, iron-rich nodules, volcanism, Basiluzzo Islet, Aeolian Volcanic Arc.*

The island of Panarea is a huge volcanic complex located to the eastern side of the Aeolian Archipelago (Tyrrhenian Sea). The island of Panarea is the largest among the islets (Fig. 1) and rocks emerging from the sea as remnants of past episodes of volcanic activity. The eruptive history evolved into six successive eruptive epochs separated by quiescence stages, the last of which contribute to the emplacement of the Basiluzzo endogenous dome ( $54 \pm 8$  ka; Favalli et al. 2005; Lucchi et al. 2003).

Gas emissions and hot springs are vented at the seafloor through cracks and fissures (Italiano and Nuccio, 1991) and after the submarine low energy blast of November 2<sup>nd</sup> 2002 (Caracausi et al., 2005), they are documented and monitored by the submarine monitoring systems of the National Institute of Geophysics and Volcanology (INGV, Italy). The recorded data are available in INGV databases (monsoon.pa.ingv.it).

The hydrothermal fluids vented at the sea floor come from high-temperature water-rock interactions in the deep geothermal system, then, they interact with the circulating sea waters and sediments at the sea-floor/sea water interface producing a large variety of hydrothermal deposits (e.g. Price et al., 2015).

The results of morphological, mineralogical and geochemical data of iron-rich nodules from a large hydrothermal area at a depth of 80 m, located SE of the Basiluzzo islet are here reported. The studied sample was recovered from a zone of ferruginous deposits, where sediments are composed of a sand made of micro-fossils and rust colored grains. The sample features were characterized by Scanning Electron Microscopy

– Energy Dispersive X Ray Spectroscopy (SEM-EDX) and X Ray Powder Diffraction (XRPD) and X Ray Fluorescence (XRF) analyses.

SEM-EDS investigations conducted on polished sections of the sand allowed to define the compositions and the morphologies of the sand grains (Fig. 2). All the analyzed grains show a more or less regular sub-spherical or elliptical shape and are characterized by the superimposition of roughly concentric iron oxides layers, from mm to cm sized, due to successive depositions by hydrothermal fluid activity. The internal portion (core) of the grains (named “iron-oids”) is commonly represented by piroclastic fragments (pumices, glass scoria, rocks) or single mineral phase phenocrysts (e.g.: clinopyroxene, plagioclase) that acted as accretion centers for the iron-oxide laminae concentric depositions.

XRPD analyses (Fig. 3) indicate the presence of oxy-hydroxide Goethite, volcanic mineral phases as Augite, anorthite, Sanidine, Quartz, Mg-Calcite. Goethite is a  $Fe^{3+}$  hydroxide with mineralogical formula  $FeO(OH)$  containing in some cases small amounts of manganese and may have an origin from primary hydrothermal fluids or formed by oxidation of iron ore (iron oxides or sulfides).

To define the bulk chemistry of the sand sample, in terms of major and trace element compositions (Table 1), XRF analyses were performed. Major oxides show higher values of  $Fe_2O_3$  (64.51 wt %),  $SiO_2$  (15.46 wt %) and  $CaO$  (11.43 wt %), trace elements high

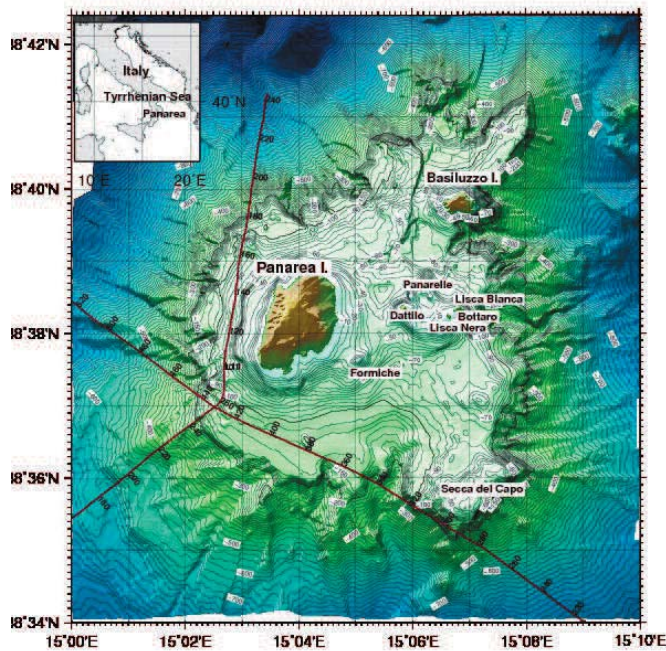


Fig. 1. The volcanic complex of Panarea and the location of the main island as well as the islets and rocks emerging from the sea surface. The main hydrothermal areas are shown (modified after Bortoluzzi et al., 2011)



Table 1. Representative XRF bulk chemistry analyses of the studied sand sample

Major Oxides Wt %	SiO <sub>2</sub>	Al <sub>2</sub> O <sub>3</sub>	Fe <sub>2</sub> O <sub>3</sub>	CaO	MgO	Na <sub>2</sub> O			
	15.46	3.35	64.51	11.43	1.26	0.70			
Major Oxides Wt %	K <sub>2</sub> O	TiO <sub>2</sub>	P <sub>2</sub> O <sub>5</sub>	MnO	SO <sub>3</sub>	Cl	Total		
	1.45	0.17	0.88	0.10	0.38	0.58	100.27		
Trace Elements ppm	V	Co	Ni	Cu	Zn	Ga	As	Rb	Sr
	39	26	28	100	4	496	76	384	33
Trace Elements ppm	Y	Zr	Nb	Cs	Ba	La	Ce	Pb	Th
	78	12	40	126	12	46	69	20	7

the hydrothermal waters rising up through the sea floor sediments as soon as the water temperature drops because of mixing processes with the shallow and cold marine waters circulating in the sediments. The concentric layering is thought to be the result of constant agitation of the ooids associated with currents and gas expulsion from the sediment

Considering 1) the extension of the “iron ooids” area, extending on the slope of the escarpment to the NE area of Basiluzzo islet from 80 to 400 meters below sea level (m bsl), and 2) the large submarine hydrothermal system located among the rocks off the coasts (Fig. 1), we argue that the hydrothermal system of the Panarea volcanic complex is one of the largest occurring in the Mediterranean area and more investigations are needed to better constrain its boundaries.

## References

- BORTOLUZZI G., ALIANI S., LIGI M., D'ORIANO F., FERRANTE V., RIMINUCCI F., CARMISCIANO C., COCCHI L., MUCCINI F. 2002. *Multidisciplinary Investigations at Panarea (Aeolian Islands) after the Exhalative Crisis of 2002*.
- CARACAUSI A., DITTA M., ITALIANO F., LONGO M., NUCCIO P.M., PAONITA A. 2005. *Massive submarine gas output during the volcanic unrest off Panarea Island (Aeolian arc, Italy): inferences for explosive conditions*. *Geochemical Journal*, 39, 5, 449-467.
- FAVALLI M., KARATSON D., MAZZUOLI R., PARESCHI M.T., VENTURA G. 2005. *Volcanic geomorphology and tectonics of the Aeolian archipelago (Southern Italy) based on integrated DEM data*. *Bull Volcanol*, 68, 157-170.
- ITALIANO F. AND NUCCIO P.M. 1991. *Geochemical investigations on submarine volcanic exhalations to the East of Panarea, Aeolian Islands, Italy*. *Jour. Volc. and Geoth. Res.*, 46, 125-141
- PRICE R. E., LA ROWE D., ITALIANO F., IVAN S., PICHLER T., AMEND J. (2015) *Subsurface hydrothermal processes 1 and the bioenergetics of chemolithoautotrophy at the shallow-sea vents off Panarea Island (Italy)*. *Chemical Geology* 407, 21-45
- SAVELLI C.; MARANI M.; GAMBERI F. 1999. *Geochemistry of metalliferous, hydrothermal deposits in the Aeolian arc (Tyrrhenian Sea)*. *Journal of Volcanology and Geothermal Research*, 88 (4), 305-323.



## Radon and CO<sub>2</sub> monitoring in Gallicano thermomineral spring, Italy

Ciolini R.<sup>1#</sup>, Pierotti L.<sup>2</sup>, D'Intinosante V.<sup>3</sup>, Facca G.<sup>2</sup>,  
Gherardi F.<sup>2</sup>, Pazzagli F.<sup>1</sup>, d'Errico F.<sup>1</sup>

<sup>1</sup> Department of Civil and Industrial Engineering, University of Pisa, Largo Lazzarino 1, I-56122 Pisa, Italy.

<sup>2</sup> CNR, Institute of Geosciences and Earth Resources, Via G. Moruzzi 1, I-56124 Pisa, Italy.

<sup>3</sup> Settore Sismica, Prevenzione Sismica, Regione Toscana, Via San Gallo 34/a, I-50129 Florence, Italy.

# corresponding author: r.ciolini@ing.unipi.it

**Keywords:** Radon, Earthquake geochemical precursors, Groundwater monitoring.

We present an automatic continuous monitoring station for radon gas (<sup>222</sup>Rn) in groundwater used to complement the study of earthquake related phenomena. Radon is a noble gas deriving from the <sup>238</sup>U decay chain and it is considered a seismic precursor (Ghosh *et al.*, 2009; Riggio and Santulin, 2015). The monitoring station has been operating since the end of 2016, measuring the radon concentration of a groundwater spring located in Gallicano, inside the Garfagnana seismic area of Tuscany in Central Italy.

Along with the radon measurement, another monitoring station developed by the CNR-IGG (National Council of research, Institute of Geosciences and Earth Resources, Italy) performs a continuous measurement of several geochemical parameters of the groundwater, i.e. temperature, pH, redox potential, electrical conductivity, CO<sub>2</sub> and CH<sub>4</sub> concentration. This station is part of a larger CNR-IGG geochemical network that has been active in Tuscany for over ten years (Cioni *et al.*, 2007) and sponsored by Tuscany Region in the within of own seismic risk reduction programs. The sampling site has been chosen on the basis of seismotectonic criteria (Pierotti *et al.*, 2015).

The radon station measures in situ the water radon concentrations every 6 hours and then transmits the data over the Internet. The radon measurement is performed by using gamma spectroscopy with a 2"x2" NaI(Tl) scintillation detector coupled to a multichannel analyzer. After the water sampling, enough time to achieve radioactive equilibrium between radon and its short decay progenies in the sample water is allowed to pass before the measurement. The detection limit is around 5 Bq/l.

The purpose of this work is to combine the radon and CO<sub>2</sub> concentration series of groundwater, searching for possible anomalies and correlations with seismic activities. Considering that CO<sub>2</sub> is frequently a radon carrier in endogenous gases,

the simultaneous measurement of both gases is expected to increase the probability of identifying earthquake-related geochemical and radioactive anomalies.

The radon measurement is performed directly in water avoiding the temporal variations due to meteorological parameters and seasonal changes which affect the radon measurements in air. Moreover, a continuous measurement is directly associated with seismic activity, avoiding the uncertainties due to long time integration measurements. The first measurement results obtained from the two type of monitors (radon and CO<sub>2</sub>) will be shown in the paper.

### References

- Cioni R., Guidi M., Pierotti L., Scozzari A., 2007. *An automatic monitoring network installed in Tuscany (Italy) for studying possible geochemical precursory phenomena*, Natural Hazards and Earth System Sciences, 7, 405–416.
- Ghosh D., Deb A., Sengupta R., 2009. *Anomalous radon emission as precursor of earthquake*, Journal of Applied Geophysics 69(2), 67–81.
- Pierotti L., Botti F., D’Intinosante V., Facca G., Gherardi F., 2015. *Anomalous CO<sub>2</sub> content in the Galliciano thermo-mineral spring (Serchio Valley, Italy) before the 21 June 2013, Alpi Apuane earthquake (M = 5.2)*. Physics and Chemistry of the Earth 85–86, 131–140.
- Riggio A., Santulin M., 2015. *Earthquake forecasting: A review of radon as seismic precursor*, Bollettino di Geofisica Teorica ed Applicata 56(2), 95–114.



## A high-temperature hydrothermal system in the Tyrrhenian offshore: the 150m deep Zannone hydrothermal field (Pontine Islands, Italy)

Italiano F.<sup>1,2#</sup>, Caruso C.<sup>1</sup>, Corbo A.<sup>1</sup>, Lazzaro G.<sup>1</sup>, Longo M.<sup>1</sup>, Nigrelli A.<sup>1</sup>

<sup>1</sup> INGV Sezione di Palermo, via Ugo La Malfa 153, Palermo, Italy,

<sup>2</sup> EMSO Interim Office, Roma, Italy

# Corresponding author: francesco.italiano@ingv.it

**Keywords:** *hydrothermal system, sea-floor observatory, Pontine Archipelago*

The hydrothermal area recently discovered in a seafloor depression (150 m water depth) offshore Zannone Island has been investigated by an oceanographic cruise for the potential connection to a deep thermal source of magmatic origin able to provide enough thermal energy to sustain the geothermal reservoir feeding the discovered vents. The island of Zannone belongs to the volcanic Pontine Archipelago located in the Tyrrhenian Sea about 30 km off the central Italy coasts, and adjacent to a wide NW-SE trending escarpment, where the last eruptive activity occurred in Pleistocene

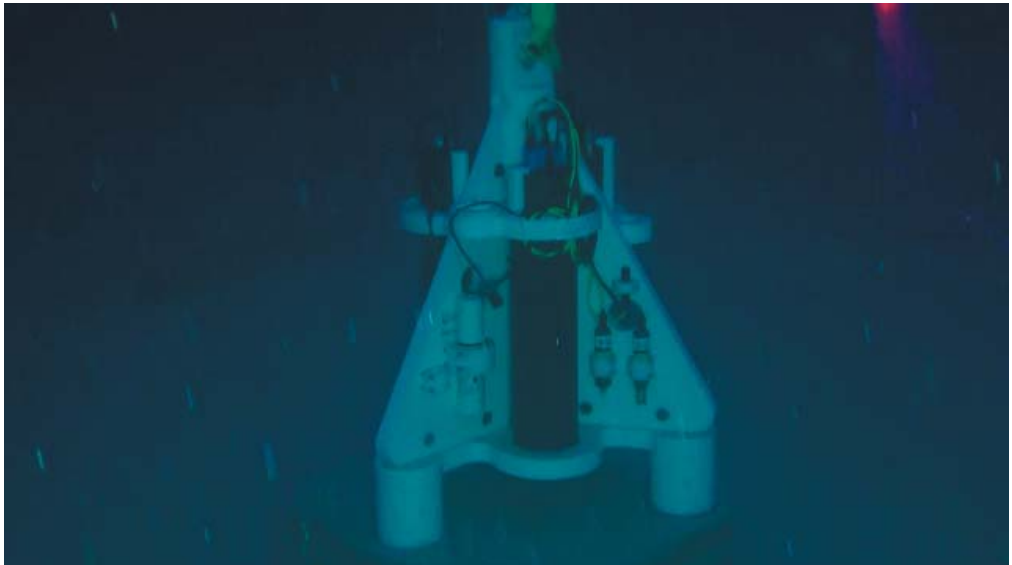
During the cruise water column profiles have been carried out to characterize the geochemical features of the dissolved gases along the water column. Bubbling gases and hot waters have been also collected at the sea-floor from hydrothermal vents. Sampling activities have been performed by a ROV (Remotely operated underwater vehicle) adaption the payload to different sampling techniques (namely bubbling gases and thermal waters collection). A customized waterproof thermometer was built by INGV researchers in order to operate directly inside the hydrothermal vents. The thermal waters were collected by a syringe operated by the ROV arm directly inserted in the vent to minimize sea water contamination.

A new “stand-alone” multidisciplinary sea-floor observatory (Ph1) developed in the mainframe of the scientific and technological activities of the EMSO – ERIC (European Multidisciplinary Seafloor and water-column Observatory, European Research Infrastructure Consortium <http://www.emso-eu.org/>). The multidisciplinary observatory, built to operate in extreme environment up to a depth of 4000 m, was deployed with the aim of gaining a better insight in the processes occurring in the submarine hydrothermal environment by collecting data of acoustics, dissolved CO<sub>2</sub>, T°C, pressure, EC, pH and turbidity. over a time period of at least six months.



Ph. 1. Seafloor observatory deployment

The chemical and isotopic analyses performed at the INGV geochemical laboratories show a dominant composition of  $\text{CO}_2$  and minor amounts of  $\text{CH}_4$  and  $\text{H}_2\text{S}$  for the bubbling gases. The isotopic composition of both  $\text{CO}_2$  and He reveal a magmatic contribution of the emitted fluids being respectively between  $-6$  and  $0 \delta^{13}\text{C} \text{ ‰}$ , and  $3 < \text{Ra} < 3,8$ . Finally the equilibrium temperatures estimated by gas-geothermometry following the indication and limitations reported by Italiano and Nuccio (1991), indicate



Ph. 2. Underwater view of deployed module



Ph. 3. Hydrothermal vent

temperatures in the range of 150-180°C, make the Zannone hydrothermal system the first deep high-temperature hydrothermal system investigated in the Tyrrhenian sea.

### References

- ITALIANO F. AND NUCCIO P.M. (1991) *Geochemical investigations on submarine volcanic exhalations to the East of Panarea, Aeolian Islands, Italy*. Jour. Volc. and Geoth. Res., 46, 125-141
- MARTORELLI E., F. ITALIANO , M. INGRASSIA, L. MACELLONI, A. BOSMAN , A. M. CONTE, S. E. BEAUBIEN , S. GRAZIANI, A. SPOSATO, and F. L. CHIOCCI. *Evidence of a shallow water submarine hydrothermal field off Zannone Island from morphological and geochemical characterization: Implications for Tyrrhenian Sea Quaternary volcanism*. Journal of Geophysical Research: Solid Earth 1 – 19.



## The influence of volcanism on the development of Chang7 black shale from Yanchang Formation in well Yaowan 1, Ordos Basin

WANG Cheng<sup>1,4</sup>, WANG Qinxian<sup>1</sup>, CHEN Guojun<sup>3</sup>,  
HE Long<sup>1,4</sup>, XU Yong<sup>3,4</sup>, CHEN Duofu<sup>1,2#</sup>

<sup>1</sup> State Key Laboratory of Organic Geochemistry, Guangzhou Institute of Geochemistry, Chinese Academy of Sciences, Guangzhou 510640, China

<sup>2</sup> Shanghai Engineering Research Center of Hadal Science and Technology, College of Marine Science, Shanghai Ocean University, Shanghai 201306, China

<sup>3</sup> Key Laboratory of Petroleum Resources Research, Chinese Academy of Sciences, Lanzhou 730000, China

<sup>4</sup> University of Chinese Academy of Sciences, Beijing 100049, China)

# Corresponding author: cdf@gig.ac.cn

**Keywords:** volcanism; hydrothermal activity; black shale; clastic influx; primary productivity; redox conditions; Late Triassic; Ordos Basin

In the geological history, volcanism was closely related to the deposition of many black shales, but its specific mechanism is still unclear. The lacustrine black shales developed in the Chang7 Member from the Upper Triassic Yanchang Formation of the Ordos Basin are considered to be the most important hydrocarbon source rocks in Central China, and it itself contained substantial gas and oils. The volcanic activities were frequent when the shales deposited, and rich volcanic ash layers were preserved in the shales, which made them as an excellent example for investigating the volcanic effect on the deposition of black shale. In this paper, three typical tuff-black shale sections of Chang7 were prepared to petrological, mineralogical and geochemical analysis. The results showed that the weathering index (WIP) of the black shales closing to the tuff decreased, the clastic influx indicators (Ti/Al and  $\Sigma$ REE), the redox indexes (V/Al, U/Al and Mo/Al), and the productivity indexes (TOC, P/Al, Ni/Al and Cu/Al) of the shales closing to the tuff increased. This suggested that the volcanic activities were likely to result in a series of environmental effects, such as the enhanced terrigenous weathering, increased debris input, water hypoxia and productivity bloom. At the same time, these environmental effects were supported by the study of the volcano eruption types of the Chang 7 period, the comparison of nutrient elements (P/Al and Fe/Al) of tuff and fresh volcanic ash, and the rich total sulfur (TS) in Chang7 black shales. Finally, this paper presented a hypothesis model of volcanism: the volcanism released a large amount of SO<sub>2</sub>, forming a large area of acid rain, which in turn accelerated the weathering of the terrestrial material and enhanced the supply of terrestrial debris and nutrients, or the

decomposition of volcanic ash released large amounts of nutrients, resulting in a bloom of biological productivity and organic matter accumulation, and then the accumulation of organic matter led to lake anoxic, and ultimately caused the development of the black shales.

This study was supported by the NSF of China (No. 41321002, 41272144) and the Strategic Priority Research Program of the Chinese Academy of Sciences (Grant No. XDB10000000).



## Radon and gas flow rates at a mofette

Heiko Woith<sup>1</sup>, Josef Vlček<sup>2</sup>, Tomáš Fischer<sup>2,3</sup>, Jens Heinicke<sup>4</sup>

<sup>1</sup> GFZ German Research Centre for Geosciences, Potsdam, Germany (radon@gfz-potsdam.de)

<sup>2</sup> Charles University in Prague, Praha, Czech Republic

<sup>3</sup> Czech Academy of Science, Prague, Czech Republic

<sup>4</sup> TU Bergakademie Freiberg, Germany

Due to its short half-life of 3.82 days (referring to the isotope <sup>222</sup>Rn) its mobility in the subsurface is limited. The diffusion length is of the order of dm to m in soil and rock (Tanner, 1964). Thus, it has been argued that radon needs a carrier fluid to migrate larger distances through the subsurface (Mogro-Campero and Fleischer, 1977). The radon carrier can be groundwater, soil gas, CO<sub>2</sub> or CH<sub>4</sub>, an overview was given by Etiope and Martinelli (2002). Experiments on the efficiency of various carrier gases have been performed by Chyi *et al.* (2010). A positive correlation between CO<sub>2</sub> flux and radon was observed in Nepal (Perrier *et al.*, 2009). Generally, radon concentration increases with increasing flow rate of the carrier fluid due to the fact that less radon decays on the way to the surface. Additionally, the mobilization of radon adsorbed on grain surfaces might change with the flow rate, as obtained experimentally by Chyi *et al.* (2010).

A natural laboratory to study gas fluxes from the mantle to the atmosphere is the NW Bohemia/Vogtland area located in the border region between the Czech Republic and Germany. More than one hundred CO<sub>2</sub>-rich springs and mofettes occur in this region (Fig. 1) with gas fluxes up to 87,000 dm<sup>3</sup>/h (Weinlich *et al.*, 1999). One of the gas emission centres within the Eger-Rift is located within the Cheb basin (Bankwitz *et al.*, 2003) with its mofette fields in Soos, Bublák, and Hartoušov. Earthquake swarms repeatedly occurred during the past century (Fischer and Horalek, 2003) and the hypothesis has been formulated that ascending/intruding magmatic fluids trigger the earthquake swarms (Parotidis *et al.*, 2005). During the past 30 years, 90% of the earthquake swarms clustered beneath the village Nový Kostel (Fig. 1) within a depth range between 6 and 12 km (Fischer *et al.*, 2014). Thus, the region had been selected to install an observatory for study of non-volcanic, mid-crustal earthquake swarms and accompanying phenomena within the frame of an ICDP-project (Dahm *et al.*, 2013).

Within the mofette field of Hartoušov the gas flow is monitored at a 30 m deep well (VP8303) since several years. A fast increase of the CO<sub>2</sub> flow rate had been observed 4 days after a local earthquake (Fischer *et al.*, 2017). During 2016 a radon detector had been installed additionally for several months to study the relation between radon concentration and gas flow rate. Air and well temperature, barometric pressure, and

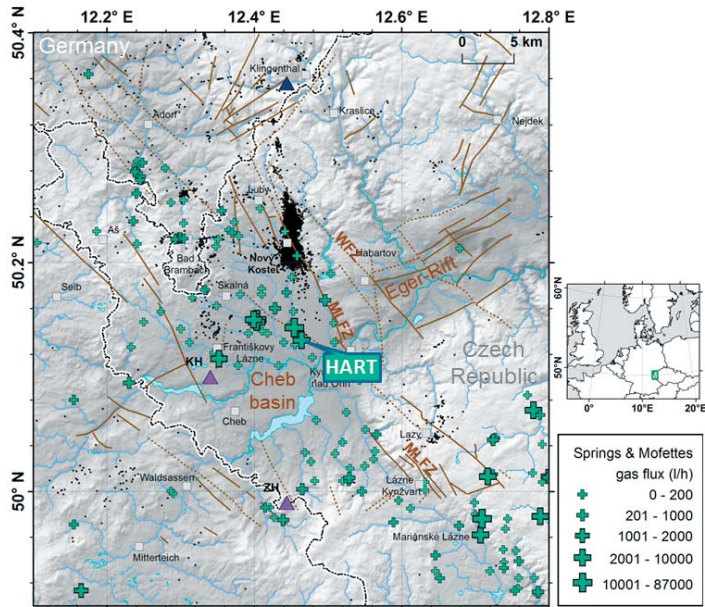


Fig. 1. Location of nearly 200 springs and mofettes in the NW Bohemia/Vogtland region (green symbols). Black dots indicate earthquake swarms between 1991 and 2007. HART indicates the location of the monitoring well VP8303 within the mofette field of Hartoušov

water level are recorded on the same datalogger. Sampling interval is 10 minutes. While similar measurements at Bad Brambach (NW of HART) showed the expected correlation between radon and flow rate (Heinicke *et al.*, 1995), both parameters are not correlated at Hartoušov.

### References:

- BANKWITZ P., SCHNEIDER, G., KAMPF, H. & BANKWITZ, E., 2003. *Structural characteristics of epicentral areas in Central Europe: study case Cheb Basin (Czech Republic)*, Journal of Geodynamics, 35, 5-32.
- CHYI L.L., QUICK, T.J., YANG, T.F. & CHEN, C.H., 2010. *The experimental investigation of soil gas radon migration mechanisms and its implication in earthquake forecast*, Geofluids, 10, 556-563.
- DAHM T., HRUBCOVÁ, P., FISCHER, T., HORÁLEK, J., KORN, M., BUSKE, S. & WAGNER, D., 2013. *Eger Rift ICDP: An observatory for study of non-volcanic, mid-crustal earthquake swarms and accompanying phenomena*, Scientific Drilling, 93-99.
- ETIOPE G. & MARTINELLI, G., 2002. *Migration of carrier and trace gases in the geosphere: an overview*, Physics of the Earth and Planetary Interiors, 129, 185-204.
- FISCHER T. & HORALEK, J., 2003. *Space-time distribution of earthquake swarms in the principal focal zone of the NW Bohemia/Vogtland seismoactive region: period 1985-2001*, Journal of Geodynamics, 35, 125-144.
- FISCHER T., HORÁLEK, J., HRUBCOVÁ, P., VAVRYČUK, V., BRÄUER, K. & KÄMPF, H., 2014. *Intra-continental earthquake swarms in West-Bohemia and Vogtland: A review*, Tectonophysics, 611, 1-27.

- FISCHER T., MATYSKA, C. & HEINICKE, J., 2017. *Earthquake-enhanced permeability – evidence from carbon dioxide release following the ML 3.5 earthquake in West Bohemia*, Earth and Planetary Science Letters, 460, 60-67.
- HEINICKE J., KOCH, U. & MARTINELLI, G., 1995. *CO<sub>2</sub> and radon measurements in the Vogtland area (Germany) - a contribution to earthquake prediction research*, Geophysical Research Letters, 22, 771-774.
- MOGRO-CAMPERO A. & FLEISCHER, R.L., 1977. *Subterrestrial fluid convection: a hypothesis for long-distance migration of radon within the Earth*, Earth & Planetary Science Letters, 34, 321-325.
- PAROTIDIS M., SHAPIRO, S.A. & ROTHERT, E., 2005. *Evidence for triggering of the Vogtland swarms 2000 by pore pressure diffusion*, Journal of Geophysical Research-Solid Earth, 110, B05S10.
- PERRIER F., RICHON, P., BYRDINA, S., FRANCE-LANORD, C., RAJAURE, S., KOIRALA, B.P., SHRESTHA, P.L., GAUTAM, U.P., TIWARI, D.R., REVIL, A., BOLLINGER, L., CONTRAIRES, S., BUREAU, S. & SAPKOTA, S.N., 2009. *A direct evidence for high carbon dioxide and radon-222 discharge in Central Nepal*, Earth and Planetary Science Letters, 278, 198-207.
- TANNER A.B., 1964. *Radon migration in the ground: a review*. in: *The natural radiation environment*, pp. 161-190, Chicago.
- WEINLICH F.H., BRÄUER, K., KÄMPF, H., STRAUCH, G., TESAŘ, J. & WEISE, S.M., 1999. *An active subcontinental mantle volatile system in the western Eger rift, Central Europe: Gas flux, isotopic (He, C, and N) and compositional fingerprints*, Geochimica et Cosmochimica Acta, 63, 3653-3671.

### **3. Gases in Petroliferous Sedimentary Basins and Reservoirs**





# Origin of Hydrocarbon Gases in the Zechstein Main Dolomite Reservoir in Wielkopolska Province of the Polish Permian Basin: Isotope and Hydrous Pyrolysis Studies

Elżbieta Bilkiewicz<sup>#</sup>, Maciej J. Kotarba

AGH University of Science and Technology, Krakow, Poland  
<sup>#</sup> corresponding author: ebil@agh.edu.pl

## Introduction

The aim of this study was to determine the origin of hydrocarbons of natural gases accumulated in the Main Dolomite (Ca<sub>2</sub>) carbonate reservoir in the Wielkopolska Petroleum Province of the Polish Upper Permian Basin (western Poland) based on the results of analytical and experimental methods of petroleum geochemistry including molecular and stable carbon (in CH<sub>4</sub>, C<sub>2</sub>H<sub>6</sub>, C<sub>3</sub>H<sub>8</sub>, *n*-C<sub>4</sub>H<sub>10</sub>, *i*-C<sub>4</sub>H<sub>10</sub>, *n*-C<sub>5</sub>H<sub>12</sub> and *i*-C<sub>5</sub>H<sub>12</sub>) and hydrogen (in CH<sub>4</sub>, C<sub>2</sub>H<sub>6</sub> and C<sub>3</sub>H<sub>8</sub>) isotope compositions of natural gas and gases generated during hydrous pyrolysis (HP) experiments.

The discussed natural gas accumulations occur within the Ca<sub>2</sub> carbonates which are underlain and overlain by impermeable sequences of evaporates forming a closed hydrodynamic system composed of both source and reservoir rocks for hydrocarbon deposits (e.g. Kotarba and Wagner, 2007).

## Discussion

Comparison of molecular and stable isotope compositions of natural gases and HP gases indicates that hydrocarbon gases have been generated during different microbial and thermogenic (thermochemical) processes. Fig. 1 shows a relationship between stable carbon isotopes of CH<sub>4</sub>, C<sub>2</sub>H<sub>6</sub> and C<sub>3</sub>H<sub>8</sub> versus reciprocal of carbon number of the analysed natural gases and gases generated during HP experiments. The plot reveals the presence of two genetic groups of analysed natural gases. The first genetic group encompasses two subgroups: subgroup A contains hydrocarbon gases generated during exclusively thermogenic processes (Jarocin and Połęcko deposits) and subgroup B comprising hydrocarbon gases produced during both microbial and thermogenic processes (Buk, Kije, Mozów, Ołobok, Radoszyn and Retno deposits). The first genetic group comprises hydrocarbon gases that originated from the Ca<sub>2</sub> source rocks and is characterized by normal order  $\delta^{13}\text{C}(\text{CH}_4) < \delta^{13}\text{C}(\text{C}_2\text{H}_6) < \delta^{13}\text{C}(\text{C}_3\text{H}_8)$  in mostly concave

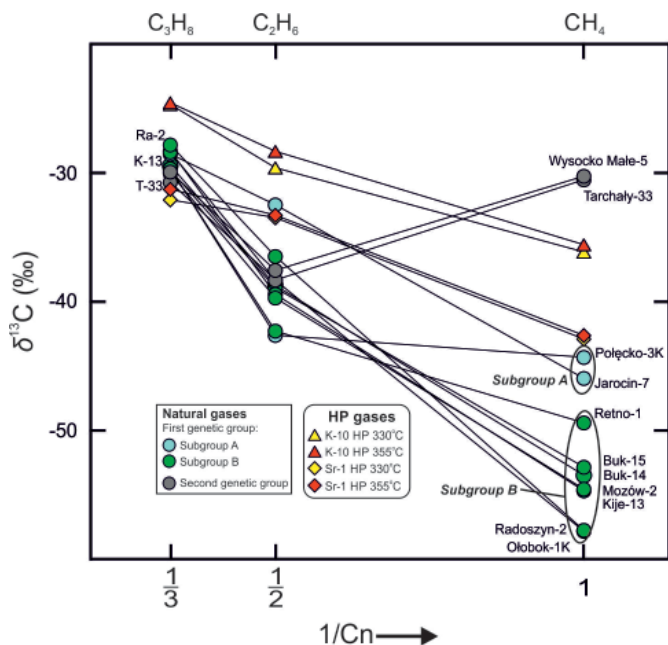


Fig. 1. Stable carbon isotope composition of  $\text{CH}_4$ ,  $\text{C}_2\text{H}_6$  and  $\text{C}_3\text{H}_8$  vs. the reciprocal of their carbon number for analysed natural gases and gases generated during HP experiments

pattern. These gases are genetically related to dispersed organic matter of Ca2 carbonates and originated from oil-prone Type-II kerogen. The second genetic group of hydrocarbon gases is represented by two gases from Wysocko Małe and Tarchały deposits. They are characterized by partial inverse  $\delta^{13}\text{C}(\text{CH}_4) > \delta^{13}\text{C}(\text{C}_2\text{H}_6) < \delta^{13}\text{C}(\text{C}_3\text{H}_8)$  order. Such partial and even complete reverse orders of natural gases generated by Carboniferous source rocks have been discovered in Polish Basin by Kotarba et al. (2014). Zumberge et al. (2012) and Kotarba et al. (2014) concluded that complete and partial reverse isotopic orders indicate very complicated generation, migration and accumulation history of natural gases. Hydrocarbon gases from these two deposits are not genetically related to dispersed organic matter of the Ca2 strata. They originated from humic source organic matter of high maturity from presumably Pennsylvanian and Mississippian strata and migrated to the Ca2 reservoir through local fault zones.

The presence of thermogenic gases of Wysocko Małe, Tarchały, Połęcko, Jarocin and Retno deposits suggests that during microbial phase traps within Ca2 carbonates had not been formed yet. Microbial component of rest of natural gases suggests that traps within the Ca2 carbonates had already been formed and sealed by the underlying evaporites which prevented its escape.

Stable carbon isotope composition of  $\text{CH}_4$ ,  $\text{C}_2\text{H}_6$ ,  $\text{C}_3\text{H}_8$  of gases generated during HP experiments plotted against the reciprocal of their carbon number showed both concave and convex trends confirming previous studies (e.g. Kotarba and Lewan, 2013)

that non-linear orders cannot be indicative for multiple thermogenic gas generation regardless of the kerogen type.

The research has been financially supported by the statutory research of the Faculty of Geology, Geophysics and Environmental Protection at the AGH University of Science and Technology in Kraków, project No. 11.11.140.626.

### References

KOTARBA, M.J., WAGNER, R., 2007. *Generation potential of the Zechstein Main Dolomite (Ca<sub>2</sub>) carbonates in the Gorzów Wielkopolski-Międzychód-Lubiatów area: geological and geochemical approach to microbial-algal source rock*. Przegląd Geologiczny 55, 1025-1035.

KOTARBA, M.J., LEWAN, M.D., 2013. *Sources of natural gases in Middle Cambrian reservoirs in Polish and Lithuanian Baltic Basin as determined by stable isotopes and hydrous pyrolysis of Lower Palaeozoic source rocks*. Chemical Geology 345, 62-76.

KOTARBA, M.J., NAGAO, K., KARNKOWSKI P.H., 2014. *Origin of gaseous hydrocarbons, noble gases, carbon dioxide and nitrogen in Carboniferous and Permian strata of the distal part of the Polish Basin: Geological and isotopic approach*. Chemical Geology 383, 164-179.

ZUMBERGE., J., FERWORN, K., BROWN, S., 2012. *Isotopic reversal ('rollover') in shale gases produced from the Mississippian Barnett and Fayetteville formations*. Marine and Petroleum Geology 31, 43-52.



## Gas diffusion causing natural gas composition and carbon isotope ratio anomalies – a case from the Carboniferous Donghe sandstone reservoir in the Hadexun oilfield, Tabei uplift, Tarim Basin, NW China

Jianfa Chen<sup>1,2#</sup>, Yangyang Wang<sup>1,2</sup>, Xiongqi Pang<sup>1,2</sup>, Baoshou Zhang<sup>3</sup>,  
Yifan Wang<sup>1,2</sup>, Liwen He<sup>1,2</sup>, Zeya Chen<sup>1,2</sup>, Guoqiang Zhang<sup>1,2</sup>

<sup>1</sup> State Key Laboratory of Petroleum Resources and Prospecting, China University of Petroleum, Changping District, Beijing, 102249, China

<sup>2</sup> College of Geosciences, China University of Petroleum, Beijing, 102249, China

<sup>3</sup> Research Institute of Exploration and Development, Tarim Oilfield Company, PetroChina, Korla, Xinjiang, 84100, China

# Corresponding author: jfchen@cup.edu.cn; phone: +8613911779822; address: China University of Petroleum, No. 18, Fuxue Road, Changping district, Beijing, P. R. China, 102249

**Keywords:** gas diffusion, carbon isotopes, natural gas, Tarim Basin.

The geochemical characteristics of natural gas have been considered as sensitive tracers for the origin of natural gas and hydrocarbon charging history due to the fact that their isotopic and compositional signatures give important information on their genetic and post-genetic histories. According to the previous published studies, many scholars believed that the genetic elements (Schoell, 1988; Chung et al., 1988; Clayton, 1991; Scott et al., 1994; Whiticar, 1994, 1999; Prinzhofer and Huc, 1995; Pan et al., 2010) including gas sources and its degree of thermal evolution were the main factors controlling compositional and isotopic characteristics of hydrocarbon gases. Hydrocarbon gaseous compounds in natural gas tend to be enriched in heavy carbon isotopes with thermal maturity increasing. Moreover, most field and laboratory observations and theoretical models of kinetic isotope effects (KIEs) created a normal sequence of carbon isotopic compositions with  $\delta^{13}\text{C}$  methane ( $\text{C}_1$ )  $< \delta^{13}\text{C}$  ethane ( $\text{C}_2$ )  $< \delta^{13}\text{C}$  propane ( $\text{C}_3$ ) and  $< \delta^{13}\text{C}$  butane ( $\text{C}_4$ ) observed in natural gas accumulations worldwide (Schoell, 1983, 1988; Pan et al., 2010). Apart from the genetic elements, some scholars had emphasized the influence of post-genetic elements on compositional and isotopic characteristics, such as migration along carrier bed (Smith et al., 1971; Prinzhofer and Huc, 1995), gas diffusion (Krooss and Schaefer, 1987; Krooss et al., 1988; Krooss and Leythaeuser, 1992), adsorption–desorption (Friedrich and Juntgen, 1972), microorganism degradation (James, 1990.; Whiticar, 1994, 1999; Pan et al., 2006; Lu et al., 2010), gas mixing (Dai et al., 2004; Burruss and Laughrey, 2010) and so on. During

studies of natural gas reservoirs of Carboniferous age in the Hadexun oilfield, Tabei uplift, Tarim Basin, NW China, we observed abnormally low total hydrocarbon gas content (< 65 %), low methane content (< 10%) and low dry coefficients (< 0.5) in the block HD4. In addition, we have observed reversal of the normal trend of carbon isotopic composition, such that  $\delta^{13}\text{C}$  methane ( $\text{C}_1$ )  $>\delta^{13}\text{C}$  ethane ( $\text{C}_2$ )  $<\delta^{13}\text{C}$  propane ( $\text{C}_3$ )  $<\delta^{13}\text{C}$  butane ( $\text{C}_4$ ). More specifically, methane had a tendency to become enriched in  $^{13}\text{C}$  (the changes of  $\delta^{13}\text{C}$  values between the gas from block HD4 and gas from the neighbouring areas reached 10‰). This type of abnormal gas had never been reported in previous studies of the Tarim Basin and such large changes in  $\delta^{13}\text{C}$  were rarely seen even in other basins. Previous observations of composition and carbon isotope ratio anomalies have been explained by mixing between gases from different sources and thermal maturities, migration along carrier bed, adsorption–desorption, microorganism degradation and so on. Whether these current models of hydrocarbon gas generation and post-genetic elements could rationally explain the composition and carbon isotope ratio anomalies in the Hadexun oilfield, it has geological and geochemical significances. Based on comprehensive analysis of gas geochemical data and the geological setting of the Carboniferous reservoirs in the Hadexun oilfield, we indicated the cause of gas composition and carbon isotope ratio anomalies in the Donghe sandstone reservoir was gas diffusion through the poorly sealed caprock rather than the microorganism degradation, the gas mixing of different kerogen types or the thermal maturity degree of gas source rocks. Our observation and interpretation that gas diffusion during post-genetic period is causing gas geochemical anomalies has important implications for natural gas resources in deeply buried sedimentary basins.

## References

- Chen, J.F., Shen, P., Huang B.J., 2000. *Application of contents of chemical components and isotopic composition of oil-gas to research on the secondary migration of Ying-qiong basin in China*. Journal of the University of Petroleum, China 24, 91-94 ( in Chinese with English abstract ).
- Chung, H.M., Gormly, J.R., Squires, R.M., 1988. *Origin of gaseous hydrocarbons in subsurface environments: Theoretical considerations of carbon isotope distribution*. Chem. Geol. 71, 97-104.
- Clayton, C.J., 1991. *Carbon isotope fractionation during natural gas generation from kerogen*. Mar. Petroleum Geol. 8, 232-240.
- Coleman, D.D., Risatti, J.B., Schoell, M., 1981. *Fractionation of carbon and hydrogen isotopes by methane-oxidizing bacteria*. Geochimica et Cosmochimica Acta 45, 1033-1037.
- Jenden, P.D., David, R., Hilton, I.R., 1993. *Abiogenic hydrocarbons and mantle helium in oil and gas fields*. United States Government Printing Office, Washington, 31-56.
- Krooss, B. M., 1988. *Experimental investigation of the molecular migration of C1-C6 hydrocarbons: Kinetics of hydrocarbon release from source rocks*. Org. Geochem. 13, 513-523.
- Krooss, B.M., Leythauser, D., 1997. *Diffusion of methane and ethane through the reservoir cap rock: Implications for the timing and duration of catagenesis discussion*. AAPG Bull. 81, 155-161.
- Lu, H., Chen, T., Liu, J., Peng, P., Lu, Z., Ma, Q., 2010. *Yields of H<sub>2</sub>S and gaseous hydrocarbons in gold tube experiments simulating thermochemical sulfate reduction reactions between MgSO<sub>4</sub> and petroleum fractions*. Org. Geochem. 41, 1189-1197.

- Pan, C., Jiang, L., Liu, J., Zhang, S., Zhu, G., 2010. *The effects of calcite and montmorillonite on oil cracking in confined pyrolysis experiments*. *Org. Geochem.* 41, 611-626.
- Prinzhofer, A., Huc, A.Y., 1995. *Genetic and post-genetic molecular and isotopic fractionations in natural gases*. *Chem. Geol.* 126, 281-290.
- Prinzhofer, A., 1997. *Isotopically light methane in natural gas: bacterial imprint or segregative migration*. *Chem. Geol.* 142, 193-200.
- Prinzhofer, A., Pernaton, E., 1997. *Isotopically light methane in natural gas: bacterial imprint or diffusive fractionation?* *Chem. Geol.* 142,193-200.
- Rooney, M.A., Claypool, G.E., Chung, H.M., 1995. *Modeling thermogenic gas generation using carbon isotope ratios of natural gas hydrocarbons*. *Chem. Geol.* 126, 219-232.
- Schoell, M., 1983. *Genetic characterization of natural gases*. *AAPG Bull.* 67, 2225-2238.
- Schoell, M., 1988. *Multiple origins of methane in the earth*. *Chem. Geol.* 71, 1-10.
- Scott, A.R., Kaiser, W.R., Ayers, W.B. Jr., 1994. *Thermogenic and secondary biogenic gases, San Juan Basin, Colorado and New Mexico implications for coal bed gas producibility*. *AAPG Bull.* 78, 1186-1209.
- Smith, J.E., Erdman, J.G., Morris, D.A., 1971. *Migration, accumulation and retention of petroleum in the earth*. *Proc. 8th World Petrol. Cong.* 2, 13-26.
- Whiticar, M.J., 1999. *Carbon and hydrogen isotope systematic of bacterial formation and oxidation of methane*. *Chem. Geol.* 161, 291-314.



## Molecular and Isotopic Compositions, Origin and Biodegradation of Natural Gas in the Central Part of the Polish Outer Carpathians

Maciej J. Kotarba, Elżbieta Bilkiewicz

AGH University of Science and Technology, Krakow, Poland

### Introduction

Origin and influence of secondary biodegradation of natural gases occurring within the Lower Cretaceous-Miocene sandstone reservoirs of the central part of the Polish Outer Carpathians, in area between meridional line Dębica-Jasło on the west and Łańcut-Dynów- Sanok on the east, based on molecular and stable C, H and N isotope ( $^{12}, ^{13}\text{C}$  in  $\text{CH}_4$ ,  $\text{C}_2\text{H}_6$ ,  $\text{C}_3\text{H}_8$ ,  $n\text{C}_4\text{H}_{10}$ ,  $i\text{C}_4\text{H}_{10}$ ,  $n\text{C}_5\text{H}_{12}$ ,  $i\text{C}_5\text{H}_{12}$  and  $\text{CO}_2$ ,  $^1, ^2\text{H}$  in  $\text{CH}_4$ ,  $\text{C}_2\text{H}_6$  and  $\text{C}_3\text{H}_8$ , and  $^{14}, ^{15}\text{N}$  in  $\text{N}_2$ ) compositions are determined and explained.

### Geological outline, petroleum occurrence and source rock

The Outer Carpathians, one of the largest petroleum provinces of Central Europe, is a fold-thrust belt of Late Jurassic-Late Miocene age rocks, up to 6 km in stratigraphic thickness. They consist of the major nappes (tectonic units) named from south to north as the Magura, Dukła, Silesian, Sub-Silesian, Skole and Zgłobice. The study area covers the central part of the Polish Outer Carpathians. Dukła, Silesian, Sub-Silesian and Magura units occur in this area. Both oil and gas are currently produced in the study area. The Oligocene Menilite Shales have the best hydrocarbon potential of formations within the Dukła and Silesian units (e.g. Kotarba et al., 2007).

### Samples and Methods

Natural gas samples from the Lower Cretaceous-Miocene sandstone reservoirs, forty three samples from Bednarka, Bóbrka-Rogi, Dobrucowa-Jaszczew, Harkłowa, Iwonicz Zdrój, Krościenko, Osobnica, Potok, Roztoki, Turaszówka petroleum deposits of the Silesian Unit, eight samples from Węglówka and Wola Jasienicka petroleum deposits of the Sub-Silesian Unit, three samples from Folusz-Pielgrzymka petroleum deposit of the Dukła Unit, and Ropianka seep of the Magura Unit (Fig. 1) were collected.

Molecular compositions of natural gases ( $\text{CH}_4$ ,  $\text{C}_2\text{H}_6$ ,  $\text{C}_3\text{H}_8$ ,  $i\text{-C}_4\text{H}_{10}$ ,  $n\text{-C}_4\text{H}_{10}$ ,  $\text{C}_5\text{H}_{12}$ ,  $\text{C}_6\text{H}_{14}$ ,  $\text{C}_7\text{H}_{16}$ , unsaturated hydrocarbons,  $\text{CO}_2$ ,  $\text{O}_2$ ,  $\text{H}_2$ ,  $\text{N}_2$ , He, Ar) were analysed in a set of columns of Hewlett Packard 5890 Series II, Hewlett Packard 6890 Series and Chrom

5 gas chromatographs equipped with flame ionization (FID) and thermal conductivity (TCD) detectors. The stable C, H and N isotope analyses were completed on a Finnigan Delta Plus and a Thermo Scientific Delta V Plus mass spectrometers. Methane, ethane, propane, butanes, pentanes and carbon dioxide for C isotopes, methane, ethane and propane for H isotopes and molecular nitrogen for N isotopes were separated chromatographically. Analytical precisions are estimated to be as follows:  $\pm 0.2\text{‰}$  of C isotopes,  $\pm 3\text{‰}$  for methane and  $\pm 5\text{‰}$  for ethane and propane of H isotopes, and  $\pm 0.4\text{‰}$  of N isotopes.

## Results

The analysed natural gases in the study area are variable both in their molecular and isotopic compositions. The molecular composition, gas indices and stable isotope ratios vary within the following ranges:  $\text{CH}_4$  from 38.3 to 98.6%,  $\text{C}_2\text{H}_6$  from 0.05 to 18.1 %,  $\text{C}_3\text{H}_8$  from 0.02 to 16.6 %,  $i\text{C}_4\text{H}_{10}$  from 0.004 to 5.1 %,  $n\text{C}_4\text{H}_{10}$  from 0.002 to 5.2 %,  $i\text{C}_5\text{H}_{12}$  from 0.003 to 1.76 %,  $n\text{C}_5\text{H}_{12}$  from 0.005 to 1.73 %,  $\text{N}_2$  from 0.12 to 22.1 %,  $\text{CO}_2$  from 0.01 to 20.9 %, hydrocarbon index [ $C_{\text{HC}} = \text{CH}_4 / (\text{C}_2\text{H}_6 + \text{C}_3\text{H}_8)$ ] from 2 to 479, carbon dioxide/methane index { $\text{CDMI} = (\text{CO}_2 / [\text{CO}_2 + \text{CH}_4]) \cdot 100$  (%) } from 0.00 to 13.4 %,  $\delta^{13}\text{C}(\text{CH}_4)$  from  $-63.4$  to  $-36.4\text{‰}$ ,  $\delta^{13}\text{C}(\text{C}_2\text{H}_6)$  from  $-44.5$  to  $-25.8\text{‰}$ ,  $\delta^{13}\text{C}(\text{C}_3\text{H}_8)$  from  $-31.4$  to  $-25.7\text{‰}$ ,  $\delta^{13}\text{C}(i\text{C}_4\text{H}_{10})$  from  $-31.7$  to  $-26.7\text{‰}$ ,  $\delta^{13}\text{C}(n\text{C}_4\text{H}_{10})$

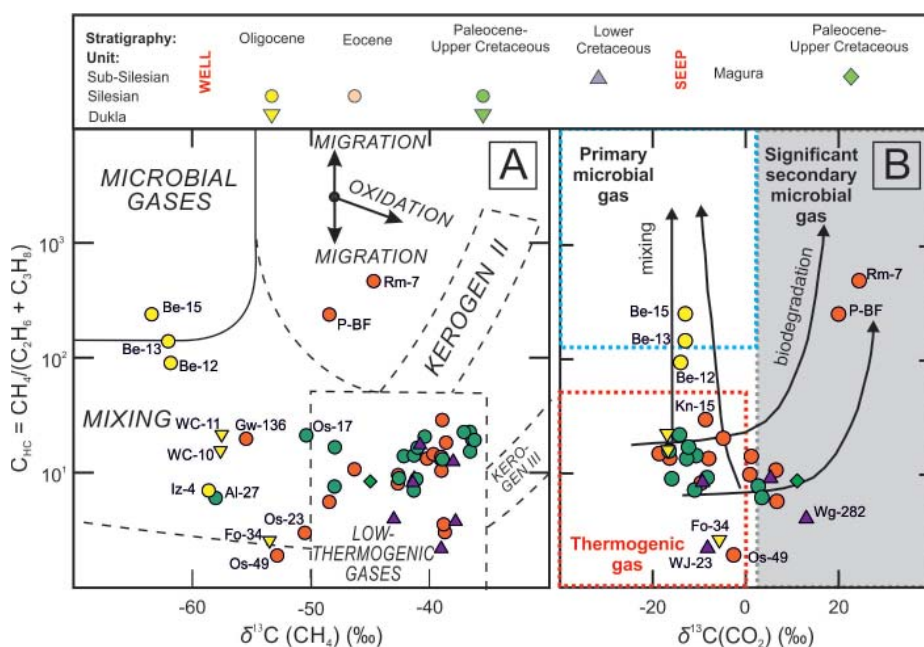


Fig. 1. Hydrocarbon index ( $C_{\text{HC}}$ ) versus (A)  $\delta^{13}\text{C}(\text{CH}_4)$  and (B)  $\delta^{13}\text{C}(\text{CO}_2)$  for analysed natural gases. Compositional fields from (A) Whitcary (1994) and (B) Milkov (2010)

from -31.0 to -24.2‰,  $\delta^{13}\text{C}(i\text{C}_5\text{H}_{12})$  from -30.0 to -25.2‰,  $\delta^{13}\text{C}(nC_5\text{H}_{12})$  from -30.0 to -24.0‰,  $\delta^2\text{H}(\text{CH}_4)$  from -218 to -153‰,  $\delta^2\text{H}(\text{C}_2\text{H}_6)$  from -171 to -126‰,  $\delta^2\text{H}(\text{C}_3\text{H}_8)$  from -166 to -113‰,  $\delta^{13}\text{C}(\text{CO}_2)$  from -18.6 to 24.4‰ and  $\delta^{15}\text{N}(\text{N}_2)$  from -4.5 to 0.5‰. The gases are wet and contain hexanes from 0.00 to 1.49 % and heptanes from 0.00 to 0.24 %.

## Conclusions

Mentioned above results of molecular and stable isotope analyses of natural gases accumulated in Silesian, Sub-Silesian, Dukla and Magura units of the central part of the Polish Outer Carpathians reveal: (i) gaseous hydrocarbons are generally related to thermogenic (thermocatalytic) processes; (ii) 3 of 55 analysed hydrocarbon gases are genetically connected with microbial carbon dioxide reduction, and further 11 of 55 analysed gases also occur genetically component of microbial (bacterial) methane (Fig. 1A), which proves that petroleum traps had already been formed and sealed before the initial microbial processes affected the organic matter of the Oligocene Menilite Shales; (iii) thermogenic gases were generated during low-temperature, and occasionally during high-temperature stages at a maturity level of 0.8 to 1.8% in vitrinite reflectance scale assuming type II and mixed type II/III kerogen of the Oligocene Menilite Shales; (iv) thermogenic gaseous hydrocarbons were generated from a single source irrespectively of kerogen type; (v) 2 of 55 analysed gases underwent the significant secondary biodegradation, and further 9 of 55 analysed gases underwent the secondary biodegradation (Fig. 1B); (vi) carbon dioxide was generated during both thermogenic and microbial processes; (vii) molecular nitrogen was generated most probably during thermal transformation of organic matter (thermogenic nitrogen), and partly has a component release from  $\text{NH}_4$ -rich illites.

The research has been financially supported by the Polish National Science Centre grant No. UMO-2014/15/B/ST10/00131 (AGH 18.18.140.666/N84).

## References

- KOTARBA M.J., WIĘCŁAW D., KOLTUN Y.V., MARYNOWSKI L., KUŚMIEREK J. & DUDOK I.V., 2007. *Organic geochemical study and genetic correlation of natural gas, oil and Menilite source rocks in the area between San and Stryi rivers (Polish and Ukrainian Carpathians)*. *Organic Geochemistry*, 38, 8, 1431-1456.
- MILKOV A.V., 2011. *Worldwide distribution and significance of secondary microbial methane formed during petroleum biodegradation in conventional reservoirs*. *Organic Geochemistry*, 42, 184-207.
- WHITICAR M.J., 1994. *Correlation of natural gases with their sources*. In: Magoon, L.B. and Dow, W.G. (Eds.), *The petroleum system - from source to trap*. AAPG Memoir 60, 261-283.



## Gas Occurrence and Accumulation Characteristics of Cambrian-Ordovician Shales in the Tarim Basin, Northwest China

Luofu LIU<sup>1,2#</sup>, Ying WANG<sup>1,2</sup>, Baojian SHEN<sup>3</sup>, Xiaoyue GAO<sup>1,2</sup>

<sup>1</sup> State Key Laboratory of Petroleum Resources and Prospecting, China University of Petroleum (Beijing), Beijing 102249, China

<sup>2</sup> Basin and Reservoir Research Center, China University of Petroleum (Beijing), Beijing 102249, China

<sup>3</sup> Wuxi Research Institute of Petroleum Geology, SINOPEC, Wuxi, Jiangsu 214126, China

# Corresponding Author: liulf@cup.edu.cn

**Keywords:** *Shale gas, Occurrence, Accumulation, Cambrian, Ordovician, Tarim Basin*

The Tarim Basin is located in the Northwest China and is the biggest basin in China with huge oil and gas resources. The Cambrian and Ordovician possess the major marine source rocks in the Tarim Basin and large shale gas resources potential. The Cambrian—Ordovician shales mainly deposited in basin—slope facies with the thickness as 30~180m. For the shales buried shallower than 4500m, they have high organic matter abundance with TOC (total organic carbon) mainly between 1.0% and 6.0%, favorable organic matter types of Type I and Type II, and high thermal maturity with  $Ro^E$  as 1.0%~2.5% (Table 1).

The mineral composition of these Cambrian—Ordovician shale samples is mainly quartz and carbonate minerals while the content of clay minerals is mostly lower than 30%, because these samples include siliceous and calcareous shale and marlstone. The Cambrian and Ordovician shales are compacted with mean porosity as 4% and 3%, permeability as  $0.0003 \times 10^{-3} \sim 0.09 \times 10^{-3} \mu\text{m}^2$  and  $0.0002 \times 10^{-3} \sim 0.11 \times 10^{-3} \mu\text{m}^2$ , density as  $2.30 \text{ g/m}^3$  and  $2.55 \text{ g/m}^3$ , respectively. The pores in these shale samples show good connectivity and are mainly mesopores in size. Different genetic types of pores can be observed such as intercrystal pore, intergranular pore, dissolved pore, organic matter pore and shrinkage joint (Fig. 1). The reservoir bed properties are controlled by the mineral composition and diagenesis. The maximum adsorption amount to methane of these shales is  $1.15 \sim 7.36 \text{ cm}^3/\text{g}$ , whose main affecting factors are organic matter abundance, porosity and thermal maturity (Fig. 2).

The accumulation characteristics of natural gas within these shales are jointly controlled by sedimentation, diagenesis, hydrocarbon-generating conditions, reservoir bed properties and occurrence process of natural gas. The natural gas underwent short-distance migration and accumulation, in-place accumulation in the early stage,

adjustment and modification in the later stage (Fig. 3). Finally, the Y1 and T1 areas are identified as the targets for shale gas exploration in the Tarim Basin (Fig. 4).

Table 1. Distribution and geochemical characteristics of Cambrian-Ordovician source rocks in Tarim Basin

Strata	Formation		Thickness (m)	Lithology	TOC (%)	Kerogen Type	Ro <sup>E</sup> (%)	Representative sections or wells
	North-west Tarim	East Tarim						
Ordovician	Upper	Saergan	30~50	Graptolite shale	0.74~4.65	Mainly I	1.58~1.61	Section E1, Section E2, T1, T2, Y1, Y2, and K1
	Middle						1.30~2.35	
	Lower	Heituwa	30~50	Dark carbonaceous, siliceous and calcareous shale	0.86~7.62		1.37~2.75	
Lower Cambrian		Xishanbulake	30~180		0.7~5.52		1.37~2.75	Section W1, Section W2, X1
		Yuertusi	30~50	Dark siliceous and carbonaceous shale	1.0~22.4	I—II	1.36~2.06	

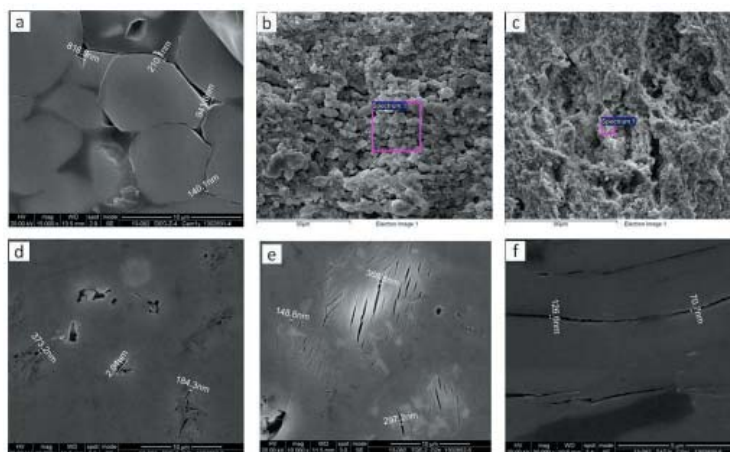


Fig. 1. Pore types of Cambrian-Ordovician shale samples in Tarim Basin: a. intercrystal pore; b. intergranular pore; c. dissolved pore; d-e. organic matter pore; f. shrinkage joint

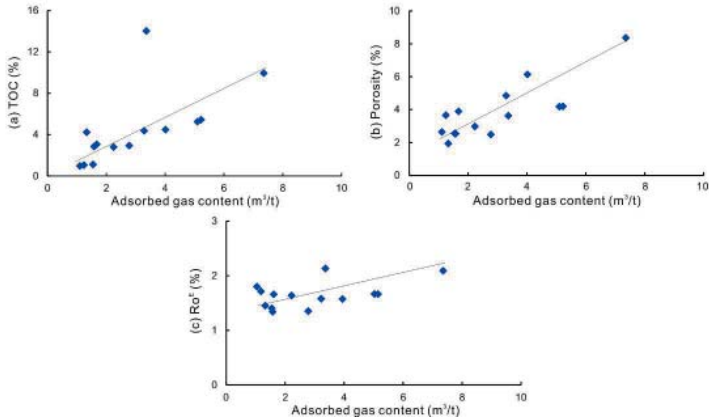


Fig. 2. Relationship of adsorbed gas content (m<sup>3</sup>/t) and controlling factors of Cambrian-Ordovician shales in Tarim Basin: a. TOC, (%); b. porosity (%); c. RoE (%)

### References

CHEN Q., QIAN Y., MA H., WANG S. 2003. *Diagenesis and porosity evolution of the Ordovician Carbonate rocks in Tahe Oilfield, Tarim Basin*. *Petroleum Geology & Experiment*. 25, 729-734 (In Chinese with English abstract).

DONG D., ZOU C., YANG H., et al. 2012. *Progress and prospects of shale gas exploration and development in China*. *Acta Petrolei Sinica*. 33, 107-114 (In Chinese with English abstract).

GUO J., CHEN J., WANG T., et al. 2008. *New progress in studying Cambrian source rock of Tarim Basin*. *Acta Sedimentologica Sinica*. 26, 518-524 (In Chinese with English abstract).

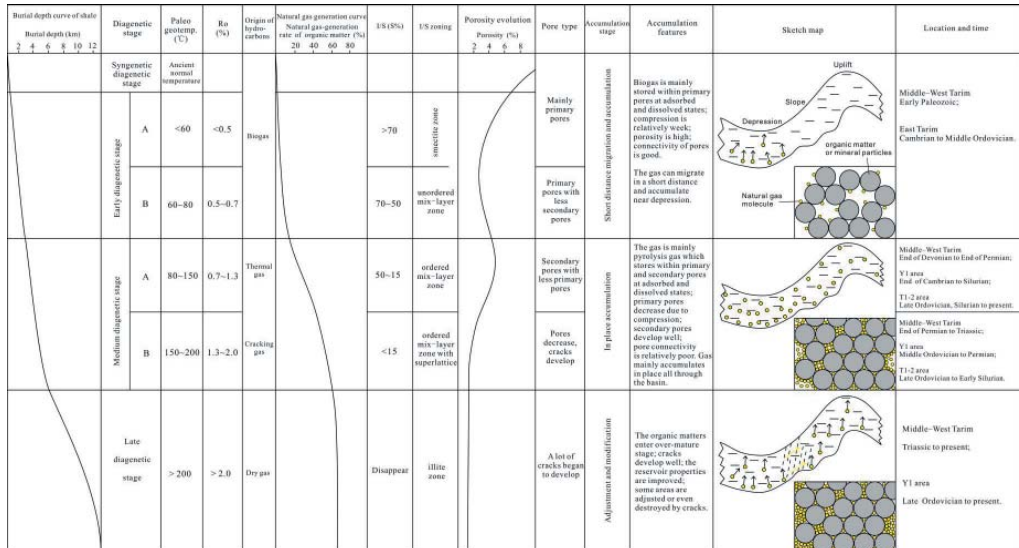


Fig. 3. Gas accumulation pattern in Cambrian—Ordovician shales of Tarim Basin

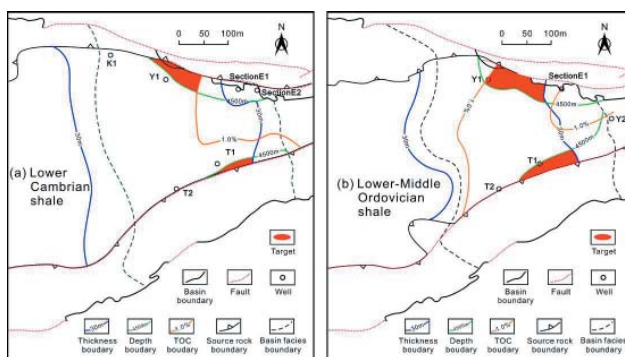


Fig. 4. Target areas for Cambrian—Ordovician shale gas exploration in Tarim Basin

JIANG C., WEI G. 2002. *Tectonic characteristics and petroleum potential of Tarim Basin*. Chinese Science Bulletin. 47, 1-8 (In Chinese)

JIN Z., WANG Q. 2004. *New progresses on petroleum accumulation studies of Chinese typical superimposed basin—Tarim Basin*. Science in China (Series D: Earth Sciences). 34, 1-12 (In Chinese).

LI H., QIU N., JIN Z., HE Z. 2005 *Geothermal history of Tarim Basin*. West China Petroleum Geosciences. 1, 15-18 (In Chinese with English abstract).

LIU L., WANG Y., GAO X. 2013. *Diagenetic Process and Pore Evolution of Jurassic Continental Shale in Tarim Basin, Northwest China*. Energy Exploration & Exploitation. 31, 899-913.

XING W., TANG D., MA X., et al. 2007. *Thermal evolution characteristics of hydrocarbon source rocks and pool-forming conditions in the Kongque river area, northeastern fringe of Tarim Basin*. Natural Gas Geoscience. 18, 57-61 (In Chinese with English abstract).

YANG W., WEI G., WANG Q., XIAO Z. 2004. *Two types of Cambrian source rocks and related petroleum systems in Tarim basin*. Oil & Gas Geology. 25, 263-267 (In Chinese with English abstract).

ZHANG J., JIANG S. H., TANG X., et al. 2009. *Accumulation types and resources characteristics of shale gas in China*. Natural Gas Industry. 29, 109-114 (In Chinese with English abstract).

ZHANG S., EANSON A. D., MOLDOWAN J. M., et al. 2000 *Paleozoic oil-source rock correlations in the Tarim Basin, NW China*. Organic Geochemistry. 31, 273-286.

ZHANG S., LIANG D., LI M., et al. 2002. *Biomarkers and oil-source correlation in the Tarim Basin*. Chinese Science Bulletin. 47, 16-23 (In Chinese).

ZOU C., YANG Z., CUI J., et al. 2013. *Formation mechanism, geological characteristics and development strategy of nonmarine shale oil in China*. Petroleum Exploration and Development. 40, 14-26 (In Chinese with English abstract).



## Effects of deep CO<sub>2</sub> on petroleum and thermal alteration: a case of Huangqiao oil and gas field

Quanyou Liu<sup>1,2</sup>, Zhijun Jin<sup>1,2,#</sup>, Bing Zhou<sup>1,2</sup>, Dongya Zhu<sup>1,2</sup>,  
Qingqiang Meng<sup>1,2</sup>, Xiaoqi Wu<sup>1,2</sup>, Hao Yu<sup>3</sup>

<sup>1</sup> State Key Laboratory of Shale Oil and Gas Enrichment Mechanisms and Effective Development, SINOPEC, Beijing 100083, China

<sup>2</sup> Petroleum Exploration & Production Research Institute, SINOPEC, Beijing 100083, China

<sup>3</sup> East China Oilfield Branch Company, SINOPEC, Nanjing 210011, China

# corresponding author: jinzj.syky@sinopec.com

**Keywords:** Huangqiao oil and gas field, mantle-derived CO<sub>2</sub> fluid, thermogenic gas, *n*-alkanes, hydrothermal-altered oil

The CO<sub>2</sub>-rich natural gas at the Huangqiao oil and gas field of the Subei Basin is produced along with crude oil. The chemical composition, carbon and hydrogen isotopic compositions and noble gas isotopes of the natural gas were analyzed. The results indicate that the gas is mainly composed of CO<sub>2</sub> with the contents ranging from 80.56% to 99.30% and an average content of 93.37%. The *n*-alkane contents are 0.51% ~10.2% with an average value of 0.37%, in which the methane contents are 0.45% ~10.2% with an average value of 0.36%. The carbon isotopic compositions of CO<sub>2</sub>, methane, ethane and propane are -20.4‰ ~ -1.7‰, -42.6‰ ~ -35.6‰ with an average of -39.7‰, -34.8‰ ~ -29.6‰ with an average of -31.9‰, and -30.0‰ ~ -28.1‰ with an average of -29‰, respectively, following the positive carbon isotopic series of gaseous alkanes, i.e.,  $\delta^{13}\text{C}_1 < \delta^{13}\text{C}_2 < \delta^{13}\text{C}_3$ . The methane hydrogen isotopic composition is between -218.5‰ and -186‰, with an average of -194.5‰. The noble gas isotope composition, <sup>3</sup>He/<sup>4</sup>He ratio, in the natural gas is  $0.94 \times 10^{-6} \sim 4.67 \times 10^{-6}$ . The gas geochemical parameters show that the CO<sub>2</sub> at the Huangqiao region is deep mantle-derived. The carbon isotopic composition of the gas indicates the alkanes at the Huangqiao region are the oil-cracking and gas/oil-cracking gases derived from the lacustrine sapropelic organic matter, which was formed in freshwater depositional environments. According to the relationships of CO<sub>2</sub>/<sup>3</sup>He vs. R/Ra and CH<sub>4</sub>/<sup>3</sup>He vs. R/Ra of the components of crust and mantle endmembers, some of the abiogenic CH<sub>4</sub> was formed by water-rock interactions of CO<sub>2</sub>. Therefore, the CH<sub>4</sub> discovered at the Huangqiao region is a mixture of biogenic oil-type gas, mantle-derived gas, and the gas generated by water-rock interactions.

The crude oil found at the Huangqiao region is light or condensate oils with low densities of 0.7933 ~ 0.8255 g/cm<sup>3</sup>. Saturated hydrocarbons are the major components

of crude oil with contents of 90.06%~97.37%. The contents of aromatic, non-hydrocarbon and asphaltene are very low. The *n*-alkanes range from C<sub>13</sub> to C<sub>34</sub>, with highest abundances at C<sub>16</sub> and C<sub>17</sub>. The abundances of the *n*-alkanes heavier than C<sub>25</sub> become very low. The carbon preference index (CPI) of the *n*-alkanes is 0.91 ~ 0.98 and its Pr/Ph ratio ranges from 1.1 to 1.47. The crude oil at the Huangqiao region showed an unresolved hump or unresolved complex mixture (UCM) distribution of a complete *n*-alkane series, non-odd/even predominance, and major *n*-alkane peaks on the highest positions of the UCM distribution in its gas chromatogram. The similarity between the crude oil in the Huangqiao area and the hydrothermal oil may be explained by that the deep mantle-derived CO<sub>2</sub> fluid formed in late stage migrated along deep faults, and extracted and accumulated the oil dispersed in the reservoirs or source rocks. In addition, the heat carried by the mantle-derived CO<sub>2</sub> fluid caused the thermal alteration of organic matters and crude oil, as well as the cracking of organic matters and water-rock interactions, during the migration.



## Geochemical characteristics of condensate oil in the tight reservoir of Xujiahe Formation in Central Sichuan, China

Shengfei Qin, Wei Li, Guanjun Xu, Peirong Wang

Research Institute of Petroleum Exploration & Development (RIPED), PetroChina, No.20 Xueyuan Road, P. O. Box 910, Beijing, 100083 China (qsf@petrochina.com.cn)

The Xujiahe Formation of the Central Sichuan is an important petroleum exploration field in the Sichuan Basin. In recent years, there were three large gas pools of Guang'an, Hechuan and Anyue had been demonstrated in the Central Sichuan area, showing rich petroleum resources in the Xujiahe Formation of Central Sichuan.

The Xujiahe Formation is a fluvial-swamp-lacustrine facies developed in a humid environment. There are several sets of coal-bearing source rocks and multiple sets of sandstone reservoirs in Xujiahe Formation. The source rocks and sandstones interbred each other, forming several sets of oil and gas system. From bottom to top, Xujiahe Formation can be subdivided into 6 sections, that is from  $T_3x^1$  to  $T_3x^6$ . Among these sections,  $T_3x^1$ ,  $T_3x^3$  and  $T_3x^5$  are mainly coal measures, and the organic matter type belongs to III type.  $T_3x^2$ ,  $T_3x^4$  and  $T_3x^6$  are mainly sandstone, and act as reservoirs. The gas reservoir is controlled by the sand body, and the porosity and permeability are relatively low. There is no uniform gas-water interface and pressure system between the gas reservoirs.

Because the source rocks of the Xujiahe coal measures are in the mature stage, the source rocks not only can generate a lot of natural gases, but also some condensate. However, little work has been done on geochemical studies of condensate, especially on light hydrocarbon studies. What are the characteristics of light hydrocarbon geochemistry in condensate oil in three reservoirs of Xujiahe Formation? Although all the condensates came from coal-bearing source rocks, is there any difference between condensate oils in different gas reservoirs? Can the difference in light hydrocarbon of condensate reflect the difference in the sedimentary environment of the corresponding three sets of source rocks? In addition, due to the Himalayan movement, there occurred about 2000 meters of the overall uplift in the Central Sichuan region. Is any influence on the light hydrocarbon geochemical characteristics of condensate caused by structural uplift? These are the problems that this paper will attempt to solve through geochemical research on the condensates.

According to chromatogram maps of the condensate oil, the condensate can be divided into single-peak and bimodal types. The number of carbon atoms in the single peak type is very low, the main peak carbon number is  $nC_6 \sim nC_8$ , mainly distributed in the upper part of the Xujiahe Formation ( $T_3x^6$ ). The double peak type has two main

peaks on the chromatogram, and the main peaks are  $nC_6 \sim nC_8$  and  $nC_{11} \sim nC_{13}$ , which are mainly distributed in the middle and lower parts of the Xujiahe Formation, namely, the second and the fourth sections of the Xujiahe Formation ( $T_3x^2$  and  $T_3x^4$ ). The “evaporative fractionation” phenomenon is more common in condensates and may be related to the uplift caused by the Himalayan Movement. In addition, all the condensates had not been washed and biologically degraded, indicating that oil and gas had been well preserved.

The methyl cyclohexane index of all the condensates is more than 50, of which the  $T_3x^2$  is among 50-60, and the  $T_3x^4$  and  $T_3x^6$  are more than 60. The cyclohexane index of condensate samples in  $T_3x^2$  is less than 40, and the  $T_3x^4$  and  $T_3x^6$  are greater than 40 instead. The methyl cyclohexane index indicates that the condensate oil is derived from the source rocks with humic organic matters, but the organic matter in the corresponding source rocks of the  $T_3x^2$  condensate is more beneficial to oil-prone than the corresponding source rocks of  $T_3x^4$  and  $T_3x^6$  condensate. Comparing studies using the family composition of  $C_7$  compound and its ratios, the source rock of condensate in  $T_3x^2$  was developed in a semi-salty to salty sedimentary environment, and the source rocks of condensates in  $T_3x^4$  and  $T_3x^6$  may be developed in a light-salty to fresh water sedimentary environment.

This study is of great significance for the study of condensate characteristics, source rock formation environment and hydrocarbon generation characteristics of Xujiahe Formation.

## Reference

- He, D., Li, D., Zhang, G., Zhao, L., Fan, C., Lu, R., Wen, Z., 2011. *Formation and evolution of multi-cycle superposed Sichuan Basin*. Chinese Journal of Geology 46(3), 589-606 (in Chinese with English Abstract).
- Hu, X., Ge, B., Zhang, Y., Liu, B., 1990. I. Experimental Petroleum Geology, 12(4): 375-394 (in Chinese with English Abstract).
- Liu, S., Sun, W., Li, Z., Deng, B., Liu, S., 2008. *Tectonic uplifting and gas pool formation since late Cretaceous epoch, Sichuan Basin*. Natural Gas Geoscience, 19(3): 293-300 (in Chinese with English Abstract).
- Mango, F. D., 1990. *The origin of light hydrocarbons in petroleum: A kinetic test of the steady-state catalytic hypothesis*. Geochimica et Cosmochimica Acta, 54(5): 1315-1323.
- Mango, F. D., 1997. *The light hydrocarbons in petroleum: A critical review*. Organic Geochemistry, 26(7-8): 417-440.
- Wang, P., Zhu, J., Fang, X., Zhao, H., Zhu, C., 1998. *A new classification of crude oils on light hydrocarbons—The classification and geochemical feature of crude oils from Tarim Basin*. Acta Petrolei Sinica, 19(1): 24-18.
- Thompson, K.F.M., 1983. *Classification and thermal history of petroleum based on light hydrocarbons*. Geochimica et Cosmochimica Acta. 47, 303-316.
- Thompson, K.F.M., 1987. *Fractionated aromatic petroleums and the generation of gas-condensates*. Organic Geochemistry. 11, 573-590.
- Thompson, K.F.M., 2010. *Aspects of petroleum basin evolution due to gas advection and evaporative 607 fractionation*. Organic Geochemistry. 41 (4), 370-385.



## Analysis on sources of oil-derived gas in Jingbian gas field, Ordos Basin, China

Han Wenxue<sup>#</sup>, Tao Shizhen, Ma Weijiao

PetroChina Research Institute of Petroleum Exploration & Development, Beijing, China

<sup>#</sup> Corresponding author: PetroChina Research Institute of Petroleum Exploration & Development, Beijing 100083, China; e-mail: vincer0543@qq.com

**Keywords:** *Jingbian gas field; Source rock-adsorbed gas; Oil-derived gas; Source rocks; Geochemical characteristics*

The Jingbian gas field, in the central Ordos Basin, resides in the middle of the Yishan slope structurally with an area of about 6000 km<sup>2</sup>. The paleogeomorphic - lithologic traps were formed in the Hercynian period. The Carboniferous Benxi Formation bauxitic mudstone and terrestrial mudstone served as the cap rocks, which are blocked laterally by the Ordovician argillaceous gypsum - dolomite (Dai et al., 2005). The 5th member of Majiagou Formation Ordovician, hereinafter referred to as Ma5 Member (including Ma5<sub>1</sub>, Ma5<sub>2</sub> and Ma5<sub>4</sub><sup>1</sup>), is the reservoir.

The Jingbian gas field has three sets of source rocks, i.e. the Upper Palaeozoic Carboniferous - Permian coal measures, the Upper Palaeozoic Carboniferous - Permian marine-terrigenous limestone, and the Lower Palaeozoic Ordovician marine carbonate rocks. The Upper Palaeozoic coal measures, with its hydrocarbon generation capacity universally recognized, is considered as the main gas source rocks in the Ordos Basin, and it is not discussed in this paper. The Ordovician and Carboniferous source rocks are controversial. The former set can be divided into two parts by the gypsum rocks. Both the Ordovician and Carboniferous source rocks reach certain thickness in the central and eastern Ordos Basin, and they are in direct contact with the Ordovician weathering crust reservoirs, with favorable source-reservoir assemblages and the possibility for hydrocarbon supply and accumulation.

Since the Jingbian gas field was put into exploration and development, its gas sources have been controversial (Yang et al., 1991; Zhang et al., 1992; Guan et al., 1993; Zhang et al., 1994; Huang et al., 1996; Ning et al., 2007; Wang et al., 2009; Yang et al., 2009; Chen et al., 2010; Ma et al., 2011). In this respect, there are mainly four views.

(a) Oil-derived gas in dominance

The gas mainly comes from the Majiagou Formation carbonate rocks, which are reservoirs of self-generation and self-storage. The pure carbonate rocks at high - over

maturity with about 0.2% organic carbon content are considered with the potential to generate natural gas.

(b) Coal-derived gas in dominance, together with a small amount of oil-derived gas

The coal-derived gas is mainly derived from the Upper Palaeozoic Carboniferous - Permian coal measures, while the small amount of oil-derived gas comes from the Carboniferous marine-terrigenous limestone.

(c) Distal mixed type gas

It is mainly the mixture of oil-derived cracking gas generated in the Ordovician marl and shale in the western-southwestern basin and coal-derived gas derived from the Carboniferous - Permian.

(d) Coal-derived gas in dominance, followed by oil-derived gas

This view is similar to (b) above, namely, natural gas mainly comes from the Upper Palaeozoic coal measures, but different in the source of oil-derived gas. Scholars holding this view believe that the oil-derived gas comes from the Lower Palaeozoic Ordovician. That is, the Upper Palaeozoic coal-derived gas was migrated into the Majiagou Formation, and mixed with the self-generated and self-accumulated oil-derived gas there. It is interfered from above views that all scholars agree on the existence of oil-derived gas in the Jingbian gas field but argue about the source of the oil-derived gas.

Based on determination of composition of source rock-adsorbed gas and carbon isotope, TOC, rock-eval, carbon isotope of kerogen, chloroform bitumen A and determination of natural gas components and stable carbon isotopes, we evaluated the potential of hydrocarbon generating of limestone from Taiyuan Formation in Upper Paleozoic and carbonate rock above and under gypsum-salt bed of Majiagou Formation in Lower Paleozoic. Meanwhile, we compared geochemical characteristics of natural gas and source rock-adsorbed gas. The results show that:

(a) The Taiyuan Formation source rocks contain Type II organic matters, and abundant sapropel components, presenting as moderate - good rocks with high - over maturity. Locally, it generates gases dominated by oil-derived gas.

(b) The source rocks from Majiagou Formation above the gypsum-salt bed have poor hydrocarbon generation capability, making it fail to be the sources for oil-derived gas in the Jingbian gas field. The under gypsum-salt bed source rocks, with certain hydrocarbon generation capability, can form self-generation and self-storage gas reservoirs, and they will be main alternative targets for further exploration and development.

(c) The Taiyuan Formation has a certain hydrocarbon generation capability, which is much less than the adjacent C-P coal measures. The generated gas is driven by the coal-derived gas generated later from the C-P coal measures to migrate to and accumulate in the Lower Palaeozoic Majiagou Formation. For this reason, part of the Ordovician Majiagou Formation above the gypsum-salt bed gas has the features of mixed gas, of which the oil-derived gas is supposed to have come from the Upper Palaeozoic Taiyuan Formation limestone.

(d) Gases in the Majiagou Formation post-salt karst reservoirs in the Jingbian gas field are mainly coal-derived gases derived from the Upper Palaeozoic C-P coal measures, with the oil-derived gases from the Taiyuan Formation but with a small proportion.

### References

- Chen A.D., Dai J.Y. and Wang W.Y. 2010. *Characteristics and origin of gas reservoirs and the favorable geological conditions in Jingbian Gasfield, Ordos Basin*. Marine Origin Petroleum Geology, 15, 45-55.
- Dai J.X., Li J., Luo X., Zhang W.Z., Hu G.Y., Ma C.H., Guo J.M. and Ge S.G. 2005. *Stable carbon isotope compositions and source rock geochemistry of the giant gas accumulations in the Ordos Basin, China*. Organic Geochemistry, 36, 1617-1635.
- Guan D.S., Zhang W.Z. and Pei G.. 1993. *Oil-gas sources of Ordovician reservoir in gas field of central Ordos Basin*. Oil & Gas Geology, 14, 191-199.
- Huang D.F., Xiong C.W., Yang J.J., Xu Z.Q. and Wang K.R.. 1996. *Gas source discrimination and natural gas genetic types of central gas field in Ordos Basin*. Natural Gas Industry, 16, 1-5.
- Ma C.S., Xu H.Z., Gong C.H. and Sun L.Z.. 2011. *Paleo-oil reservoir and Jingbian natural gasfield of Ordovician weathering crust in Ordos Basin*. Natural Gas Geoscience, 22, 280-286.
- Ning N, Chen M.J., Sun F.J. and Xu H.Z. 2007. *Determination and its significance of ancient oil pools in Ordovician weathering crust, Ordos Basin*. Oil & Gas Geology, 28, 280-286.
- Wang C.G., Wang Y., Xu H.Z., Sun Y.P., Yang W.L. and Wu T.H. 2009. *Discussion on evolution of source rocks in Lower Paleozoic of Ordos Basin*. Acta Petrolei Sinica, 30, 38-45.
- Yang H, Zang W.Z., Zan C.L. and Ma J. 2009. *Geochemical characteristics of Ordovician subsalt gas reservoir and their significance for reunderstanding the gas source of Jingbian Gasfield, East Ordos Basin*. Natural Gas Geoscience, 20, 8-14.
- Yang J.J. 1991. *Discovery of the natural gas in Lower Palaeozoic in Shanganning Basin*. Natural Gas Industry, 11, 1-6.
- Zhang S.Y. 1994. *Natural gas source and explorative direction in Ordos Basin*. Natural Gas Industry, 14,1-4.
- Zhang W.Z., Pei G and Guan D.S. 1992. *Carbon isotope study of light hydrocarbon monomer Series in Mesozoic-Paleozoic oil in Ordos Basin*. Chinese Science Bulletin, 37, 248-251.



## Hydrocarbon seeps in petroliferous basins in China: a first inventory

Guodong Zheng<sup>1#</sup>, Wang Xu<sup>1</sup>, Giuseppe Etiope<sup>2</sup>, Xiangxian Ma<sup>1</sup>,  
Shouyun Liang<sup>3</sup>, Qiaohui Fan<sup>1</sup>, Wasim Sajjad<sup>1</sup>, Yang Li<sup>1</sup>

<sup>1</sup> Key Laboratory of Petroleum Resources, Gansu Province/Key Laboratory of Petroleum Resources Research, Institute of Geology and Geophysics, Chinese Academy of Sciences, Lanzhou 730000, PR China

<sup>2</sup> Istituto Nazionale di Geofisica e Vulcanologia, Sezione Roma 2, Rome, Italy and Faculty of Environmental Science and Engineering, Babes-Bolyai University, Cluj-Napoca, Romania

<sup>3</sup> Key Laboratory of Mechanics on Disaster and Environment in Western China (Lanzhou University), Ministry of Education, Lanzhou 730000, P.R. China

# Corresponding author: gdzhhbj@mail.iggcas.ac.cn

**Keywords:** *seeps, hydrocarbons, methane, petroliferous basin, China, mud volcano*

Natural hydrocarbon seepage is a widespread phenomenon in sedimentary basins, with important implications in petroleum exploration and emission of greenhouse gases to the atmosphere. China has vast petroleum (crude oils and natural gases) bearing sedimentary basins but hydrocarbon seepage has rarely been the object of systematic studies and measurements. Based on the available Chinese literature, we report a first inventory of 931 hydrocarbon seeps or seepage zones (709 onshore seeps and 222 offshore seeps), including 81 mud volcanoes, 449 oil seeps, 214 gas seeps, and 187 solid seeps (bitumen outcrops). The seeps are located within the main 19 Mesozoic-Cenozoic petroliferous sedimentary basins, especially along the marginal, regional and local faults. The type of manifestations (oil, gas or mud volcano) reflects the type and maturity of the subsurface petroleum system and the sedimentary conditions of the basin. Oil seeps are particularly abundant in the Junggar Basin. Gas seeps are mostly developed in the Lunpola Basin, in smaller basins of the eastern Guizhou and Yuannan provinces, onshore Taiwan and in the offshore Yinggehai Basin. Mud volcanoes are developed in basins (Junggar, Qaidam, Qiangtang, onshore and offshore Taiwan) that experienced rapid sedimentation, which induced gravitative instability of shales and diapirism. In comparison to available global onshore seep data-bases, China is a country with the highest number of seeps in the world. The massive gas seepages in China may represent a considerable natural source of methane to the atmosphere and a key indicators for future hydrocarbon exploration.

**Acknowledgments:** This study was supported by China National Major S&T Projects (2016ZX05007-001), the National Natural Science Foundation of China (41273112; 41402129; 41020124002)



## **4. Gases in Groundwater and Crystalline Rocks**





## Chemical and carbon isotopic compositions and implications of volatiles in the Poyi Permian mafic magmatism in the Northeastern Margin of Tarim Craton, China

Pengyu Feng, Ming Yu, Mingjie Zhang\*, Yuekun Wang, Xiaodong Wang, Fei Hu

School of Earth Sciences & Key Lab of Mineral Resources in Western China, (Gansu) Lanzhou University, Lanzhou, 730000

\* Corresponding author: mjzhang@lzu.edu.cn

**Key words:** magmatic condition, C isotope, volatile, the Poyi mafic-ultramafic complex in China

### Introduction

The large Poyi Permian layered ultramafic mafic-ultramafic complex in the Beishan terrane, the northeastern part of the Tarim block, western China is related temporally and spatially to adjacent coeval Tarim Large Igneous Province (LIP), and hosted Ni-Cu sulfide deposit. A integrated study of chemical compositions, carbon isotope of volatiles have been carried for the Poyi mafic-ultramafic complex to reveal source characteristics, the condition and process of volatiles during magma evolution, and provide insight into the dynamic setting of mafic magmatism of Poyi mafic-ultramafic complexes.

### Geological background

The Poyi complex is located in the middle of the Pobei complexes with an exposed area about 3.6km<sup>2</sup>, the plane shape of the complex is irregular trapezoid, the east-west length is 3.2 km, the north-south width is 1.08 km, it intruded into the Hongliuyuan Formation of Carbonic period and well differentiated. It is composed of dunite, wehrlite, olivine clinopyroxenite and troctolite. SIMS zircon U-Pb isotope ages SIMS zircon U-Pb isotope age shows  $278 \pm 2$  Ma for gabbro and  $269.9 \pm 1.7$  Ma for the Poyi ultramafic-troctolitic intrusion (Xue et al., 2016).

### Samples and analytical methods

Samples used in this study were collected from different drill cores at different exploration line, including ultramafic-troctolitic and gabbroic rocks. All of the rock samples were examined using microscopy, and the least altered samples based on the microscopic observations were selected for mineral separation. The olivine (Olv),

pyroxene (Pyx) and plagioclase (Pl) separates were selected by magnetic separation and followed by hand picking under a binocular microscope.

The volatiles in olivine, pyroxene and plagioclase separates have been determined for chemical compositions by a MAT-271 mass spectrometer, Carbon isotopes of CO<sub>2</sub> and CH<sub>4</sub> were analyzed by a GC-C-MS system using a Delta plus XP mass spectrometer. The detailed experimental method and relative errors were described in Zhang et al. (2007) and Tang et al. (2013).

### The chemical and carbon isotopic compositions of volatiles

The volatiles in olivine, pyroxene and plagioclase separates in the Poyi complex are released at 200–400°C, 400–700°C and 700–1200°C interval during stepwise heating. The conspicuous feature of the volatiles in the Poyi complex is that H<sub>2</sub>O is a dominant component (av. 4082 mm<sup>3</sup>/g), which is similar to that from the Siberian LIP (Tang et al., 2013). The proportions of the H<sub>2</sub> and CO<sub>2</sub> in the ultramafic-troctolitic rocks are lower than in the gabbroic rocks. The H<sub>2</sub>S contents in the ultramafic-troctolitic rocks are lower than H<sub>2</sub>S in the gabbroic rocks.

The  $\delta^{13}\text{C}_{\text{CO}_2}$  values ranged from -4.0‰ to ~-33.7‰, and the  $\delta^{13}\text{C}_{\text{CH}_4}$  values varied from -10.4‰ to ~-29.1‰. The values are within the range of mantle, crust and thermogenic components. The  $\delta^{13}\text{C}$  values of CO<sub>2</sub> (av. (-24.8 ‰~ -2.2 ‰)) is reduced from 700–1200°C, 400–700°C to 200–400°C. The Pobei ultramafic-troctolitic samples have relatively heavy  $\delta^{13}\text{C}_{\text{CH}_4}$  values at 700–1200°C (-29.5‰ to -10.3‰) and 400–700°C (-34.9‰ to -12.5‰), and 200–400°C (av. -36.1‰ to -10.4‰). The  $\delta^{13}\text{C}$  values of CO<sub>2</sub> and CH<sub>4</sub> range among mantle, crust, carbonatite and thermogenic values.

The  $\delta^{13}\text{C}$  of CH<sub>4</sub>, C<sub>2</sub>H<sub>6</sub>, C<sub>3</sub>H<sub>8</sub>, and C<sub>4</sub>H<sub>10</sub> methane homologue for the ultramafic-troctolitic rocks range from -33.5 to -12.8 ‰. The  $\delta^{13}\text{C}$  values of methane homologue for the gabbroic rocks vary from -33.5 to -10.7 ‰. The  $\delta^{13}\text{C}$  values of methane homologue show a normal carbon isotopic distribution patterns among CH<sub>4</sub> to C<sub>4</sub>H<sub>10</sub> with lighter  $\delta^{13}\text{C}_{\text{CH}_4}$  values (-35‰), and partial reversal distribution pattern with heavier  $\delta^{13}\text{C}_{\text{CCH}_4}$  values (-25‰), imply different origins of volatiles in the Pobei complex.

### The compositions and origins of magmatic volatiles

The volatiles released from magmatic minerals in the Poyi complex are intrinsically stored in the constituent minerals, because volatiles absorbed on mineral surfaces and filled in cracked inclusions have been removed by sample heating at 100°C and pumping out under a high vacuum prior to analysis. The volatiles released at the 400-700°C and 700-1200°C intervals could be derived from primary fluid inclusions, and can represent the volatiles of Poyi magmatism (Miller and Pillinger, 1997; Zhang et al., 2009).

The magmatic volatiles in the Poyi complex are mainly composed of H<sub>2</sub>O (av. 3284.3 mm<sup>3</sup>/g) and H<sub>2</sub> (449.1) and CO<sub>2</sub> (449.3 mm<sup>3</sup>/g). SO<sub>2</sub> are not detected in Poyi complex. The troctolitic rocks and gabbroic rocks show similar chemical compositions of magmatic volatiles.

The variation between  $\delta^{13}\text{C}_{\text{CO}_2}$  values and  $\text{CO}_2$  contents in Poyi mafic-ultramafic rocks at different temperature intervals does not well correspond with Rayleigh model of carbon isotope fractionation, indicating that degassing cannot be the reason for observed  $\delta^{13}\text{C}$  variations. Therefore,  $\delta^{13}\text{C}_{\text{CO}_2}$  values can be used to reveal the source of volatiles in the Poyi complex. The  $\delta^{13}\text{C}_{\text{CO}_2}$  and  $\delta^{13}\text{C}_{\text{CH}_4}$  at 400-700 and 700-1200°C of Poyi ultramafic- troctolitic and gabbroic rocks are plotted in the ranges of mantle, crustal and carbonatite/ thermogenic origins (Sherwood et al., 2008).

The addition of component with low  $\delta^{13}\text{C}$  to the melt may contribute to the low  $\text{CO}_2$  contents and variable  $\delta^{13}\text{C}_{\text{CO}_2}$  values. The normal distribution pattern of  $\delta^{13}\text{C}$  values of methane homologue with carbon number were attributed to the contribution of thermogenic hydrocarbon gases from oceanic organic materials. The partial reversal carbon isotopic distribution pattern indicated that the methane homologue may be originated from abiogenic origin or the deep mantle (Ueno et al., 2006).

### The implications of the Poyi mafic magmatism

High contents of  $\text{H}_2$  at 700-1200°C suggested a relatively reduced environment for parental magma, and volatile escaped during magma evolution. The carbon isotopes of  $\text{CO}_2$  and methane homologue indicated that magma originated from the mantle, mixed with the crustal components, and thermogenic components of sedimentary organic matter. The crust-derived component was derived from either sedimentary organic matter of subduction in the source or contamination from country rocks in magma chambers.

The  $\text{H}_2\text{O}$  contents in the Poyi magma volatiles decreased from olivine (av. 2235.7  $\text{mm}^3/\text{g}$ ), to pyroxene (av. 1491.1  $\text{mm}^3/\text{g}$ ) and plagioclase (2111.7  $\text{mm}^3/\text{g}$ ), indicated that parental magma was rich in  $\text{H}_2\text{O}$ , and dehydration or volatile ( $\text{H}_2\text{O}$ ) losing existed during magma evolution. On the contrary,  $\text{CO}_2$  contents in the Poyi magmatic volatiles increased from olivine (av. 264.5  $\text{mm}^3/\text{g}$ ), pyroxene (av. 307.7  $\text{mm}^3/\text{g}$ ) to plagioclase (av. 1098.6  $\text{mm}^3/\text{g}$ ).  $\text{H}_2\text{S}$  contents increase from olivine in peridotite (16.1  $\text{mm}^3/\text{g}$ ), olivine in troctolite (28.2  $\text{mm}^3/\text{g}$ ) and plagioclase in troctolite (27.7  $\text{mm}^3/\text{g}$ ), to pyroxene in pyroxenite (62.5  $\text{mm}^3/\text{g}$ ) in the ultramafic rocks. These indicated the addition of  $\text{CO}_2$  and sulfur-rich volatiles into the magma during crystallization.

In addition,  $\text{H}_2\text{S}$  contents showed a weak positive correlation with  $\text{CO}_2$  and  $\text{H}_2$  contents, indicating the addition of  $\text{H}_2\text{O}$ ,  $\text{CO}_2$  and  $\text{H}_2$  is helpful to sulfide segregation. The crustal contamination and addition of  $\text{H}_2\text{O}$  and  $\text{CO}_2$ -rich volatiles are the key factor controlling the sulfur saturation and the formation of sulfide deposit.

### Conclusion

(1) The volatiles in the Poyi ultramafic complex are mainly composed of  $\text{H}_2\text{O}$  and minor  $\text{H}_2$  and  $\text{CO}_2$ . The  $\delta^{13}\text{C}$  of  $\text{CO}_2$  and  $\text{CH}_4$  were plotted in the range among crust, carbonate and mantle. The  $\delta^{13}\text{C}$  values of  $\text{CH}_4$  to  $\text{C}_4\text{H}_{10}$  showed normal and partial reversal distribution pattern with carbon number.

(2) The  $\delta^{13}\text{C}$  values of olivine, pyroxene and plagioclase from different types of rocks in Poyi mafic-ultramafic complex showed that mantle-derived magma volatiles were mixed with the crustal components, and thermogenic components of sedimentary organic matter.

### References

- Sherwood Lollar, B., Lacrampe-Couloume, G., Voglesonger, K., Onstott, T.C., Pratt, L.M., Slater, G.F., 2008. *Isotopic signatures of  $\text{CH}_4$  and higher hydrocarbon gases from Precambrian Shield sites*. *Geochim. Cosmochim. Acta* 72, 4778–4795.
- Tang, Q., Zhang, M., Li, C., Yu, M., Li, L. 2013. *The chemical compositions and abundances of volatiles in the Siberian large igneous province*. *Chem. Geol.* 339, 84–91.
- Ueno, Y., Yamada, K., Yoshida, N., Maruyama, S., Isozaki, Y., 2006. *Evidence from fluid inclusions for microbial methanogenesis in the early Archaean era*. *Nature* 440, 516–519.
- Xue, S.C., Qin, K.Z., Li, C., Tang, D.M., Mao, Y.J., Qi, L., Ripley, E.M., 2016. *Geochronological, petrological and geochemical constraints on Ni–Cu sulfide mineralization in the Poyi ultramafic–troctolitic intrusion in the northeast rim of the Tarim Craton, western China*. *Economic Geology*, 111, 1465–1484.
- Zhang, M.J., Hu, P.Q., Niu, Y., Su, S.G. 2007. *Chemical and stable isotopic constraints on the origin and nature of volatiles in sub-continental lithospheric mantle beneath eastern China*. *Lithos* 96, 55–66.

## **5. Gases migration and mechanism of Earth Degassing**





## The role of mantle-derived gases with respect to the geodynamic situation in the western Eger Rift, central Europe

Karin Bräuer<sup>1#</sup>, Horst Kämpf<sup>2</sup>, Samuel Niedermann<sup>2</sup>, Gerhard Strauch<sup>1</sup>

<sup>1</sup> UFZ Helmholtz Centre of Geochemistry, Environmental Res, D-06120 Halle, Germany

<sup>2</sup> GFZ German Research Centre for Geosciences, D-14473 Potsdam, Germany

# corresponding author: karin.braeuer@ufz.de

The Vogtland (Germany) and NW Bohemia (Czech Republic) belong to the European Cenozoic Rift System and are characterised by Quaternary volcanism, CO<sub>2</sub>-rich mineral springs and mofettes, and the occurrence of earthquake swarms. Comprehensive isotopic studies of free fluids have been carried out during the last 25 years, including three monitoring studies lasting for several years each.

As a result of the gas and isotopic composition studies combined with measurements of the gas flow, three degassing centres (Cheb Basin (CB), Mariánské Lázně and surroundings (MB) and Karlovy Vary (KV)) have been distinguished. These centres are characterised by high gas flow and the exhalation of nearly pure CO<sub>2</sub>. Their δ<sup>13</sup>C values encompass a small range, whereas clear differences in the proportion of mantle-derived helium were observed. From the degassing centres to the peripheries, the fraction of mantle-derived fluids decreases (Weinlich et al., 1999). A surprising result of the regional characterisation of the gas signatures was the finding of mantle-derived degassing in a clay pit (Figure 1, location no. 91 in Fig. 2).

The first indications of a seismically triggered release of crustal gas components were found in the course of weekly fluid monitoring before, during and after a small earthquake swarm in December 1994 (Weise et al., 2001; Bräuer et al., 2003). Two further monitoring studies accompanying the earthquake swarms in 2000 (Bräuer et al., 2008) and 2008 (Bräuer et al., 2014) confirmed and extended our knowledge about the behaviour of the fluids in relation to the occurrence of earthquake swarms in the western Eger Rift. Related to the 2008 swarm, seismically triggered anomalies of the gas signatures were recorded along the Počátky-Plesná Fault zone (PPZ) and the Mariánské Lázně fault (MLF). However, the temporal relation to the seismic events and the magnitude of the anomalies was variable (Bräuer et al., 2014). Throughout our investigation period (25 years), the seismicity was concentrated on the Nový Kostel focal zone (Figure 2). Interestingly, directly above the focal zone no gas exhalation has been found. Besides that, the seismic activity observed near the three degassing centres was substantially different (CB >> ML ≈ KV).



Fig. 1. Mantle-derived degassing observed in an open clay pit Nová Ves II near Skalná in the Cheb Basin

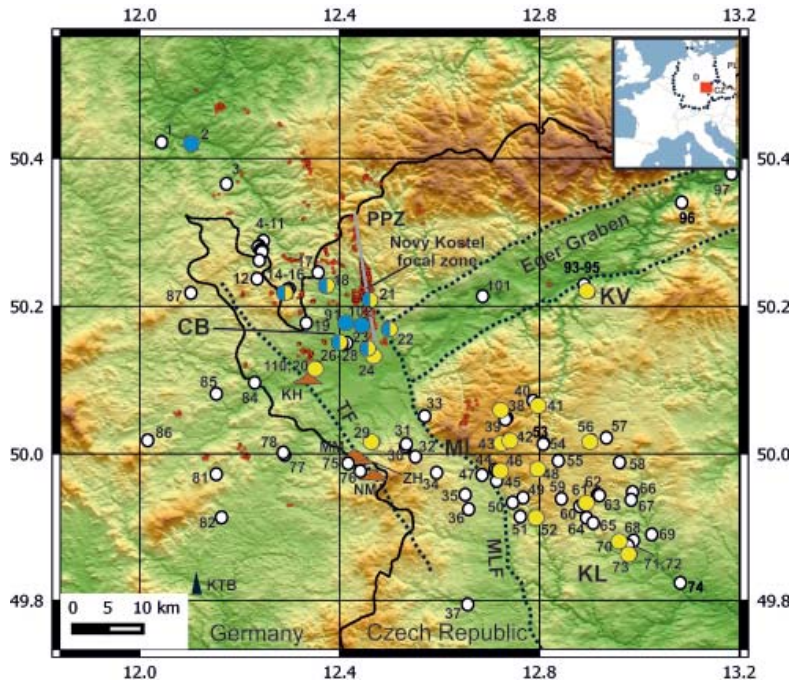


Fig. 2. Topography of the western Eger Rift area together with the distribution of the studied degassing sites (numbers according to Geissler et al., 2005). The bigger circles correspond to sites where long-term studies of the gas signature (yellow), weekly/monthly monitoring studies (blue) or both (blue/yellow) were carried out. Four Quaternary volcanoes (KH - Komorní Hůrka, ZH - Železná Hůrka, MM - Mýtina Maar, NM - Neualbenreuth Maar) and the major fault zones (MLF - Mariánské Lázně Fault, TF - Tachov Fault, PPZ - Počátky-Plesná Zone) are indicated. The small red dots correspond to epicenters of local swarm earthquakes. CB - Cheb Basin, ML - Mariánské Lázně, KV - Karlovy Vary, KL - Konstantinovy Lázně. The inset shows the location of the investigation area in central Europe

As a result of the comprehensive gas studies, first evidence for ascending magma beneath the CB was found, expressed by a temporary increase of the  $^3\text{He}/^4\text{He}$  ratios several months before the 2000 and the 2008 earthquake swarms (Bräuer et al., 2008, 2014). Superimposed on that, a long-term increase of mantle-derived helium contributions was also observed, but only at locations in the eastern part of the Cheb Basin (Bräuer et al., 2005, 2009).

The degassing behaviour at the locations marked by larger circles in Figure 2 was investigated in detail. Here we present new data of the gas and isotopic compositions from these sites recorded between 2014 and 2016 as well as monitoring data from the clay pit degassing site (no. 91). Since the time of the first regional characterisation of the gas signatures (1992-1994), the contribution of mantle-derived helium has remained nearly the same at locations belonging to the ML degassing centre and its periphery as well as in the KV degassing centre. In the eastern part of the CB however, the increase of the  $^3\text{He}/^4\text{He}$  ratios has continued and the latest data confirm the Bublák mofette as being connected to the fluid-injection zone by deep-reaching pathways (down to the upper mantle).

## References

- BRÄUER K., KÄMPF H., STRAUCH G. & WEISE S. 2003. *Isotopic evidence ( $^3\text{He}/^4\text{He}$ ,  $^{13}\text{C}_{\text{CO}_2}$ ) of fluid-triggered intraplate seismicity*. Journal of Geophysical Research 108, doi:10.1029/2002JB002077.
- BRÄUER K., KÄMPF H., NIEDERMANN S. & STRAUCH G. 2005. *Evidence for ascending upper mantle-derived melt beneath the Cheb basin, central Europe*. Geophysical Research Letters 32, doi:10.1029/2004GL022205.
- BRÄUER K., KÄMPF H., NIEDERMANN S., STRAUCH G. & TESAŘ J. 2008. *Natural laboratory NW Bohemia: Comprehensive fluid studies between 1992 and 2005 used to trace geodynamic processes*. Geochemistry Geophysics Geosystems 9, doi:10.1029/2007GC001921.
- BRÄUER K., KÄMPF H. & STRAUCH G. 2009. *Earthquake swarms in non-volcanic regions: What fluids have to say*. Geophysical Research Letters 36, doi:10.1029/2009GL039615.
- BRÄUER K., KÄMPF H. & STRAUCH G. 2014. *Seismically triggered anomalies in the isotope signatures of mantle-derived gases detected at degassing sites along two neighboring faults in NW Bohemia, central Europe*. Journal of Geophysical Research 119, doi:10.1002/2014JB011044.
- GEISSLER H., KÄMPF H., KIND R., BRÄUER K., KLINGE K., PLENEFISCH T., HORÁLEK J., ZEDNIK J. & NEHYBKA V. 2005. *Seismic location of a  $\text{CO}_2$  source in the upper mantle of the western Eger rift, Central Europe*, Tectonics 24, doi:10.1029/2004TC001672.
- WEINLICH F.H., BRÄUER K., KÄMPF H., STRAUCH G., TESAŘ J. & WEISE S.M. 1999. *An active subcontinental mantle volatile system in the western Eger rift, Central Europe: Gas flux, isotopic (He, C, and N) and compositional fingerprints*. Geochimica et Cosmochimica Acta 63, 3653-3671.
- WEISE S.M., BRÄUER K., KÄMPF H., STRAUCH G. & KOCH U. 2001. *Transport of mantle volatiles through the crust traced by seismically released fluids: A natural experiment in the earthquake swarm area Vogtland-NW-Bohemia, Central Europe*. Tectonophysics 336, 137-150.



## Gas geochemistry of shallow submarine vents in the Aegean sea (Greece)

Daskalopoulou K.<sup>1,2</sup>, Longo M.<sup>3</sup>, Calabrese S.<sup>1</sup>, Gagliano A.L.<sup>3</sup>,  
Kyriakopoulos K.<sup>2</sup>, Italiano F.<sup>3</sup>, D'Alessandro W.<sup>3#</sup>

<sup>1</sup> University of Palermo, Dept. DiSTeM, via Archirafi 36, 90123 Palermo, Italy

<sup>2</sup> National and Kapodistrian University of Athens, Dept. of Geology and Geoenvironment, Greece

<sup>3</sup> Istituto Nazionale di Geofisica e Vulcanologia – Sezione di Palermo, Via U. La Malfa 153, 90146 Palermo, Italy

# corresponding author: walter.dalessandro@ingv.it

**Keywords:** *submarine degassing, stable isotopes, environmental impact, ocean acidification*

The Aegean area, which is geodynamically very active, is characterised by intense seismic activity, presence of active volcanic systems and anomalous geothermal gradients. Like other regions of intense geodynamic activity it is also characterized by extensive geogenic degassing. Gas manifestations are not only widespread on land but are also very frequent underwater. Many of these, as for example those of Milos and Santorini, are known since long time and have been previously studied although the targets were generally the hot waters or the sediments affected by the emissions (Smith and Cronan 1978, Dando et al. 1995, Price et al. 2013, Megalovassilis 2014).

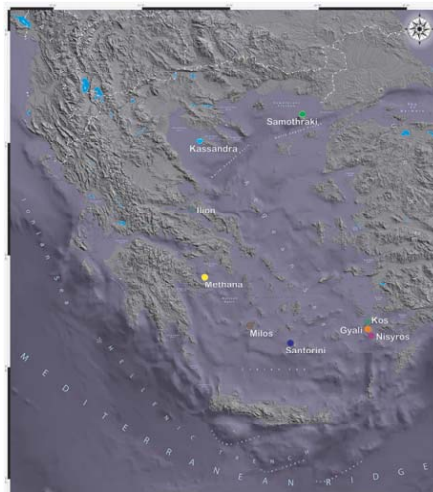


Fig. 1. Geographic distribution of the sampling areas

Table 1. Geographic coordinates of the sampling sites

Area	Site	UTM coordinates (WGS84)		
		Sector	E	N
Evia	Ilion	34S	684788	4302532
Kassandra peninsula	Ag. Pareskevi	34S	721293	4422552
Kassandra peninsula	Xyna	34S	731638	4423292
Samothraki	Therma Limani	35T	381584	4484685
Methana	Pausanias	34S	708237	4168275
Methana	Thiafi	34S	712355	4163870
Milos	Paleochori	35S	272157	4068098
Milos	Skinopi	35S	270211	4067712
Milos	Adamas	35S	278078	4061694
Santorini	Palea Kameni	35S	354725	4029380
Santorini	Nea Kameni	35S	356561	4030695
Nisyros	Katsouni	35S	517346	4051911
Nisyros	Lies	35S	518202	4050287
Gyali	Gyali	35S	511048	4057840
Gyali	Gyali nord	35S	510958	4058232
Gyali	Gyali west	35S	510511	4055549
Kos	Bros Therma	35S	528308	4077682
Kos	Paradise beach	35S	500794	4068393
Kos	Kefalos	35S	497339	4065831
Kos	Ag. Irini 1	35S	520916	4075676
Kos	Ag. Irini 2	35S	521910	4075843

The present study aims at producing the first catalogue of the shallow submarine gas manifestations of the Aegean Sea and to characterize geochemically the emitted gases. To this end, 61 samples at 21 different sites have been collected by diving at depth between 1 and 15 m. Figure 1 shows the geographic distribution of the sampling areas and the UTM coordinates of the 21 sites are shown in Table 1. Most of the samples were collected along the south Aegean active volcanic arc (SAAVA) close to the coasts of Methana, Milos, Santorini, Nisyros, Gyali and Kos. The remaining samples have been collected at Evia, Kassandra peninsula and Samothraki.

The sites displayed very different gas fluxes. Most of them showed a very sluggish gas bubbling while a few show strong bubbling over a larger area. The most intense manifestation was found at Kos Island along Paradise beach. There, in September 2016, a preliminary CO<sub>2</sub> flux survey was made with 12 measurements covering an area of about 250 m<sup>2</sup>. Flux values ranged from 500 to 50,000 g/m<sup>2</sup>/day from which a total output of about 3 tons/day has been estimated.

Gas samples have been analysed for their chemical (He, Ne, O<sub>2</sub>, N<sub>2</sub>, H<sub>2</sub>, H<sub>2</sub>S, CH<sub>4</sub> and CO<sub>2</sub>) and isotopic (He, CO<sub>2</sub>-C, CH<sub>4</sub>-C, CH<sub>4</sub>-H) composition by gas chromatography

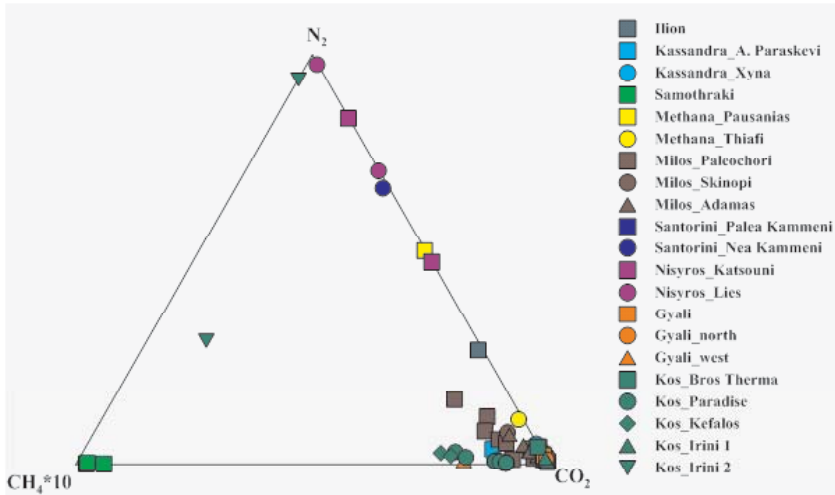


Fig. 2. CO<sub>2</sub>-N<sub>2</sub>-CH<sub>4</sub> triangular graph

and mass-spectrometry methodologies. The chemical composition of almost all samples was dominated by CO<sub>2</sub> (Fig. 2).

Only 11 samples, collected at very low flux vents, had CO<sub>2</sub> contents lower than 50%. Three of these samples derive from a CH<sub>4</sub>-dominated reservoir (Samothraki) while the remaining show clear signs of CO<sub>2</sub> loss due to dissolution processes being sometimes highly enriched in less soluble gas species (He, N<sub>2</sub>, CH<sub>4</sub>). In one case (sample Irini2 of Sep. 2016) the dissolution process is so extreme that only 900 ppm of extremely fractionated CO<sub>2</sub> (δ<sup>13</sup>C -20.1‰) is left over (Fig. 3). The helium isotopic composition, ranging from 0.74 to 6.73, points to a significant mantle contribution (5-95%) especially along the SAAVA (Fig. 4). Also the δ<sup>13</sup>C-CO<sub>2</sub> values (mostly between -5 and 0 ‰) indicate an important mantle contribution although CO<sub>2</sub> deriving from crustal limestones is often prevailing (Fig. 3).

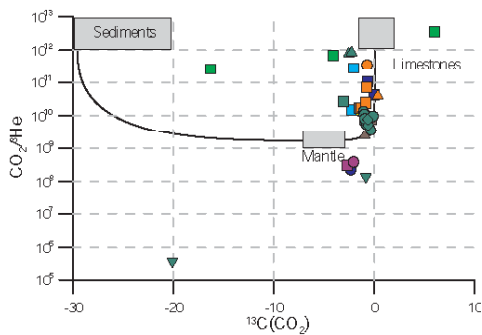


Fig. 3. CO<sub>2</sub>/<sup>3</sup>He vs. δ<sup>13</sup>C-CO<sub>2</sub>

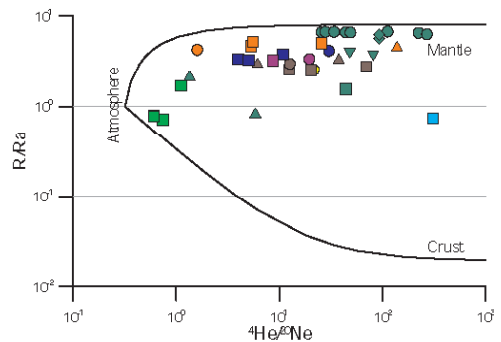


Fig. 4. R/Ra vs. He/Ne

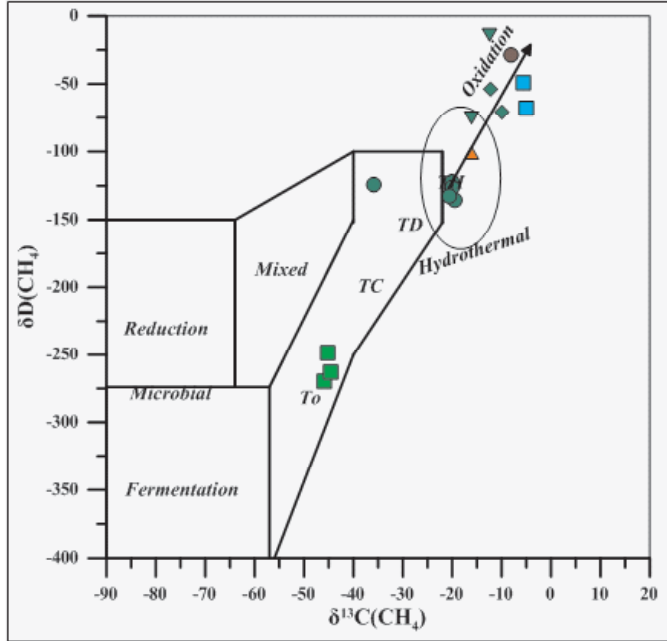


Fig. 5.  $\delta^{13}\text{C}$  vs.  $\delta\text{D}$  of methane

Isotopic composition of methane indicates mostly a hydrothermal origin either abiogenic or thermogenic (Fig. 5). Only the samples taken at Samothraki indicate a clear thermogenic origin (Fig. 5). Some sample shows more positive isotopic values pointing to possible biogenic methane oxidation processes.

Hydrogen sulphide, being highly soluble, was found only in three samples in concentrations ranging from 16 to 8200 ppm indicating a hydrothermal contribution.



Fig. 6. Underwater sampling at Methana and Gyalí

The present study highlighted a widespread submarine degassing activity in the Aegean Sea mainly along the active volcanic systems of the volcanic arc. The gas composition highlights their tight relationships with the volcanic and geothermal systems of the area. Gases from hydrocarbon fields are on the contrary rare. Although the gases emitted are sometimes quantitatively small they should not be disregarded because their environmental impact can be locally important. Furthermore these areas, especially those where nearly pure CO<sub>2</sub> is emitted, could be the sites where the impact on the marine environment of ocean acidification due to future increased atmospheric CO<sub>2</sub> levels or gas leakage from geologic CO<sub>2</sub> storage sites can be studied.

### References

- DANDO P. R., HUGHES J. A., LEAHY Y., NIVEN S. J., TAYLOR L. J. & SMITH C. 1995. *Gas venting rates from submarine hydrothermal areas around the island of Milos, Hellenic Volcanic Arc*. *Continental Shelf Research* 15, 913–929.
- MEGALOVASILIS P. 2014. *Partition geochemistry of hydrothermal precipitates from submarine hydrothermal fields in the Hellenic Volcanic Island Arc*. *Geochemistry International* 52, 992–1010.
- PRICE R. E., SAVOV I., PLANER-FRIEDRICH B., BÜHRING S. I., AMEND J. & PICHLER T. 2013. *Processes influencing extreme As enrichment in shallow-sea hydrothermal fluids of Milos Island, Greece*. *Chemical Geology* 348, 15–26
- SMITH P. A. & CRONAN D. S. 1978. *The geochemistry of metalliferous sediments and waters associated with shallow submarine hydrothermal activity, Santorini, Aegean Sea*. *Chemical Geology* 39, 241–262.



## Origin of methane and light hydrocarbons in the gas manifestations of Greece

Daskalopoulou K.<sup>1-2#</sup>, Calabrese S.<sup>1</sup>, Fiebig J.<sup>3</sup>, Grassa F.<sup>4</sup>,  
Kyriakopoulos K.<sup>2</sup>, Longo M.<sup>4</sup>, Parello F.<sup>1</sup>, Tassi F.<sup>5</sup>, D'Alessandro W.<sup>4</sup>

<sup>1</sup> Università degli Studi di Palermo, DiSTeM, via Archirafi, 36, 90123, Palermo, Italy, kyriaki.daskalopoulou@unipa.it,

<sup>2</sup> National and Kapodistrian University of Athens, Dept. of Geology and Geoenvironment, Panepistimioupolis, Ano Ilissia, 15784, Athens, Greece

<sup>3</sup> Goethe-Universität, Institut für Geowissenschaften, Altenhöferallee 1, 60438 Frankfurt am Main, Germany

<sup>4</sup> Istituto Nazionale di Geofisica e Vulcanologia, Sezione di Palermo, via Ugo la Malfa 153, 90146, Palermo, Italy

<sup>5</sup> Università degli Studi di Firenze, Dipartimento della Terra, via G. La Pira 4, 50121, Florence, Italy

The geologic emissions of greenhouse gases (CO<sub>2</sub> and CH<sub>4</sub>) give an important natural contribution to the global carbon budget. However, the contribution of these emissions to the global carbon cycle and their possible role on the climate change remain still poorly quantified (Guliyev and Feizullayev, 1997; Milkov, 2000; Etiope et al., 2015 and references therein). Methane, the most abundant organic compound in Earth's atmosphere, may be created either from existing organic matter or synthesized from inorganic molecules. Accordingly, it can be differentiated in two main classes: a) biotic (either microbial or thermogenic) and b) abiotic.

For this study, 115 gas samples of fumarolic, thermal and cold discharges from all over the Hellenic territory were collected and both chemical (CO<sub>2</sub>, H<sub>2</sub>S, CH<sub>4</sub>, N<sub>2</sub>, O<sub>2</sub>, Ar, H<sub>2</sub> and light hydrocarbons) and isotopic ( $\delta^{13}\text{C-CO}_2$ ,  $\delta^{13}\text{C-CH}_4$ ,  $\delta\text{D-CH}_4$ ) analyses were performed, in order to investigate the genetic processes that produced CH<sub>4</sub> in fluids related with the complex geodynamic setting of Greece. On the basis of the spatial distribution of the gas discharges and their type of emission, the whole dataset was subdivided into 3 main "domains", as follows: 1) Volcanic Arc (VA) - 34 samples; 2) External Hellenides (EH) - 23 samples of cold emissions and of hyperalkaline aqueous solutions; 3) Internal Hellenides (IH) - 62 samples of cold and geothermal emissions. Almost each group is characterized, as long as subdivided in 3 groups based on the type of emission (on-land free or dissolved gases and subaqueous gases) and a 4<sup>th</sup> group includes literature data.

Samples collected from cold manifestations in the internal Hellenides and the Volcanic Arc mostly have CO<sub>2</sub> as the main species, whereas gases associated with

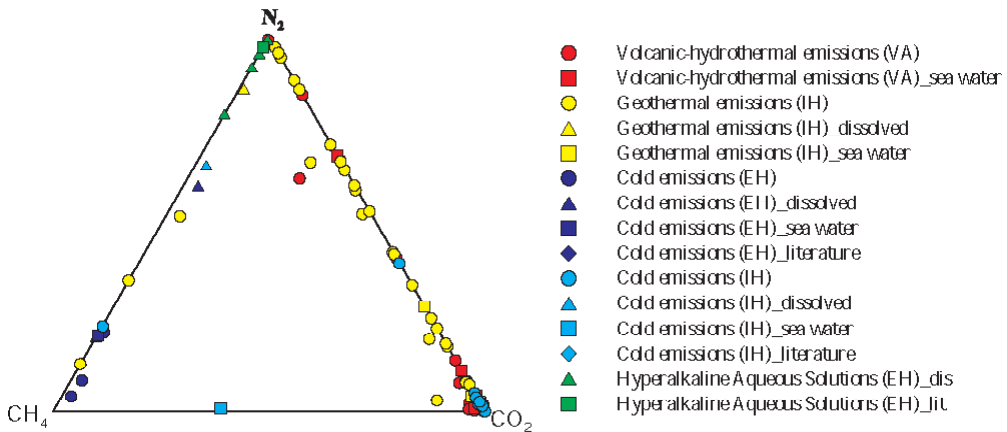


Fig. 1. Chemical composition of the gas manifestations in Greece.  
VA = volcanic arc; IH = internal Hellenides; EH = external Hellenides

hyperalkaline waters are  $N_2$  dominated sometimes with significant  $CH_4$  contributions. In the cold manifestations collected from the external Hellenides the prevailing gas is  $CH_4$ . The remaining gas samples collected from the geothermal emissions that occur in the Hellenic territory are showing a mixed  $N_2$  -  $CO_2$  composition (Figure 1).

The present study highlights a widespread continental and underwater degassing activity along the Hellenic territory. Both chemical and isotopic compositions of  $CH_4$  underscore the different primary sources and the secondary post-generic processes (oxidation) that can significantly affect the origin of this gas compound (Figure 2a, 2b). Hydrocarbons in the  $CH_4$ -dominated gases from the external Hellenides are showing a clear biotic origin. In particular, those collected in the Gavrovo-Tripolis zone are showing a dominating thermogenic origin, whereas it is also noticeable that some of the samples of the Ionian zone are produced by both microbial activity and thermal maturation of sedimentary organic matter. The  $CO_2$ -dominated gas discharges from the main geothermal systems of the Internal Hellenides and from the Volcanic Arc most likely predominantly contain abiogenic  $CH_4$  deriving from  $CO_2$  reduction. This process seems to have a lower effectiveness in producing higher hydrocarbons, such as  $C_2H_6$ ,  $C_3H_8$  and  $C_6H_6$ . However, some of the  $CO_2$ -rich gas discharges of the geothermal and volcanic-hydrothermal systems located in the sedimentary Pelagonian and the Gavrovo-Tripolis zones, seem to exhibit significant contributions from thermogenic sources. This is likely due to 1) low temperatures of the fluid reservoirs, i.e. too low to promote an efficient  $CO_2$  to  $CH_4$  conversion, and 2) the large amounts of organic matter that were buried in the sedimentary formations and that is available for thermal degradation processes. The presence of abiogenic methane

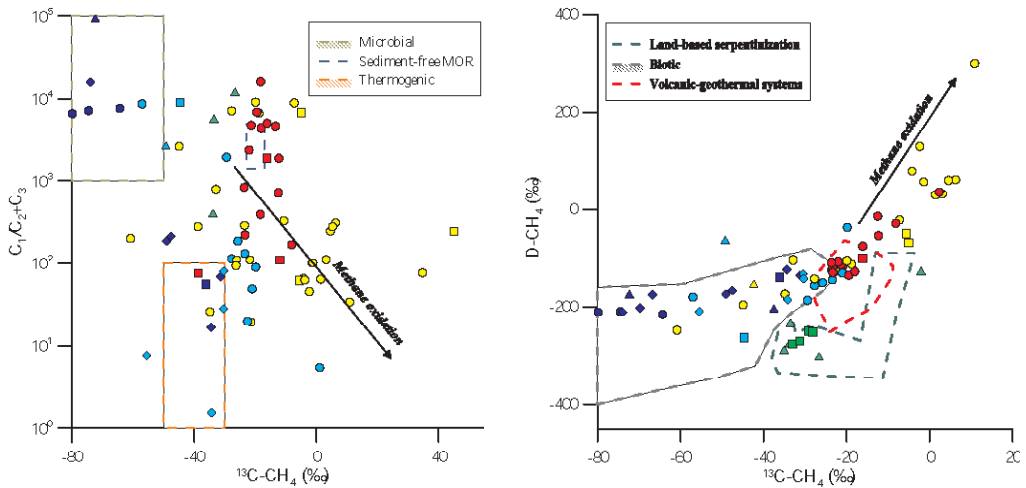


Fig. 2. a) Bernard classification diagram (Bernard et al., 1978) that is correlating the  $\text{CH}_4/(\text{C}_2\text{H}_6+\text{C}_3\text{H}_8)$  concentration ratios with the  $\delta^{13}\text{C}-\text{CH}_4$  ratios for the Hellenic gas discharges. Values for gases of biogenic origin (microbial and thermogenic) and from unsedimented mid-oceanic ridges are reported (McCollom and Seewald, 2007, and references therein) for comparison; b) Schoell binary diagram (Etiope and Schoell, 2014) which is correlating  $\delta\text{D}-\text{CH}_4$  with  $\delta^{13}\text{C}-\text{CH}_4$  ratio for the Hellenic gas discharges

was also recognized in the hyperalkaline aqueous solutions that are issuing from the ophiolites of Othrys and Argolida (Etiope et al., 2013; D'Alessandro et al., 2017).

Most of the geothermal gases of central Greece (internal Hellenides) and some of the volcanic- hydrothermal ones show lower Bernard ratios ( $\text{CH}_4/[\text{C}_2\text{H}_6+\text{C}_3\text{H}_8]$  – Fig. 2a) and strongly positive isotopic ratios of  $\text{CH}_4$  ( $\delta^{13}\text{C}$  up to +45‰ and  $\delta\text{D}$  up to 301‰ – Fig. 2). Such chemical and isotopic features can be explained by microbial oxidation of  $\text{CH}_4$ . In these environments microbes obtain energy from aerobic or anaerobic  $\text{CH}_4$  oxidation (Murrell and Jetten, 2009), preferentially consuming  $\text{CH}_4$  with respect to higher hydrocarbons and preferring light isotopes. This results in a noticeable decrease in the Bernard ratio and a progressive enrichment in heavy isotopes (both  $^{13}\text{C}$  and D) in the residual  $\text{CH}_4$ .

## References

- BERNARD, B.B., BROOKS, J.M., SACKETT, W.M., 1978. *A geochemical model for characterization of hydrocarbon gas sources in marine sediments*. Offshore Technology Conference, Houston, USA, 435-438.
- D'ALESSANDRO, W, DASKALOPOULOU, K., CALABRESE, S., BELLOMO, S., 2017. *Water chemistry and abiogenic methane content of a hyperalkaline spring related to serpentinization in the Argolida ophiolite (Ermioni, Greece)*. Marine and Petroleum Geology, doi: 10.1016/j.marpetgeo.2017.01.028.
- ETIOPE, G., 2015. *Natural Gas Seepage. The Earth's Hydrocarbon Degassing*. Springer International Publishing Switzerland, e- book. DOI 10.1007/978-3-319-14601-0.
- ETIOPE, G., SCHOELL, M., 2014. *Abiotic gas: atypical but not rare*. Elements 10, 291-296.

- ETIOPE, G., TSIKOURAS, B., KORDELLA, S., IFANDI, E., CHRISTODOULOU, D., PAPTAEODOROU, G., 2013. *Methane flux and origin in the Othrys ophiolite hyperalkaline springs, Greece* Chemical Geology 347, 161–174.
- GULIYEV, I. S. AND FEIZULLAYEV, A. A., 1997. *All about mud volcanoes*. Baku Pub. House, NAFTA-Press, 120.
- MCCOLLOM, T.M., SEEWALD, J.S., 2007. *Abiotic synthesis of organic compounds in deep-sea hydrothermal environments*. Chemical Reviews 107, 382-401.
- MILKOV, A. V., 2000. *Worldwide distribution of submarine mud volcanoes and associated gas hydrates*, Marine Geology 167 (1 – 2), 29 – 42.
- MURRELL, C. J. AND JETTEN, M. S. M., 2009. *The microbial methane cycle*, Environ. Microbiol. Reports 1, 279–284.



## Seamount-like Structure (?) in the SE Tyrrhenyan Sea: Constraints from Fluid Emission Data and Mineralogical Features of Dradged Sample

Di Bella Marcella<sup>1</sup>, Sabatino Giuseppe<sup>2</sup>, Nigrelli Alessandra<sup>1</sup>, Francesco Italiano<sup>1#</sup>

<sup>1</sup> National Institute of Geophysics and Volcanology, Via Ugo La Malfa, Palermo, Italy

<sup>2</sup> Department of Mathematics and Computer Science, Physics and Earth Sciences, University of Messina, Italy

# Corresponding author: francesco.italiano@ingv.it

**Keywords:** *seamount-like structure, mantle degassing, Biotite, XRPD, SEM-EDS, Tyrrhenian Sea*

In the SE Tyrrhenian Sea, about 6 miles off the Calabrian shoreline, the presence of a seamount-like structure was recently suggested (Fig. 1). De Ritis et al. (2010), through aeromagnetic data collected between the Aeolian volcanoes (SE Tyrrhenian Sea) and the Calabrian Arc (Italy) highlight a WNW-ESE elongated positive magnetic anomaly centered on the Capo Vaticano morphological ridge (Tyrrhenian coast of Calabria). High-intensity positive magnetic anomaly lies in correspondence of the CV morphological ridge, highlighting the presence of a noticeable magnetization contrast in an area strongly affected by tectonic structures. They suggest that the magnetic properties of this body are consistent with those of the medium to highly evolved volcanic rocks of the Aeolian Arc (i.e., dacites and rhyolites) and define it as a “buried volcano”. Loreto et al. (2015) taking into account the geophysical and fluid-geochemistry data (fig. 2) suggest the presence of mantle degassing enhanced by the two fault systems that could have controlled former magma migration and/or fluid upwelling. The geochemical analyses revealed a significant enrichment in CO<sub>2</sub> and CH<sub>4</sub> contents as well as in the mantle-derived <sup>3</sup>He of the fluids dissolved in the surrounding marine waters. All the available literature data point to a volcanic origin of the geological structure defining it as a *seamount-like structure*.

In order to gain a better understanding of the origin and nature of the investigated submarine structure, we combined the geochemical features of the fluids proposed by Loreto et al. (2015) with the mineralogical data of a dredged sample (-80 m) in correspondence of the top of the seamount-like structure. Minerals were analyzed by a combination of Scanning Electron Microscopy – Energy Dispersive X Ray Spectroscopy (SEM-EDX) and X Ray Powder Diffraction (XRPD) analyses.

The materials are a mixture of biogenic and inorganic components. The inorganic compounds consist of a fine grained fraction containing magnetic and not-magnetic mineral phases ( $< 63 \mu\text{m}$ ) and a not-magnetic, coarse grained ( $< 1 \text{ mm}$ ), phyllosilicatic (single crystals) rich fraction. XRPD analysis of the  $< 63 \mu\text{m}$  fraction, highlights the presence of Quartz, Phlogopite, Albite, Calcite, Clinocllore and significant amount of Magnetite. XRPD analyses of the single crystals occurred in the coarse grained phyllosilicatic fraction, suggesting the presence of prevalent phlogopite and minor amount of phlogopite/chlorite laminae. The SEM-EDS analysis allowed to classify the dark mica laminae as Mg-rich solid solutions of the Annite  $[\text{KFe}_2+3\text{AlSi}_3\text{O}_{10}(\text{OH})]$  - Phlogopite  $[\text{KMg}_3\text{AlSi}_3\text{O}_{10}(\text{OH})_2]$  series.

The composition of biotite reflects primarily the nature of the host magmas (Shabani et al., 2003). Trioctahedral micas such as Annite–Phlogopite solid solutions, are found in nearly all types of granites and granitic rocks. The dark mica from the studied sample compare well with those of documented continental calcalkaline plutonic rocks from the Calabrian Peloritani Arc Orogen. On the mineralogical point of view this feature added to the presence of the other identified mineral phases such as Quartz, Albite and Magnetite support this hypothesis.

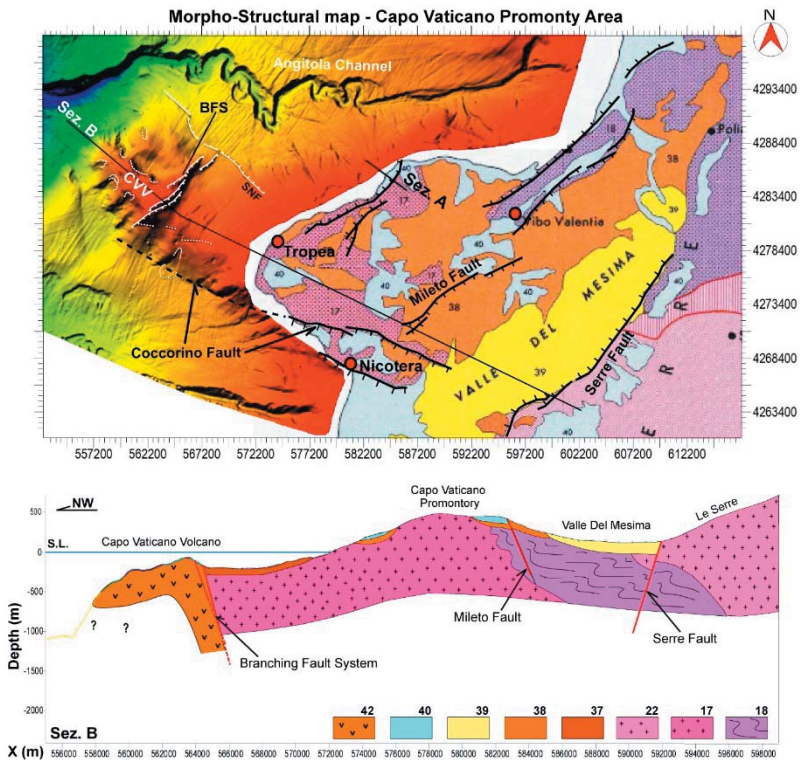


Fig. 1. Location of the submarine structure (CVV on the map) crossed by the main faults (Coccorino fault and BFS). The geological sketch is also shown

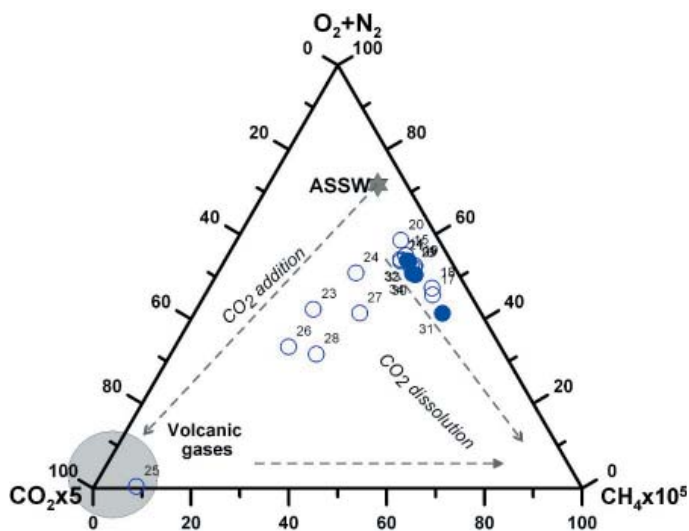


Fig. 2. Geochemical features of the fluids dissolved in the sea-water. A clear enrichment in deep-originated  $\text{CO}_2$  is quite evident

The significant magnetite content detected in the magnetic fine grained fraction could explain the high values of magnetic susceptibility measured by De Ritis et al. (2010). Furthermore, the minor biotite laminae partially replaced by chlorite can be interpreted as evidence of incipient hydrothermal alteration process due to interaction of the involved rocks and the fluid emissions located at the top of the seamount-like structure (Loreto et al., 2015).

The literature multidisciplinary data and the historical information point to a volcanic origin of the seamount located offshore the Calabrian shoreline. If the identified minerals assemblage of this study is representative of the seamount-like rock parageneses, we suggest a plutonic calcalkaline composition, e.g. Biotite granodiorites, and granites similar to those of the Serre Massif and the Capo Vaticano area, crossed by the main active faults of the area that allow the upraising of deep-originated fluids.

## References

- SHABANI A.T., LALONDE A.E., WALEN J.B. (2003) - *Composition of biotite from granitic rocks of the Canadian Appalachian orogen: a potential tectonomagmatic indicator?* The Canadian Mineralogist, 41, 1381-1396.
- DE RITIS, R., DOMINICI, R., VENTURA, G., NICOLOSI, I., CHIAPPINI, M., SPERANZA, R., DE ROSA, R., DONATO, P. AND SONNINO, M. (2010) - *A buried volcano in the Calabrian Arc (Italy) revealed by high-resolution aeromagnetic data.* J. Geophys. Res., 115(B11), B11101.
- LORETO M. F., ITALIANO F., DEPONTE D., FACCHIN L., ZGUR F. (2015) - *Mantle degassing on a near shore volcano, SE Tyrrhenian Sea.* Terra Nova, 27, No. 3, 195-205.



## CO<sub>2</sub> Dynamics in Mofettes

Antoine Kies<sup>1</sup>, Olivier Hengesch<sup>1</sup>, Zornitza Tosheva<sup>1</sup>, Hardy Pfanz<sup>2</sup>

<sup>1</sup> University of Luxembourg, 162a, av. Faïencerie, L-1511 Luxembourg, (antoine.kies@uni.lu)

<sup>2</sup> Chair of Applied Botany, Faculty of Biology, University of Duisburg-Essen, 45117 Essen, Germany; (hardy.pfanz@uni-due.de)

**Key words:** Bossoleto, carbon dioxide, CO<sub>2</sub>, gas lake, infrared absorption, mofette

We report continuous carbon dioxide measurements in mofettes in the Democratic Republic of Congo (Goma), in Czech Republic (Eger-Graben) and Italy (Rapolano).

Mofettes are characterized by enhanced CO<sub>2</sub> degassing from focused emissions (vents), diffuse soil exhalation and sometimes CO<sub>2</sub>-enriched groundwater, connected to geothermal fluids. Often mofettes are part of a depression and CO<sub>2</sub> concentrations can reach at night very high levels especially close to the ground. Mofettes are very capricious, agreeable to live in at daytime being sheltered from the environment; deadly traps at night-time. Our measurements show very low carbon dioxide concentrations at daytime before increasing, often to lethal levels, during the night. North of the Kivu lake, in the vicinity of the Nyiragongo and Nyamuragira, the most active African volcanoes, CO<sub>2</sub> emitting mofettes, locally called mazuku (evil wind), cause regular casualties, especially to fugitives not aware of the danger.

Strong, subcontinental mantle-dominated CO<sub>2</sub> degassing occurs in the Bublák mofette field in the western Eger Rift in Czech Republic. Here in two mofettes, over weeks, continuous CO<sub>2</sub> measurements were linked to temperature and humidity.

In the Bossoleto, a mofette close to Rapolano (Tuscany, Italy) a 6 m tower was mounted close to the mofette center. The CO<sub>2</sub> vents occur both at the bottom and on the flanks of a circular doline; some 70 m in diameter and 6 m depth. From the bottom of the tower to the top, at each 40 cm air was sucked successively each 10 minutes to a pressure-temperature compensated CO<sub>2</sub> meter, based on infrared absorption. At the same elevations air temperature was measured. On top of the tower a weather station monitored barometric pressure, temperature, humidity, rainfall, wind speed and direction and solar irradiation.

Mostly over the day, CO<sub>2</sub> concentrations in the mofettes are very low. CO<sub>2</sub> accumulation starts precisely at reversal of the vertical temperature gradient, this happens in the afternoon when solar irradiance decreases sufficiently and bottom air in contact with the soil cools down getting heavier than the upper warmer air. As air movements are restricted, the seeping CO<sub>2</sub> is retained in the mofette.



Fig. 1. Observation tower in the Bossoleto doline; the picture, taken in the morning, shows the visible boundary separating the homogeneous CO<sub>2</sub> gas lake (up to 80 %) and air with low CO<sub>2</sub> levels above

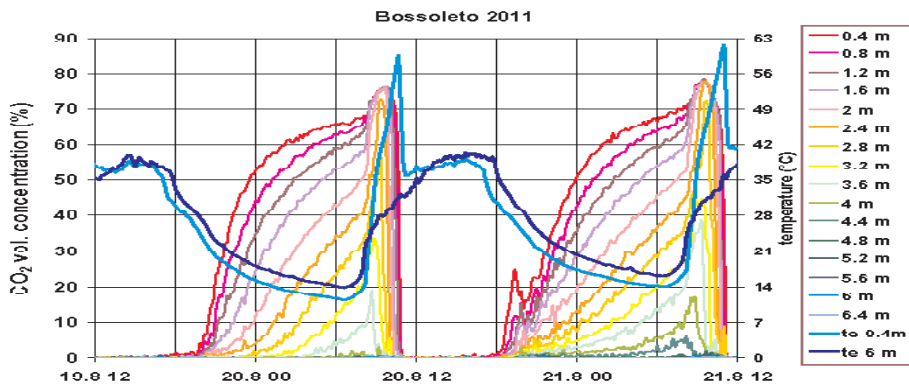


Fig. 2: Typical variation of CO<sub>2</sub> levels at the monitoring elevations, added is the temperature at 2 different heights

During the night a layered CO<sub>2</sub> gas lake will built up, reaching concentrations up to 80 %. In the morning a transition from the layered gas lake evolves into a homogeneous gas lake characterized by high CO<sub>2</sub> concentrations and high internal temperature before CO<sub>2</sub> drops rapidly to low harmless levels.

## References

- Etiopio G., Guerra M., Raschi A., 2005: *Carbon Dioxide and Radon Geohazards Over a Gas-bearing Fault in the Siena Graben (Central Italy)*, TAO, Vol. 16, No. 4, 885-896.
- Kies A., Hengesoch O., Tosheva Z., Raschi A., Pfanz H., 2015: *Diurnal CO<sub>2</sub>-cycles and temperature regimes in a natural CO<sub>2</sub> gas lake*. Int. J. Greenh. Gas Control 37, 142 –145.
- Pfanz H (2008): *Mofetten –kalter Atem schlafender Vulkane*. German Volcanological Society (eds.)RVVDL. Verlag, Köln
- Raschi, A., F. Miglietta, R. Tognetti, and P. R. van Gardingen, 1997: *Plant responses to elevated CO<sub>2</sub>. Evidence from natural springs*. Cambridge Univ. Press., 272 pp.



## **The effect of iron-bearing minerals on gaseous hydrocarbon generation**

Xiangxian Ma<sup>1</sup>, Guodong Zheng<sup>1</sup>, Wasim Sajjad<sup>1,2</sup>, Wang Xu<sup>1,2</sup>,  
Qiaohui Fan<sup>1</sup>, Jianjing Zheng<sup>1</sup>, Yanqing Xia<sup>1</sup>

<sup>1</sup> Key Laboratory of Petroleum Resources, Gansu Province / Key Laboratory of Petroleum Resources Research, Institute of Geology and Geophysics, Chinese Academy of Sciences, Lanzhou 730000, China

<sup>2</sup> University of Chinese Academy of Sciences, Beijing 100049, China

Numerous studies have been established that the mineral matrixes and transition metals are important factors to control the processes of hydrocarbon gases generation, and even influence the resources evolution of crude oils and natural gases. Iron-bearing minerals (pyrite and siderite) were one kind of these important minerals. However, the catalytic effect of iron-bearing minerals has been limitedly studied and the action mechanism is still unclear. One kerogen sample was used in this study, which was obtained from a brown coal from the eastern Junggar Basin, NW China. It was a low-matured sample dominated by humic matters (type III) and suitable for the study on hydrocarbon gases generation by pyrolysis experiment. The results showed that both pyrite and siderite could be able to improve the 0.5 - 1.5 times yields of gaseous hydrocarbons, but the effect mechanism of them was different. Pyrite may act indirectly as a catalytic agent or inducer via sulfur, which may enhance free radical formation and hydrocarbons generation, siderite is related with salt of organic acid formation and hydrogenation.

This work was supported by National Natural Science Foundation of China (41402129).



## Updated Versions of Methane Genetic Diagrams

Alexei V. Milkov<sup>1</sup>, Giuseppe Etiope<sup>2#</sup>

<sup>1</sup> Colorado School of Mines, USA

<sup>2</sup> Istituto Nazionale di Geofisica e Vulcanologia, Italy

# giuseppe.etiope@ingv.it

Empirical diagrams based on the stable C and H isotope composition of methane ( $\delta^{13}\text{C}$  vs  $\delta^2\text{H}$  of  $\text{CH}_4$ ) and molecular ratios ( $\delta^{13}\text{C}\text{-CH}_4$  vs  $\text{CH}_4/(\text{C}_2\text{H}_6+\text{C}_3\text{H}_8)$ ), often referred as Schoell, or Whiticar, and Bernard plots, are widely used as basic tool to interpret natural gas origin (microbial, thermogenic, abiotic), maturity and alteration. Since their early publications and versions proposed in widely cited works (e.g. Bernard et al. 1977; Whiticar, 1999 and references therein), thousands of natural gas samples were collected, either from sedimentary (conventional and unconventional) petroleum systems and igneous-metamorphic systems (Precambrian shields, ophiolites, peridotite massifs, geothermal systems). As more gas data became available, some genetic (isotopic) fields evolved. For example, Milkov (2011) introduced genetic fields to identify secondary microbial gas and early thermogenic gas, and Etiope and Sherwood Lollar (2013) and Etiope and Schoell (2014) expanded the genetic field of abiotic gas. We have revised the two diagrams using a larger global dataset of natural gases to encompass the entire variety of natural gas compositions and origins known to date.

The global dataset includes >15,000 gas samples from petroleum systems, using >400 published papers, reports and government databases, and >200 data from dominantly abiotic gas from published works. Using these datasets, we propose a new version of the empirical genetic fields for primary microbial, secondary microbial, thermogenic and abiotic gases. We also found that gases originating from Type II and Type III kerogen sufficiently overlap on the “Bernard” plot and cannot be reliably distinguished.

### References

- Bernard et al. (1977) *9<sup>th</sup> Annual OTC Conference* 435-438 (OTC 2934).  
Etiope and Schoell (2014) *Elements*, 10, 291-296.  
Etiope and Sherwood Lollar (2013) *Rev. Geophys.* 51, 276-299.  
Milkov A.V. (2011) *Org. Geochem.* 42, 184-207.  
Whiticar, M.J. (1999) *Chem. Geol.* 161, 291-314,



## **Chemical and isotope composition of fluids related to travertine formation in Western and Central Turkey: inferences on the role of tectonics in fluid circulation**

Andrea Luca Rizzo<sup>1#</sup>, Kadir Dirik<sup>2</sup>, I. Tonguc Uysal<sup>3</sup>, Antonio Caracausi<sup>1</sup>,  
Francesco Italiano<sup>1</sup>, Mariagrazia Misseri<sup>1</sup>, Galip Yuce<sup>2</sup>, Halim Mutlu<sup>4</sup>,  
Ezgi Unal-Imer<sup>2</sup>, Abidin Temel<sup>2</sup>, Serdar Bayari<sup>2</sup>, Nur Ozyurt<sup>2</sup>

<sup>1</sup> Istituto Nazionale di Geofisica e Vulcanologia, Sezione di Palermo, Via Ugo La Malfa 153, 90146 Palermo (Italia)

<sup>2</sup> Hacettepe University, Geological Engineering Department, Beytepe, Ankara, Turkey

<sup>3</sup> CSIRO Energy, The University of Queensland Kensington, Western Australia, Perth, Australia

<sup>4</sup> Ankara University, Geological Engineering Department, Golbasi, Ankara, Turkey

# corresponding author: andrea.rizzo@ingv.it

The study of chemical and isotope composition of fluids trapped in travertine may give important clues on the origin of fluids circulating during travertine formation as well as on the processes that controlled this formation (e.g., Pik and Marty, 2009 and references therein). This type of investigation becomes even more important when travertine forms in areas where tectonic activity is still active and may produce catastrophic earthquakes, such as in Turkey.

In this work, we focus on the travertine deposits of Pamukkale and Resadiye, which are in proximity of still active thermal springs. The former, is located within Denizli basin and is one of best-known travertine deposits of the world, which covers an area of more than 100 km<sup>2</sup> with thickness up to 60 m (Ozkul et al., 2013 and references therein). The latter, is located within the Kelkit valley in Central Turkey along the North Anatolian Fault Zone. Samples collected at Pamukkale and Resadiye have been previously dated based on U-Th isotope measurements and show ranges of age of ~24500-50000 and ~240-14600 ky, respectively. These estimations are in agreement with previous measurements made by Ozkul et al. (2013, and references therein). In these samples, we determined the H<sub>2</sub>O, CO<sub>2</sub> and O<sub>2</sub>+N<sub>2</sub> content, and the elemental and isotope composition of noble gases (He, Ne, and Ar) in fluid inclusions. We used single-step crushing technique in order to minimize the contribution of cosmogenic <sup>3</sup>He and radiogenic <sup>4</sup>He potentially accumulated in the matrix, according with protocol reported in Rizzo et al. (2015), Gennaro et al. (2017), and Robidoux et al. (2017). Selected grains of bulk travertine have been also analyzed for δ<sup>13</sup>C and δ<sup>18</sup>O of calcite, which is the dominant component of these rocks.

The H<sub>2</sub>O and CO<sub>2</sub> content measured in fluid inclusions from Pamukkale vary from 5.6 · 10<sup>-10</sup> to 5.1 · 10<sup>-4</sup> mol g<sup>-1</sup> and from 6.3 · 10<sup>-9</sup> to 3.8 · 10<sup>-7</sup> mol g<sup>-1</sup>, respectively; from Resadiye, H<sub>2</sub>O and CO<sub>2</sub> move from 5.6 · 10<sup>-9</sup> to 1.8 · 10<sup>-6</sup> mol g<sup>-1</sup> and from 2.6 · 10<sup>-9</sup> to 3.3 · 10<sup>-8</sup> mol g<sup>-1</sup>, respectively. Helium varies from 4.2 · 10<sup>-14</sup> to 1.6 · 10<sup>-12</sup> mol g<sup>-1</sup> in Pamukkale, while from 3.6 · 10<sup>-15</sup> to 4.4 · 10<sup>-14</sup> mol g<sup>-1</sup> in Resadiye. This suggests that H<sub>2</sub>O is generally the major component followed by CO<sub>2</sub>, with the highest gas content generally measured in Pamukkale travertine. Neon and argon, together with O<sub>2</sub>+N<sub>2</sub> indicate that all the samples suffered high atmospheric contribution, which reasonably occurred during fluids circulation in crustal layers.

Carbon and oxygen isotope composition of calcite varies in a narrow range (5‰ < δ<sup>13</sup>C < 6.8‰, -16.8‰ < δ<sup>18</sup>O < -12.8‰), with a general overlapping between the two studied areas. Our results are comparable to the measurements carried out by Kele et al. (2011), who indicated an active degassing of deep CO<sub>2</sub> through the local faults.

The <sup>3</sup>He/<sup>4</sup>He ratio not corrected for air contamination varies from 0.5 to 1.4 Ra (where Ra is the <sup>3</sup>He/<sup>4</sup>He of air equal to 1.39 · 10<sup>-6</sup>) in Pamukkale, while from 0.9 to 4.4 Ra in Resadiye. It is important to highlight that values >1 Ra are generally found in samples showing the lowest He content, which suggests the reasonable addition of cosmogenic <sup>3</sup>He to the pristine He content of fluid inclusions. In fact, this effect is more evident in Resadiye rather than in Pamukkale travertine, although the former are younger. On the other hand, <sup>3</sup>He/<sup>4</sup>He ratio <1Ra are generally independent on the He content, as confirmed by the negligible production of radiogenic <sup>4</sup>He calculated from the measured U and Th content and assuming the travertine ages calculated from U-Th isotope systematics. He isotope ratios <0.7 Ra are measured in correspondence of the highest <sup>4</sup>He/<sup>20</sup>Ne (i.e., ratios >0.6).

These preliminary results indicate that fluids trapped in Pamukkale travertine result from the mixing of a deep and hot fluid crustal-derived with cold and shallow waters bearing atmospheric-like dissolved gases. It is remarkable that the deep fluids do not show a typical radiogenic signature (<sup>3</sup>He/<sup>4</sup>He=0.01-0.05 Ra), while show a clear mantle-derived (<sup>3</sup>He) input. A previous study carried out by Gulec and Hilton (2016) confirms the presence in the area of fluids with magmatic <sup>3</sup>He/<sup>4</sup>He (up to 3.7 Ra). This implies that travertine formed in an active fault zone connected at depth with levels (lower crust) where mantle-derived He was trapped. On the contrary, the more atmospheric signature of fluids trapped in Resadiye travertine would suggest that their formation occurred in an environment dominated by shallow waters bearing atmospheric-like dissolved gases. This could imply that any faulty activity would regard the upper crust.

Acknowledgments: We wish to thank Fausto Grassa, Aldo Sollami, Mariano Tantillo, and all the other INGV colleagues that helped in the isotope analysis. This research is funded by TUBITAK 114Y544.

## References

- Correale A., Rizzo A.L., Barry P.H., Lu J., Zheng J. 2016. *Refertilization of lithospheric mantle beneath the Yangtze craton in south-east China: Evidence from noble gases geochemistry*. *Gondwana Research* 38, 289-303.
- Gennaro M.E., Grassa F., Martelli M., Renzulli A., Rizzo A.L. 2017. *Carbon isotope composition of CO<sub>2</sub>-rich inclusions in cumulate-forming mantle minerals from Stromboli volcano (Italy)*. *Journal of Volcanology and Geothermal Research* in press.
- Gulec N. & Hilton D.R. 2016. *Turkish geothermal fields as natural analogues of CO<sub>2</sub> storage sites: Gas geochemistry and implications for CO<sub>2</sub> trapping mechanisms*. *Geothermics* 64, 96-110.
- Kele S., Ozkul M., Forizs I., Gokgoz A., Oruc Baykara M., Nemeth T. 2011. *Stable isotope geochemical study of Pamukkale travertines: New evidences of low-temperature non-equilibrium calcite-water fractionation*. *Sedimentary Geology* 238, 191-212.
- Ozkul M., Kele S., Gokgoz A., Shen C., Jones B., Oruc Baykara M., Forizs I., Nemeth T., Chang Y., Cihat Alcicek M. 2013. *Comparison of the Quaternary travertine sites in the Denizli extensional basin based on their depositional and geochemical data*. *Sedimentary Geology* 294, 179-204.
- Pik R. & Marty B. 2009. *Helium isotopic signature of modern and fossil fluids associated with the Corinth rift fault zone (Greece): Implication for fault connectivity in the lower crust*. *Chemical Geology* 266, 67-75.
- Rizzo A.L., Barberi F., Carapezza M.L., Di Piazza A., Francalanci L., Sortino F., D'Alessandro W., 2015. *New mafic magma refilling a quiescent volcano: Evidence from He-Ne-Ar isotopes during the 2011–2012 unrest at Santorini, Greece*. *Geochemistry, Geophysics, Geosystems*. doi:10.1002/2014GC005653
- Robidoux P., Aiuppa A., Rotolo S.G., Rizzo A.L., Hauri E.H., Frezzotti M.L. (2017). *Volatile contents of mafic-to-intermediate magmas at San Cristóbal volcano in Nicaragua*. *Lithos* 272-273, 147-163.



## **Anomalous zones of light hydrocarbon recorded in the soil gas samples above Mszana Dolna tectonic window – Polish Outer Carpathians**

Anna Twaróg<sup>#</sup>, Henryk Sechman, Piotr Guzy, Adrianna Góra

AGH University of Science and Technology, Faculty of Geology, Geophysics and Environmental Protection, al. A. Mickiewicza 30, 30-059 Krakow, Poland.

<sup>#</sup> Corresponding author: [twarog@agh.edu.pl](mailto:twarog@agh.edu.pl)

**Keywords:** *soil gas, light hydrocarbons, tectonic window, Carpathian oil basin*

From the very beginning of the oil exploration, the presence of hydrocarbons seepages in the near-surface zone was a direct indicator of subsurface accumulations. The hydrocarbons migration to the surface may be done by cracks, fissures or faults (Brown, 2000; Etiope, 2015) using the mechanisms associated with diffusion and effusion processes. The oil and gas macro-seeps (focused, visible leakage) and gas microseepage (invisible, wide spread) are the surface expressions of hydrocarbons migration (Etiope, 2015). The Outer Carpathians are characterized by a very complex, disturbed structures and occurrence of reservoir and source rocks exposed on the surface. Therefore, the geochemical signal recorded in the near-surface zone may be an evidence of the tectonic structure presence and hydrocarbon potential of the study area. This is confirmed by the results of the previous research conducted in the Polish Flysch Carpathians (Celary et al., 1961; Dzieniewicz et al., 1978, 1979; Sechman and Dzieniewicz, 2009).

The purpose of the study was to determine the correlation between light hydrocarbons concentration recorded in soil gas and the tectonics of the study area in order to indicate the zones of highest hydrocarbon potential.

Surface geochemical survey was carried out in 2016 in the area of the Mszana Dolna tectonic window and the Magura Nappe, using the free-gas method. The soil gas samples were collected with a patented probe and using a specific procedure (Dzieniewicz and Sechman, 2001, 2002). In total, 576 soil gas samples were collected along 4 sampling lines. The spacing between sampling sites was 100 m. The soil gas samples were analyzed for concentrations of methane and its homologues (ethane, propane, i-butane, n-butane, neo-pentane, i-pentane, n-pentane) and gaseous alkenes (ethylene, propylene, 1-butene) using the gas chromatograph with the flame-ionization detector (FID).

In the collected soil gas samples the highest variability was recorded for methane, with concentrations ranging from 0.92 ppm to 38.21 %vol. While, the maximum

values of total alkanes  $C_2-C_5$  and total alkenes  $C_2-C_4$  were: 1.67 %vol. and 146.42 ppm, respectively. In order to visualize the variability of recorded concentrations in the study area, the histograms of  $CH_4$  and total alkanes  $C_2-C_5$  were made, additionally dividing data into two areas: Mszana Dolna tectonic window (MDW) – 197 sampling points (Fig. 1A, B) and Magura Nappe (MN) – 379 sampling points (Fig. 1C, D). The histograms of methane and total alkanes  $C_2-C_5$  concentrations in the MN area are right-skewed, with modal classes within the intervals: 2-3 ppm and 0.05-0.1 ppm, respectively (Fig. 1C, D). Whereas, the distribution of  $CH_4$  and total alkanes  $C_2-C_5$  concentrations in the MDW area are characterized by open classes with a high frequency occurrence of the data: >18 ppm, >0.8 ppm, respectively (Fig. 1B, D). These relationships suggest that the anomalous  $CH_4$  and total alkanes  $C_2-C_5$  concentrations are dominant in the MDW area. In order to select the objective anomalous values, the background values were determined by the iterative method (Sechman and Dzieniewicz 2011). The background values of methane, total alkanes  $C_2-C_5$  and total alkenes  $C_2-C_4$  were: 2.74 ppm, 0.094 ppm and 0.013 ppm, respectively. The “true anomaly” ( $>3\sigma$ ) (Elkins, 1940) for  $CH_4$  and total alkanes  $C_2-C_5$  occurred in 243 (42%) and 224 (39%) of gas samples, respectively.

To illustrate the surface distribution of total alkanes  $C_2-C_5$  anomalies, the anomalous values above  $3\sigma$  were plotted in the tectonic sketch of study area (Fig. 2). Anomalous zones occur throughout almost entire length of sampling lines located above MDW. In the Northern part of study area, only single small anomalies associated with the outcrops of the Grybow Nappe were recorded. The soil gas samples collected in the MN area are generally characterized by lack of the increased values of total alkanes  $C_2-C_5$ . On the BB'

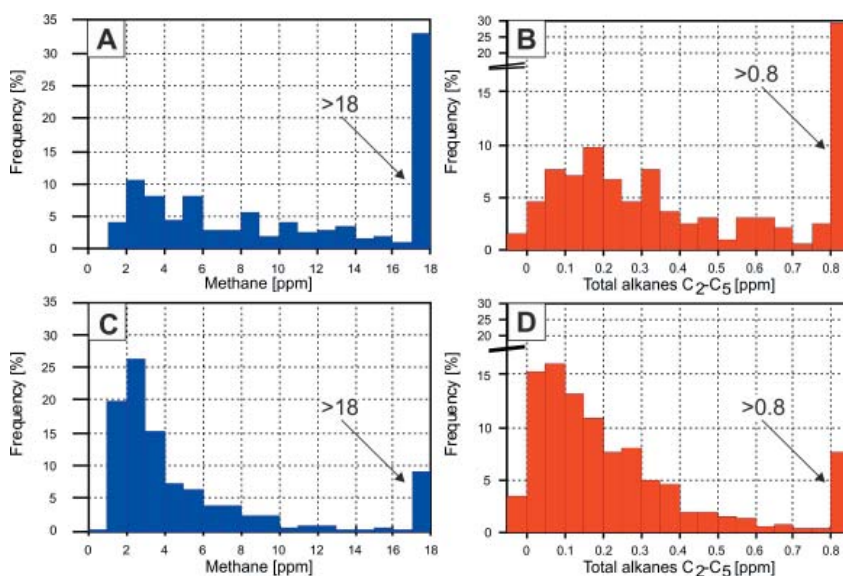


Fig. 1. Histograms of methane and total alkanes  $C_2-C_5$  concentrations recorded in the soil gas samples above Mszana Dolna tectonic window (A, B) and Magura Nappe (C, D)

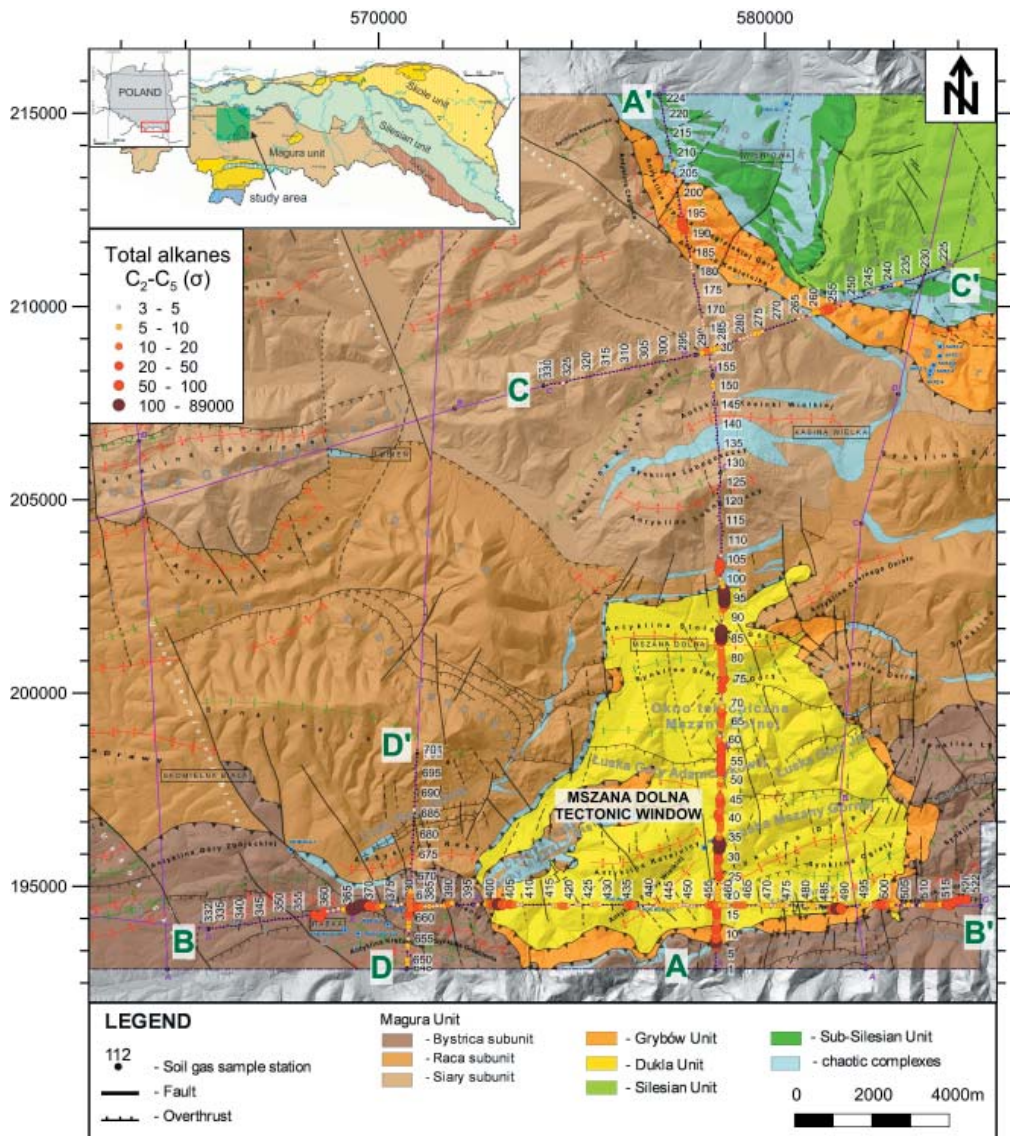


Fig. 2. Distribution of surface geochemical anomalies superimposed on the tectonic sketch of the study area (tectonic sketch after Geokrak, 2015).

sampling line located in the Southern part of study area, the anomalous zones occur also in the Bystrica subunit – in the Rabka area and in the Eastern part of line.

The surface distribution of light hydrocarbons indicates the strong correlation between the anomalous zones and deep tectonic structures. Obtained results confirm the sealing character of the Magura Nappe (Dzieniewicz et al., 1979). Simultaneously, the occurrence of hydrocarbon anomalies on practically entire area of the Mszana

Dolna tectonic window, may suggest relatively good hydrocarbon potential of the exposed Dukla Nappe layers. Increased hydrocarbons concentrations values registered in the Bystrica subunit area, may determine deep tectonic discontinuities intersecting the Dukla unit layers and the overlapping Magura complex.

Preliminary results show that the highest hydrocarbon potential may occur in contact zones of the Western and Eastern parts of the Mszana Dolna tectonic window with the Magura Nappe overlap. The detailed geochemical and geological analysis should be conducted in the Mszana Dolna tectonic window and Bistrica subunit area.

*The research was funded as a part of the Blue Gas project of the National Centre for Research and Development (BG2/ShaleCarp/14).*

### **Bibliography**

BROWN A. 2000. *Evaluation of possible gas microseepage mechanisms*. American Association of Petroleum Geologists Bulletin 84, 1778-1789.

CELARY M., LENK T., SZURA T. 1961. *Przykład powierzchniowego zdjęcia gazowego w warunkach karpackich*. Nafta 8, 209-211 (in Polish).

DZIENIEWICZ M., KUŚMIEREK J., POTERA J., SEMYRKA R. 1978. *Perspektywy naftowe fałdu Suchych Rzek w świetle badań geochemicznych (Bieszczady)*. Geologia 4, 37-51 (in Polish).

DZIENIEWICZ M., KUŚMIEREK J., RUSTA T. 1979. *Porównanie wyników powierzchniowych badań geochemicznych z budową struktur podmagurskich w południowo-zachodnim obrzeżeniu „okna tektonicznego” Mszany Dolnej*. Nafta 5, 145-149 (in Polish).

DZIENIEWICZ M. & SECHMAN H. 2001. *Design of a Driving Rod for Soil Studies. Utility model no 58584*, WUP, 05/2001 (in Polish).

DZIENIEWICZ M. & SECHMAN H. 2002. *Tool kit for manual gas sampling of near-surface soil horizons. Patent no. PL 184080*, WUP, 08/2002 (in Polish).

ELKINS T. A. 1940. *The reliability of geophysical anomalies on the basis of probability considerations*. Geophysics 5, 321-336.

ETIOPE G. 2015. *Natural Gas Seepage. The Earth's Hydrocarbon Degassing*. Springer, Switzerland.

GEOKRAK 2015. *Tectonic sketch of Jordanów-Limanowa area* (unpublished material).

SECHMAN H. & DZIENIEWICZ M. 2009. *Analysis of results of surface geochemical surveys in the transfrontier zone of the Polish and Ukrainian Carpathians*. Geologia 35, 109-127 (in Polish).

SECHMAN H. & DZIENIEWICZ M. 2011. *The example of background determination and mathematical processing of data from surface geochemical survey for the purposes of petroleum exploration*. Journal of Petroleum Science and Engineering 78, 396-406.



## Reservoir geochemical characteristics and fluid system of the Sinian Dengying and Cambrian Longwangmiao Formation in Sichuan Basin, China

XU Fanghao, XU Guosheng<sup>#</sup>, YUAN Haifeng, LIANG Jiaju, LIU Yong

State Key Laboratory of Oil and Gas Reservoir Geology and Exploitation, Chengdu University of Technology, Chengdu, 610059, Chengdu, China

<sup>#</sup> corresponding author: xgs@cduet.edu.cn

**Keywords:** *Sichuan Basin, the Sinian Dengying and Cambrian Longwangmiao Formation, Geochemical characteristics, Fluid system, Pressure evolution*

The oil and gas exploration of the Sinian and Cambrian has always been a focus in Sichuan Basin since 1950s, and the Dengying and Longwangmiao Formation in central Sichuan area has become the research hotspot in recent years.

Microscopy shows that there are signs of multi-stage fluid charging in the Sinian Dengying and Cambrian Longwangmiao Formation. Specifically, the first stage fine-grained dolomite grew along vug margin, second stage bitumen distributed along vug margin, third stage coarse-grained dolomite and fourth stage bitumen filled within pore space, fifth stage quartz or calcite also developed within pore space. They represent first stage brine water, first stage crude oil, second stage brine water, second stage oil and gas and third stage natural gas charging, respectively.

Based on Sr, C, O isotope analysis of dolomite, calcite and quartz filled in vugs, results indicates that during the period of the Qiongzhusi Formation oil generation window, the Sinian Dengying Formation and the lower Cambrian shares one connected and open fluid system, hydrocarbon-bearing and Sr-rich formation fluid laterally traveled from the Sinian Dengying Formation to the Cambrian Longwangmiao Formation along the paleo weathering crust between them. While after the period of gas generation window, the Cambrian Longwangmiao Formation transformed into an isolated fluid system with overpressure kept till now, as well as the Sinian Dengying Formation.

Under isovolumetric and closed condition, the relationship between pressure and Raman peak value could be illuminate by a unified equation. Based on laser Raman spectrum analysis and homogeneous temperature of the gas hydrocarbon fluid inclusion, combined with series of geochemical methods and related plots, the paleo fluid pressure of different stage of source rock evolution could be recovered. As a result, when  $R_o$  value is 0.5, 1.3, 1.7, 2.0 and  $>2.8$ , the pressure coefficient of the Sinian Dengying and

Cambrian Longwangmiao Formation is from 1.0, 1.1–1.2, 1.2, 1.2–1.3 to 1.0–1.1 and 1.0, 2.1–2.2, 1.8–1.9, 1.6–1.8 to 1.55–1.75, respectively.

Pressure recovering results reveals that over high pressure has never occurred in the geologic history of the Sinian Dengying Formation, but overpressure kept occurred in the geologic history of the Cambrian Longwangmiao Formation in Sichuan Basin. Pressure evolution processes in Sichuan Basin matched with the exploration situation at present. In Gaoshiti-Moxi area, the Cambrian Longwangmiao overpressure gas reservoirs preserved until now and with high reserves, the Sinian Dengying gas pools remained normal pressure, and also with natural gas reserves. In general, with favorable lithology and overpressure sealing, natural gas of the Sinian and Cambrian Formations in the Sichuan Basin accumulated perfectly and with great exploration potential.



## The Effect of Maturation on Gas Carbon Isotope in Different Types of Hydrocarbon Source Rocks

Yingqin Wu<sup>1#</sup>, Yanhong Liu<sup>1,2</sup>, Yongli Wang<sup>1</sup>,  
Zuodong Wang<sup>1</sup>, Tianzhu Lei<sup>1</sup>, Yanqing Xia<sup>1</sup>

<sup>1</sup> Gansu Provincial Key Laboratory of Petroleum Resources; Key Laboratory of Petroleum Resources Research, Institute of Geology and Geophysics, Chinese Academy of Sciences, Lanzhou 730000, China

<sup>2</sup> University of Chinese Academy of Sciences, Beijing 100049, China

# corresponding author: wuyingqin001@163.com

Abundances of stable isotopes distribution and evolution are widely used to the research of natural gas exploration and development. They can be used to clarify gas generation processes, deduce gas type and maturity and investigate the gas migrational processes. Hydrous pyrolysis experiments, as an important means to know about the natural evolution of geochemical characteristics, make multi-parameter analysis possible in controlled system and analytical results can be applied to actual production. In the present work, hydrous pyrolysis, using progressive heating from 250 to 550 °C, conducted on several immature organic sources to study the carbon isotopic composition and evolution of hydrocarbon gas.

Three different types of samples were selected in this study. A shale from the Green River Formation (Eocene) containing Type-I kerogen, a coal gangue from Huang County Basin (Tertiary) of Type-III kerogen, a Huaan carbonaceous shale (Jurassic) with Type-III kerogen, a shale from Minqin area (Jurassic) containing Type-II<sub>2</sub> kerogen and Pine needle powder were selected for thermal experiments (Table 1). All five samples are in the immature and low mature stage. The gas compositions were analyzed by GC/MS and the stable carbon isotope was analyzed by GC/IRMS.

Concentrations of the gaseous components varied substantially at different temperature and pressure conditions. Carbon dioxide was the most abundant gas produced in the hydrous pyrolysis experiments without taking into account the large amounts of CO<sub>2</sub> that can be dissolved in the water (Lewan *et al.*, 2011). Concentration of propane was too low to determine isotope composition in several samples, which was due to the excessive carbon dioxide generated in the corresponding system.

Methane, ethane and propane carbon isotope values were determined as a function of increasing temperature with two trends in  $\delta^{13}\text{C}$  values observed (Fig. 1). Early in the pyrolysis process, methane, ethane and propane were enriched in  $^{13}\text{C}$  in most cases. We showed that the phenomenon is similar to those reported by Liu *et al.* (2012) for hydrous pyrolysis experiments. The temperature which the most negative  $^{13}\text{C}$  value was

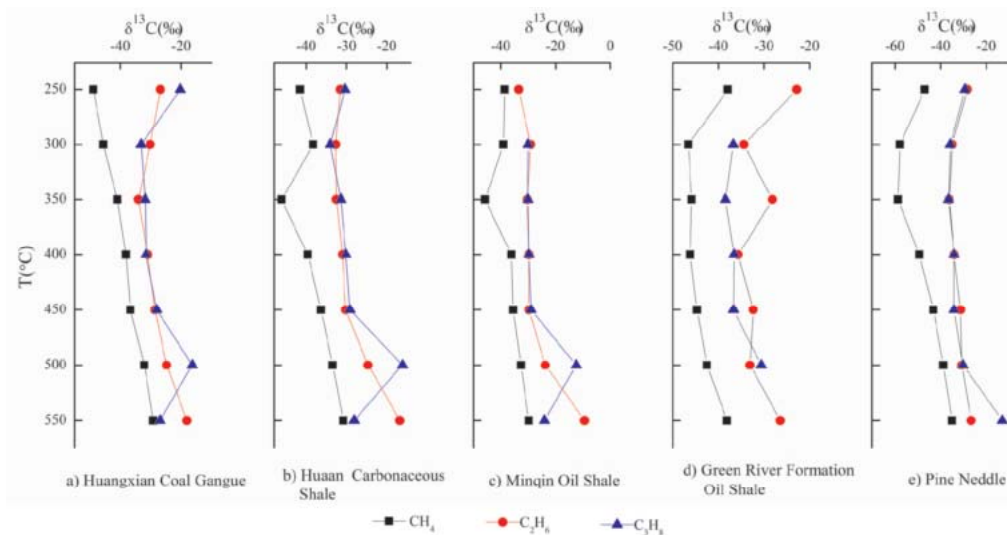


Fig. 1. The  $\delta^{13}\text{C}$  values trend of methane, ethane and propane with increasing temperature

observed was almost about 300 or 350 °C. After reaching a  $^{13}\text{C}$  minimum, they became enriched in  $^{13}\text{C}$  as temperature increasing other than propane of the samples contained type-II<sub>2</sub>, and type-III kerogen, which shifted to  $^{13}\text{C}$  enrichment at 550 °C.

The difference and relationship between the “normal” and “reversed” distributions were shown clearly in plots of  $\delta^{13}\text{C}$  vs. Carbon-number reciprocal (Fig. 1). Type-I kerogen and Pine needle at 250-450 °C, type-II<sub>2</sub> and Type-III kerogen at 300, 550 °C exhibited a “reversed” isotope distribution pattern. The  $\delta^{13}\text{C}$  values of ethane produced from the hydrous pyrolysis are more positive than those of methane and propane, showing significant “dogleg” trends. The reversal isotope trend of Type-I and III kerogen, Pine needle pronounced with increasing temperature from 250 to 350 °C and weakened or even disappeared with increasing temperature from 350 to 500 °C. The change in the carbon isotope compositions was substantial when the temperature changed from 500 to 550 °C. They showed more significant reversal for Huangxian coal gangue, Huanan carbonaceous shale, Minqin oil shale at 550 °C due to the degree of ethane enriching

Table 1. Sample description: All five samples are in the immature and low mature stage

Sample	Age code Strata	Kerogen
Green river formation oil shale	Eocene	Type-I
Minqin oil shale	Jurassic	Type-II <sub>2</sub>
Huangxian coal gangue	Tertiary	Type-III
Huanan carbonaceous shale	Jurassic	Type-III
Pine needle	Morden	Higher plant

$^{13}\text{C}$  was far more than methane and propane, while pine needles behaved differently and they showed positive serial because that the  $^{13}\text{C}$  enrichment of propane occurs far more than methane and ethane. The magnitude of difference between  $^{13}\text{C}$  ethane and  $^{13}\text{C}$  methane or  $^{13}\text{C}$  propane changed with temperature increasing in a closed hydrous system and led to the carbon isotope evolution.

In addition, we concluded that the temperature which the most negative  $\delta^{13}\text{C}$  value was almost about 300 or 350 °C. After reaching a  $\delta^{13}\text{C}$  minimum, they became enriched in  $\delta^{13}\text{C}$  as temperature increasing other than propane of the samples contained type-II<sub>2</sub>, and type-III kerogen, which shifted to  $\delta^{13}\text{C}$  enrichment at 550 °C. It is likely that thermal pressure, kinetic isotope fractionation, water, organic matter type and thermal maturation caused comprehensively the change of evolution characteristics of gas  $\delta^{13}\text{C}$  values. The research would provide more thoughts to explain gas “reversed” isotope distribution.

Supported by NSFC No. (41272147, 41172169, 41202093) and the Key Laboratory Project of Gansu Province (Grant No. Y621JJ1WYQ; Y530JJ1WZD).

### Reference

- Lewan M.D. and Roy S., 2011. *Role of water in hydrocarbon generation from Type-I kerogen in Mahogany oil shale of the Green River Formation*. Org. Geochem. 42, 31-41.
- Liu W.H., Wang J., Teng G.E., Qin J.Z. and Zheng L.J., 2012. *Stable carbon isotopes of gaseous alkanes as genetic indicators inferred from laboratory pyrolysis experiments of various marine hydrocarbon source materials from southern China*. Sci. China Earth Sci. 55, 966-974. (in Chinese).



## Is Australia a stable or moving continent? Recent findings in Eastern and South-Central Australia

Galip Yüce<sup>1#</sup>, Uwe Ring<sup>2</sup>, I.Tonguç Uysal<sup>3</sup>, Francesco Italiano<sup>4</sup>

<sup>1</sup> Department of Geological Engineering, Hacettepe University, Ankara 06800, Turkey

<sup>2</sup> Department of Geological Sciences, Stockholm University, 10691 Stockholm, Sweden

<sup>3</sup> The Commonwealth Scientific and Industrial Research Organisation, Energy, Perth, Kensington, Western Australia, Australia

<sup>4</sup> Istituto Nazionale di Geofisica e Vulcanologia, Sezione di Palermo, Italy

# corresponding author: galipyuce@gmail.com

**Keywords:** Australia, fluid's geochemistry, active faults, noble gas isotopes

Most of the interior of Australia is a Precambrian craton that is considered tectonically stable. However, in contrast to this belief, a number of recent studies suggest that Australia is actually less stable than commonly assumed. Herein, we report two recent studies showing that the Great Artesian Basin (GAB) in the Australian craton is tectonically active.

Basen on the first comprehensive gas geochemistry study (Italiano et al., 2014) carried out over three sedimentary basins of the GAB (Galilee, Cooper and Millungera basins) mantle helium is degassing from boreholes. This shows that the mantle is being tapped and neotectonical activity releases volatiles upward to the surface along fault zones. The He isotope values ( $R/R_a$ ) range between 0.02 and 0.21 while the  $\delta^{13}C_{TDIC}$  values in the range from -16.9 ‰ to 0.18 ‰. Mantle-derived volatiles are believed to have penetrated the crust due to extensional and/or transtensional deformation and further migrated to the surface through active faulting. A small amount of mantle contribution in a crustal-fluid system with a substantial radiogenic He accumulation cannot be determined easily based on only the He isotope ratios. Therefore, fluid's geochemistry is the most important tool to delineate the origin of fluids which associated with geo-tectonical settings.

A second study was performed along a major strike-slip fault at the southeastern margin of the GAB, the Norwest Fault Zone in south-central Australia (Ring et al., 2016). Geochemical data collected from very young travertine mounds showed a contribution of mantle volatiles ( $R/R_{ac}$ : 0.06-0.08) to the precipitating carbonate. Mantle degassing along the Norwest fault zone indicates recent tectonic activity.

These two geochemical studies provide strong evidence show recent tectonical activity prevailing in Eastern and South-central parts the Australian craton.

## References

- ITALIANO, F., YUCE, G., UYSAL, I.T., GASPARON, M., MORELLI, G. 2014. *Insights into mantle-type volatiles contribution from the dissolved gases in artesian waters of the Great Artesian Basin, Australia*, *Chemical Geology*, 378-379, 75-88, <http://dx.doi.org/10.1016/j.chemgeo.2014.04.013>
- RING, U., UYSAL, I.T., YUCE, G., UNAL-IMER, E., ITALIANO, F., IMER, A., ZHAO, J. 2016. *Recent mantle degassing recorded by carbonic spring deposits along sinistral strike-slip faults, south-central Australia*, *Earth and Planetary Science Letters* 454, 304-318



## **6. Noble Gases Applications**





## Applying $^{222}\text{Rn}$ to $^{226}\text{Ra}$ activity concentration measurements in environmental water samples by using an Ultra Low Level Liquid Scintillation Spectrometer

Tadeusz A. Przylibski, Stanisław Żak, Elżbieta Domin, Agata Kowalska

Wrocław University of Science and Technology, Faculty of Geoengineering, Mining and Geology, Division of Geology and Mineral Waters; Wybrzeże S. Wyspiańskiego 27, 50-370 Wrocław, POLAND; e-mail: Tadeusz.Przylibski@pwr.edu.pl, Stanislaw.Zak@pwr.edu.pl, Elzbieta.Domin@pwr.edu.pl, Agata.Kowalska@pwr.edu.pl

**Keywords:** radon, radium, natural hazard, water, groundwater, mineral water

The pair of  $^{222}\text{Rn}$  and  $^{226}\text{Ra}$  radionuclides in the Earth's hydrosphere only rarely lies in the radioactive equilibrium. That is why this pair of radionuclides can be used to monitor different processes occurring in groundwater and surface water and in the mixing zones of these two types of waters (Przylibski, 2011; Girault et al., 2016). The  $^{222}\text{Rn}$  nuclide, being a direct product of an alpha nuclear transformation of  $^{226}\text{Ra}$ , may be used for measuring its parent  $^{226}\text{Ra}$  activity concentration. The advantage of using  $^{222}\text{Rn}$  for measuring  $^{226}\text{Ra}$  activity concentration is an ease of detection with different types of detectors, including scintillation detectors. The absence of chemical preparation of the samples is undoubtedly an advantage (Przylibski et al., 2014; Perrier et al., 2016). An additional advantage of the scintillation technique is the small volume of water sample collected for analysis. The disadvantage, however, is a relatively high limit of detection. Therefore, it is necessary to use a spectrometer capable of measuring very small  $^{222}\text{Rn}$  activity concentration.

The authors use an Ultra Low Level Liquid Scintillation  $\alpha/\beta$  Spectrometer Quantulus 1220 for  $^{226}\text{Ra}$  (via  $^{222}\text{Rn}$ ) activity concentration measurements in liquid samples. Three scintillation vessels of 20 cm<sup>3</sup> each are used for the measurement of one sample. They are filled with 10 cm<sup>3</sup> of the analyzed water and 10 cm<sup>3</sup> of the liquid scintillator InstaFLUOR PLUS'. The measurement is carried out twice. During each of the two measurements 9 times for 60 minutes, the activity concentration of  $^{222}\text{Rn}$  in the water sample in each vessel is measured. In total this gives two sets of 27 measurement results at different times from the collection of the water sample. Using equations describing activity concentration of  $^{222}\text{Rn}$  and  $^{226}\text{Ra}$  as a function of time (Figure 1), activity concentration of  $^{222}\text{Rn}$  and  $^{226}\text{Ra}$  in the analyzed water sample can be determined. At the same time it is possible to obtain the information on what part of the  $^{222}\text{Rn}$  atoms comes from the alpha nuclear transformation of  $^{226}\text{Ra}$  dissolved in water, and which results from the

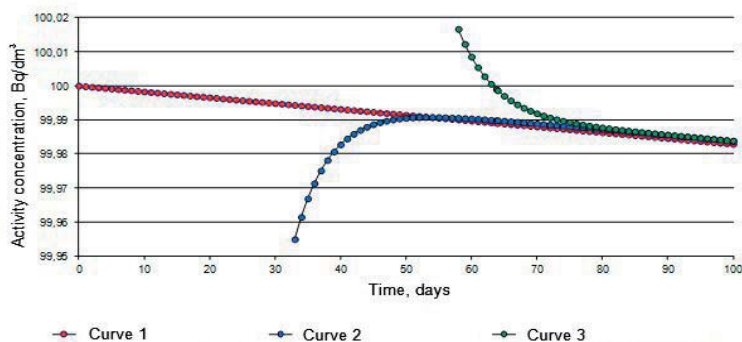


Fig. 1. The  $^{226}\text{Ra}$  and  $^{222}\text{Rn}$  activity concentration in a sample of groundwater as a function of time. Curve 1 –  $^{226}\text{Ra}$  activity concentration. Curve 2 –  $^{222}\text{Rn}$  activity concentration, assuming that at the time of water sampling, the activity concentration of  $^{222}\text{Rn}$  was lower than that resulting from the radioactive equilibrium between the  $^{226}\text{Ra}$  and  $^{222}\text{Rn}$  nuclides. Curve 3 –  $^{222}\text{Rn}$  activity concentration, assuming that at the time of water sampling, the activity concentration of  $^{222}\text{Rn}$  was higher than that resulting from the radioactive equilibrium between the  $^{226}\text{Ra}$  and  $^{222}\text{Rn}$  nuclides

dissolution of  $^{222}\text{Rn}$  atoms formed in the reservoir rocks, which then released from the rock and dissolved in the water.

The method developed in our laboratory allows us to obtain the results of  $^{226}\text{Ra}$  activity concentration fully satisfactory and comparable to other methods used in other laboratories for different type of samples including groundwater, surface, mineral, medicinal, bottled, tap, and thermal water or brine. The lower limit of detection for our method is  $0.05 \text{ Bq/dm}^3$ .

**Acknowledgements:** The abstract was written in the framework of internal research projects 0402/0115/16, 0401/0158/16, 0401/0190/16 financed by the Polish Ministry of Science and realized at the Division of Geology and Mineral Waters, Faculty of Geoenvironment, Mining and Geology, Wrocław University of Science and Technology.

## References

- Girault F, Perrier F, Przylibski T.A., 2016 – *Radon-222 and radium-226 occurrence in water: a review*. [in]: Gillmore, G. K., Perrier, F. E. & Crockett, R. G. M. (eds): *Radon, Health and Natural Hazards*. Geological Society, London, Special Publications, 451, <https://doi.org/10.1144/SP451.3>.
- Perrier F, Aupiais J, Girault F, Przylibski T.A., Bouquerel H., 2016 – *Optimized measurement of radium-226 concentration in liquid samples with radon-222 emanation*. *Journal of Environmental Radioactivity*, Vol. 157, pp. 52-59.
- Przylibski T.A., 2011 – *Shallow circulation groundwater – the main type of water containing hazardous radon concentration*. *Natural Hazards and Earth System Sciences*, Vol. 11, pp. 1695-1703.
- Przylibski T.A., Gorecka J., Kula A., Fijałkowska-Lichwa L., Zagożdżon K., Zagożdżon P., Miśta W., Nowakowski R., 2014 –  *$^{222}\text{Rn}$  and  $^{226}\text{Ra}$  activity concentrations in groundwaters of southern Poland: new data and selected genetic relations*. *Journal of Radioanalytical and Nuclear Chemistry*, Vol. 301, No. 3, pp. 757-764.



## Radon as a monitoring tool of atmospheric influx to landfill gas

Solecki A.T.<sup>1#</sup> Tchorz-Trzeciakiewicz D. E.<sup>1</sup>, Kowalczyk Ł.<sup>2</sup>

<sup>1</sup> Institute of Geological Sciences University of Wrocław,

<sup>2</sup> K35 Usługi przyjazne środowisku

# Corresponding author: andrzej.solecki@uwr.edu.pl

**Keywords:** landfill, radon, methane, CO<sub>2</sub>

CH<sub>4</sub>, CO<sub>2</sub>, O<sub>2</sub>, N<sub>2</sub> and Rn activity concentrations have been analyzed in landfill gases collected at 28 monitoring wells of the reclaimed municipal waste landfill in Wrocław. Minimum and maximum values of concentrations are shown in Tab. 1.

Tab. 1. Minimum and maximum concentrations of analyzed gases

	CH <sub>4</sub> (%)	CO <sub>2</sub> (%)	N <sub>2</sub> (%)	O <sub>2</sub> (%)	Rn(kBq m <sup>-3</sup> )
Max.	67.1	42.3	78.8	20.9	8.5
Min.	0.2	0.0	0.0	0.0	0.1

Nitrogen and oxygen maximum values are at the normal atmospheric level, while CH<sub>4</sub> and CO<sub>2</sub> reach maximum concentrations of 67.1 and 42.3 respectively. Rn activity concentration varies in the range of 0.1 to 8.5 kBq m<sup>-3</sup> what is normal for soil gas concentration.

Cross plots of gases concentrations are shown in Fig.1. CH<sub>4</sub> and CO<sub>2</sub> are positively correlated especially in the lower range of concentrations. In the case of high CH<sub>4</sub> concentrations, CO<sub>2</sub> concentration cannot exceed values higher than 100 - CH<sub>4</sub> concentration.

Methane evidently dominates gas composition and CO<sub>2</sub> presence is the result of the fact that the fraction of the methane in the gas is oxidized microbially to CO<sub>2</sub> (see Scheutz et al. 2009).

O<sub>2</sub>, N<sub>2</sub> contents are inversely correlated with CH<sub>4</sub> and CO<sub>2</sub> and if CH<sub>4</sub> and CO<sub>2</sub> c CH<sub>4</sub> probably due to the fact that the increased CH<sub>4</sub> content requires longer residence of gas in underground environment necessary for collecting emanated radon. Low values of radon activity concentrations which correlate with low CH<sub>4</sub> and CO<sub>2</sub> content indicate that sampled gas consisted of unmodified atmospheric air of short underground residence time.

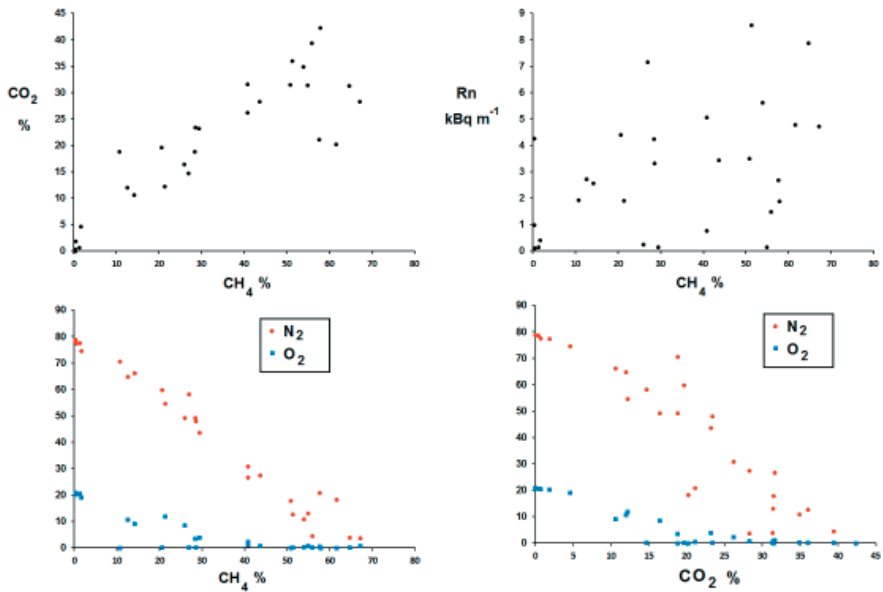


Fig. 1. Crossplots of analyzed gases concentrations

## References

- PARAJULI P, THAPA D., SHAH BR. 2016. *Assessment of residential radon concentration in the dwellings near Sisdol Landfill Site using solid state nuclear track detector (SSNTD)*, Journal of Applied Research 2016; 2(7): 425-427
- WALTER GARY R. , BENKE ROLAND R. & PICKETT DAVID A. 2012. *Effect of biogas generation on radon emissions from landfills receiving radium-bearing waste from shale gas development*, Journal of the Air & Waste Management Association, 62:9, 1040-1049, DOI: 10.1080/10962247.2012.696084
- SCHEUTZ, C., KJELDEN, P., BOGNER, J.E., DE VISSCHER, A., GEBERT, J., HILGER, H.A. & SPOKAS, K. 2009. *Microbial methane oxidation processes and technologies for mitigation of landfill gas emissions*. Waste Manage. Res. 27:409-455.



## Geochemical characteristics and their differences of helium and argon in coal-derived gases and oil-typed gases, China

Wang Xiaobo<sup>#</sup>, Li Jian, Li Zhisheng, Xie Zengye, Wang Yifeng, Wang Zhihong, Cui Huiying, Ma Wei, Hao Aisheng, Qi Xuening

Langfang Branch of PetroChina Research Institute of Petroleum Exploration & Development, CNPC Key Laboratory of Gas Reservoir Formation and Development, Langfang, Hebei, 065007 China

<sup>#</sup> First author: Wang Xiaobo, Engineer. Engage in Natural gases geology and geochemistry.

Add: P.O.B.44, Wanzhuang, Langfang, Hebei 065007, P.R. China. Phone: +861069213131.

E-mail: Wangxb69@petrochina.com.cn

Coal-derived gases take the main position in natural gases resources and play a vital role on promoting gas industry development in China<sup>[1-4]</sup>. Noble gases are important components of natural gases, and have great relationship with hydrocarbon gases. So, it is of great significances in guiding gas exploration by comprehensively understanding noble gases geochemical differences of coal-derived gases and oil-typed gases. Based on researches on noble gases geochemistry of coal-derived gases and oil-typed gases in China, geochemical characteristics differences of helium and argon are comparatively studied and their geologic implicating significances on gases genesis are discussed. The main recognitions are followed as:

1. The helium(He) content mainly ranges from 31 to 1626 ppm with main frequency distributed from 40 to 800 ppm in coal-derived gases in China, while it usually ranges from 30 to 3420 ppm with main frequency distributed around 100~500 and 1000~3000ppm in oil-typed gases. The argon (Ar) content generally ranges from 14.7 to 394.2 ppm with main frequency distributed from 10 to 70 ppm in coal-derived gases in China, while it mainly ranges from 10.2 to 497.3 ppm with two main frequencies distributed around 10~80ppm and 120~300ppm in oil-typed gases. Generally, the He and Ar contents in coal-derived gases are relative lower than these of oil-typed gases in China.

2. The  $^3\text{He}/^4\text{He}$  value of coal-derived gases in China generally ranges around  $(1.84 \sim 83.6) \times 10^{-8}$  with main frequency distributed around  $(2 \sim 8) \times 10^{-8}$ , While it mainly ranges around  $(0.28 \sim 14.6) \times 10^{-8}$  with main frequency distributed around  $(1 \sim 7) \times 10^{-8}$  in oil-typed gases. The  $^{40}\text{Ar}/^{36}\text{Ar}$  value of coal-derived gases in China usually ranges around 387 ~ 1940 with main frequency distributed around 400 ~ 1400, while it mainly ranges around 389 ~ 9559 with main frequency distributed around 500 ~ 2500 in oil-typed gases. The  $^3\text{He}/^4\text{He}$  value of coal-derived gases is relative wider than that of oil-typed gas, but their main frequencies are close to each other. The  $^{40}\text{Ar}/^{36}\text{Ar}$  value of oil-typed gases is generally higher than that of coal-derived gases.

3. The noble gases of coal-derived gases and oil-typed gases in China are generally typical crustal genesis, mainly originating from radioactive decay of U, Th and K elements in source rocks and closed formation.

4. The crustal and mantled genesis of noble gases have important indirect indicating effects on hydrocarbon and non-hydrocarbon gases, namely organic gases usually accompany with typical crustal genetic noble gases and inorganic gases generally mix with obvious mantled noble gases. According to differences on geochemical characteristics of Helium and Argon in coal-derived gases and oil-typed gases, the identified index and chart of oil-typed gases identification is established: When  $R/R_a$  is less than 0.1 (Noble gas is typical crustal genesis can make sure that hydrocarbon gases in natural gases is crustal organic genesis) and  $^{40}\text{Ar}/^{36}\text{Ar}$  is larger than 2000, the natural gases are usually can be identified as oil-typed gases. It provides a new technical method for oil-typed gases identification, having great significances in understand gas origination and guiding natural gases exploration.

Fund project: Special and Significant Project of National Science and Technology “Development of Large Oil/gas Fields and Coalbed Methane” (No.:2016ZX05007-002); Project of Petrochina, No.:2016B-0601.

## References

- [1]. Dai J, Li J, Hu G, et al. 2007. Geological characteristics of natural gas at giant accumulation in China. *Journal of Petroleum Geology*, 30(3): 275-288.
- [2]. Dai J X, Zou C N, Li J, et al. 2009. Carbon isotopes of Middle-Lower Jurassic coal-derived alkane gases from the major basins of northwestern China. *International Journal of Coal Geology*, 80: 124-134.
- [3]. Dai J X, Gong D Y, Ni Y Y, et al. 2014. Genetic types of the alkane gases in giant gas fields with proven reserves over 1000X10<sup>8</sup>m<sup>3</sup> in China. *Energy Exploration & Exploitation*, 32(1): 1-18.
- [4]. Li Jian, Li Jin, Li Zhisheng, et al. 2014. The hydrogen isotopic characteristics of the Upper Paleozoic natural gas in Ordos Basin, *Organic Geochemistry*, 74: 66-75.

## **7. Gases and Geo-hazards**





## **Two years of geochemical monitoring along the Alto Tiberina Fault (Italy): new inferences on fluids and seismicity in central Apennines**

Camarda Marco<sup>1</sup>, Caracausi Antonio<sup>1#</sup>, Chiaraluca Lauro<sup>2</sup>,  
De Gregorio Sofia<sup>1</sup>, Favara Rocco<sup>1</sup>

<sup>1</sup> Istituto Nazionale di Geofisica e Vulcanologia, Sezione di Palermo, via Ugo La Malfa 153, Palermo, Italy.

<sup>2</sup> Istituto Nazionale di Geofisica e Vulcanologia, Centro Nazionale Terremoti, Via di Vigna Murata, 605, Roma, Italy.

# Corresponding author, antonio.caracausi@ingv.it

Crustal faults are complex natural systems whose mechanical properties evolve over time. Hence the understanding of the multiscale chemico-physical processes, which control rock deformation, faulting and seismicity, requires investigating processes at the boundaries between different research fields and the availability of long term series of data.

With this aim it was created the TABOO near fault observatory within the inner sector of the northern Apennines (Italy). TABOO has been created to permanently monitor at high resolution a relatively small and actively deforming area (120km x 120km) by means of state of art geophysical networks comprising multidisciplinary instruments (Chiaraluca et al., 2014).

In this area it is documented the existence of a 60km long extensional fault named Alto Tiberina Fault (ATF) and it has accumulated a minimum time-averaged long term slip rate of about 1-3mm/year in the last 2Myear without large historical events unambiguously associated with this fault (Mirabella et al., 2011). In contrast a set of synthetic and antitethic high angle faults generated moderate seismic events.

The region is characterized by high pressure fluids (mainly CO<sub>2</sub>) at depth and very high flux CO<sub>2</sub> emissions (up to 5800 t/yr) on the surface in absence of any evidences of active or quiescent volcanism. The fluid over-pressure is proposed as one of the main triggering mechanisms of Apennine earthquakes (Chiodini et al., 2004). Furthermore long-term geochemical investigations in central Apennine highlighted the sensitivity of both the outgassing volatiles and the circulating groundwater to regional seismicity (Italiano et al., 2009).

Recently, we deployed a network of 3 automatic stations along the ATF to monitor the soil CO<sub>2</sub> flux. These stations were installed in correspondence of areas characterized by high flux of CO<sub>2</sub>. Notwithstanding these areas are far from the Italian volcanic provinces the measured CO<sub>2</sub> flux is comparable to those measured in the volcanic districts in

the Apennine. In addition periodically we also collected fluids released at these sites to investigate their chemical composition and the isotopic signature of noble gases (He, Ne and Ar) and carbon of CO<sub>2</sub> and CH<sub>4</sub>. These measurements allow us to get new insight on a) the origin of outgassing volatiles, b) the role of the tectonic discontinuities in the transfer of volatiles towards the surface and c) the main processes (e.g., atmospheric contamination, gas-water interaction) that occur in the crust. These investigations are well integrated with the multidisciplinary monitoring carried out in TABOO Near Fault Observatory.

The result of this monitoring show a co-variation of the CO<sub>2</sub> fluxes in all the investigated sites before the seismic sequences that occurred in the central Apennine between August and November 2016. We recognized an increase of the soil CO<sub>2</sub> flux in all the stations even if these are localized up to 140km away the hypocentres of the high magnitude earthquakes (M>5). We firstly recognized the increase of the CO<sub>2</sub> flux at the southernmost station in the TABOO area (100 km from the epicentre of the high magnitude summer 2016 earthquakes, M>5) and after two it occurred in the northernmost station (140 km from the epicentre of the high magnitude summer 2016 earthquakes, M>5).

Moreover the volatiles that we collected periodically highlighted that the increase of soil CO<sub>2</sub> flux was not coupled to variations of the chemical and isotopic compositions of the fluids emitted from the main vents in the region. So the nature of these fluids was not modified by the seismicity occurred in 2016 in central Italy.

This study proves that crustal deformation associated with seismogenic processes control the gas transfer on regional scale along the Apennine. It is worthy of note that the increase of the soil CO<sub>2</sub> flux anticipated the high magnitude earthquakes in central Italy from one week to one month.

The geochemical investigations in ATF coupled to the availability of multidisciplinary and high resolution data of TABOO Near Fault Observatory supports that the ATF is an ideal site for studying the relationship between fluids, crustal deformations and seismicity patterns and contributing to fill the lack of a plausible physico-chemical basis to explain the worldwide recognized geochemical variations in relation to crustal deformations and faulting.

## References

- CHIARALUCE ET AL. 2014, The Alto Tiberina Near Fault Observatory (northern Apennines, Italy). *Annals of Geophysics*, 57, S0327, 1-16.
- CHIODINI G., CARDELLINI C., AMATO A., BOSCHI E., CALIRO S., FRONDINI F. & VENTURA G. 2004. Carbon dioxide Earth degassing and seismogenesis in central and southern Italy. *Geophysical Research Letters*, 31, L07615, 1-4.
- ITALIANO F., MARTINELLI G., BONFANTI P. & CARACAUSI A. 2009. Long-term (1997-2007) geochemical monitoring of gases from the Umbria-Marche region. *Tectonophysics*, 476, 282-296.
- MIRABELLA F., BROZZETTI F., LUPATELLI A. & BARCHI M.R. 2011. Tectonic evolution of a low angle extensional faults system from restored cross sections in the northern Apennines (Italy). *Tectonics*, 30, TC6002.



## Radon and gamma rays anomalies in northern Taiwan and its tectonic Implications

Ching-Chou Fu<sup>1#</sup>, Lou-Chuang Lee<sup>1</sup>, Tsanyao Frank Yang<sup>2</sup>, Peng-Kang Wang<sup>1</sup>,  
Cheng-Horng Lin<sup>1</sup>, Vivek Walia<sup>3</sup>, Cheng-Hong Chen<sup>2</sup>, Arvind Kumar<sup>3</sup>

<sup>1</sup> Institute of Earth Sciences, Academia Sinica, Taiwan

<sup>2</sup> Department of Geosciences, National Taiwan University, Taiwan

<sup>3</sup> National Center for Research on Earthquake Engineering, NARL, Taiwan

# corresponding author

**Keywords:** radon, gamma ray, earthquake, subduction

Taiwan is tectonically situated in a terrain resulting from the oblique collision between the Philippine Sea plate (PHS) and the Eurasian plate (EU). The continuous observations of soil radon for earthquake studies at the Tapingti station (TPT) have been recorded and are compared with the data from gamma rays observations at the Taiwan Volcano Observation station (YMSG), located north to the TPT station. Some anomalous high radon concentrations and gamma-ray counts at certain times can be identified. It is noted that the significant increase of soil radon concentrations were observed and followed by the increase in gamma-ray counts several days before the earthquakes, which occurred in northeastern Taiwan. These earthquakes are usually located within the subducting PHS beneath the EU to the north along the Ryukyu trench in northern Taiwan (e.g.,  $M_L = 6.3$  April 20, 2015). It is suggested that the pre-seismic activities of an earthquake may be associated with slow geodynamic processes at the subduction interface, leading to the PHS movement to trigger radon enhancements at TPT station. Furthermore, the further movement of PHS may be locked by EU and accumulate elastic stress resulting in the increase of gamma rays due to an increase in the porosity and fractures below the YMSG station. The continuous monitoring on the multiple parameters can improve our understanding of the relationship between the observed radon and gamma-ray variations and the regional crustal stress/strain in the area.



## Increased fluid emission after a $M_L$ 3.5 event in the earthquake swarm region of NW-Bohemia/ Vogtland

J. Heinicke<sup>1#</sup>, T. Fischer<sup>2,3</sup>, J. Vlček<sup>2</sup>, C. Matyska<sup>4</sup>

<sup>1</sup> TU Bergakademie Freiberg, Institute of Geophysics and Geoinformatics, Germany

<sup>2</sup> Charles University in Prague, Faculty of Science, Czech Republic

<sup>3</sup> Institute of Geophysics, Czech Academy of Science, Czech Republic

<sup>4</sup> Charles University in Prague, Faculty of Mathematics and Physics, Czech Republic

# corresponding author: Jens.heinicke@geophysik.tu-freiberg.de

Fluid pore pressure variations in the upper crust are considered as an important factor to induce seismicity. The earthquake swarm activity in our region of interest can be interpreted as an interaction of tectonic stress accumulation and pore pressure perturbations as discussed in several publications. The relevant fluid component is a mixture of water and CO<sub>2</sub> of mantle origin. Effects of these interactions could be also transmitted to the surface via the fluid migration path along deep reaching fracture zones. In comparison to well known water level variations in wells during co- or post-seismic periods, an extra ordinary increase of CO<sub>2</sub> gas flow rate was observed 4 days after a  $M_L$  3.5 earthquake in May 2014 in the Hartoušov mofette, 9 km from the epicentres (NW Bohemia). During the subsequent 150 days the flow reached sixfold of the original level, and has been slowly decaying until present. Similar behaviour was observed during and after the swarm in 2008 suggesting a repeated fault-valve mechanism in long-term. We present a discussion about the mechanisms to induce these anomalous CO<sub>2</sub> emissions.

### Reference

FISCHER, T., MATYSKA, C. & HEINICKE, J, 2017. *Earthquake-enhanced permeability – evidence from carbon dioxide release following the  $M_L$  3.5 earthquake in West Bohemia*. EPSL 460, 60-67.



## **Fluids Geochemistry and Tectonics: What we have Learned from the Last Central Italy Seismic Crisis**

Francesco Italiano<sup>1#</sup>, Antonio Caracausi<sup>1</sup>, Alessandra Nigrelli<sup>1</sup>,  
Giovanni Martinelli<sup>2</sup>, Sergio Bovini<sup>3</sup>, Margherita Lemmi<sup>4</sup>

<sup>1</sup> INGV, Sezione di Palermo, via U. La Malfa 153, 90146 Palermo, Italy.

<sup>2</sup> ARPA Emilia Romagna, Via Amendola 2, 42100 Reggio Emilia (Italy)

<sup>3</sup> Geologo, via Marche Foligno, (PG, Italy)

<sup>4</sup> Geologo, via Ponte Lato, Visso (MC, Italy)

# Corresponding author: francesco.italiano@ingv.it

The last seismic sequence that strongly struck for the third time in 20 years the Central Apennines (Italy), started on August 24<sup>th</sup> 2016 with a Mw6 event and is still ongoing. More than 1000 Mw>3 events have been recorded in 8 months, 9 of them with magnitude above 5. The strongest Mw6.5 shock occurred on October 30, 2016. The sequence started close to the village of Amatrice (see fig. 1) and evolved toward NW following the Apenninic SE-NW trend over an area about 60km long across the Italian regions of Latium, Abruzzo, Marche and Umbria. With the last significant event (Mw6) the sequence moved back to the SE and occurred in between the tectonic structures responsible for the L'Aquila 2009 and the Amatrice 2016 crises (Fig. 1)

The fluids vented over those areas had been investigated during and after the previous seismic sequences by long-term geochemical monitoring (Fig. 1). Two decades of geochemical investigations on regional scale allowed us to recognize geochemical features of the circulating fluids and temporal changes of both thermal and cold waters from springs and wells as well as of free and dissolved gases. This allowed us to model the origin and circulation of the fluids and to interpret their variations over time (Italiano et al., 2004; Italiano et al., 2009). Coinciding with the seismic crisis, the recorded temporal changes of the geochemical features highlighted the occurrence of tectonics-related phenomena having regional interest besides modification only locally detected.

All the sequences were characterized by an enhanced CO<sub>2</sub> degassing at regional scale (Italiano et al., 2001; Heinicke et al., 2006; Bonfantiet al., 2012). CO<sub>2</sub> always represents the major component of both the vented and dissolved gases with variable CH<sub>4</sub> and N<sub>2</sub> contents. The recorded changes of the gas geochemistry in CH<sub>4</sub>, N<sub>2</sub> and He contents (Fig. 2) allowed to recognize the gas composition as a mixture of different components originated in different crustal layers, which mixing ratio changes as a function of the crustal permeability. The isotopic composition of helium testifies a major crustal component of the released gases.

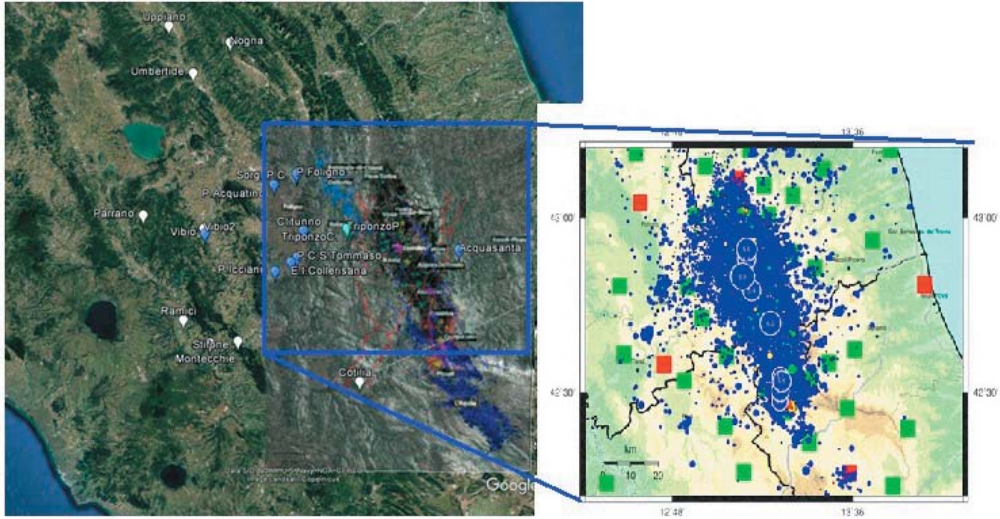


Fig. 1. Distribution of the investigated sampling sites over Central Italy during the three seismic crises. The box shows the epicenters of the Amatrice seismic crisis from a map dated April 25, 2017. The 9 Mw>5 events are shown in white circles

The chemical composition of the waters circulating over the Umbria region displayed large changes during the 1997-98 seismic crisis (Heinicke et al., 2000; Caracausi et al., 2005) that have not been recorded during the recent Amatrice crisis (Fig 3). Significant changes in the temperature and composition of shallow groundwaters, often used for human consumption purposes, were recorded either during the 1997-98 and the 2017 crises as a consequence of the upraising of thermal waters from selenitic levels (about 3km deep)

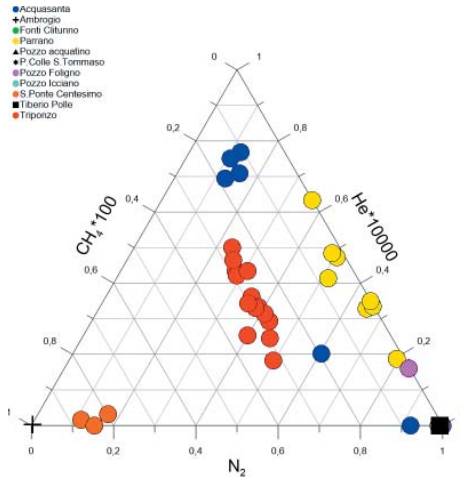


Fig. 2. Triangular diagram of the dissolved gases. The occurrence of changes as He increase within the same site is evident

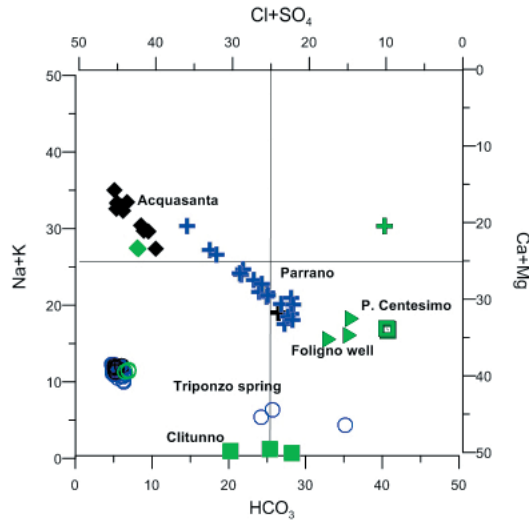


Fig. 3. Langelier classification diagram of some of the sampled waters. The changes in the main geochemical features is evident for every single site.  $\text{HCO}_3^-$  increase content can be related to an enhanced  $\text{CO}_2$  dissolution. The green, blue and black symbols refer to the Amatrice, Colfiorito and L'Aquila crises respectively

The depth of the hypocenters of the Amatrice sequence, located between 8 and 10 km, implies that the ruptures involved only the shallower portion of the crustal thickness being the crust-mantle transition located at a depth of about 25km. Coherently, the fluids vented during in the seismic sequence denote a crustal signature. Any contribution of mantle-derived fluids would indicate an active role of lithospheric structures, which seems unlikely during the Amatrice seismic crisis.

It is accepted that at least a part of a tectonic line under stress deforms before undergoing rupture, and causes modifications to the fluids circulation and their geochemical features during the whole seismogenesis. The modifications recorded so far during the Amatrice crisis indicate increases of the permeability well before the rupture (shown by the increase of the degassing rates) have not been accompanied by significant changes in the geochemical features of the gas phase, posing limits on the possible origin and provenance of the emitted fluids. This effect could be related to the geographical location of the investigated gases to the respect of the main shocks (Fig. 1)

## References

BONFANTI P., GENZANO N., HEINICKE J., ITALIANO F., MARTINELLI G., PERGOLA N., TELESCA L., TRAMUTOLI V. (2012) *Evidences of  $\text{CO}_2$ -gas emission variations in Central Apennines (Italy) during the L'Aquila seismic sequence (March-April 2009)*. *Boll.Geof.Teor. Appl.*, 53, 1, 147-168

- CARACAUSI A., ITALIANO F., MARTINELLI G., PAONITA A., RIZZO A. (2005) *Long-term geochemical monitoring and extensive/compressive phenomena: case study of the Umbria region (Central Apennines, Italy)*. *Annals of Geophysics*, 48, 1, 43-53
- HEINICKE J., ITALIANO F., LAPENNA V., MARTINELLI G., NUCCIO P.M. (2000) *Coseismic geochemical variations in some gas emissions of Umbria region (Central Italy)*. *Phys. Chem. Earth*, 25, 289-293
- HEINICKE J., T. BRAUN, P. BURGASSI, F. ITALIANO AND G. MARTINELLI. (2006) *Gas flux anomalies in seismogenic zones in the Upper Tiber Valley, Central*. *Geophysical Journal International*, 167, 794-806
- ITALIANO, F.; MARTINELLI, G.; NUCCIO, P. M. (2001). *Anomalies of mantle-derived helium during the 1997-1998 seismic swarm of Umbria-Marche, Italy*. *Geophys. Res. Lett.* Vol. 28, No. 5, p. 839-842
- ITALIANO F., MARTINELLI G., PLESCIA P. (2008) *CO2 degassing over seismic areas: the role of mechanochemical production at the study case of Central Apennines*. *Pageoph*, Vol. 165, 1, 75 - 94
- ITALIANO F., MARTINELLI G., RIZZO A. (2004) *Geochemical evidence of seismogenic-induced anomalies in the dissolved gases of thermal waters: A case study of Umbria (Central Apennines, Italy) both during and after the 1997–1998 seismic swarm*. *G-Cubed*, vol. 5, 11, doi: 101029/2004GC000720
- ITALIANO F., MARTINELLI G., BONFANTI P., CARACAUSI A. (2009) *Long-term geochemical monitoring of gases from the seismic area of the Umbria region: 1997-2007*. *Tectonophysics*, 476 (2009) 282–296
- ITALIANO F., BONFANTI P., M. DITTA, R. PETRINI, F. SLEJKO (2009) *Helium and carbon isotopes in the dissolved gases of Friuli region (NE Italy): geochemical evidence of CO2 production and degassing over a seismically active area*. *Chem. Geol.* 266 (2009) 76–85, doi: 101016 /j.chemgeo.2009.05.022



## Earthquake impact on iron isotope signatures recorded in mineral spring water

Horst Kämpf<sup>#</sup>, Jan Schüssler<sup>1</sup>, Karin Bräuer<sup>2</sup>, Ulrich Koch<sup>3</sup>, Mashal Alawi<sup>1</sup>

<sup>1</sup> GFZ German Research Centre for Geosciences, Telegrafenberg, 14473 Potsdam, Germany ()

<sup>2</sup> UFZ Helmholtz Centre of Environmental Research, D-06120 Halle, Germany

<sup>3</sup> August-Bebel-Str. 97, 08525 Plauen, Germany

#kaempf@gfz-potsdam.de

There are a lot of studies of earthquake-related impacts on water compositions and isotope ratios highlight the potential of geochemical investigations to decipher seismically induced changes in fluid-rock interactions. Previous studies found strong changes in dissolved element concentrations prior, during, or after an earthquake. For example, chloride concentration and lead isotope anomalies were found in spring water starting a few days prior to the 1996 earthquake (magnitude ML = 5.2) in the Pyrenean (Poitrasson et al., 1999; Toutain et al., 2006) and the major M= 7.2 Kobe earthquake in 1995 (Tsunogai and Wakita, 1995), respectively, and were attributed to preseismic strain changes inducing mixing of different aquifers. Such earthquake-related hydrochemical signals were also observed in other tectonically active regions. Several anomalies in hydrogen and oxygen stable isotope composition of water occurred immediately after seismic events near Acapulco, Mexico (Taran et al., 2005), and related to a M= 5.1 earthquake in 2005 at Koyna, India (Reddy et al., 2011), respectively. Similarly, a transient geochemical groundwater anomaly occurred after the 1998 Adana earthquake in Turkey (Woith et al., 2013).

Swarm earthquake triggered isotopic anomalies in the Vogtland area, central Europe were identified for the first time during and after the strong swarm earthquake period 1985/86 by monitoring of the hydrogen and oxygen isotope composition of spring water (Kämpf et al., 1989). More recently, chemical and isotopic time series data of groundwater samples were obtained over several years combined with detailed petrological studies on drill cores related to consecutive M>5 earthquakes in northern Iceland (e.g., Skelton et al., 2014; Wasteby et al., 2014; Andrén et al., 2016). There, dissolved element concentrations, as well as oxygen and hydrogen stable isotope ratios studied in groundwater, showed pre-earthquake anomalies, and their subsequent decay was related to mixing of different groundwater components variably affected by water rock interaction, nonstoichiometric mineral dissolution, and mineralogical alteration reactions in the fractured rock aquifer, respectively. These processes were explained by

expansion of the rock volume (dilation), therefore enhancing permeability. Generally, previous studies highlight the specific behavior of different elements and their isotopes in aquifers affected by earthquakes...

The activity of the deep subsurface biosphere is increasingly explored, revealing the significance of this habitat for biogeochemical cycles and evidence for deep biosphere activity related to earthquakes (Bräuer et al., 2005; Kietavainen and Purkamo, 2015; Pedersen, 2012; Sherwood Lollar et al., 2014).

Particularly, iron plays an important role in the abiotic and biotic reactions in the subsurface, and therefore, Fe isotope measurements in groundwater offer the possibility to reveal insights into earthquake-triggered changes of water-rock interactions. However, the potential impact of earthquakes on Fe isotope signatures in deep aquifers—and the associated spring water emanating at the surface—has not been investigated to date. The objective of this study is to test whether Fe isotopes in mineral spring water trace earthquake-induced changes in water-rock interaction and in biogeochemical cycles that are active in a fissured granitic aquifer. For this study we used a unique “natural laboratory” setting (Wettnquelle, Bad Brambach, Germany), where long-term geophysical and geochemical monitorings were carried out (Koch et al., 2003; Bräuer et al., 2007; Horalek et al., 2013).

We monitored the iron isotope signatures in the water of the Wettnquelle mineral spring (Bad Brambach) before, during and after the seismically active period 2000. . Our objective was to test whether Fe isotopes trace earthquake-induced changes in the water-rock interaction of the deep, fissured, granitic aquifer.

We found that the Fe isotope signatures in spring water are distinct from the granitic source signature ( $\delta^{56}\text{Fe} = +0.09 \text{ ‰}$ ). Particularly, we discovered that water  $\delta^{56}\text{Fe}$  values are remarkably stable ( $-0.01 \pm 0.11 \text{ ‰}$ , 2SD,  $n = 4$ ) before and during a strong seismic swarm period in 2000 (local magnitudes  $M_L > 3$ ), while  $\text{O}_2$  and  $\text{H}_2$  concentrations in water decrease and dissolved Fe content increases. Later, recurring events of lower  $\delta^{56}\text{Fe}$  values down to  $-0.3 \text{ ‰}$  are observed in the period from 2001 to 2003 with intermittent seismic events ( $1 < M_L < 3.2$ ). Our observations indicate a time lag between tectonic forcing and Fe isotope response. The role of abiotic water-rock interaction and Fe-utilizing bacteria identified in the mineral spring water on Fe isotope fractionation is discussed and a conceptual model scenario of earthquake-triggered changes in biogeochemical processes is proposed.

## References

- ANDREN M., et al. 2016. *Coupling between mineral reactions, chemical changes in groundwater, and earthquakes in Iceland*, Journal of Geophysical Research Solid Earth, 121, 2315–2337, doi:10.1002/2015jb012614.
- BRÄUER K., KÄMPF H., FABER E., KOCH U., NITZSCHE H.M. & STRAUCH G. 2005. *Seismically triggered microbial methane production relating to the Vogtland—NW Bohemia earthquake swarm period 2000, Central Europe*, Geochemical Journal, 39(5), 441–450, doi:10.2343/geochemj.39.441.

- BRÄUER K., KÄMPF H., FABER E., KOCH U., NITZSCHE H.M. & STRAUCH G. 2007. *Seismically induced changes of the fluid signature detected by a multi-isotope approach (He, CO<sub>2</sub>, CH<sub>4</sub>, N<sub>2</sub>) at the Wettinquelle, Bad Brambach (central Europe)*, Journal of Geophysical Research, 112, B04307, doi:10.1029/2006JB004404.
- HORALEK J. & ŠILENY J. 2013. *Source mechanisms of the 2000-earthquake swarm in the West Bohemia/Vogtland region (Central Europe)*. Geophysical Journal International 194, 979–999. <http://dx.doi.org/10.1093/gji/ggt138>.
- KÄMPF H., STRAUCH G., VOGLER P., & MICHLER W. 1989. *Hydrologic and hydrochemic changes associated with the December 1985/January 1986 earthquake swarm activity in the Vogtland/NW Bohemia seismic area*, Zeitschrift für Geologische Wissenschaften, 17, 685–698.
- KOCH U., HEINICKE J. & VOSSBERG M. 2003. *Hydrogeological effects of the latest Vogtland- NW Bohemian swarmquake period (August to December 2000)*. Journal of Geodynamics 35,107–121.
- KIETAVAINEN R. & PURKAMO L. 2015. *The origin, source, and cycling of methane in deep crystalline rock biosphere*, Frontiers of Microbiology, 6, 16, doi:10.3389/fmicb.2015.00725.
- PEDERSEN K. 2012. *Subterranean microbial populations metabolize hydrogen and acetate under in situ conditions in granitic groundwater at 450 m depth in the Aspo Hard Rock Laboratory, Sweden*, Fems Microbiology and Ecology, 81(1), 217–229, doi:10.1111/j.1574-6941.2012.01370.x.
- POITRASSON F., DUNDAS S.H., TOUTAIN J.P., MUNOZ M., & RIGO A. 1999. *Earthquake-related elemental and isotopic lead anomaly in aspringwater*, Earth and Planetary Science Letter, 169(3–4), 269–276, doi:10.1016/s0012-821x(99)00085-0.
- REDDY D. V., NAGABHUSHANAM P. & SUKHIJA B.S. 2011. *Earthquake (M5.1) induced hydrogeochemical and delta O-18 changes: Validation of aquifer breaching-mixing model in Koyna, India*, Geophysical Journal International, 184(1), 359–370, doi:10.1111/j.1365-246X.2010.04838.x.
- SHERWOOD LOLLAR B.T. ONSTOTT C., LACRAMPE-COULOUME G. & BALLENTINE C.J. 2014. *The contribution of the Precambrian continental lithosphere to global H-2 production*, Nature, 516(7531), 379–382, doi:10.1038/nature14017.
- SKELTON A., et al. 2014. *Changes in groundwater chemistry before two consecutive earthquakes in Iceland*, Nature Geoscience, 7(10), 752–756, doi:10.1038/ngeo2250.
- TARAN Y. A., RAMIREZ-GUZMAN A., BERNARD R., CIENFUEGOS E., & MORALES P. 2005. *Seismic-related variations in the chemical and isotopic composition of thermal springs near Acapulco, Guerrero, Mexico*, Geophysical Research Letters, 32, L14317, doi:10.1029/2005GL022726.
- TOUTAIN J. P., MUNOZ M., PINAUD JL, LEVET S, SYLVANDER M, RIGO A, & ESCALIER J 2006. *Modelling the mixing function to constrain coseismic hydrochemical effects: An example from the French Pyrenees*, Pure and Applied Geophysics, 163(4), 723–744, doi:10.1007/s00024-006-0047-9.
- TSUNOGAI U., & WAKITA H. 1995. *Precursory chemical-changes in-ground water—Kobe earthquake, Japan*, Science, 269(5220), 61–63.
- WASTEBY N., SKELTON A., T OLLEFSEN E., ANDREN M., STOCKMANN G., LILJEDAHL L.C., STRUKELL E., & MORTH M 2014. *Hydrochemical monitoring, petrological observation, and geochemical modeling of fault healing after an earthquake*, Journal of Geophysical Research Solid Earth, 119, 5727–5740,doi:10.1002/2013jb010715.
- WOITH H., WANG R.J., MAIWALD U., PEKDEGER A., & ZSCHAU J. 2013. *On the origin of geochemical anomalies in groundwaters induced by the Adana 1998 earthquake*, Chemical Geology, 339, 177–186, doi:10.1016/j.chemgeo.2012.10.012.



## Earthquake-related signals simultaneously detected in Central Italy by geochemical, hydrogeologic and satellite techniques in the period 2006-2016

Martinelli G.<sup>1#</sup>, Facca G.L.<sup>2</sup>, Genzano N.<sup>3</sup>, Gherardi F.<sup>2</sup>, Lisi M.<sup>3</sup>,  
Pierotti L.<sup>2</sup>, Tramutoli V.<sup>3,4,5</sup>.

<sup>1</sup> ARPAE Environmental Protection Agency of Emilia Romagna Region, Via Amendola 2, 42100 Reggio Emilia, Italy

<sup>2</sup> CNR Institute of Geosciences and Earth Resources, Via G.Moruzzi 1, 56124 Pisa, Italy

<sup>3</sup> University of Basilicata, School of Engineering, Viale dell'Ateneo Lucano 10, 85100 Potenza

<sup>4</sup> CNR Institute of Advanced Environmental Methodologies, 85050, Tito Scalco, Potenza, Italy

<sup>5</sup> International Space Science Institute, Beijing, China.

# corresponding author: giovanni.martinelli15@gmail.com

**Keywords:** *degassing processes, crustal deformations, satellite techniques, Central Italy earthquakes, earthquake precursors*

Central Italy is affected by intense crustal deformation processes due to active tectonics driven by the relative motions between the African and the Eurasia plates. In this area extensional tectonics is responsible for strain values of 1.5-2 cm/year (Carafa and Bird, 2016 and references therein) and for intense CO<sub>2</sub> gaseous emissions. Free CO<sub>2</sub> emissions and groundwaters affected by CO<sub>2</sub> discharges introduce in the atmosphere of central Italy over 20 Mt/year of CO<sub>2</sub>, about 1/3 of the total geological CO<sub>2</sub> degassed in Italy (e.g. Chiodini et al., 2013). Fluctuations of the stress field could be, in principle, revealed by GPS or by InSAR techniques but technological constraint factors may often limit these researches. Further monitoring techniques which include geochemical and hydrogeologic parameters revealed intense concentration fluctuations in past ten years (Pierotti et al., 2017). Satellite techniques able to detect thermal anomalies due to possible geochemical variations of the atmospheric composition induced by degassing phenomena have been utilized (e.g. Tramutoli et al., 2013). About in the same periods variations in various parameters evidenced possible crustal deformative processes. Part of the observed signals have been detected before mainshocks and could be related to aseismic slip (e.g. Johnston and Linde (2002) or to seismic slip eventually induced by fluctuations in minor seismicity. Crustal rheological characteristics linked to shallow depth of earthquakes and to intense circulation of deep originated geofluids could have allowed the recording of described parameters (Martinelli and D'Adamo, 2017).

Earthquake forecasting researches could benefit by the joint utilization of different monitoring techniques applied to geofluids.

### References

- Carafa M.M.C., Bird P. 2016 *Improving deformation models by discounting transient signals in geodetic data, 2: Geodetic data, stress directions, and long-term strain rates in Italy*. Journal of Geophysical Research: Solid Earth, 121, 5557-5576.
- Chiodini G., Aiuppa A., Cardellini C. 2013 *MaGa: Mapping Gas Emissions*. Wwww.magadb.net.
- Johnston M., Linde A. 2002 *Implications of crustal strain during conventional slow and silent earthquakes*. In: Lee WHK et al. (Eds) *International Handbook for Earthquake and Engineering Seismology, Part A*. International Geophysical Services, 81, 589-605, Elsevier New York.
- Martinelli G., D'Amico A. 2017 *Factors constraining the geographic distribution of earthquake geochemical and fluid-related precursors*. Chemical Geology, DOI: <http://dx.doi.org/10.1016/j.chemgeo.2017.01.006>
- Pierotti L., Gherardi F., Facca G., Piccardi L., Moratti G. 2017 *Detecting CO<sub>2</sub> anomalies in a spring on Mt. Amiata Volcano (Italy)*. Physics and Chemistry of the Earth, Parts A/B/C, DOI: <http://dx.doi.org/10.1016/j.pce.2017.01.008>.
- Tramutoli V., Aliano C., Corrado R., Filizzola C., Genzano N., Lisi M., Martinelli G., Pergola N. 2013 *On the possible origin of thermal infrared radiation (TIR) anomalies in earthquake-prone areas observed using robust satellite techniques (RST)*, Chemical Geology, 339, 157-168.



## Earthquake-related signals recorded in Central Italy, Southern Italy and in Sicily by geochemical and hydrogeologic methods

Martinelli G.<sup>1#</sup>, Ciolini R.<sup>2</sup>, Facca G.L.<sup>4</sup>, Fazio F.<sup>3</sup>, Gherardi F.<sup>4</sup>, Heinicke J.<sup>5</sup>, Pierotti L.<sup>4</sup>

<sup>1</sup> ARPAE Environmental Protection Agency of Emilia Romagna Region, Via Amendola 2, 42100 Reggio Emilia, Italy ()

<sup>2</sup> University of Pisa, Department of Civil and Industrial Engineering, Largo Lucio Lazzarino 1, 56122 Pisa, Italy

<sup>3</sup> GEODIXI, Via Alfonzetti 46, 95121 Catania, Italy

<sup>4</sup> CNR Institute of Geosciences and Earth Resources, Via G. Moruzzi 1, 56124 Pisa, Italy

<sup>5</sup> Technische Universität, Institute of Geophysics and Geoinformatics, Gustav-Zeuner-Str.12, D-09596 Freiberg, Germany

# corresponding author: giovanni.martinelli15@gmail.com

**Keywords:** *fluid geochemistry, water level, crustal deformations, earthquake precursors*

Crustal deformative processes are usually monitored by GPS or by satellite-based techniques. Significant signals have been recorded in many places of the world after strong earthquakes. Only in a few cases similar signals were detected before seismic events due to the relatively low sensitivity of equipments (Roeloffs, 2006; Cicerone et al., 2009). Due to the about non compressible character of water and to deep origin of CO<sub>2</sub>, deep originated fluid monitoring could be more sensitive in revealing weak signals related to crustal deformations and contribute to earthquake precursors researches (Martinelli and Albarello, 1997; Martinelli and Dadomo, 2017). Dissolved and bubbling CO<sub>2</sub> and related gases (e.g. Pierotti et al., 2017) have been automatically monitored in thermal spring waters located in selected areas of Tuscany and Umbria regions (Central Italy). Water level has been automatically recorded in deep wells located in Eastern Sicily and in Southern Italy (Campania region). Recorded data do not show significant dependence to meteorological or artificial parameters. Part of the observed signals have been detected before mainshocks and could be related to aseismic slip (e.g. Johnston and Linde (2002) or to seismic slip eventually induced by fluctuations in minor seismicity. Earthquake forecasting researches could benefit by the joint utilization of different monitoring techniques applied to geofluids.

### References

Cicerone R.D., Ebel J.E., Britton J.(2009) *A systematic compilation of earthquake precursors*. Tectonophysics, 476, 371-396.

- Johnston M., Linde A. (2002) *Implications of crustal strain during conventional slow and silent earthquakes*. In: Lee WHK et al. (Eds) *International Handbook for Earthquake and Engineering Seismology*, Part A. International Geophysical Services, 81, 589-605, Elsevier New York.
- Martinelli G., Albarello D. (1997) *Main constraints for siting monitoring network devoted to the study of earthquake related hydrogeochemical phenomena in Italy*. *Annals of Geophysics*, 40, 1505-1525.
- Martinelli G., Dadomo A. (2017) *Factors constraining the geographic distribution of earthquake geochemical and fluid-related precursors*. *Chemical Geology*, DOI: <http://dx.doi.org/10.1016/j.chemgeo.2017.01.006>
- Pierotti L., Gherardi F., Facca G., Piccardi L., Moratti G. (2017) *Detecting CO2 anomalies in a spring on Mt. Amiata Volcano (Italy)*. *Physics and Chemistry of the Earth, Parts A/B/C*, DOI: <http://dx.doi.org/10.1016/j.pce.2017.01.008>.
- Roeloffs E. (2006) *Evidence for Aseismic Deformation Rate changes Prior to Earthquakes*. *Annual Review of Earth and Planetary Sciences*, 34, 591-627.



## Mofettes as ancient gates to hell

Hardy Pfan<sup>1</sup>, Galip Yüce<sup>2</sup>

<sup>1</sup> Institute of Applied Botany and Volcano Biology, University of Duisburg-Essen, 45117 Germany; hardy.pfan@uni-due.de

<sup>2</sup> Hacettepe University, Department of Geological Engineering, 06800, Beytepe, Ankara, Turkey

In Greek mythology, the entrance to hell (Plutonium) is often located in valleys, caves or places of natural extremes. Oracles and Plutonia (the gates to the Underworld) are therefore found within seismic graben structures often associated with escaping geo-gases. Delphi and Chimaira in Greece, Lago Averno or Mefite D'Ansanto in Italy are well known mythological sites where due to geological fractures and fissures carbon dioxide or methane emissions can be measured (Etiopie et al. 2006). Yet, it is still a matter of debate, whether observations and descriptions published 2000 years ago can be verified with modern techniques. Here we report on our finding of a deadly CO<sub>2</sub> atmosphere at two famous temples within the Sanctuary of Hierapolis (Turkey) where ancient writers (Strabo, Plinius) describe the entrance to hell below the Apollo temple and an adjacent sanctuary of Pluto/Hades. Up to 91% of CO<sub>2</sub> gas was found within the Plutonium below the Apollo temple and the newly excavated sanctuary. The corpses of dead birds and hundreds of dead insects surrounding the gate to hell had already shown the presence of toxic gases. Mammals would not tolerate more than 5-7% CO<sub>2</sub> for some minutes. Our findings clearly proved not only the existence of the famous entrance to hell (Charonium, Plutonium) but also corroborate the precise descriptions already made by ancient writers like Strabo, Plinius and Cassius Dio. The finding of a diurnal CO<sub>2</sub>-gas lake close to the grotto also underlines the plausibility that during ceremonies, bulls and goats were ushered into the room close to the Plutonium where they asphyxiated within minutes. The Eunuch priests knowing about the dangers of the devil's breath avoided poisoning by keeping the heads way above the deadly CO<sub>2</sub>-gas lake.

### References

Cassius Dio's Epitome 68.27.3

Etiopie G, Papatheodorou G, Christodoulou D, Geraga M, Favali P (2006): *The geological links of the ancient Delphic Oracle (Greece): A reappraisal of natural gas occurrence and origin*. *Geology* 34, 821-824

Plinius the Elder (Nat. Hist. V, 105)

Strabo (XII, 8, 17)



## **Mofette bowls as deadly CO<sub>2</sub>-gas traps for animals – an example for a “recent” autochthonic thanatocoenosis**

Hardy Pfanz, Olivier Ruiz, Laura Siegert, Annika Thomalla

Institute for Applied Botany and Volcano Biology, Universität Duisburg-Essen, Universitätsstr. 5,  
45117 Essen, Germany

In tectonically active regions and in areas with pre- or post-volcanic activity, degassing of geogenic CO<sub>2</sub> leads to extremely increased CO<sub>2</sub> concentrations within pedosphere and atmosphere. As carbon dioxide is specifically heavier than air, it forms permanent and transient gas lakes within pits and depressions. CO<sub>2</sub> accumulates therein forming deadly gas lakes with concentrations of up to 100% CO<sub>2</sub>. A great number of asphyxiated animals is found in such mofette bowls. The animals were attracted to the deadly lake by trophic or behavioral reasons or just by pure accident. The carcasses form an exciting autochthonous thanatocoenosis. In our case, 123 asphyxiated determinable species were detected in a mofette bowl with a surface area of only 0.3 m<sup>2</sup>. The corpses belonged to 23 orders, 70 families and 115 different genera. The different reasons for the attraction of the CO<sub>2</sub> lake to the different animal taxa are discussed.



## Geogenic CO<sub>2</sub>-degassing and its effects on environment and organisms

Pfanz, H.

Chair of Applied Botany and Volcano Biology, University of Duisburg-Essen, 45117 Essen, Germany.  
hardy.pfanz@uni-due.de

The geogenic CO<sub>2</sub> emitted from magma chambers or seismic structures degasses and influences organismic life on the earth's surface. It irritates (8-10% CO<sub>2</sub>) or kills most animals (15-20%), yet some soil-specific animals (collembolan, nematodes) survive [1]. Plants are not that sensitive and some species transiently tolerate CO<sub>2</sub> concentrations even as high as 100%. Mofette areas are characterized by bare soil, if CO<sub>2</sub> fluxes are extremely high. Surrounding these extreme CO<sub>2</sub>-spots, specific vegetation occurs, showing adaption to hypoxic and acidic soils [2,3]. Several distinct plant species are even indicative for mofette fields and hint to the presence of CO<sub>2</sub> gas (mofettophilic plants). Sedges and rushes growing azonally in mofette areas hint to geogenic carbon dioxide emissions. Additionally, a special mofettophobic vegetation type occurs. These plants border degassing areas and cannot grow on soils with a CO<sub>2</sub> concentration higher than 2-3%. Aside from changes in species composition, plants occurring within mofettes reveal differences in habitus and growth. They stay smaller, have less and smaller leaves, and a reduced number of flowers and seeds. Furthermore, most species show a reduced photosynthetic ability, while chlorophyll and nutrient contents are lower than in control plants. Soil fungi react to enhanced CO<sub>2</sub> emissions with a reduction in species number.

### References

- [1] Hohberg K et al (2015), *Soil Biology & Biochemistry* 88, 420-42
- [2] Pfanz H et al (2004), *Progress in Botany* 65, 499-538
- [3] Vodnik D et al (2006), *Geoderma* 133 (3-4), 309-319



## Thoron ( $^{220}\text{Rn}$ ) exhalation into room air of earthen dwellings in northern Vietnam: Recognition of health geohazard and strategy for remediation

Arndt Schimmelmann<sup>1#</sup>, Dương Nguyễn-Thùy<sup>2</sup>, Hương Nguyễn-Văn<sup>2</sup>,  
Nguyễn Thị Ánh Nguyễn<sup>2</sup>, Minh Ngọc Schimmelmann<sup>1</sup>

<sup>1</sup> Indiana University, Department of Earth and Atmospheric Sciences, Bloomington, Indiana 47405-1403, USA; aschimme@indiana.edu

<sup>2</sup> Faculty of Geology, VNU University of Science, 334 Nguyễn Trãi, Thanh Xuân District, Hanoi, Vietnam; duongnt\_minerals@vnu.edu.vn; huongtectonics@vnu.edu.vn; nguyetdiachat@gmail.com

\* corresponding author: aschimme@indiana.edu

**Keywords:** exhalation, mud house, radiation hazard, radon, remediation, thoron

Low-cost housing construction in developing countries often relies on the use of local soil or clay that is compacted and dried to form the walls of dwellings (Fig. 1). Depending on the local geological context, the soil and clay building materials may contain enough thorium and uranium to produce significant exhalation of radon isotopes. Unlike their metallic precursor elements, monoatomic noble gas radon can diffuse into the room air where it can be inhaled by humans, dissolve in lymph fluid, and pose a radiation health hazard not only due to radon's own radioactive decay, but also due to the subsequent radioactive decay chains of their unstable metallic daughter nuclides in the human body (UNSCEAR, 1993; WHO, 2009).

Utilizing RAD7 and SARAD<sup>®</sup> RTM2200 instruments, thoron concentrations in excess of 1000 Bq m<sup>-3</sup> were frequently encountered in room air close to mud surfaces of northern Vietnamese mud houses (Fig. 2). Inhabitants often place beds near walls of mud houses where thoron concentrations are much higher than elsewhere in rooms. In contrast to thoron ( $^{220}\text{Rn}$ ) with its short half-life of ~55 seconds, the longer-lived  $^{222}\text{Rn}$  with a half-life of ~3.8 days is rarely of concern in mud houses because their typically drafty construction allows for fast ventilation of room air. An inhaled atom of  $^{222}\text{Rn}$  will likely be exhaled over the next day before it decays in a human body. In contrast, an inhaled atom of thoron that readily dissolved in the lung's fluid will almost certainly decay in the human body and contribute to radiation damage in tissue. Neither the population nor governmental and public health authorities in Vietnam are sufficiently aware of the wide-spread thoron geohazard. Enhanced ventilation of rooms is unable to significantly decrease the concentration of thoron near mud surfaces.



Figure 1. Traditional mud house in northern Vietnam

A detailed study by Meisenberg et al. (2017) laid the foundation for accurate measurements of the  $^{220}\text{Rn}$  inhalation hazard in mud houses, yet it seems that no feasible remediation strategy has been available to fit the needs of developing countries. A promising strategy is a diffusion barrier on inside walls to delay the escape of  $^{220}\text{Rn}$  until the short half-life of  $\sim 55$  seconds has caused safe decay within the porous mud wall.

Our group performed numerous practical tests of surface sealing techniques both in an authentic mud house in northern Vietnam and using standard-sized artificial mud bricks in the laboratory in Hanoi. Abundant deep cracks in most mud walls prevent layers of paint to provide an adequate seal. Hung tapestry, sheets of paper, and foil pinned to walls also proved to be inadequate. Isolated renovation efforts in historic mud houses sealed interior walls and unwittingly remediated the  $^{220}\text{Rn}$  problem, but the high



Fig. 2. *Left:* Measurement chamber with optional internal fan is pressed against wall to seal a defined volume of air in contact with a standardized surface area of mud; air is recirculated at  $1 \text{ L min}^{-1}$  through instruments. *Right:* SARAD<sup>®</sup> RTM2200 and two RAD7 units measuring radon and thoron during daytime in the room air of a northern Vietnamese mud house

costs of drywall, plastering, wall paper and paint make such approaches unaffordable for most inhabitants of mud houses.

In December 2016, our alternative strategy in an authentic mud house reduced the thoron concentration in room air close to walls from above 1000 Bq m<sup>-3</sup> to below detection limit. The applied diffusion barrier is inexpensive, non-toxic, non-flammable, resistant to biodegradation, and easily applicable using regionally available materials. The final application can be pigmented or include a dye. The material cost to remediate an average mud house in northern Vietnam is estimated to US \$25. A crew of two low-skilled workers can remediate an average mud house in two days using simple tools. Mud houses are abundant in many parts of the world, and mud-based 'green' building technologies are gaining acceptance in developed countries. Effective outreach and remediation need to be customized for each country.

### References

MEISENBERG O., MISHRA R., JOSHI M., GIERL S., ROUT R., GUO L., AGARWAL T., KANSE S., IRLINGER J., SAPRA B. K., TSCHIERSCH J. (2017) *Radon and thoron inhalation doses in dwellings with earthen architecture: Comparison of measurement methods*. Science of the Total Environment 579, 1855 – 1862. <http://dx.doi.org/10.1016/j.scitotenv.2016.11.170>

UNSCEAR (1993) The United Nations Scientific Committee on the Effects of Atomic Radiation 1993 Report. In: Sources, vol. I. United Nations, New York, 1993. <http://www.unscear.org/unscear/en/publications/1993.html>

WHO (2009) WHO Handbook on Indoor Radon: a Public Health Perspective. World Health Organization (WHO, Eds. H. Zeeb, F. Shannoun), 1–94. [http://apps.who.int/iris/bitstream/10665/44149/1/9789241547673\\_eng.pdf](http://apps.who.int/iris/bitstream/10665/44149/1/9789241547673_eng.pdf)



## **8. Shale Gas and Tight Gas**





## Gas Geochemistry Characteristics of Shale Gas in Changning-Weiyuan Area, Sichuan Basin, China

Chunhui Cao<sup>1,2#</sup>, Mingjie Zhang<sup>2</sup>, Li Du<sup>1</sup>, Liwu Li<sup>1</sup>

<sup>1</sup> Key Laboratory of Petroleum Resources, Gansu Province/Key Laboratory of Petroleum Resources Research, Institute of Geology and Geophysics, Chinese Academy of Sciences, Lanzhou 730000

<sup>2</sup> School of Earth Sciences & Key Lab of Mineral Resources in Western China, Gansu Province, Lanzhou University, Lanzhou 730000

# Corresponding author: caochunhui@lzb.ac.cn

**Keywords:** Noble gas isotope, Carbon Isotopic Reversal, Longmaxi formations, Shale gas,; Sichuan Basin in China

An enormous amount of potential shale gas resources exist in the Sichuan Basin, China.  $(4.1-10.3) \times 10^{12}$  m<sup>3</sup> of shale gas resource reserves in the Longmaxi Formation stratum, lying at a burial depth of less than 4000 m (Wang et al. 2015). Results of carbon isotope analysis for shale gas from Longmaxi Formation in the Changning-Weiyuan area indicate that the carbon isotopic reversal has the following order:  $\delta^{13}\text{C}_1 > \delta^{13}\text{C}_2 > \delta^{13}\text{C}_3$ . And, there is an evident difference in the carbon isotope composition between the areas of Changning and Weiyuan: the  $\delta^{13}\text{C}_1$  and the  $\delta^{13}\text{C}_2$  values in the Weiyuan area are roughly 8‰ and 6‰ lighter, respectively, than in the Changning area (Cao et al., 2016; Dai et al., 2014). Furthermore, such differences in isotopic composition are continually being found during the manufacturing processes conducted in the two areas (Cao et al., 2017; Zhang et al., 2017).

Differences in the carbon isotope composition of methane between Changning and Weiyuan could possibly be attributed to the following two causes: firstly, it is possible that the shale gas went through different geochemical processes during its generation and evolution in these two areas, and secondly, shale gas possibly currently undergoes different physical processes (adsorption/desorption) during the storage and exploitation processes conducted in these two areas (Zhang et al., 2017). Noble gases (He, Ne, Ar, Kr, Xe) are chemically inert and are not affected by secondary chemical processes (chemical reactions or microbial activity) (Ozima et al., 2004). Additionally, physical processes would not fractionate helium and argon in the range of the variations observed above (Ballentine et al., 1991; Ozima et al., 2002). In this respect, noble gases can be used as natural tracers for studying the physical processes that shale gas has undergone (Hilton et al., 2003; Warrier et al., 2013). In recent years, stable isotopes and noble gases isotopes have been used to discuss natural gas geochemistry, and have particularly been used to

distinguish bacterial and thermogenic gas origins where characterization of parameters relate to the genesis of thermogenic gas (such as primary versus secondary cracking, system openness, relations between gas isotope signatures, and biodegradation) (Prinzhofer et al., 2003; Kotarba et al., 2008, 2012, 2014; Schlegel et al., 2011).

Twenty-two shale gas samples collected from Lower Silurian Longmaxi Formation (Marine black shale) of Southern Sichuan Basin in Changning and Weiyuan were analyzed for stable isotope composition of noble gases (He, Ne, Ar) and molecular composition, stable carbon isotope composition of hydrocarbons ( $\text{CH}_4$ ,  $\text{C}_2\text{H}_6$ ,  $\text{C}_3\text{H}_8$ ) and  $\text{CO}_2$ , stable hydrogen isotope composition of methane and ethane. All the analyzed hydrocarbon gases reveal complete [ $\delta^{13}\text{C}(\text{CH}_4) > \delta^{13}\text{C}(\text{C}_2\text{H}_6) > \delta^{13}\text{C}(\text{C}_3\text{H}_8)$ ] and partial inversed isotopic trends from methane to propane thus they have a very complicated generation, migration and accumulation history and range of their source rock horizons. Analysis results indicate that: Longmaxi shale gas is a mixture of cracking gasses that were produced in various thermal evolution stage, including kerogen initial cracking gasses, liquid hydrocarbons secondary cracking gas, and gaseous hydrocarbons secondary cracking gas. About 6-8‰ difference in carbon isotopes between the Changning shale gas and the Weiyuan shale gas mainly attributes to the mixing of oil cracking gas and kerogen cracking gas at high-over mature stage.

Small fluctuations of the carbon isotopes and  $\text{CH}_4 / (\text{C}_2\text{H}_6 \text{ and } \text{C}_3\text{H}_8)$  ratios display during 3.5 years period of shale gas production from year 2012 to 2016, showing an adequate gas supply from matrix to fracture network.

High concentrations of He in analyzed gases are mostly a product of  $\alpha$ -decay of U and Th enriched in crustal materials.  $\text{CO}_2$  from analyzed gases was mainly generated during thermogenic processes of transformation of organic matter, although some gases can contain components from endogenic processes and from thermal destruction of carbonates.

In Changning-Weiyuan area, shale gas are mainly crustal origin (including degassing from organic matter rich shales, surrounding strata, inter-bedded carbonate as well as basin base) with minor air and radiogenic components mixing. There are obvious differences in noble gas geochemistry between the Weiyuan and Changning shale gases. The Weiyuan shale gases show low and uniform  $^3\text{He}/^4\text{He}$  ratios, high  $^{40}\text{Ar}/^{36}\text{Ar}$  ratios with varying  $^4\text{He}$  and  $^{40}\text{Ar}$  abundances, in contrast, the Changning shale gases have high and uniform  $^4\text{He}$  and  $^{40}\text{Ar}$  abundances but varied  $^3\text{He}/^4\text{He}$  ratios. The regional heterogeneity and gas mixing of different origins in varied proportion are main causes to noble gas geochemical difference between two areas. The Weiyuan shale gases show an increased  $^{40}\text{Ar}$  contents but a slight decrease in  $^{40}\text{Ar}/^{36}\text{Ar}$  during shale gas production, suggesting the insufficient free gas supply. In contrast, the Changning shale gases display small fluctuations in radiogenic  $^{40}\text{Ar}$  and  $^4\text{He}$  contents during shale gas production, indicating abundant gas supply source from mineral matrix to fracture network system because of high in-situ gas content or better connectivity of hydraulic fracture networks.

This study is financially supported by the National Science Foundation (NO. 41502143).

## References

- BALLENTINE C.J. O'NIONS R.K. OXBUGH E.R. HORVATH F. & DEAK J. 1991. *Rare gas constraints on hydrocarbon accumulation, crustal degassing and groundwater flow in the Pannonian Basin*. Earth and Planetary Science Letters 105, 229-246.
- CAO C.H. LV, Z.G. LI L.W. & DU, L. 2016. *Geochemical characteristics and implications of shale gas from the Longmaxi Formation, Sichuan Basin, China*. Journal of Natural Gas Geoscience 1, 131-138.
- CAO C.H. ZHANG M.J. TANG Q.Y. YANG Y. LV Z.G. ZHANG T.W. CHEN C. YANG H. & LI L.W. 2017. *Noble gas isotopic variations and geological implication of Longmaxi shale gas in Sichuan Basin, China*. Marine and Petroleum Geology, In Press.
- DAI J.X. ZOU C.N. LIAO S.M. DONG D.Z. NI, Y.Y. HUANG J.L. WU W. GONG D.Y. HUANG S.P. & HU G.Y. 2014. *Geochemistry of the extremely high thermal maturity Longmaxi shale gas, southern Sichuan Basin*. Organic Geochemistry 74, 3-12.
- HILTON D.R. & PORCELLI D. 2003. *Noble gases as mantle tracers, in the mantle and core*. In: Holland, H.D., Turekian, K.K. (Eds.), *Treatise on Geochemistry*. Elsevier, New York.
- KOTARBA M.J. & NAGAO K. 2008. *Composition and origin of natural gases accumulated in the Polish and Ukrainian parts of the Carpathian region: Gaseous hydrocarbons, noble gases, carbon dioxide and nitrogen*. Chemical Geology 255, 426-438.
- KOTARBA M.J. 2012. *Origin of natural gases in the Paleozoic–Mesozoic basement of the Polish Carpathian Foredeep*. Geologica Carpathica 63, 307–318.
- KOTARBA M.J. NAGAO K. & KARNKOWSKI P.H. 2014. *Origin of gaseous hydrocarbons, noble gases, carbon dioxide and nitrogen in Carboniferous and Permian strata of the distal part of the Polish Basin: Geological and isotopic approach*. Chemical Geology 383, 164-179.
- OZIMA M. & PODOSEK F. A. 2002. *Noble Gas Geochemistry*. Noble Gas Geochemistry, (2nd Edition). Cambridge University Press, 286.
- PRINZHOFER A. & BATTANI A. 2003. *Gas isotopes tracing: An important tool for hydrocarbons exploration*. Oil & Gas Science and Technology-Rev. IFP. 58, 299–311.
- SCHLEGEL M.E. ZHOU Z. MCINTOSH J.C. BALLENTINE C.J. & PERSON M.A. 2011. *Constraining the timing of microbial methane generation in an organic-rich shale using noble gases, Illinois Basin, USA*. Chemical Geology 287, 27-40.
- WANG S.F. ZOU C.N. DONG D.Z. WANG Y.M. LI, X.J. HUANG J.L. & GUAN Q.Z. 2015. *Multiple controls on the paleoenvironment of the Early Cambrian marine black shales in the Sichuan Basin, SW China: Geochemical and organic carbon isotopic evidence*. Marine and Petroleum Geology 66, 660-672.
- WARRIER R.B. CASTRO M.C. HALL C.M. & LOHMANN K.C. 2013. *Large atmospheric noble gas excesses in a shallow aquifer in the Michigan Basin as indicators of a past mantle thermal event*. Earth Planet. Science Letters 375, 372–382.
- ZHANG M.J. TANG Q.Y. CAO C.H. LV Z.G. ZHANG T.W. ZHANG D.K. LI Z.P. & DU L. 2017. *Molecular and carbon isotopic variation in 3.5 years shale gas production from Longmaxi Formation in Sichuan Basin, China*. Marine and Petroleum Geology, In press.

## Geochemical characteristics of Longmaxi Formation shale gas in Weiyuan area that located the China's oldest gas field, Sichuan Basin

Ziqi Feng<sup>1#</sup>, Weilong Peng<sup>2</sup>, Shipeng Huang<sup>2</sup>

<sup>1</sup> China University of Petroleum, Qingdao, Shandong 266580, China

<sup>2</sup> China Research Institute of Petroleum Exploration and Development, PetroChina, Beijing 100083, China

# Corresponding author: ziqi0314@163.com

**Keywords:** Geochemical characteristics; Longmaxi Formation; shale gas; Weiyuan area; Sichuan Basin

Weiyuan gas field is the first gas field found in the Sichuan Basin, and the oldest reservoirs (Sinian) in China. In recent years, Longmaxi Formation (Silurian) shale gas exploration has made a breakthrough in the southwest of the field. The following understanding is obtained by analysis:

Longmaxi shale gas in the Weiyuan area is dominated by methane, with an average wetness coefficient ( $C_{2-4}/C_{1-4}$ , %) of 0.57% ( $\delta^{13}C_1 = -36.9\text{‰}$  to  $-34.0\text{‰}$ ), with minor amounts of  $CO_2 = 0.46\%$  that most likely derived from the high temperature decomposition of carbonate sediments,  $N_2 = 0.56\%$ , and ethane ( $\delta^{13}C_2 = -42.8\text{‰}$  to  $-37.5\text{‰}$ ) and traces of propane. The gas is predominantly oil-associated originating

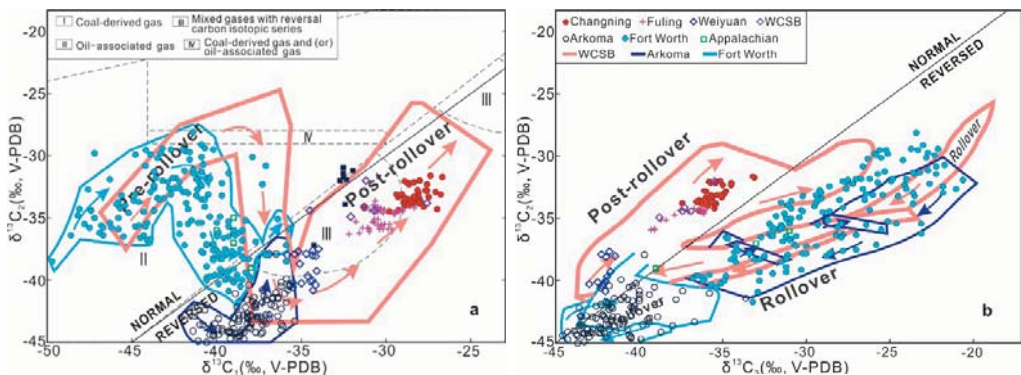


Fig 1. Generalized summary plots of  $\delta^{13}C_1$ - $\delta^{13}C_3$ , and  $\delta^{13}C_2$ - $\delta^{13}C_3$  showing a comparison of data from shale gas of Longmaxi Formation in Sichuan Basin (modified from Tilley and Muehlenbachs, 2013; Dai, 1992)

from late Ordovician- early Silurian sapropelic source rocks. The carbon isotope series includes reversals, with  $\delta^{13}\text{C}_2 < \delta^{13}\text{C}_1$  and rare  $\delta^{13}\text{C}_3 < \delta^{13}\text{C}_2 < \delta^{13}\text{C}_1$ . The enriched  $\delta^{13}\text{C}_1$  value is a result of the extremely high thermal maturity, and the complex carbon isotope reversals result from the combined effects of several secondary reactions such as the mixing of gases from different origin (kerogen, retained oil and wet gas) under such extremely high thermal maturity.

### Reference

- Wei G, Chen G, Du S, et al. 2008. *Petroleum systems of the oldest gas field in China: Neoproterozoic gas pools in the Weiyuan gas field, Sichuan Basin*. Marine & Petroleum Geology 25(4): 371–386.
- Tilley B, & Muehlenbachs K. 2013. *Isotope reversals and universal stages and trends of gas maturation in sealed, self-contained petroleum systems*. Chemical Geology, 339: 194-204.
- Dai J. 1992. *Identification and distinction of various alkane gases*. Science in China (series B) 35(10): 1246-1257.



## **Geochemical, Physical Properties and Shale Gas Exploration Prospects of the Longmaxi Shale in Nanchuan, Southeast Margin of the Sichuan Basin**

Yuhong Liao<sup>#</sup>, Yijun Zheng, Yunpeng Wang, Weiming Liu,  
Yongqiang Xiong, Ping'an Peng

The State Key Laboratory of Organic Geochemistry, Guangzhou Institute of Geochemistry, Chinese Academy of Sciences, 511 Kehua Street, Wushan Road, Tianhe District, Guangzhou, GD 510640, PR China

<sup>#</sup> corresponding author: liaoyh@gig.ac.cn

Nanchuan District of Chongqing City is located at southeast margin of the Sichuan Basin. Thick marine shales occur in both the Wufeng Formation ( $O_3w$ ) and the Lower Longmaxi Formation ( $S_1l$ ) of Nanchuan, and they are usually combined and called the Longmaxi shale. In geological times of Late Ordovician and Early Silurian, the sedimentary environment and tectonic settings of Nanchuan used to be similar to those of the Jiaoshiba shale gas field in Fuling District of Chongqing Province, which is located in the Eastern Sichuan Basin and famous for shale gas production in China (Guo et al., 2014). However, geochemical characteristics and physical properties of the Wufeng-Longmaxi marine shales in Nanchuan are rarely reported in previous studies.

In this study, in order to evaluate shale gas exploration prospects of the Longmaxi shale in Nanchuan, a well about 100 m deep was drilled at Sanquan town of Nanchuan District. The geochemical characteristics of the Longmaxi shales, such as total organic carbon content (TOC) and mineral compositions, together with physical properties including porosity, specific surface area, pore volume and pore-size distribution were measured (Fig .1).

The results indicated that geochemical characteristics and physical properties of the Longmaxi shale varied with ancient sedimentary environment. Deep-water shelf facies were more conducive to the accumulation of organic matter and excess silica. Additionally, TOC values also have strong positive relationship with silica content. Katian, Hirnantian in the Wufeng Formation, Rhuddanian in the Longmaxi Formation (TOC > 2%, clay < 40%) were mainly high-quality shale intervals. The high-quality shale with TOC > 2% is about 24 m thick, with an average TOC value of 2.99%. It indicates that the Longmaxi shale in Nanchuan should have considerable shale gas exploration prospects. Basically, most geochemical characteristics and physical properties of Wufeng-Longmaxi shales in Nanchuan were similar to but no better than those in Jiaoshiba shale gas field.

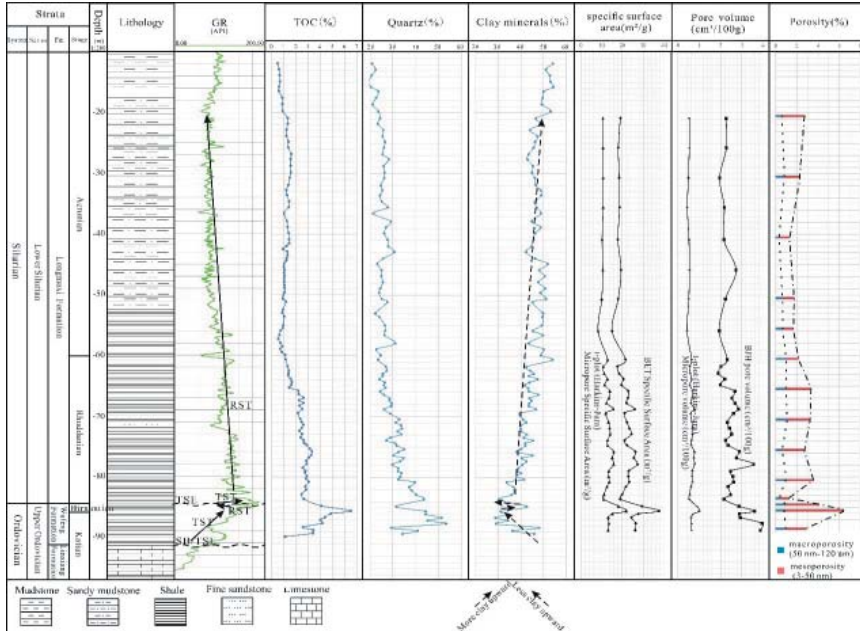


Fig. 1. A comprehensive histogram of Well SY-1 logs, lithology, geochemical parameters and physical properties

From bottom to top, the geochemical and physical properties of the Longmaxi shale varied significantly. In fact, sedimentary environment controls the development of high quality shale in the Wufeng Formation and Longmaxi Formation. High TOC, high quartz and brittle mineral contents, excess silica, high porosity and better kerogen type are mainly developed in TST and the early stages of RST of the Longmaxi shale. Fig. 1 shows that the variation curves of the quartz contents and TOC are basically similar to those of API. While, there is a negative relationship between API values and clay contents. Variations in porosity, especially of micropores, were mainly related to changes in TOC in that high TOC shales usually have high pore volume and high surface area (Fig. 2). Abundant micropores and mesopores could be produced through

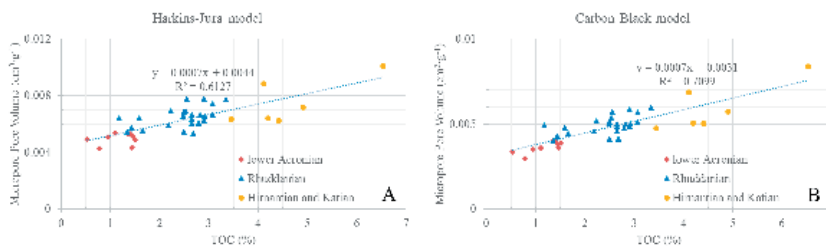


Fig. 2. The relationships of  $V_{mic}$  with TOC for the Longmaxi shale

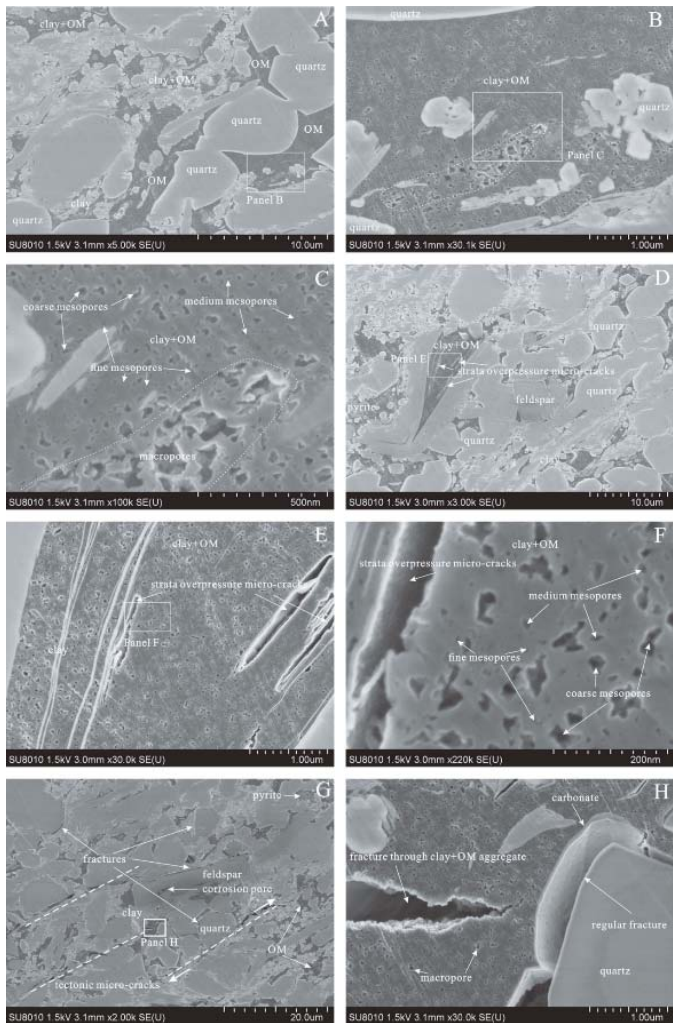


Fig. 3. FE-SEM images of the Longmaxi shale in Hirnantian

both thermogenic cracking of kerogen and secondary cracking of retained bitumen in those high TOC shales (Jarvie et. al., 2007). FE-SEM imaging also suggests that organic matter is rich in micropores and mesopores (Fig. 3).

### References

Guo, T.L., Zhang, H.R., 2014. *Formation and enrichment mode of Jiaoshi shale gas field, Sichuan Basin*. Petroleum Exploration and Development. 41, 31-40.

Jarvie, D.M., Hill, R.J., Ruble, T.E., Pollastro, R.M., 2007. *Unconventional shale-gas systems: The Mississippian Barnett Shale of north-central Texas as one model for thermogenic shale-gas assessment*. AAPG Bull. 91, 475-499.

## Factors affecting chemical composition analysis of gases released by crush methods from rocks

Yan Liu<sup>#</sup>, Liwu Li, Jincan Tuo, Zhongping Li, Yingqin Wu, Hui Yang, Xianbin Wang

Key Laboratory of Petroleum Resources Research, Institute of Geology and Geophysics, Chinese Academy of Sciences, Lanzhou in Gansu Province, China;

<sup>#</sup> yanliu@lzb.ac.cn

Chemical composition analysis of gases released by crush methods is useful to shale-gas assessment and research. Although these methods can avoid the affection of pyrolysis, the released gases will be absorbed on the particles secondarily. So it is necessary to do some experimental research and find out the factors affecting chemical composition analysis of released gases by crushing rocks.

We connected the vacuum crush system with *Swagelok* valves to analysis equipment on line in order to decrease cross contamination (Fig. 1). Both quadrupole mass spectrometer and high sensitive GC were furnished to improve the accuracy by reference gas test. Electromagnetic crush with the frequency 50Hz showed high crush efficiency, and the temperature of the crush pot was tested synchronously.

The chemical composition of released gases varied with the different crush time when the sample and the temperature were kept the same (Fig. 2). The total quantity of gases reached the biggest when crush time was 3min according to this sample. Gases would not increase after more than 3min. For different samples with different physicochemical properties, the crush time for the biggest gas quantity will be different.

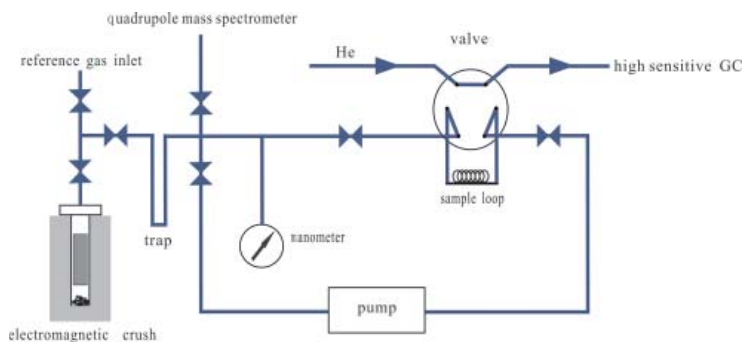


Fig. 1. system of chemical composition analysis of gases released by crush methods from rocks

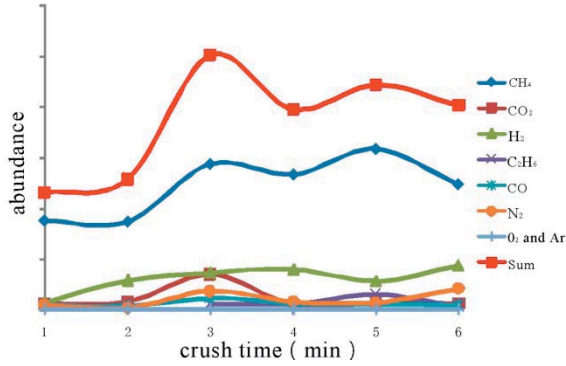


Fig. 2. chemical composition of released gases with different crush time

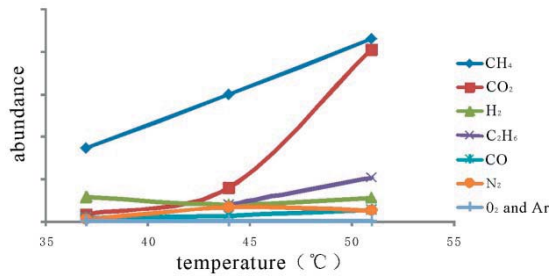


Fig. 3. chemical composition of released gases with different temperature

The chemical composition of released gases varied with the different temperature when the sample and the crush time were kept the same (Fig.3). The results showed that the quantities of methane and carbon dioxide would increase fast when the temperature only had slightly change. We inferred that the secondary absorption between gases and particles was very sensitive to the temperature. So it was necessary to test the temperature synchronously and keep the temperature same during a batch of sample analysis.

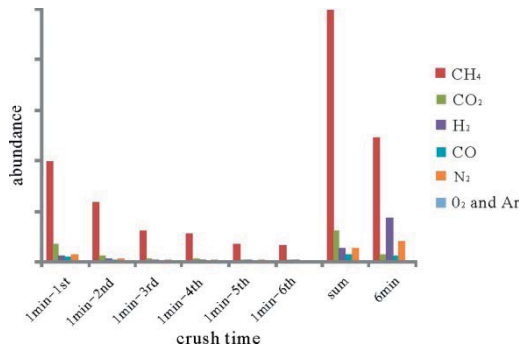


Fig. 4. chemical composition of released gases with different crush mode

The chemical composition of released gases varied with the different crush mode, such as sectionalized crush and consecutive crush, when the sample and the temperature were kept the same (Fig.4). Gases, such as methane, carbon dioxide and carbon monoxide, released by sectionalized crush were more than consecutive crush, while gases, such as hydrogen and nitrogen, showed contrary results. We inferred that pressure decrease might lead to desorbing of polar molecule.

In the following work, the particle size will be tested and the relationship between particle size and chemical composition of released gases will be observed.

This research was supported by Natural Science Foundation of China (No. 41202093, 41272146, 41572136).

### References

- ZHANG T. W., YANG R. S., MILLIKEN K. L., et al. 2014. *Chemical and isotopic composition of gases released by crush methods from organic rich mudrocks*. *Organic Geochemistry* 73, 16-28.
- SUN M. L., CHEN J. F. 1998. *Study on the salt deposit crushing by the vacuum-electricmagnetic- breaker and measurement of noble gas isotope composition*. *Acta Sedimentologica Sinica* 16, 103-106.
- LI L. W., ZHANG M. J., DU L., et al. 2005. *A heated extracting device for analyzing carbon and hydrogen isotopes in rock*. *Rock and Mineral Analysis* 24,135-137.



## Characteristics and origin of desorption gas of the Permian Shanxi Formation shale in the Ordos Basin, China

Zepeng Sun<sup>1,2</sup>, Yongli Wang<sup>1,#</sup>, Zhifu Wei<sup>1,#</sup>,  
Mingfeng Zhang<sup>1</sup>, Gen Wang<sup>1,2</sup>, Liang Xu<sup>1,2</sup>

<sup>1</sup> Key Laboratory of Petroleum Resources, Gansu Province/Key Laboratory of Petroleum Resources Research, Institute of Geology and Geophysics, Chinese Academy of Sciences, Lanzhou 730000, China

<sup>1</sup> University of Chinese Academy of Sciences, Beijing 100049, China

# Corresponding authors: wyll6800@lzb.ac.cn, weizf@lzb.ac.cn

**Keywords:** *Marine-continental transitional shale; Desorbed gas; Gas origin; Shanxi Formation; Ordos Basin*

Shale gas, a significant unconventional hydrocarbon resources, is derived from the biodegradation and/or the thermal maturation of organic matter and stored mainly as free gas, desorbed gas, and slightly dissolved gas (Jarvie et al., 2007; Strapoc et al., 2010). In contrast to shales developed in foreland marine settings in the U.S., China has more types of organic-rich shale according to the depositional environment including marine, transitional and lacustrine shale (Zou et al., 2010). After nearly ten years of exploration, gas has been discovered in multiple shale units in China, including the Paleozoic marine shale in southern Sichuan Basin and the Mesozoic terrestrial shale in the Ganquan Xiasiwan area of Ordos Basin (Dai et al., 2016). There are multiple transitional organic-rich shales that were deposited from the Carboniferous to Permian in northern and northwestern China and on the Yangtze Platform that possess large potentials for shale gas exploration (Jiang et al., 2016). However, owing to the complex geological conditions of marine-continental transitional shale, commercial success has not been achieved in this field (Dang et al., 2016). The Lower Permian Shanxi Formation organic-rich shale in the southeastern margin of Ordos Basin was deposited in a marine-continental transitional environment. This shale, which is usually interlayered with coal beds, provides an ideal formation to investigate the properties of transitional shale gas. A series of studies have been carried out on the gas generation, resource potential and reservoir characterization of marine-continental transitional shale in the southeastern Ordos Basin (Tang et al., 2016; Yan et al., 2015). However, less work has been done and little attention has been paid to the gas content and the geochemical characteristics, as well as the origin and formation mechanism of gases in this field, which limit the understanding of gas generation and exploration. Based on 17 core samples of Shanxi Formation from well SL-1 in the southeastern margin of

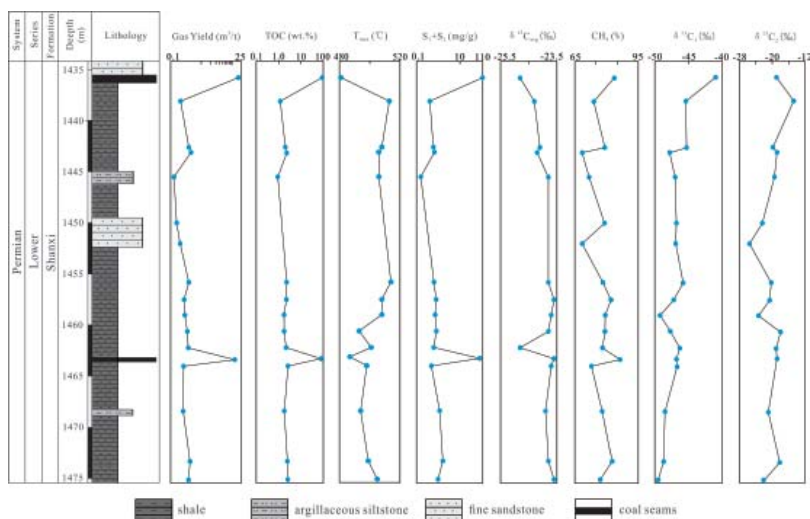


Fig. 1. Petrological characterization and geochemical log column of the drilling section (SL-1 well) in this study.

Ordos Basin, the geochemical characteristics, the content and origin of desorbed gas are analyzed in this paper (Fig. 1). The results show that the shales of Shanxi Formation in the study area are characterized by high TOC values (1.17-2.63%), type III organic matter, and high  $T_{max}$  values (493-514 °C). The desorbed gas content varies from 0.13  $m^3/t$  to 20.36  $m^3/t$  with an average value of 2.39  $m^3/t$ , and shows a positive correlation with TOC contents. The gases are dominated by methane (69.47-93.12%), with small amounts of ethane (0.01-0.10%). The  $\delta^{13}C_1$  values range from -49.5‰ to -41.0‰ and the  $\delta^{13}C_2$  values range from -25.5‰ to -14.7‰. In addition, it is believed that the gases released from the Shanxi Formation core samples are of thermogenic origin and are

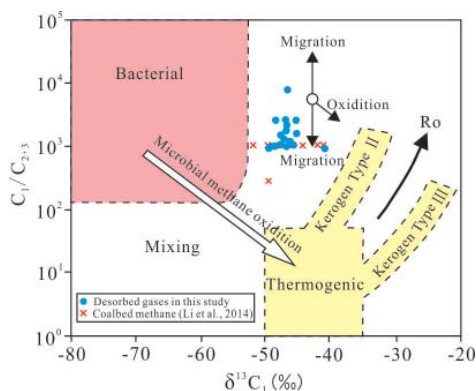


Fig. 2.  $C_1/C_{2+3}$  versus  $\delta^{13}C_1$  for gases from the Shanxi Formation core samples

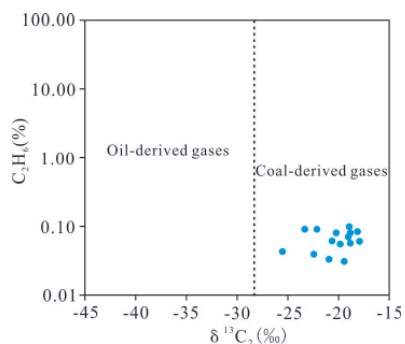


Fig. 3. Plot of  $\delta^{13}\text{C}_2$  versus  $\text{C}_2\text{H}_6$  of desorbed gases from the Shanxi Formation

coal-derived by the Whiticar chart board (Fig. 2) and the diagram of  $\text{C}_2\text{H}_6$  versus  $\delta^{13}\text{C}_2$  (Fig. 3).

### References

- DAI J. X., ZOU C. N., DONG D. Z., NI Y. Y., WU W., GONG D. Y., WANG Y. M., HUANG S. P., HUANG J. L., FANG, C. C. & LIU D. 2016. *Geochemical characteristics of marine and terrestrial shale gas in China*. *Marine and Petroleum Geology* 76, 444-463.
- DANG W., ZHANG J. C., TANG X., CHEN Q., HAN S. B., LI Z. M., DU X. R., WEI X. L., ZHANG, M. Q., LIU J., PENG J. L. & HUANG Z. L. 2016. *Shale gas potential of Lower Permian marine-continental transitional black shales in the Southern North China Basin, central China: Characterization of organic geochemistry*. *Journal of Natural Gas Science and Engineering* 28, 639-650.
- JARVIE D. M., HILL R. J., RUBLE T. E. & POLLASTRO R. M. 2007. *Unconventional shale-gas systems: The Mississippian Barnett Shale of north-central Texas as one model for thermogenic shale-gas assessment*. *AAPG Bulletin* 91, 475-499.
- JIANG S., XU Z. Y., FENG Y. L., ZHANG J. C., CAI D.S., CHEN L., WU Y., ZHOU D. S., BAO S. J. & Long S. X. 2016. *Geologic characteristics of hydrocarbon-bearing marine, transitional and lacustrine shales in China*. *Journal of Asian Earth Sciences* 115, 404-418.
- STRAPOC D., MASTALERZ M., SCHIMMELMANN A., DROBNIK A. & HASENMUELLER N. R. 2010. *Geochemical constraints on the origin and volume of gas in the New Albany Shale (Devonian-Mississippian), eastern Illinois Basin*. *AAPG Bulletin* 94, 1713-1740.
- TANG X., ZHANG J.C., DING W.L., YU B.S., WANG L., MA Y.L., YANG Y.T., CHEN H.Y., HUANG H. & ZHAO P.W. 2016. *The reservoir property of the Upper Paleozoic marine-continental transitional shale and its gas-bearing capacity in the Southeastern Ordos Basin*. *Earth Science Frontiers* 23, 147-157.
- YAN D. Y., HUANG W. H. & ZHANG J. C. 2015. *Characteristics of marine-continental transitional organic-rich shale in the Ordos Basin and its shale gas significance*. *Earth Science Frontiers* 22, 197-206.
- ZOU C. N., DONG D. Z., WANG S. J., LI J. Z., LI X. J., WANG Y. M., LI D. H. & CHENG K. M. 2010. *Geological characteristics, formation mechanism and resource potential of shale gas in China*. *Petroleum Exploration and Development* 37, 641-653.



## Isotopic and Molecular Compositions of Shale Gas from the Silurian Longmaxi Shale of the Sichuan Basin: maturation or accumulation control?

Yunpeng Wang<sup>1#</sup>, Lingling Liao<sup>1</sup>, Chensheng Chen<sup>1</sup>, Shuyong Shi<sup>1</sup>,  
Shengfei Qin<sup>2</sup>, Ziqi Feng<sup>2</sup>, Jinxing Dai<sup>2</sup>

<sup>1</sup> State Key Laboratory of Organic Geochemistry, Guangzhou Institute of Geochemistry, Chinese Academy of Sciences, 511 Kehua Street, Wushan Road, Tianhe District, Guangzhou, GD 510640, PR China

<sup>2</sup> Research Institute of Petroleum Exploration and Development, PetroChina, 20 Xueyuan Road, Beijing 100083, China

# corresponding author: wangyp@gig.ac.cn

Sichuan Basin is a primary gas-producing area in China. The black shale deposited in marine environment of Upper Ordovician Wufeng Formation and Lower Silurian Longmaxi Formation (O3w-S1l) is the potential source rocks of shale gas in Sichuan Basin. Till to now, China has begun exploiting shale gas in Jiaoshiba, Changnin, Weiyuan, and also drilled and evaluated in some out-basin areas such as Dingshan and Heye areas. In general, the Silurian Longmaxi shale gas exhibits the unique geochemical characteristics, such as high methane, low C2+ gases, higher  $\delta^{13}\text{C}_1$  and relatively lower  $\delta^{13}\text{C}_2$ , and the hydrogen isotopes of gases also show special trends. In the above gases fields and prospecting areas, isotopic and molecular compositions of shale gas also show different variations. What is the main control of compositions of shale gas: maturation or accumulation? This is a very important question for shale gas study in high-maturated marine shale area of southern China.

In this paper around 40 samples of shale gas was taken and analyzed. The isotopic and molecular compositions of shale gas were measured. Combining the previous publication of Dai et al., (2014), the following characteristics of geochemical compositions of shale gas can be observed: (1) the shale gas is mainly composed of methane with a wide variation of gas wetness (0.29 to 0.74%). The concentration of C2 and C3 are very low. The main inorganic gases are N2 and CO2 without H2S. (2) The carbon isotopic compositions of all the alkane gases are characterized by  $\delta^{13}\text{C}_1 > \delta^{13}\text{C}_2$  showing a typical reversal phenomenon. Relationship between  $\delta^{13}\text{C}_2$  values and wetness show a special “roll-over” pattern. (3) Compare with the shale gas, the Longmaxi shale gases are located the area of the second turning point after the “roll-over” (Fig. 1). The reversal and “roll-over” of carbon isotopes are caused by the higher maturation of the shale gas in this area. (4) Interesting thing is that Longmaxi shale gases show a typical “roll-over”

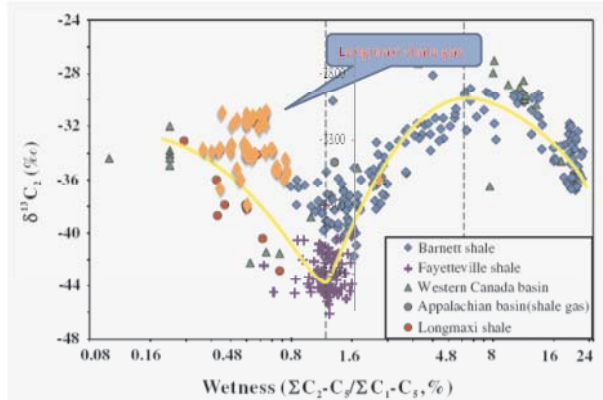


Fig. 1. The plot between the  $\delta^{13}C_1$  and wetness values based on the data from typical marine shale gas in China, Canada and America in which a typical “roll-over” could be observed in  $\delta^{13}C_2$  values with the increase of wetness values after Dai et al (2014)

for gas hydrogen isotopes. In Fig. 2, the distribution of Longmaxi shale gases along the trend of maturation in “roll-over” variations for gas hydrogen isotope while it deviates the trend of maturation in “roll-over” for gas carbon isotopes.

For better recovering the history of gas generation and isotopic evolution, we firstly built the basin model in five typical areas using the representative wells and PetroMod software. The burial and thermal histories, which control the timing of hydrocarbon generation and expulsion as well as gas isotopes, are the most important parameters for source rock evaluation and hydrocarbon dynamic accumulation in oil-gas-bearing basin. The detailed construction procedures can be found in Yao et al. (2016a and 2016b). For studying the maturation trends of the gas isotopes, we found that the carbon isotopes of both C1 and C2 are controlled by source rock maturation while the hydrogen shows similar trends. However, we found that the gas wetness show great variations in

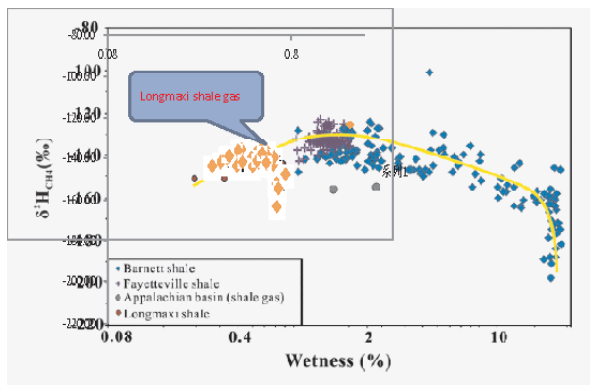


Fig. 2. The plot between the  $\delta^2H_{CH_4}$  and wetness values based on the data from Longmaxi shale gas in southern Sichuan Basin and shale gas in America after Dai et al (2014)

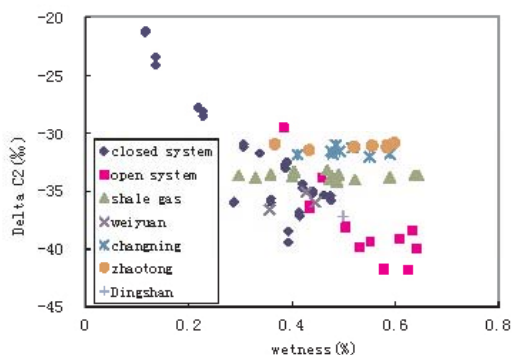


Fig. 3. The plot between the  $\delta^{13}C_2$  and wetness values based on the pyrolysis results and shale gas compositions of Longmaxi shale

one gas field even they show similar maturities, which are mainly controlled by gas accumulation.

And we also conducted a kinetic experiment for deriving kinetics of gas generation and isotopes. A low matured marine shale sample of Middle Ordovician Pingliang formation in Northern China was used as an analogue to conduction the pyrolysis using gold tube system. From Fig. 3, it is clear that the Longmaxi shale gas are mainly located the transitional zone of closed system and open one, but showing great variations along wetness direction. It indicates that as the accumulation process changes, the shale gas will show great variations of gas wetness, which also controls both carbon and hydrogen isotopes to some extent. One obvious fact is that Longmaxi shale gas shows great variation of carbon isotope than hydrogen one and methane carbon isotope became heavier and heavier as the maturation while ethane carbon isotope ceased at the secondary cracking window.

**Acknowledgments:** The Strategic Priority Research Program of the Chinese Academy of Sciences (XDB10010300), NSFC Project (41372137), CNPC-CAS strategic cooperation project (No. RIPED-2015-JS-255) and GIG 135 project (No. 135TP201602) are acknowledged for the financial supports.

## References

- Jinxing Dai, Caineng Zou, Shimeng Liao, Dazhong Dong, Guoyi Hu, *Geochemistry of the extremely high thermal maturity Longmaxi shale gas, southern Sichuan Basin*, Organic Geochemistry, 2014, Volume 74, Pages 3-12.
- Xiulian Yao, Yunpeng Wang, *Assessing Shale Gas Resources of Wufeng-Longmaxi shale (O3w-S11) in Jiaoshiba area, SE Sichuan (China) using PetroMod: Burial and Thermal Histories*, Petroleum Science and Technology, 2016, 34 (11-12): 1000-1007.
- Xiulian Yao, Yunpeng Wang, *Assessing Shale Gas Resources of Wufeng-Longmaxi Shale (O3w-S11) in Jiaoshiba area, SE Sichuan (China) using PetroMod: Gas Generation and Adsorption*, Petroleum Science and Technology, 2016, 34 (11-12): 1008-1015.



## **9. Techniques of measurements**





## **Testing device for radon migration experiments – the construction and preliminary results**

Bonczyk M.<sup>#</sup>, Chałupnik S., Smoliński A., Wysocka M., Howaniec N.

Silesian Centre for Environmental Radioactivity  
Central Mining Institute, Katowice, Poland  
<sup>#</sup> mbonczyk@gig.eu

The main goal of the research activity is to estimate the time and diffusion length for radon in the geological structures of Upper Silesian Coal Basin (USCB) and advection of Rn-222 with other gases like carbon dioxide or methane, occurring in the Carboniferous strata in USCB. This knowledge will support the precision of the assessment of radon hazard in dwellings. Moreover, it should give an answer to some questions, related to the radon migration issues – if the results of measurements of an adhesive transport of radon with other gases in the strata could be applied for the prediction of geodynamic phenomena in the mining areas like tremors and outbursts.

For this purpose a special device has been designed and constructed. This device consists of a container for the sample of the coal, mineral or rock and two reservoirs – inlet and outlet ones. The gas (air, carbon dioxide, methane) with radon is introduced into inlet reservoir, while the content of marker gases and radon is monitored in the outlet reservoir. The device has been built and preliminary experiments will be started soon. In the literature, there are only rare results of such investigations, while our previous research in USCB region showed some correlation between sudden changes of radon level and geodynamic events. Therefore we would like to use results of our investigations for the improvement of the models of these phenomena.



## **Comparative study on the gas released from rock samples by pyrolysis using mass spectrometry**

Li Du<sup>#</sup>, Xuan Fang

<sup>1</sup> Key Laboratory of Petroleum Resources, Gansu Province/Key Laboratory of Petroleum Resources Research, Institute of Geology and Geophysics, Chinese Academy of Sciences, Lanzhou 730000, China;  
<sup>#</sup> Corresponding author: storm1983hui@163.com

### **Research Purpose**

In order to understand the experiences of adsorption hydrocarbon in the process of Calcite samples which coexistence with dense sandstone, we carried out the segmented heat simulation experiment. So we can restore and research the geological background of the sample.

### **Sample background**

5 Calcite samples (60 ~ 80 mesh), collected from five different formations of Devonian in Mohe Basin.

### **Experiment condition**

Gas chromatography – Carbon isotope mass spectrometry system (GC/C/delta Plus XP) is a new type instrument, which made by ThermoFinnigan company. Gas chromatography conditions: HP - 5 quartz capillary chromatographic column (60 m × 0.25mm × 0.32 mm), temperature program: keep 80 °C for 5 min, then warming up to 300 °C by 3 °C/ min, and then keep 300 °C for 30 min; Carrier gas: high purity He (99.999%). Carbon isotope ratio is corrected by PDB.

MAT271 Gas isotope mass spectrometer is developed by the U.S. Company of Finnigan MAT. It is a kind of magnetic mass spectrometer. The ionization source is electron impact (EI) type. The detector is Faraday cup. The scan range of MAT 271 is 1 ~ 350 amu (atomic mass units). Linear range is no more than 3% within three orders of magnitude. Detection range of routine concentration is 0.0001 ~ 100%. The instrument, with high sensitivity ( $10^{-3}$  A/Torr) and good linear range, is suitable for gas chemical and isotopic composition analysis.

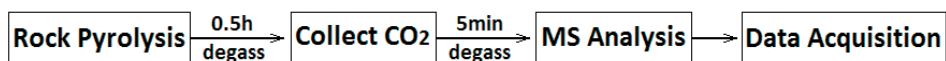


Fig. 1. Calcite samples pyrolysis experiment and gas analysis

## Results

Experimental methods and process are described in Fig. 1. The analysis results are list in Table 1, Table 2 and Table 3.

Table 1. Gas production rate of Calcite samples by heating with different temperatures table ( $\mu\text{L/g}$ )

Samples	200 °C			300 °C		
	$\text{CH}_4$	$\text{C}_2\text{H}_6$	$\text{C}_3\text{H}_8$	$\text{CH}_4$	$\text{C}_2\text{H}_6$	$\text{C}_3\text{H}_8$
Fang-1	0.02	0.18	0.00	0.13	0.36	0.02
Fang-2	0.03	0.44	0.02	0.19	1.14	0.05
Fang-3	0.02	0.17	0.00	0.13	0.01	0.00
Fang-4	0.00	0.00	0.00	0.09	0.73	0.04
Fang-5	0.05	0.14	0.03	0.22	0.01	0.17
Samples	400 °C			500 °C		
	$\text{CH}_4$	$\text{C}_2\text{H}_6$	$\text{C}_3\text{H}_8$	$\text{CH}_4$	$\text{C}_2\text{H}_6$	$\text{C}_3\text{H}_8$
Fang-1	0.25	0.08	0.08	1.21	0.06	0.05
Fang-2	0.32	0.31	0.23	1.29	0.12	0.33
Fang-3	0.44	0.14	0.11	1.02	0.1	0.09
Fang-4	0.23	0.04	0.06	1.57	0.04	0.02
Fang-5	0.58	0.16	0.32	3.46	0.31	0.21

Table 2. Gas production rate of Calcite samples at 500 °C

Samples	Content/ $\mu\text{L}$	$\text{CH}_4/\%$	$\text{C}_2\text{H}_6/\%$	$\text{C}_3\text{H}_8/\%$
Fang-1	70.26	2.99	0.25	0.14
Fang-2	84.74	3.11	0.19	0.05
Fang-3	62.89	3.09	0.21	0.1
Fang-4	53.16	2.31	0.08	0.08
Fang-5	91.58	5.4	0.51	0.43

Table 3. Carbon isotope composition of Calcite adsorbed gas (500 °C)

Samples	$\delta^{13}\text{CH}_4$	$\delta^{13}\text{C}_2\text{H}_6$	$\delta^{13}\text{C}_3\text{H}_8$
Fang-1	-39.85	-30.97	-33.41*
Fang-2	-39.86	-30.25	-29.51
Fang-3	-38.84	-29.81	-28.65
Fang-4	-45.77	-30.62	-30.59 *
Fang-5	-39.32	-31.43	-31.69 *

## Conclusions

The five Calcite samples were carried pyrolysis experiments respectively. The released gases were analysed by MAT-271 mass spectrometer for chemical composition and by GC/C/delta Plus XP for carbon isotope composition. For Table 1, we found that Calcite samples gradually release hydrocarbon gas in the process of heat, and the volume increase with temperature rising, which prove that this sample adsorbed hydrocarbon fluid in the process of geological formation. Table 2 showed that the gas released from the five samples have a common rule, methane content is the highest, the volume of n-hexane and propane present decrease trend. Only when heating temperature reached 500 °C, all the 5 Calcite samples can release enough methane gas for carbon isotope analysis (Table 3). From the carbon isotope data we can determine the origin of the sample and geological background.



## Gas chromatography combined mass spectrometry for the chemical composition of gases from rock samples

Li Liwu<sup>1#</sup>, Cao Chunhui<sup>1</sup>, Li Zhongping<sup>1</sup>,  
Xing Lantian<sup>1</sup>, Zhang Mingjie<sup>2</sup>, Wang Xianbin<sup>1</sup>

<sup>1</sup> Key Laboratory of Petroleum Resources, Gansu Province/ Key Laboratory of Petroleum Resources Research, Institute of Geology and Geophysics, CAS, Lanzhou 730000, PR China

<sup>2</sup> School of Earth Sciences, Lanzhou University, Lanzhou 730000, China

# corresponding author: llwu@lzb.ac.cn

The chemical composition of gases trapped in rocks is important information sought in a wide variety of earth science studies, therefore gases are usually extracted from rock samples and analyzed. Gas chromatography and mass spectrometry are the two methodologies most frequently used for analysis of gases extracted from rock samples, but the two methodologies scarcely worked together in the past. For gas chromatography, the mainly used detector is thermal conductivity detector (TCD) because of its sense for all kinds of gas, while the sensitivity of TCD is not enough to test trace gases extracted from some rock samples. Therefore, we build a new device, with which gases extracted from rock samples are test by gas chromatograph (GC) and mass spectrometer (MS) together, and a pulsed discharge detector (PDD) is used as the detector of GC because PDD is sensible for almost all kinds of gas and its sensitivity is much higher than that of TCD. In this device, a rock sample can be heated or crushed in vacuum to release gases from. The pressure of gases released from rock samples is measured by a diaphragm gauge. We've investigated some samples, such as serpentinized peridotites in Inner Mongolia, volcanic rocks from Wudalianchi, shale rocks in Sichuan basin and reservoir rocks from Song Liao basin. The chemical contents of H<sub>2</sub>, CH<sub>4</sub>, H<sub>2</sub>O, CO, N<sub>2</sub>, C<sub>2</sub>H<sub>4</sub>, C<sub>2</sub>H<sub>6</sub>, O<sub>2</sub>, H<sub>2</sub>S, Ar, CO<sub>2</sub>, C<sub>3</sub>H<sub>8</sub>, COS and SO<sub>2</sub> could be measured at once.

Figure 1 and 2 are shown the results of a serpentinized peridotite sample gathered in Inner Mongolia.

Two columns are used in the GC. No absorbent is in GC sample loop. To show the test ability, only 0.01g rock sample was used in figure 1 and 2. Some gases, such as CO, C<sub>2</sub>H<sub>4</sub> and SO<sub>2</sub>, are not existed in figure 1. SO<sub>2</sub> is found at 1000 in figure 2. Water can easily be absorbed by pipeline; the device here is not suitable for measuring H<sub>2</sub>O content when the water partial pressure is high. In this case, Raman spectroscopy or Fourier transformed infrared spectroscopy is recommended for measuring H<sub>2</sub>O content.

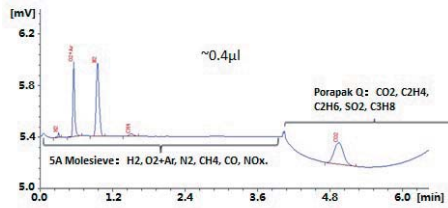


Fig. 1. The gas chromatography of gases released from a 0.01g serpentinized peridotite sample at 200 °C, the total gas quantity is about 0.4mm<sup>3</sup>(at room temperature and standard pressure)

Acknowledgements: This study is supported financially by NSF of China (No.41473062) and the Key Laboratory Project of Gansu Province (Grant No.1309RTSA041)

### Reference

Klein, F., Bach, W., McCollom, T. M., 2013. *Compositional controls on hydrogen generation during serpentinization of ultramafic rocks*. *Lithos* 178: 55 - 69.

Wang, X. B., Ouyang, Z. Y., Zhuo, S. G., et al., 2014. *Serpentinization, abiogenic organic compounds, and deep life*. *Science China (Earth Sciences)* (05): 878-887.

Pearson, D. G., Brenker, F. E., Nestola, F., et al., 2014. *Hydrous mantle transition zone indicated by ringwoodite included within diamond*. *Nature* 507: 221-224.

Doucet, L. S., Peslier, A. H., Ionov, D. A., et al., 2014. *High water contents in the Siberian cratonic mantle linked to metasomatism: An FTIR study of Udachnaya peridotite xenoliths*. *Geochimica et Cosmochimica Acta* 137: 159-187.

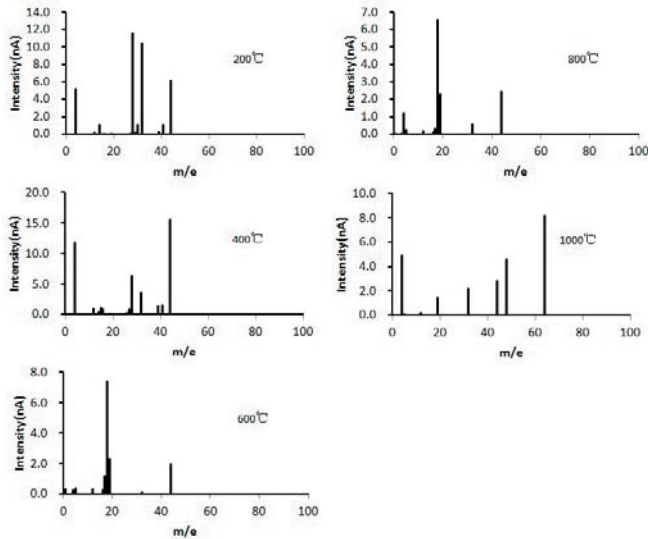


Fig. 2. The mass spectrometry of gases released from a 0.01g serpentinized peridotite sample by stepwise heating. Large amount of water is released at 600 and 800 °C



## Natural and artificial constraints to detectability of anomalous Thermal Infrared Signals by satellite techniques

Martinelli G.<sup>1#</sup>, Dadomo A.<sup>2</sup>

<sup>1</sup> ARPAE Environmental Protection Agency of Emilia Romagna Region, Via Amendola 2, 42100 Reggio Emilia, Italy

<sup>2</sup> Geoinvest, Via della Conciliazione 45/A, 29100 Piacenza, Italy

# corresponding author: giovanni.martinelli15@gmail.com

**Keywords:** *Greenhouse natural gas emissions, Greenhouse artificial gas emissions, CO<sub>2</sub>, TIR, satellite techniques*

Satellite techniques have been widely utilized to detect possible increase of atmospheric temperature due to greenhouse effects induced by CO<sub>2</sub> or CH<sub>4</sub> generated by geological processes. These signals have been widely utilized to detect tectonically active processes (e.g. Tramutoli et al., 2013 and references therein). These processes are usually monitored by GPS or by satellite-based techniques like InSAR. Significant signals have been recorded in many places of the world after strong earthquakes. Only in a few cases similar signals were detected before seismic events due to the relatively low sensitivity of equipments (Roeloffs, 2006; Cicerone et al., 2009) or to unsuitability of monitored areas (Martinelli and Dadomo, 2017). Satellite techniques able to identify TIR or AIRS signals (Cui et al., 2013) are able, in principle, to identify weak degassing activities linked to tectonic processes and could contribute to the geochemical monitoring of wide areas. Part of these signals has been detected before mainshocks and could be related to tectonic pumping phenomena induced by aseismic slip (e.g. Johnston and Linde, 2002) or by seismic slip eventually induced by fluctuations in minor seismicity. The satellite monitoring of geochemical parameters could offset the relatively poor sensitivity of GPS techniques. Anyway CO<sub>2</sub> and CH<sub>4</sub> artificially injected in the atmosphere by human activities could seriously hamper correct data interpretation in densely populated areas. The knowledge of natural and artificial constraint factors may strongly contribute to a better understanding of geochemical data recorded by satellite techniques. Researches oriented to earthquake forecasting could benefit by gas geochemical monitoring of large areas once removed possible sources of error.

### References

Cicerone R.D., Ebel J.E., Britton J. 2009, *A systematic compilation of earthquake precursors*. *Tectonophysics*, 476, 371-396.

Cui Y., Du J., Zhang D., Sun Y. (2013) Anomalies of total column CO and O<sub>3</sub> associated with great earthquakes in recent years. *Natural Hazards and Earth System Sciences*, 13, 2513-2519.

Johnston M., Linde A. 2002. *Implications of crustal strain during conventional slow and silent earthquakes*. In: Lee WHK et al. (Eds) *International Handbook for Earthquake and Engineering Seismology*, Part A. International Geophysical Services, 81, 589-605, Elsevier New York.

Martinelli G., Dadomo A. 2017 Factors constraining the geographic distribution of earthquake geochemical and fluid-related precursors. *Chemical Geology*, DOI: <http://dx.doi.org/10.1016/j.chemgeo.2017.01.006>

Roeloffs E. 2006. *Evidence for Aseismic Deformation Rate changes Prior to Earthquakes*. *Annual Review of Earth and Planetary Sciences*, 34, 591-627.

Tramutoli V., Aliano C., Corrado R., Filizzola C., Genzano N., Lisi M., Martinelli G., Pergola N. 2013. *On the possible origin of thermal infrared radiation (TIR) anomalies in earthquake-prone areas observed using robust satellite techniques (RST)*, *Chemical Geology*, 339, 157-168.



## Preliminary research on the effects of microbial methane oxidation on drill-core head-space gas analysis

Kazuya Miyakawa<sup>1#</sup>, Fumiaki Okumura<sup>2</sup>

<sup>1</sup> Horonobe Underground Research Center, Japan Atomic Energy Agency, Hokushin 432-2, Horonobe-cho, Hokkaido 098-3224, JAPAN

<sup>2</sup> JAPEx Research Center, Japan Petroleum Exploration Co., Ltd, Chiba, Japan

\* Corresponding author: miyakawa.kazuya@d.nagoya-u.jp

**Keywords:** head-space gas, carbon isotope ratio, microbial methane oxidation

### Introduction

Investigations into the origin of deep hydrocarbons is an important aspect of exploring resources and understanding geological environments. In this investigation, gases adsorbed on rock fragments or bore cores were studied by head-space gas analysis (e.g., Schoell, 1983). Gas samples from the Horonobe area, Hokkaido, were collected using IsoJar<sup>TM</sup> plastic containers (Funaki et al., 2012). Head-space analyses of gases dissolved in groundwater were also undertaken, by using an evacuated-vial (EV) method (Miyakawa et al., 2017). Measured  $\delta^{13}\text{C}_{\text{CH}_4}$  and  $\delta^{13}\text{C}_{\text{CO}_2}$  ratios for gases from the Horonobe area are shown in Fig. 1. Differences between data reported by Funaki et al. (2012) and Miyakawa et al. (2017) have been attributed to microbial methane oxidation.

In this study, the effects of methodology, sampling procedures, and sample storage were investigated as possible causes of these differences. Deep-bore gases from the Horonobe area were sampled by using the methods of Funaki et al. (2012) and Miyakawa et al. (2017). The effects of sampling method on carbon isotope ratios and isotopic fractionation were investigated. Finally, head-space gas analysis techniques are summarized.

### Methods

#### Sampling location

The Horonobe area is located in northwestern Hokkaido, in a Neogene–Quaternary sedimentary basin. Since August 2006, the Japan Atomic Energy Agency (JAEA) has been excavating an underground research laboratory (URL) for a generic research associated with development of technologies to be used in the geological disposal

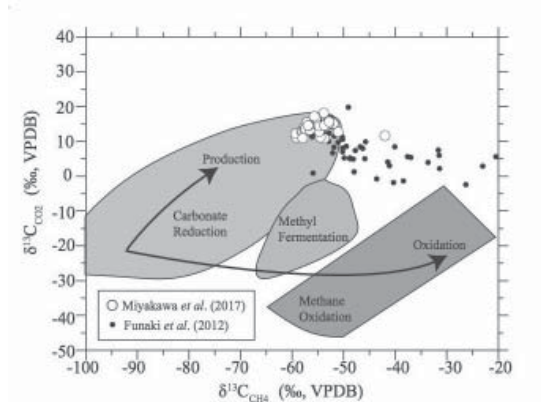


Fig. 1. Plot of  $\delta^{13}\text{C}_{\text{CH}_4}$  vs  $\delta^{13}\text{C}_{\text{CO}_2}$  in co-existing gases, showing fields relating to different gas sources, and isotopic shifts resulting from production and oxidation (adapted from Whiticar, 1999)

of radioactive waste. The associated high-pressure boreholes have steel casings, with valves allowing sampling from multiple depths or zones (e.g., Mezawa et al., 2016). In this study, groundwater was sampled from boreholes drilled in the 250 m and 350 m galleries where the surrounding geology is of the Wakkanai Formation, which comprises Neogene siliceous mudstone.

### Sampling method

The IsoJar™ (Isotech Laboratories and Humble Instruments, USA) technique involved approximately 300–400 g of rock fragments or bore cores, crushed to pieces roughly 30–50 mm diameter, and placed in an IsoJar™ with 250–300 g of groundwater or drilling fluid. In the URL, shallow groundwater (53.5–64.5 m) was used as drilling fluid. The rock fragments were obtained from the 350 m gallery, and the bore cores were from ~400 m depth.  $\text{HgCl}_2$ -saturated or 10% benzalkonium chloride (BKC) solution (~1 ml of either) was poured into the jars to suppress microbial activity, and the jars

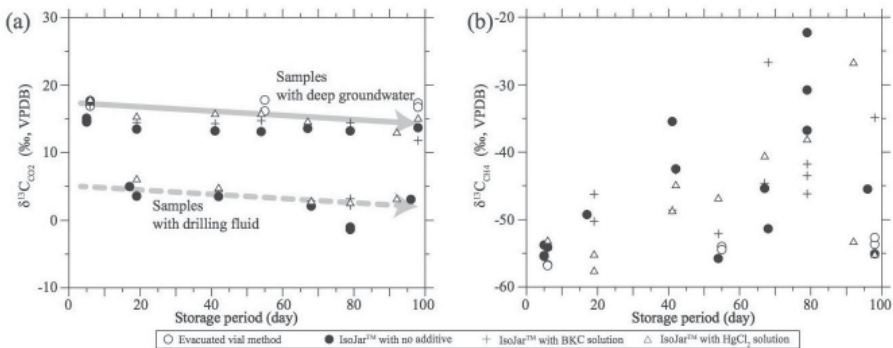


Fig. 2. Time variation of (a)  $\delta^{13}\text{C}_{\text{CO}_2}$  and (b)  $\delta^{13}\text{C}_{\text{CH}_4}$  after sampling

sealed with an air head-space. The samples were kept in the dark at room temperature for 5 to 98 days before analysis.

The EV sampling procedure involved preliminary evacuation of septum-topped 50 ml glass vials containing ~1 ml phosphoric acid (85 wt%; to remove any inorganic carbon as CO<sub>2</sub>). Groundwater (15–30 ml) was introduced with syringe needle, through a 0.22 μm membrane filter. Samples were kept in the dark at room temperature for 5 to 98 days, after which ultra-pure He was added by syringe to atmospheric pressure, the sample was left to stand overnight (for gas exchange equilibrium between head-space and dissolved gases), and the composition of the head-space gas was determined.

### Analytical method

Concentrations of O<sub>2</sub>, N<sub>2</sub>, CO<sub>2</sub>, CH<sub>4</sub>, C<sub>2</sub>H<sub>6</sub>, C<sub>3</sub>H<sub>8</sub>, i-C<sub>4</sub>H<sub>10</sub>, n-C<sub>4</sub>H<sub>10</sub>, i-C<sub>5</sub>H<sub>12</sub>, n-C<sub>5</sub>H<sub>12</sub>, and n-C<sub>6</sub>H<sub>14</sub> were determined by gas chromatography (GC) by using a GC7890A Valve System (Agilent Technologies, USA). Carbon isotopic ratios ( $\delta^{13}\text{C}_{\text{CH}_4}$  and  $\delta^{13}\text{C}_{\text{CO}_2}$ ) were determined by GC combustion isotope-ratio mass spectrometry (GC–IRMS), by using an IsoPrime GC–MS system (GV Instruments, UK). Isotopic ratios are expressed in the usual VPDB  $\delta$  notation. Details of the GC and GC–IRMS procedures can be found in Waseda and Iwano (2008).

### Results

Time variations of  $\delta^{13}\text{C}_{\text{CO}_2}$  and  $\delta^{13}\text{C}_{\text{CH}_4}$  ratios are shown in Fig. 2a and 2b, respectively. The  $\delta^{13}\text{C}_{\text{CO}_2}$  ratios (Fig. 2a) of gases from all IsoJar<sup>TM</sup> samples decreased slightly as time increased, and showed different trends for deep-groundwater (solid arrow) and drilling-fluid (dashed arrow) samples. Because amounts of CO<sub>2</sub> dissolved in water are much larger than those of CO<sub>2</sub> adsorbed onto cores, the  $\delta^{13}\text{C}_{\text{CO}_2}$  ratios represent dissolved gases in water. The  $\delta^{13}\text{C}_{\text{CH}_4}$  ratios (Fig. 2b) of IsoJar<sup>TM</sup> samples increased markedly with time, and fluctuated by more than 30‰ after 80 days. Because amounts of CH<sub>4</sub> dissolved in water are smaller than those of adsorbed CH<sub>4</sub>, the  $\delta^{13}\text{C}_{\text{CH}_4}$  ratios obtained by the IsoJar<sup>TM</sup> technique represent adsorbed gases onto cores. Relatively large amounts of CO<sub>2</sub> also diminish an isotope fractionation of  $\delta^{13}\text{C}_{\text{CO}_2}$  although  $\delta^{13}\text{C}_{\text{CH}_4}$  ratios are easily affected by an isotope fractionation due to small amount of CH<sub>4</sub>.

The  $\delta^{13}\text{C}_{\text{CO}_2}$  and  $\delta^{13}\text{C}_{\text{CH}_4}$  ratios for all EV gases were relatively constant although the  $\delta^{13}\text{C}_{\text{CH}_4}$  ratios showed small variation less than 4.2‰ (Fig. 2), which are good agreement with those by Miyakawa et al. (2017). IsoJar<sup>TM</sup> samples with deep groundwater stored for less than one week showed almost the same values of EV samples.

### Discussions and conclusion

A bivariate plot of  $\delta^{13}\text{C}_{\text{CH}_4}$  vs  $\delta^{13}\text{C}_{\text{CO}_2}$  is shown in Fig. 3. IsoJar<sup>TM</sup> samples stored for longer than one week and those with drilling fluid showed two trends as in Fig. 2a, which suggests that both trends indicate isotopic fractionation by methane oxidation. Variations in  $\delta^{13}\text{C}_{\text{CH}_4}$  and  $\delta^{13}\text{C}_{\text{CO}_2}$  ratios reported by Funaki et al. (2012) can be explained

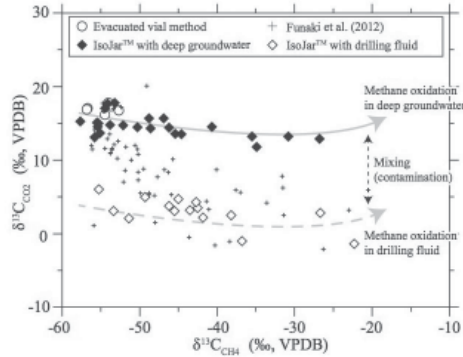


Fig. 3. Plot of  $\delta^{13}\text{C}_{\text{CH}_4}$  vs  $\delta^{13}\text{C}_{\text{CO}_2}$  in co-existing gases, as obtained in this study

by the mixing of the two trends shown in Fig. 3, indicating effects of both microbial activity and contamination of drilling fluid.

Despite the addition of BKC and  $\text{HgCl}_2$  solutions, significant isotopic fractionation was observed in the IsoJar™ samples, especially in the  $\delta^{13}\text{C}_{\text{CH}_4}$  ratios which represent adsorbed gases onto cores, suggesting that the amounts of additives used were insufficient to suppress microbial activity. To obtain original *in situ* values using IsoJar™ containers, it is therefore necessary to analyze immediately after sampling cores with groundwater, not with drilling fluid.

**Acknowledgement:** The author is grateful to A. Waseda (JAPEx), H. Funaki, E. Ishii (JAEA), T. Ishikawa and Y. Kitagawa (Mitsubishi Materials Techno: MMT) for providing helpful information regarding sampling methods.

## References

- Funaki H., Ishiyama K., Waseda A., Kato S. & Watanabe K. 2012. *Molecular and carbon isotope compositions of hydrocarbon gas in Neogene sedimentary rocks in Horonobe area, northern Hokkaido, Japan*. Journal of Geography (Chigaku Zasshi) 121, 929–945.
- Mezawa T., Miyakawa K., Sasamoto H. & Soga K. 2016. *Development and improvement of geochemical monitoring system for groundwater installed in the 350 m gallery of the Horonobe underground research laboratory*. JAEA-Technology 2016-003, Japan Atomic Energy Agency.
- Miyakawa K., Ishii E., Hirota A., Komatsu D. D., Ikeya K. & Tsunogai U. 2017. *The role of low-temperature organic matter diagenesis in carbonate precipitation within a marine deposit*. Applied Geochemistry 76, 218–231.
- Waseda A. & Iwano H. 2008. *Characterization of natural gases in Japan based on molecular and carbon isotope compositions*. Geofluids 8, 286–292.
- Whiticar M. J. 1999. *Carbon and hydrogen isotope systematics of bacterial formation and oxidation of methane*. Chemical Geology 161, 291–314.
- Schoell M. 1983. *Isotope techniques for tracing migration of gases in sedimentary basins*. Journal of the Geological Society of London 140, 414–422.



## Depth oriented measurement of $^{222}\text{Rn}$ and $\text{CO}_2$ concentration and fluxes with a novel measuring device and a modular probe system

Sauer, U.<sup>1</sup>; Streil, T.<sup>2#</sup>; Borsdorf, H.<sup>1</sup>; Horak, G.<sup>2</sup>;

<sup>1</sup> UFZ- Helmholtz Center für Environmental Research, Permoserstr. 18, 04315 Leipzig, Germany  
uta.sauer@ufz.de

<sup>2</sup> SARAD GmbH, Wiesbadener Str. 20, 01159 Dresden, streil@sarad.de

# corresponding author

Radon is a naturally occurring radioactive gas which is distributed throughout soil and rocks in Germany in varying concentrations. Although there is only little public attention, radon gas and its decay products are due to migration processes into houses one of the most toxic indoor air pollution sources.

The radon concentration in soil gas varies between 10,000 to 100,000 Bq/m<sup>3</sup> in Germany and is seen as the main source of indoor air pollution. The radon gas migrates in the soil and seepages into the atmosphere through diffuse and passive advective transport processes. Studies show that the mobility of the radon gas rises to higher levels when this gas is mixed with other carrier gases e.g.  $\text{CO}_2$  and  $\text{CH}_4$ . The primary problem is that  $^{222}\text{Rn}$  migrates along geological gas permeable fault zones (e.g. permeable rock layers, gaps or gravel deposits) into soil layers near surface and enters buildings through potential weaknesses such as leaking foundations or cracks in masonry. In order to avoid cost-intensive restructuring measures at later times it is necessary to evaluate the radon activity already during site investigations, and to take special sealing and ventilation techniques into account in the planning process.

Monitoring results indicate that gas concentrations have distinct spatial variability caused by several geological and petrophysical parameters such as soil permeability, geological structure and soil moisture content. E.g. high soil moisture content in a soil layer causes gas accumulation and acts as a gas barrier to some extent. Therefore, the detailed depth oriented monitoring of varying gas concentrations and its influencing parameters are necessary to evaluate the accumulation/migration processes of radon gas and to establish mitigation options. The knowledge of small-scale variations is particularly important in the evaluation of individual properties or for site development with regard to special preventive precautions.

Therefore, a measuring device and a modular probe system to measure depth oriented both soil gas concentration and fluxes (especially  $\text{CO}_2$  and  $^{222}\text{Rn}$ ) and

other relevant influencing parameters (e.g. soil temperature, and soil moisture) was developed within the RATIEF project, funded by the German Federation of Industrial Research Associations (AIF). The simultaneous depth oriented measurement of soil gas concentration and other parameters allows the assessment of  $^{222}\text{Rn}$  concentration variations and other influencing parameters such as soil moisture, soil permeability and soil temperature. Hence, a detailed image of the subsurface is provided which is important for a comprehensive risk analysis with respect to radon migration processes.

In the project, a robust, easy-to-use and suitable for use in the field measuring instrument for the combined determination of radon and other carrier gas concentrations ( $\text{CO}_2$ ,  $\text{CH}_4$ ) was developed and implemented into a functional modular probe system, which ensures a representative depth-oriented measurement or sampling. Publication of Shahrokhi et al. (2015) showed that an increased  $\text{CO}_2$  concentration leads to an under- or overestimation of the measured  $^{222}\text{Rn}$  concentration with certain radon measuring devices. Experimental data show a short-term reduction in the concentration of  $^{222}\text{Rn}$  with increasing  $\text{CO}_2$  content. However, data analysis point out that the decrease is mainly related to neutralization processes of  $^{218}\text{Po}$  due to moisture and there is no direct influence of  $\text{CO}_2$  on radon gas measurements. The developed modular telescopic probe system can also be applied by common Direct Push machines allow measurements in deeper layers of the vadose zone. A special focus of the conceptual and practical development was the minimization of the gas loss as well as the prevention of atmospheric gas influx. This could be achieved by the optimization and coupling of a four part-divided packing system, which therefore allows an exact determination of the gas concentration in different depth horizons.

In addition to gas concentration, the migration rate of geogenic gases also represents an important parameter for risk assessment. Gas flux measurements can be used to determine the ascent rates of the gases. The gas flow is primarily controlled by the gas diffusion gradient. The flux measurement is based on the accumulation chamber method where the soil gas is directed into a measuring chamber placed on the ground or at a certain depth below. The gas flow is determined from the increase in gas concentration as a function of time ( $dC / dt$ ) with a defined chamber volume ( $V_{\text{acc}}$ ) and a defined gas-effective area ( $A_{\text{acc}}$ ). Since, after a sufficiently long time, a saturation value is reached, the chamber must be flushed with atmospheric fresh air at periodic intervals. With help of experimental data both optimal flush rates as well as optimal regression algorithms for the determination of the flux from concentration changes with time could be determined.

Permeability is a relevant influencing parameter to determine indoor radon concentrations. The emanation of the  $^{222}\text{Rn}$  and the migration in the soil are significantly influenced by the soil permeability, while varying climatic factors significantly influencing the further transport. The EC Directive 2013/59 / Euratom of 5 Dec 2013 pointed out that the determination of permeability is essential for radon measurements. Analysis of two different methods of permeability determination assessed the sensitivity

to small changes in input parameters. It will be shown that the accuracy of the pressure measurement is significantly better than that of the fall time measurement and the presentation will show results of permeability measurement with help of pressure difference measurements. The applied method of permeability measurement represents a time efficient method with increased measurement accuracy by simultaneous measurement of pressure difference and gas concentration.

The measuring device and a modular probe system and some results of field tests will be presented. Experiments show good results of flux determination and it can be concluded that the dimensions of the sampling probe are optimal for flow measurements. If depth-oriented soil gas measurements are required, the use of the modular probe system is very effective because of a significant reduction in personnel, material and time.



## **Radon Scout Home**

### **The Radon Recorder For Your Home**

T. Streil, V. Oeser

SARAD GmbH, Wiesbadener Str. 10, 01159 Dresden Germany  
streil@sarad.de; www.sarad.de

The radioactive noble gas radon counts as the major cause of lung cancer besides smoking. Because of this, a maximum of  $300\text{Bq/m}^3$  will be defined until 2018 by European law. Radon gets from ground or construction materials into buildings and leads to higher concentrations depending on availability and air exchange.

The Radon Scout Home is used for long-term monitoring of the legal reference value for the radon concentration in breathing air. The device was specially designed for homeowners as well as tenants, lessors and housing companies. The Radon Scout Home records the transient behaviour of the radon concentration over many years reliably, meaning that influences on weather conditions and seasonal changes are safely recorded. Sensors for temperature and humidity provide information about a healthy indoor climate. The measurement data can be read out at any time for preservation of evidence.

It is characterized by

- High-quality case
- Alphanumeric display
- Humidity and temperature measuring
- Battery/mains-powered operation
- USB port
- Time-resolved measurement
- Professional Software Radon Vision
- Developed & manufactured in Germany
- Based on the professional Radon Scout instruments

Technical data on the device are available on the website: [www.sarad.de](http://www.sarad.de).



## Resolution of small neon isotope anomaly in helium rich gas samples from Kii peninsula, Japan by a NGX multi-collector noble gas mass spectrometer

Hajimu Tamura<sup>1</sup>, Yoko Saito-Kokubu<sup>2</sup>, Koji Umeda<sup>3</sup>

<sup>1</sup> PESCO Co. Ltd., tamura.hajimu@jaea.go.jp

<sup>2</sup> Japan Atomic Energy Agency

<sup>3</sup> Hiroasaki University

**Keywords:** neon, isotope, multi-collector noble gas mass spectrometer, magmatic

Age and origin of groundwater estimated from isotopic composition of rare gases are needed to evaluate geosphere stability for long-term isolation of high-level radioactive waste. Neon has three isotopes of  $^{20}\text{Ne}$ ,  $^{21}\text{Ne}$  and  $^{22}\text{Ne}$  and isotope ratios of  $^{20}\text{Ne}/^{22}\text{Ne}$  and  $^{21}\text{Ne}/^{22}\text{Ne}$  are widely used to analyze mixing of multiple endmembers such as Earth's atmosphere, continental crust, or upper and lower mantles in rock geochemical study. In many cases, neon isotope difference from atmospheric composition is subtle in groundwater and gas, which requires measurement of the isotope ratios with high precision.

Multi-collector isotope analysis by high mass resolution mass spectrometer enhances precision of measurement of isotope ratio, and it causes better resolution on data analysis. A NGX multi-collector noble gas mass spectrometer in the Tono Geoscience Center, Japan Atomic Energy Agency has six collectors and three of them are configured for neon isotope measurement: a faraday with 100 G $\Omega$  amplifier for  $^{20}\text{Ne}$ , a secondary electron multiplier for  $^{21}\text{Ne}$ , a faraday with 1 T $\Omega$  amplifier for  $^{22}\text{Ne}$ , respectively.

Two gas samples from Yuasa and Ninomaru hot springs in Kii peninsula, Japan were analyzed by the NGX noble gas mass spectrometer. They had 4 times  $^4\text{He}/^{20}\text{Ne}$  ratio to atmospheric abundance and their isotopic composition were magmatic (3 Ra for Yuasa and 2 Ra for Ninomaru). Isotope ratios of  $^{20}\text{Ne}/^{22}\text{Ne}$  and  $^{21}\text{Ne}/^{22}\text{Ne}$  in the samples of Yuasa and Ninomaru were  $9.893 \pm 0.002$ ,  $9.855 \pm 0.002$ ,  $0.3012 \pm 0.0009$  and  $0.3001 \pm 0.0003$ , respectively. From the results, contribution of mantle neon is 3-4% and is small to resolve by conventional single collector mass spectrometer. These results suggest that this estimate of the origin of the gas is enabled with the neon isotope ratios with high precision measured by the NGX noble gas mass spectrometer.

This study was carried out under a contract with Ministry of Economy, Trade and Industry of Japan as a part of its R&D supporting program for developing geological disposal technology.



## **10. Coal-derived Gases and Coalbed Methane**





## Geochemical Characteristics and Sources of Natural Gas in the Southern Margin of Junggar Basin

Jianping Chen<sup>1,2,3#</sup>, Yunyan Ni<sup>1,2,3</sup>, Chunping Deng<sup>1,2,3</sup>, Xulong Wang<sup>4</sup>

<sup>1</sup> Research Institute of Petroleum Exploration and Development, PetroChina, Beijing, 100083, China

<sup>2</sup> State Key Laboratory of Enhanced Oil Recovery, Beijing, 100083, China

<sup>3</sup> Key Laboratory of Petroleum Geochemistry of CNPC, Beijing, 100083, China

<sup>4</sup> PetroChina Xinjiang Oilfield Company, Karamay, 834000, China

# Corresponding author, email: chenjp@petrochina.com.cn

The southern margin of the Junggar Basin, China is very complex and has many structural traps, and plenty of oils and gases have been found in these traps. At present, the Hutubi and Manas anticlines have discovered natural gas fields with commercial reserves, and other anticline structures also contain natural gas to varying degrees.

The natural gases discovered in the southern margin are dominated by hydrocarbon and alkane gas accounts more than 90% with an average of 97%. Other nonhydrocarbon gases are mainly nitrogen, accounting for 0.5% to 8.5% with an average of 2.2%, followed by carbon dioxide, accounting for 0 to 2% with an average of 0.19%. Among the hydrocarbon gases, methane accounts for 40% to 99%, with a majority from 50% to 95% and an average of 81.73%; the content of ethane varies from 0.5% to 35% with an average of 9.21%; propane varies from 0.1% to 25% with an average of 3.87%. In general, natural gas in the southern margin is dominated by wet gas, with small amount of dry gas.

The carbon isotopic composition of natural gas in the southern margin is relatively heavy. The carbon isotopic value ( $\delta^{13}\text{C}$ ) of methane ranges from -47‰ to -29‰, and the vast majority is between -42‰ and -31‰; the carbon isotopic value ( $\delta^{13}\text{C}$ ) of ethane is between -30 ‰ and -21 ‰, and the vast majority is from -28‰ to -22‰. In general, the carbon isotopic composition of the gas from west to east presents a tendency to becoming heavier gradually.

The natural gas in the south margin can be divided into three types: the oil-type gas, mixed-type gas and coal-type gas, among which the mixed-type gas and coal-type gas are dominant, with only a small amount of oil-type gas. The majority of natural gas in the central part of the southern margin is typical coal-type gas, with methane carbon isotope value ranging from -35‰ to -33‰, ethane  $\delta^{13}\text{C}$  value basically from -24‰ to -22.5‰, propane from -24‰ to -20‰, and it is mainly derived from the Jurassic coal measures source rock. The minority of natural gas has methane carbon isotope value less than -35 ‰ and ethane  $\delta^{13}\text{C}$  value less than -25‰, which belongs to the mixed-type

gas, and is derived from the Jurassic coal measures source rocks and the Cretaceous lacustrine source rocks.

The majority of natural gas in the west part of the southern margin is mixed-type gas, with methane  $\delta^{13}\text{C}$  value around -35‰, ethane  $\delta^{13}\text{C}$  value about -26.5‰, propane around -24‰, and is derived from the Jurassic coal measures source rocks and the Permian lacustrine source rocks. The minority of natural gas has ethane  $\delta^{13}\text{C}$  value less than -29‰ and propane  $\delta^{13}\text{C}$  value less than -26‰, belonging to the oil-type gas, and is derived from the Permian lacustrine source rocks. Another minority of natural gas has heavy ethane and propane  $\delta^{13}\text{C}$  values and is derived from the Jurassic coal measures source rocks.



## Geochemical characteristics of natural gases related to Late Paleozoic coal measures in China

Deyu Gong<sup>#</sup>, Jinxing Dai, Yanzhao Wei

Research institute of petroleum exploration and development, PetroChina, Beijing 100083 China  
<sup>#</sup>deyugong@petrochina.com.cn

**Keywords:** Late Paleozoic; coal measures; natural gas; stable carbon isotopes; TSR

Lithologically, coal measures are primarily composed of coal, black mudstone, and carbonaceous shales characterized by kerogen type II<sub>2</sub>–III and gases generated from such humic source rocks are usually defined as coal-type gas. In contrast, gases generated from sapropelic source rocks characterized by kerogen type I–II<sub>2</sub> are usually defined as oil-type gas. As early as the 1940s, German scholars had realized that coal measures could form commercial gas accumulations. Research on coal measures and related natural gas started in China in 1979 resulting in remarkable achievements in coal-type gas prospecting over the past 30 years. By 2011, the total proven reserves and yearly production of coal-type gas reached  $5813.5 \times 10^9 \text{ m}^3$  and  $64.8 \times 10^9 \text{ m}^3$ , respectively, accounting for 69.72% and 63.23% of their respective totals in China.

From the Early Cambrian to the Tertiary, there are eight major coal-forming periods in China, of which the Late Carboniferous–Early Permian and the Late Permian are the most significant. The Late Paleozoic coal measures primarily occur in the Upper Carboniferous Benxi Formation (C<sub>2</sub>b Fm) and Lower Permian Shanxi (P<sub>1</sub>s) and Taiyuan (P<sub>1</sub>t) Fms in East and Central China, the Lower Carboniferous Dishuiquan (C<sub>1</sub>d) and Upper Carboniferous Bashan (C<sub>2</sub>bs) Fms in Northwest China, and the Upper Permian Longtan (P<sub>2</sub>l) Fm in South China. In addition, a set of humic source rocks interbedded with coal seams and fragments of charring plants developed in the Middle Permian Wuerhe (P<sub>2</sub>w) Fm with a huge thickness in the Junggar Basin.

By 2013, more than 20 gas fields related to the Late Paleozoic coal measures had been discovered in China, distributed in the Bohai Bay, Ordos, Sichuan, and Junggar Basins. The total proven reserves of these gas fields is more than  $3200 \times 10^9 \text{ m}^3$ , accounting for 30% of the proven gas reserves in China. Of these gas fields, 12 have proven reserves of more than  $30 \times 10^9 \text{ m}^3$ , including the Sulige gas field, the largest gas field in China, whose gas production reached  $21.2 \times 10^9 \text{ m}^3$  in 2013 and accounts for 17.6% of the total gas production in China. Clearly, the gas fields related to the Late Paleozoic coal measures play an important role in the Chinese natural gas industry.

These gas fields experienced complex geological processes resulting in their gas origins and relevant secondary alterations still being much debated. Previous studies primarily focused on geochemical characteristics of natural gases from some specific gas fields, which lacked the comparison between gases from different gas fields or different prolific basins. After 30 years of exploration, more and more wells have been in these fields, promising us a more comprehensive understanding of the geochemical characteristics of the natural gas.

After analyzing the molecular compositions, stable carbon isotopes, and helium isotopes of 375 gas samples, genetic types and origins of the natural gas, as well as the secondary alterations it experienced, are discussed in this study. Most of the natural gas related to the Late Paleozoic coal measures are coal-type gas, with some of the gases from the Sichuan Basin and the Jingbian gas field in the Ordos Basin being oil-type gases generated from marine mudstones in the Permian Longtan Formation and marine carbonates in the Ordovician Majiagou Formation, respectively. The vitrinite reflectance values of natural gas vary from 0.8% to 2.5%, indicating the mature-over mature stage. Because the carbon isotopes of the higher hydrocarbon gases are only slightly affected by thermal maturity, they can be used as an effective criterion to distinguish coal-type and oil-type gases. Positive carbon isotopic series are observed in most gas samples, and carbon isotopic reversals occur in the forms of  $\delta^{13}\text{C}_1 > \delta^{13}\text{C}_2$  and  $\delta^{13}\text{C}_1 < \delta^{13}\text{C}_2 > \delta^{13}\text{C}_3$ . The former resulted from the admixture of oil-type and coal-type gases, while the latter resulted from the admixture of coal-type gases of different maturities. High concentrations of hydrogen sulfide in natural gas from the Sichuan Basin and the Chenghai gas field in the Bohai Bay Basin resulted from thermochemical sulfate reduction (TSR), which causes, to some extent, the fractionation of ethane carbon isotopes. By contrast, the fractionation of methane carbon isotopes resulting from the TSR effect is not clear. Carbon dioxide from the Bohai Bay and Junggar Basins is primarily biogenic, generated via the thermal decomposition of organic matter, while that from the Ordos Basin, Sichuan Basin, and Chenghai gas field is generated via the thermal decomposition of carbonates. Carbon dioxide related to the TSR effect has also contributed to the Sichuan Basin and Chenghai gas field.

In the 21st century, oil and gas exploration is becoming increasingly difficult as the target strata grow older and deeper. Our study is not only of great significance for the future gas exploration in China but can also shed light on gas exploration in other worldwide areas which share a similar geological background.



## Geochemical characteristics of carbon dioxide and their differences in coal-derived and oil-type gases, China

Li Jian<sup>#</sup>, Wang Xiaobo, Li Zhisheng, Xie Zengye, Wang Yifeng, Li Jin,  
Ma Chenghua, Cui Huiying, Qi Xuening

Langfang Branch of PetroChina Research Institute of Petroleum Exploration & Development,  
CNPC Key Laboratory of Gas Reservoir Formation and Development, Langfang, Hebei, 065007 China

<sup>#</sup> First author: Li Jian, Professor Senior engineer. Engage in petroleum geologic and Geochemistry research. Add: P.O.B.44, Wanzhuang, Langfang, Hebei 065007, P.R. China. Phone: +861069213414.  
E-mail: Lijian69@petrochina.com.cn

Coal-derived gases are the main body in Chinese's natural gases resources and play an important role on gas industry development in China<sup>[1-4]</sup>. Non-hydrocarbon gases are important components of natural gases and have great relationship with hydrocarbon gases. So, it has great effect in comprehensively understanding geochemical differences of non-hydrocarbon gases and their origination of coal-derived gases and oil-typed gases in China. Based on researches on non-hydrocarbon gases geochemistry of coal-derived gases and oil-typed gases in China, geochemical characteristics differences of non-hydrocarbon gases in coal-derived gases and oil-typed gases are comparatively studied and their geologic implicating significances on gases genesis are discussed. The main recognitions are followed as:

1. The CO<sub>2</sub> content mainly ranges from 0.1% to 80.42% with main frequency distributed from 0 to 2% in coal-derived gases, while it usually ranges from 0.09% to 22.76% with main frequency distributed from 0 and 5% in oil-typed gases in China. Generally, the CO<sub>2</sub> has a relative wide component concentration distribution area in coal-derived gases but a relative narrow distribution area in oil-typed gases.

2. The  $\delta^{13}\text{C}_{\text{CO}_2}$  value of coal-derived gases generally ranges from -26.4‰ to -2.6‰ with main frequency distributed from -20‰ to -2‰, while it mainly ranges from -15.8‰ to 1.9‰ with main frequency distributed from -15‰ to 2‰ in oil-typed gases in China. The  $\delta^{18}\text{O}_{\text{CO}_2}$  value of coal-derived gases usually ranges from 4.05‰ to 29.2‰ with main frequency distributed from 4‰ to 16‰, while it mainly ranges from 12.2‰ to 32.5‰ with main frequency distributed 12‰~32‰ in oil-typed gases in China. The  $\delta^{13}\text{C}_{\text{CO}_2}$  and  $\delta^{18}\text{O}_{\text{CO}_2}$  values of coal-derived gases are generally relative lighter than that of oil-typed gases.

3. The CO<sub>2</sub> in coal-derived gases is mainly organic genesis originated from pyrolysis of humic organic matter. The CO<sub>2</sub> in oil-typed gases not only has organic genesis

originated from sapropelic organic matter, but also has inorganic genesis originated from pyrolysis of carbonate or carbonate cement.

4. Based on the geochemical differences of CO<sub>2</sub> in coal-derived gases and oil-typed gases in China, it can be concluded that the coal-derived gases generally has relative light carbon isotope values and oil type gases usually has relative heavy carbon isotopes in oil-typed gases. It possibly has some indicating effect on coal-derived gases and oil-typed gases identification. According to above differences of CO<sub>2</sub> in coal-derived gases and oil-typed gases and combing noble gases index (make sure that natural gases have no mantled inorganic gases), the new identified index and chart of coal-derived gases and oil-typed gases from He and CO<sub>2</sub> are established: When R/Ra is less than 0.1 (Noble gases are typical crustal genesis can make sure that hydrocarbon gases in natural gases are crustal organic genesis) ,if δ<sup>13</sup>C<sub>CO2</sub> is less than -15‰, the natural gas are usually can be identified as coal-derived gases, if δ<sup>13</sup>C<sub>CO2</sub> is larger than -2.5‰, the natural gas are usually can be identified as oil-typed gases. It provides a new technical method for coal-derived gases and oil-typed gases identification, having great significances in understand CO<sub>2</sub> origination and guiding natural gas exploration.

Fund project: Special and Significant Project of National Science and Technology “Development of Large Oil/gas Fields and Coalbed Methane” (No.:2016ZX05007-002); Project of Petrochina, No.: 2016B-0601.

## References

- [1] Dai J, Li J, Hu G, et al. 2007. *Geological characteristics of natural gas at giant accumulation in china*[J]. Journal of Petroleum Geology, 30(3): 275-288.
- [2] Dai J X, Zou C N, Li J, et al. 2009. *Carbon isotopes of Middle-Lower Jurassic coal-derived alkane gases from the major basins of northwestern China*. International Journal of Coal Geology, 80: 124-134.
- [3] Dai J X, Gong D Y, Ni Y Y, et al. 2014. *Genetic types of the alkane gases in giant gas fields with proven reserves over 1000X108m3 in China*. Energy Exploration &Exploitation, 32(1): 1-18.
- [4] Li Jian, Li Jin, Li Zhisheng, et al. 2014. *The hydrogen isotopic characteristics of the Upper Paleozoic natural gas in Ordos Basin*, Organic Geochemistry, 74: 66-75.



## Genetic mechanism of the carbon isotope reversal in over-mature coal-derived gas in Ordos Basin, China

Liu Dan<sup>1,3\*</sup>, Dai Jinxing<sup>2</sup>, Liu Jiaqi<sup>1</sup>, Li Jian<sup>3</sup>, Feng Ziqi<sup>3</sup>

<sup>1</sup> Institute of Geology and Geophysics, Chinese Academy of Science, Beijing, 100029, China

<sup>2</sup> PetroChina Research Institute of Petroleum Exploration and Development-Langfang, Langfang, Hebei, 065007, China

<sup>3</sup> Research Institute of Petroleum Exploration and Development, PetroChina, Beijing, 100083, China

# corresponding author: liudan@igccas.ac.cn

### Introduction

For many years, carbon isotopic reversal has been attributed to abiogenic gases. However, recent exploration for shale gas and recently published works suggest that it may also be generated by: (a) mixed gases that are derived from different source rocks, or from the same source at different stages of maturity; (b) Rayleigh fractionation during redox reactions; (c) the secondary cracking of wet gas at high thermal stress; and (d) the interaction between water and organic matter at high temperatures. In addition, after a comparative study of previous published work and their new data, Dai et al (2016) reported that the carbon isotopic reversal can be divided into primary and secondary origins. The primary was a typical characteristic of abiogenic gases, while the secondary, which usually observed in over-mature shale gas and coal-derived gas, was controlled by high temperature (>200 °C) during which secondary cracking, diffusion and Rayleigh fractionation could happen separately or together.

Jingbian gas field was the first giant gas accumulation of the Ordos Basin. Most of the upper Paleozoic gases in Jingbian gas field have been generated from the Carboniferous–Permian coaly source rock (Dai et al., 2005), while the gas of lower Paleozoic reservoirs in the Jingbian gas field is mixture of coal-derived gas from C-P humic source rock and Ordovician sapropelic source rock. In this paper, a large suite of gases from the south Jingbian have been isotopically and chemically characterized and previous interpretations are reviewed, in order to discuss the potential controls on isotopic reversals at the over-mature stage (i.e. Ro>2.0%).

A distinct feature of the natural gas of southern Jingbian is that the carbon isotopes show a reversal (Fig. 1). The lower Paleozoic gas shows a partial reversal ( $\delta^{13}\text{C}_1 > \delta^{13}\text{C}_2 < \delta^{13}\text{C}_3$ ), while upper Paleozoic gas shows both partial and full ( $\delta^{13}\text{C}_1 > \delta^{13}\text{C}_2 > \delta^{13}\text{C}_3$ ) reversals. The partial carbon isotope reversals occur in areas where Ro < 2.8%, while

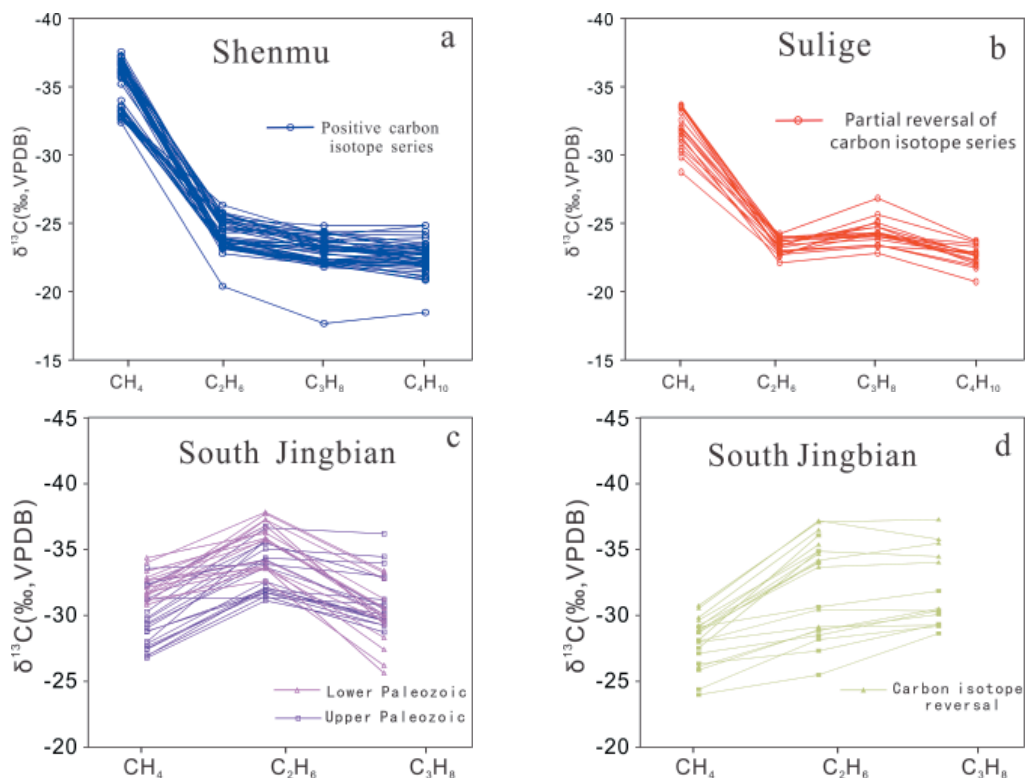


Fig. 1. Carbon isotope series of gas fields with different maturity in the Ordos Basin

the full reversals occur where  $R_o > 2.8\%$ . In addition, gases with the lowest maturity in the Shenmu gas field exhibit a positive carbon isotope series, while mature gases (2.2%–2.6%) in the Sulige gas field show partial reversals, with propane lighter than ethane. The correlation between carbon isotope systematics and gas maturity indicates that the carbon isotope reversal of Paleozoic gas was formed as a result of elevated temperatures.

## Genetic of isotopic reversal

### Abiogenic origin

Inorganic gas is formed by Fischer–Tropsch synthesis when mantle degassing releases  $\text{CO}_2$  or  $\text{CO}$ , forming hydrocarbons with reversed carbon isotopes by reduction. These gases are typically characterized by  $\delta^{13}\text{C}_1 > \delta^{13}\text{C}_2 > \delta^{13}\text{C}_3 > \delta^{13}\text{C}_4$ ,  $\delta^{13}\text{C}_1$  greater than  $-25\%$ , and  $R/R_a > 0.1$ . The samples of the present study did not yield  $\delta^{13}\text{C}_4$  data due to their high drying coefficient. Among the 47 Paleozoic gas samples from southern Jingbian, 11 showed a complete carbon isotope reversal ( $\delta^{13}\text{C}_1 > \delta^{13}\text{C}_2 > \delta^{13}\text{C}_3$ ), while the others showed a partial reversal, with  $\delta^{13}\text{C}_1 > \delta^{13}\text{C}_2 < \delta^{13}\text{C}_3$ . The  $\delta^{13}\text{C}_1$  value is less than

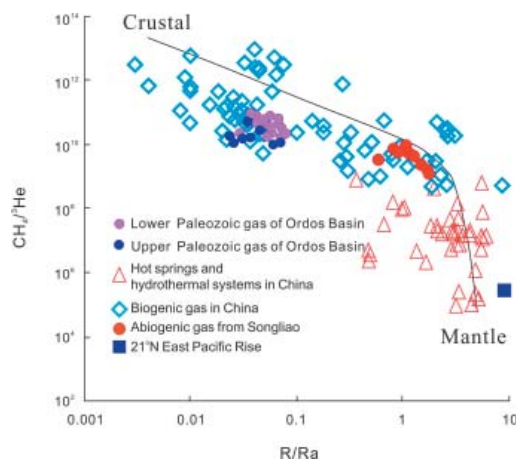


Fig. 2. R/Ra-CH<sub>4</sub>/<sup>3</sup>He diagram

-25‰ for all except three of the samples. Since the <sup>3</sup>He/<sup>4</sup>He value of mantle helium is higher than shell source helium, R/Ra, a comparison of the He isotope composition of the sample against that of air can be used to ascertain whether mantle-derived inorganic gas was injected into the natural-gas-producing system. Figure 2 shows that the distribution of C and He isotopes in Paleozoic gas of the Ordos Basin is different from that of inorganic gas of the Songliao Basin; however, the distribution of these isotopes is similar to other organic gases from other basins in China, indicating the Paleozoic gas of southern Jingbian is of organic thermogenic. In addition, the Paleozoic reservoir rocks of the Ordos Basin were deposited on a stable cratonic basement that has not been affected by large deep-seated faults connecting the Paleozoic reservoirs to a source of mantle-derived inorganic gas. Thus, we conclude that the carbon isotope reversal of the Paleozoic gas of southern Jingbian is not of inorganic origin.

### Gas mixing

Mixing processes involve the mixing of gas produced by source rocks of different maturities, or from different types of parent materials. Sapropel-type source rocks of the Carboniferous Benxi Formation, the Permian Taiyuan Formation, and the lower Paleozoic Majiagou Formation have the potential to generate oil-type gas, and the carbon isotope reversals of the present study may have been caused by the mixing of a coal gas containing very small amounts of heavy hydrocarbon gas with a large amount of oil-type gas containing light δ<sup>13</sup>C<sub>2</sub>. In this study, the carbon isotope range of mixed gas was calculated by using the typical Paleozoic coal gas and oil-type gases of the Ordos Basin as two end-members. For coal gas, δ<sup>13</sup>C<sub>1</sub> = -30‰ and δ<sup>13</sup>C<sub>2</sub> = -25‰ at C<sub>1</sub> = 0.995% and C<sub>2</sub> = 0.005%, while oil-type gas yields δ<sup>13</sup>C<sub>1</sub> = -35‰ and δ<sup>13</sup>C<sub>2</sub> = -31‰ at C<sub>1</sub> = 0.900% and C<sub>2</sub> = 0.100%. Simple calculation shows that regardless of the relative

proportions of hydrocarbons in the gas, the carbon isotope value of methane remains lower than that of ethane, indicating a carbon isotope reversal between methane and ethane is impossible. Furthermore, negative carbon isotope series are formed through mixing of coal-derived gas containing heavy  $\delta^{13}\text{C}_2$  with oil-type gas containing light  $\delta^{13}\text{C}_2$ . The  $\delta^{13}\text{C}_2$  value of self-generated and self-preserved lower Paleozoic gas ranges from  $-30.0\text{‰}$  to  $-32.0\text{‰}$ . However, all gases with carbon isotope reversal have  $\delta^{13}\text{C}_2$  lighter than  $-32.0\text{‰}$ . Therefore, the carbon isotope values and isotope series of the natural gas could not have resulted from mixing processes.

### Wet gas cracking

Previous studies have suggested that carbon isotope reversals in shale gas are caused by secondary cracking, as isotope fractionation can occur during the expulsion or diffusion of hydrocarbons; however, the effects of fractionation are not substantial enough to cause carbon isotope reversals (Xia et al., 2013). Therefore, it may be possible that shale gas with negative carbon isotope series forms during the generation of hydrocarbons. Condensate oil or wet gas is generated during secondary cracking in the over-mature stage, when extensive carbon isotope fractionation produces large amounts of  $\text{C}_2$  and  $\text{C}_3$ . The wet gas contains light carbon isotopes and mixes with dry natural gas containing heavy carbon isotopes generated by the initial cracking of kerogen. The resultant shale gas has a negative carbon isotope series. Secondary cracked gas typically has the following characteristics: (1)  $\delta^{13}\text{C}_1$  increases and  $\delta^{13}\text{C}_2$  decreases with a reduction in gas wetness associated with rising temperature; and (2) since  $i\text{C}_4$  is less stable than  $n\text{C}_4$  in the over-mature stage, the  $i\text{C}_4/n\text{C}_4$  value of secondary cracked gas decreases when wetness ( $\text{C}_{2-5}/\text{C}_{1-5}$ ) falls below 5% (Zumberge et al., 2012).

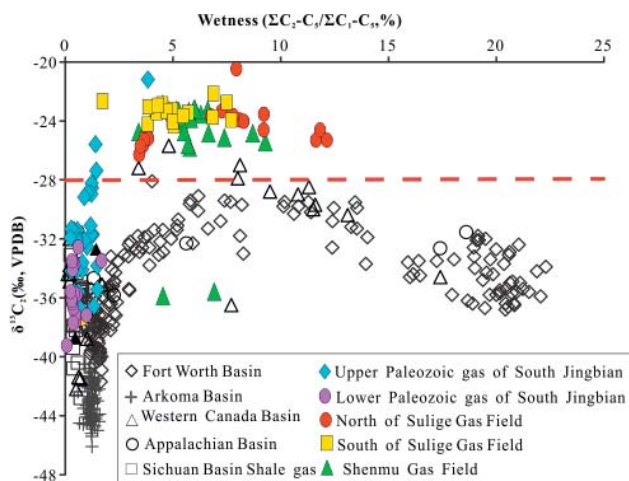


Fig. 3. Diagram of  $\delta^{13}\text{C}_2$  versus gas wetness (data of shale gas are from Wu et al., 2015)

The relationship between  $\delta^{13}\text{C}_1$ ,  $\delta^{13}\text{C}_2$ , and wetness of the Paleozoic natural gas in different areas in the Ordos Basin, and Chinese and global shale gas show that the conventional Paleozoic gas of the Ordos Basin evolved in a similar way to shale gas. In the Shenmu and Sulige gas fields, the  $\delta^{13}\text{C}_1$  and  $\delta^{13}\text{C}_2$  values of the natural gas that is not highly evolved become heavier with a decrease in wetness, whereas in southern Jingbian the  $\delta^{13}\text{C}_1$  of highly evolved gas increases with decreasing wetness, and  $\delta^{13}\text{C}_2$  decreases, causing similar carbon isotope reversals to those observed in shale gas. This late-stage isotopic reversal may be the result of the secondary cracking of coal-derived liquid or light hydrocarbons.

Because  $i\text{C}_4$  is less stable than  $n\text{C}_4$ , its cracking rate is greater during secondary cracking, resulting in a decrease in  $i\text{C}_4/n\text{C}_4$  with increasing maturity. Figure 8 shows that the  $i\text{C}_4/n\text{C}_4$  value of the Paleozoic natural gas in southern Jingbian decreases rapidly with decreasing wetness, consistent with the evolution trends of secondary cracked shale gas. Thus, the negative carbon isotope series of the Paleozoic natural gas in southern Jingbian may have resulted from secondary cracking.

Given that the Ordos Basin is located on stable basement, it does not contain large faults that could have facilitated gas migration. As a result, Paleozoic gas accumulated near its source. In the case that the source was upper Paleozoic coal seams, natural gases were generated by initial cracking and secondary cracking, and these gases mixed with each other in Paleozoic reservoirs. Upper Paleozoic natural gas with negative carbon isotope series that occurs in the Yan'an gas field (southeastern Ordos Basin) is thought to have formed by similar processes (Wu et al., 2015).

## References

- DAI J, LI J, LUO X. 2005. *Stable carbon isotope compositions and source rock geochemistry of the giant gas accumulations in the Ordos Basin, China*. *Organic Geochemistry* 36, 1617-1635.
- DAI J., NI Y., HUANG S, GONG D., LIU Dan, FENG Z., PENG W., HAN W. 2016. *Origins of secondary negative carbon isotopic series in natural gas*. *Natural Gas Geoscience* 27, 1-7.
- WU W, DONG D, YU C, LIU D. 2015. *Geochemical characteristics of shale gas in Xiasiwan area*. *Energy Exploration & Exploitation* 33, 25-42.
- XIA X, CHEN J, BRAUN R. 2013. *Isotopic reversals with respect to maturity trends due to mixing of primary and secondary products in source rocks*. *Chemical Geology* 339, 205-212.
- ZUMBERGE J, FERWORN K, BROWN S. 2012. *Isotopic reversal ('rollover') in shale gases produced from the Mississippian Barnett and Fayetteville formations*. *Marine and Petroleum Geology* 31, 43-52.



## **Geochemical characteristics of the typical coal-derived early thermogenic gas with extremely low $\delta^{13}\text{C}$ values from the Turpan-Hami Basin, China**

Yunyan Ni<sup>#</sup>, Fengrong Liao, Deyu Gong, Jianping Chen, Dijia Zhang

Research Institute of Petroleum Exploration and Development, PetroChina, Beijing, 100083, China

<sup>#</sup> Corresponding author, email: niyy@petrochina.com.cn

The widely accepted concept of hydrocarbon formation is that thermogenic gas forms at the relatively late stage of geochemical transformation of organic matter. At the great depth, the main gas generation will come after the stage of oil formation and extensive vertical gas migration will occur after the gas generation. However, Galimov (1988) proposed that humic organic matter, in general, has a high methane-generating capacity at comparably low maturities of organic matter equivalent to 0.5-0.7% on the vitrinite reflectance scale. Therefore, except the supergiant gas fields in West Siberia such as the Urengoy which comprise 30% of the proven gas reserves of the world, are there any other gas fields consisting of early thermogenic gases? Here we investigate systematically the geochemical characteristics and geological conditions of the gaseous hydrocarbons in the Turpan-Harmi Basin, Northwest China and make a detailed study on the gas origin and gas-source correlations.

The Turpan-Harmi Basin is located in Northwest China and is one of the three largest sedimentary basins in the Xinjiang Uygur Autonomous Region, China with an area of  $5.35 \times 10^4 \text{ km}^2$ . It not only has abundant coal with reserves exceeding  $5.3 \times 10^{11} \text{ t}$ , but also is famous for its coal-sourced oils and the early coal-derived gases. In the basin, potential source rocks include the marine carbonates in the Lower Permian-Carboniferous, the Pre-Jurassic lacustrine mudstones in the Triassic Huangshanjie Formation and the Upper Permian Taodonggou Formation, the coal measures in the Middle-Lower Jurassic Xishanyao and Badaowan Formations and the black lacustrine mudstones in the Middle Jurassic Qiketai Formation. The Permian and Triassic source rocks are mainly at mature to over-mature stage. While for the Jurassic, only source rocks from Badaowan Formation nearly reaches mature stage and all others are at immature stage, e.g., source rocks of Xishanyao Formation have thermal maturity from 0.4%~0.8%. Therefore, it has long been a hot debate about the origin of the oils and gases in the basin.

We collected 23 gas samples from Baka, Qiuling, Shanshan and Wenmi oil fields in the north of the basin. These gases have very low gas dryness coefficient ( $C_1/C_{1-5}$ ), varying from 0.66 to 0.98, and belong to wet gas. The calculated gas maturity is around

0.5% Ro indicating the very low maturity of the gas. The gases have  $\delta^{13}\text{C}_{\text{CH}_4}$  of -44.9‰ ~ -37.2‰ with an average of -41.0‰,  $\delta^{13}\text{C}_{\text{C}_2\text{H}_6}$  of -28.2‰ ~ -24.9‰ with an average of -27.0‰,  $\delta^{13}\text{C}_{\text{C}_3\text{H}_8}$  of -27.1‰ ~ -18.0‰ with an average of -25.1‰,  $\delta^{13}\text{C}_{\text{C}_4\text{H}_{10}}$  of -26.7‰ ~ -22.0‰ with an average of -25.0‰. The hydrogen isotopes are of -272‰ ~ -248‰ with an average of -261‰, -236‰ ~ -200‰ with an average of -225‰, -222‰ ~ -174‰ with an average of -210‰ for methane, ethane and propane, respectively. No partial isotopic reversal has been found in either carbon or hydrogen isotopes. In general, all the gas samples are determined to be coal-derived gases sourced from the Jurassic coal measures which were generated at relatively low mature stage. The relatively low hydrogen isotopes of methane indicate the water medium of depositional environment to be freshwater.



## Geochemical Characteristics of Light Hydrocarbons in the Natural Gas and Their Influencing Factors of the Kuqa Depression, NW China

Weilong PENG<sup>1#</sup>, Guoyi HU<sup>1</sup>, Ziqi FENG<sup>2</sup>, Shipeng HUANG<sup>1</sup>

<sup>1</sup> Research Institute of Petroleum Exploration and Development, PetroChina, Beijing 100083, China

<sup>2</sup> China University of Petroleum, Qingdao, Shandong 266580, China

# Corresponding author: pengwl26@yeah.net

**Keywords:** *Natural gas; Light hydrocarbons; Geochemical characteristics; Source rock; Kuqa Depression; China*

Kuqa depression is the deepest gas exploration area in China. Large amount of high-over matured gas has been discovered in the depression. In order to study the geochemical characteristics and source of the natural gas light hydrocarbons in Kuqa Depression, the light hydrocarbons and their influencing factors were discussed based on the analysis of the natural gas samples from 19 wells in Kuqa Depression, combining with previous studies on natural gas components and isotope analysis.

The results show that for the natural gas of Kuqa Depression, C7 light hydrocarbon series compounds have methyl cyclohexane advantages (37.5%~60.3%) and heptanes (25.0%~54.8%) is high in content. The C6-7 light hydrocarbon series compounds have abnormally high aromatic hydrocarbon content (26.2%~83.8%). Heptane value (13.31%~37.77%) and isoheptane value (2.10%~7.64%) indicate that the gas in the depression is of high maturity (Fig.1). The study reveals that the natural gas in the depression is typical coal-derived gas, but its light hydrocarbons represent mixed-source parent material characteristics. Specifically, the light hydrocarbons in Dina 2 gas field represent coal-derived gas characteristics; the light hydrocarbons in Dabei gas field represents oil type gas characteristics, while the light hydrocarbons in Kela 2 and Keshen 2 gas field and Well Yangta 101 represent mixed source characteristics. The abnormally high content of the aromatic hydrocarbons in the natural gas in the depression is mainly resulted from the high productivity of aromatic hydrocarbons during the thermal evolution of humic type parent material and the gas accumulation of late stage (Fig.2). The different relative contents of the aromatic hydrocarbons in different oil and gas fields are resulted from the different organic matter types, maturity and distribution patterns of source rocks.

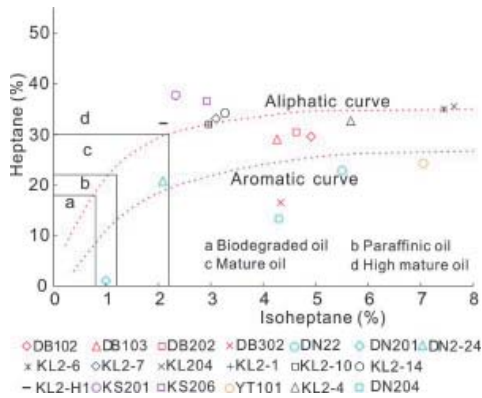


Fig. 1. Cross plot of heptane and isoheptane values of gases from the Kuqa Depression (diagram after Thompson, 1983)

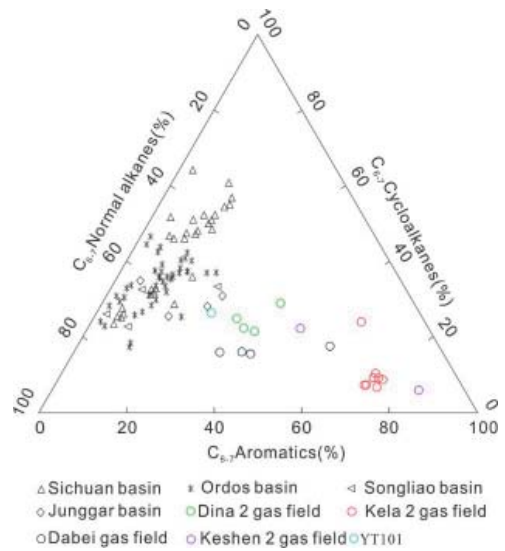


Fig. 2. Ternary diagram of chain alkanes, cycloalkanes and aromatics of the total  $C_{6-7}$  compounds of the Kuqa Depression and other typical coal derived gases in China (modified after Hu et al., 2014)

## Reference

- THOMPSON K. F. M. 1983. *Classification and thermal history of petroleum based on light hydrocarbons*. *Geochimica Et Cosmochimica Acta* 47: 303-316.
- HU G., YU C. & TIAN X. 2014. *The origin of high benzene in light hydrocarbons associated with gas from the Kuqa depression in the Tarim Basin, China*. *Organic Geochemistry*, 74: 98-105.



## 11. CO<sub>2</sub> and Greenhouse Gases





## Bottom-up characterization of largest anthropogenic methane source in Europe: Upper Silesian Coal Basin, Southern Poland

J. Nęcki<sup>1#</sup>, M. Zimnoch<sup>1</sup>, M. Gałkowski<sup>1</sup>, Ł. Chmura<sup>1,2</sup>, A. Jasek<sup>1,2</sup>,  
M. Kotarba<sup>1</sup>, K. Różański<sup>1</sup>, W. Wołkowicz<sup>3</sup>

<sup>1</sup> AGH – University of Science and Technology, Kraków, Poland

<sup>2</sup> IMGW – NRI, branch in Kraków, Poland

<sup>3</sup> Polish Geological Institute PGI – NRI, Warszawa, Poland

# corresponding author: necki@agh.edu.pl

**Keywords:** Greenhouse effect, methane balance, atmospheric methane, methane anthropogenic emissions

Methane is the second most important greenhouse gas. Its atmospheric concentration has been increasing steadily during the 20th century till late 1990s when its level has stabilized. The last decade renewed build-up of this gas in the global atmosphere was observed and causes of this recent increase are the subject of vigorous scientific debate. Methane emissions associated with coal production (mining, transport and storage on the surface) are responsible for approximately 35% of the global anthropogenic flux of methane to the atmosphere associated with fossil fuel production and usage [1]. In regions of active coal mining methane emissions may lead to elevated concentration of this gas in the near-ground atmosphere. Restructuring of coal mining industry in some countries and shifts of major coal production centers results in transient character of this global CH<sub>4</sub> flux.

The presented work was launched with the main objective of providing a comprehensive assessment of methane flux into the atmosphere during the period 2001-2014, associated with the Upper Silesian Coal Basin (USCB). The Upper Silesia region is located in southern Poland and constitutes a unique example in Europe of the impact over two centuries of heavy industry (coal, lead and zinc mining industry, steelworks, machine building industry) and dense urbanization on the land-use evolution. With 19 interconnected cities, approximately 3.5 million inhabitants, and 20 active coal mines, it presents the most heavily transformed landscape in Poland. The assessment comprised thorough characterization of CH<sub>4</sub> emissions from coal mines of the region, supplemented by carbon isotope measurements of coal-bed methane inside the mines, in the boreholes drilled from the surface, as well as in the ventilation shafts. Spatial and temporal variability of CH<sub>4</sub> mixing ratios in the lower atmosphere of the region have been quantified through mobile measurement campaigns, supplemented by sampling

of air for  $\delta^{13}\text{C}$  and  $\delta^2\text{H}$  measurements of methane for source isotope fingerprinting. Ground-level transects of atmospheric  $\text{CH}_4$  mixing ratios in the region were compared with regional, free-tropospheric concentrations of methane obtained from high-altitude mountain station located at Kasprowy Wierch, Tatra Mountains, ca. 150 km south-east of USCB. The bottom-up assessment of regional flux of  $\text{CH}_4$  included also other sources of this gas in the region, such as landfills, leaking city gas networks,  $\text{CH}_4$  emissions from livestock and other biogenic sources. Comprehensive bottom-up estimate of regional  $\text{CH}_4$  flux performed in the framework of the present work was compared with the most recent  $\text{CH}_4$  emission inventories for the Silesia region [2, 3].

### References

- [1] Saunio et al. (2016). *The global methane budget 2000-2012*. Earth Syst. Sci. Data, 8, 697-751.
- [2] EDGAR, (2013). European Commission, Joint Research Centre (JRC)/Netherlands Environmental Assessment Agency (PBL). Emission Database for Global Atmospheric Research (EDGAR), release EDGARv4.2 FT2010, <http://edgar.jrc.ec.europa.eu>.
- [3] Bun, R. et al. (2016). *Modeling of greenhouse gas emissions from stationary sources*. Ukrainian Ministry of Education and Science, ISBN 978-966-2598-74-2.

## Index

Aisheng Hao	117	Dicu T.	15
Alawi Mashal	129	Dirik Kadir	96
Bayari Serdar	96	Domin Elżbieta	113
Beldean S.	15	Du Li	145, 166
Bilkiewicz Elżbieta	47, 53	Etiopie Giuseppe	67, 94
Bonczyk M.	165	Facca G.L.	35, 132, 134
Bonfanti P.	27	Fan Qiaohui	67, 95
Borsdorf, H.	177	Fang Xuan	166
Bovini Sergio	125	Favara Rocco	121
Bräuer Karin	77, 129	Fazio F.	134
Burghele B.	15	Feng Pengyu	71
Calabrese S.	80, 85	Feng Ziqi	148, 159, 198
Camarda Marco	121	Fiebig J.	85
Cao Chunhui	145	Fijałkowska-Lichwa Lidia	11
Caracausi Antonio	96, 121, 125	Fischer Tomáš	42, 124
Caruso C.	27, 31, 37	Fu Ching-chou	123
Chałupnik S.	165	Gagliano A.I.	80
Chen Cheng-hong	123	Gałkowski M.	203
Chen Chensheng	159	Gao Xiaoyue	56
Chen Duofu	40	Genzano N.	132
Chen Guojun	40	Gherardi F.	35, 132, 134
Chen Jianfa	50	Goliáš Viktor	9
Chen Jianping	185, 196	Gong Deyu	187, 196
Chen Zeya	50	Góra Adrianna	99
Chenghua Ma	189	Grassa F.	85
Chiaraluce Lauro	121	Guzy Piotr	99
Chmura Ł.	203	He Liwen	50
Chunhui Cao	169	He Long	40
Ciolini R.	35, 134	Heinicke J.	42, 124, 134
Corbo A.	37, 31	Hengesch Olivier	92
Cucoş A.	15	Horak G.	177
Čurda Michal	9	Howaniec N.	165
D'alessandro W.	80, 85	Hu Fei	71
D'errico F.	35	Hu Guoyi	198
D'intinosante V.	35	Huang Shipeng	148, 198
Dadomo A.	171	Huiying Cui	117, 189
Dai Jinxing	159, 187	Italiano F.	27, 31, 37, 80, 89, 96, 108, 125
Dan Liu	191	Jasek A.	203
Daskalopoulou K.	80, 85	Jian Li	117, 189, 191
De Gregorio Sofia	121	Jiaqi Liu	191
Deng Chunping	185	Jin Li	189
Di Bella Marcella	31, 89	Jin Zhijun	60

Jinxiang Dai	191	Ni Yunyan	185, 196
Kämpf Horst	77, 129	Niedermann Samuel	77
Kies Antoine	92	Nigrelli Alessandra	31, 37, 89, 125
Koch Ulrich	129	Oeser V.	180
Kotarba Maciej J.	47, 53, 203	Okumura Fumiaki	173
Kowalczyk Ł.	115	Olszewski Jerzy	19
Kowalska Agata	113	Olszewski Sławomir	17
Kumar Arvind	123	Ozyurt Nur	96
Kyriakopoulos K.	80, 85	Pang Xiongqi	50
Lantian Xing	169	Papp B.	15
Lazzaro Gianluca	31, 37	Parello F.	85
Lee Lou-chuang	123	Pazzagli F.	35
Lei Tianzhu	105	Peng Ping'an	150
Lemmi Margherita	125	Peng Weilong	148, 198
Li Liwu	145, 153	Pfanz Hardy	92, 136, 137, 138
Li Wei	62	Pierotti L.	35, 132, 134
Li Yang	67	Przylibski Tadeusz A.	11, 113
Li Zhongping	153	Qin Shengfei	62, 159
Liang Jiaju	103	Ring Uwe	108
Liang Shouyun	67	Rizzo Andrea Luca	96
Liao Fengrong	196	Romano Davide	31
Liao Lingling	159	Róžański K.	203
Liao Yuhong	150	Ruiz Olivier	137
Lin Cheng-horng	123	Sabatino Giuseppe	31, 89
Lisi M.	132	Sainz C.	15
Liu Luofu	56	Saito-Kokubu Yoko	181
Liu Quanyou	60	Sajjad Wasim	67, 95
Liu Weiming	150	Sauer U.	177
Liu Yan	153	Schimmelmann Arndt	139
Liu Yanhong	105	Schimmelmann Minh Ngoc	139
Liu Yong	103	Schüssler Jan	129
Liwu Li	169	Sechman Henryk	99
Longo M.	37, 80, 85	Shen Baojian	56
Lopez M.	27	Shi Shuyong	159
Ma Xiangxian	67, 95	Shizhen Tao	64
Martinelli Giovanni	125, 132, 134, 171	Siegert Laura	137
Matyska C.	124	Smoliński A.	165
Meng Qingqiang	60	Solecki A.T.	115
Milkov Alexei V.	94	Stępnik Maciej	19
Mingjie Zhang	169	Strauch Gerhard	77
Misseri Mariagrazia	96	Streil T.	177, 180
Miyakawa Kazuya	173	Sun Zepeng	156
Moldovan M.	15	Szacsvai K.	15
Mutlu Halim	96	Tamura Hajimu	181
Nęcki J.	203	Tassi F.	85
Nguyễn Nguyệt Thị Ánh	139	Tchorz-Trzeciakiewicz Dagmara	17, 115
Nguyễn-thùy Dương	139	Temel Abidin	96
Nguyễn-văn Hương	139	Teñter A.	15

Thomalla Annika	137	Xia Yanqing	95, 105
Tosheva Zornitza	92	Xianbin Wang	169
Tramutoli V.	132	Xiaobo Wang	117, 189
Tuo Jincan	153	Xiong Yongqiang	150
Twaróg Anna	99	Xu Fanghao	103
Umeda Koji	181	Xu Guanjun	62
Unal-imer Ezgi	96	Xu Guosheng	103
Uysal I. Tonguç	96, 108	Xu Liang	156
Vlček Josef	42, 124	Xu Wang	67, 95
Walczak Katarzyna	19	Xu Yong	40
Walia Vivek	123	Xuening Qi	117, 189
Wang Cheng	40	Yang Hui	153
Wang Gen	156	Yang Tsanyao Frank	123
Wang Peirong	62	Yifeng Wang	117, 189
Wang Peng-kang	123	Yu Hao	60
Wang Qinxian	40	Yu Ming	71
Wang Xianbin	153	Yuan Haifeng	103
Wang Xiaodong	71	Yüce Galip	96, 108, 136
Wang Xulong	185	Zachariáš Jiří	9
Wang Yangyang	50	Zengye Xie	117, 189
Wang Yifan	50	Zhang Baoshou	50
Wang Ying	56	Zhang Dijia	196
Wang Yongli	105, 156	Zhang Guoqiang	50
Wang Yuekun	71	Zhang Mingfeng	156
Wang Yunpeng	150, 159	Zhang Mingjie	71, 145
Wang Zuodong	105	Zheng Guodong	67, 95
Wei Ma	117	Zheng Jianjing	95
Wei Yanzhao	187	Zheng Yijun	150
Wei Zhifu	156	Zhihong Wang	117
Weijiao Ma	64	Zhisheng Li	117, 189
Wenxue Han	64	Zhongping Li	169
Woith Heiko	42	Zhou Bing	60
Wołkowicz Stanisław	22	Zhu Dongya	60
Wołkowicz W.	203	Zimnoch M.	203
Wu Xiaoqi	60	Ziqi Feng	191
Wu Yingqin	105, 153	Zmysłony Marek	19
Wysocka M.	165	Żak Stanisław	113



## Spis treści

### 1. Radon in environment

- Michal Čurda, Viktor Goliáš, Jiří Zachariáš  
*Mineralogical and structural aspects of the radioactive therme formation  
on the hydrogeological structure Geschieber in Jáchymov, Czech Republic.* . . . . . 9
- Lidia Fijałkowska-Lichwa, Tadeusz A. Przylibski  
*Radon risk in underground tourist routes: the Książ Castle case study* . . . . . 11
- B. Papp, A. Cucuș, T. Dicu, B. Burgehele, M. Moldovan, A. Țenter, K. Szacsvai, S. Beldean,  
C. Sainz  
*Comprehensive indoor radon study in Romanian urban agglomerations within  
SMART\_RAD\_EN European Project* . . . . . 15
- Dagmara Tchorz-Trzeciakiewicz, Sławomir Olszewski  
*Indoor radon concentration in Wrocław (SW Poland)* . . . . . 17
- Katarzyna Walczak, Jerzy Olszewski, Marek Zmyślony, Maciej Stępnik  
*Preliminary results of blood tests in people with elevated radon concentrations  
in dwellings* . . . . . 19
- Stanisław Wołkowicz  
*Variability of the Radon Potential of Granitoids and Gneisses of the Polish Part  
of the Sudetes and Fore-sudetic Block* . . . . . 22

### 2. Gases in Volcanoes and Geothermal Systems

- Caruso C., Italiano F., Lopez M., Bonfanti P.  
*Geochemical survey of soil Rn and CO<sub>2</sub> gas emissions at Salina Island (Aeolian arc,  
Italy): correlation to structural vs volcanic origin* . . . . . 27
- Caruso Cinzia, Corbo Andrea, Di Bella Marcella, Lazzaro Gianluca, Nigrelli Alessandra,  
Romano Davide, Sabatino Giuseppe Francesco Italiano  
*Hydrothermal Fluids and Sea-water Interactions: Geochemical and Mineralogical  
Characterization of Iron-ooids from the Submarine Hydrothermal Area  
off Panarea Island (Aeolian Arc, Italy)* . . . . . 31
- Ciolini R., Pierotti L., D'Intinosante V., Facca G., Gherardi F., Pazzagli F., d'Errico F.  
*Radon and CO<sub>2</sub> monitoring in Galliciano thermomineral spring, Italy* . . . . . 35
- Italiano F., Caruso C., Corbo A., Lazzaro G., Longo M., Nigrelli A.  
*A high-temperature hydrothermal system in the Tyrrhenian offshore: the 150 m deep  
Zannone hydrothermal field (Pontine Islands, Italy)* . . . . . 37
- Wang Cheng, Wang Qinxian, Chen Guojun, He Long, Xu Yong, Chen Duofu  
*The influence of volcanism on the development of Chang 7 black shale from Yanchang  
Formation in well Yaowan 1, Ordos Basin* . . . . . 40

Heiko Woith, Josef Vlček, Tomáš Fischer, Jens Heinicke <i>Radon and gas flow rates at a mofette</i> .....	42
<b>3. Gases in Petroliferous Sedimentary Basins and Reservoirs</b>	
Elżbieta Bilkiewicz, Maciej J. Kotarba <i>Origin of Hydrocarbon Gases in the Zechstein Main Dolomite Reservoir in Wielkopolska Province of the Polish Permian Basin: Isotope and Hydrous Pyrolysis Studies</i> .....	47
Jianfa Chen, Yangyang Wang, Xiongqi Pang, Baoshou Zhang, Yifan Wang, Liwen He, Zeya Chen, Guoqiang Zhang <i>Gas diffusion causing natural gas composition and carbon isotope ratio anomalies – a case from the Carboniferous Donghe sandstone reservoir in the Hadexun oilfield, Tabei uplift, Tarim Basin, NW China</i> .....	50
Maciej J. Kotarba, Elżbieta Bilkiewicz <i>Molecular and Isotopic Compositions, Origin and Biodegradation of Natural Gas in the Central Part of the Polish Outer Carpathians</i> .....	53
Luofu Liu, Ying Wang, Baojian Shen, Xiaoyue Gao <i>Gas Occurrence and Accumulation Characteristics of Cambrian-Ordovician Shales in the Tarim Basin, Northwest China</i> .....	56
Quanyou Liu, Zhijun Jin, Bing Zhou, Dongya Zhu, Qingqiang Meng, Xiaoqi Wu, Hao Yu <i>Effects of deep CO<sub>2</sub> on petroleum and thermal alteration: a case of Huangqiao oil and gas field</i> .....	60
Shengfei Qin, Wei Li, Guanjun Xu, Peirong Wang <i>Geochemical characteristics of condensate oil in the tight reservoir of Xujiatahe Formation in Central Sichuan, China</i> .....	62
Han Wenxue <sup>#</sup> , Tao Shizhen, Ma Weijiao <i>Analysis on sources of oil-derived gas in Jingbian gas field, Ordos Basin, China</i> .....	64
Guodong Zheng, Wang Xu, Giuseppe Etiope, Xiangxian Ma, Shouyun Liang, Qiaohui Fan, Wasim Sajjad <sup>1</sup> , Yang Li <i>Hydrocarbon seeps in petroliferous basins in China: a first inventory</i> .....	67
<b>4. Gases in Groundwater and Crystalline Rocks</b>	
Pengyu Feng, Ming Yu, Mingjie Zhang, Yuekun Wang, Xiaodong Wang, Fei Hu <i>Chemical and carbon isotopic compositions and implications of volatiles in the Poyi Permian mafic magmatism in the Northeastern Margin of Tarim Craton, China</i> .....	71
<b>5. Gases migration and mechanism of Earth Degassing</b>	
Karin Bräuer, Horst Kämpf, Samuel Niedermann, Gerhard Strauch <i>The role of mantle-derived gases with respect to the geodynamic situation in the western Eger Rift, central Europe</i> .....	77
Daskalopoulou K., Longo M., Calabrese S., Gagliano A.L., Kyriakopoulos K., Italiano F., D'Alessandro W. <i>Gas geochemistry of shallow submarine vents in the Aegean sea (Greece)</i> .....	80

Daskalopoulou K., Calabrese S., Fiebig J., Grassa F., Kyriakopoulos K., Longo M., Parello F., Tassi F., D'Alessandro W. <i>Origin of methane and light hydrocarbons in the gas manifestations of Greece.</i> . . . . .	85
Di Bella Marcella, Sabatino Giuseppe, Nigrelli Alessandra, Francesco Italiano <i>Seamount-like Structure (?) in the SE Tyrrhenyan Sea: Constraints from Fluid Emission Data and Mineralogical Features of Dradged Sample</i> . . . . .	89
Antoine Kies, Olivier Hengesch, Zornitza Tosheva, Hardy Pfan <i>CO<sub>2</sub> Dynamics in Mofettes.</i> . . . . .	92
Xiangxian Ma, Guodong Zheng, Wasim Sajjad, Wang Xu, Qiaohui Fan, Jianjing Zheng, Yanqing Xia <i>The effect of iron-bearing minerals on gaseous hydrocarbon generation.</i> . . . . .	95
Alexei V. Milkov, Giuseppe Etiope <i>Updated Versions of Methane Genetic Diagrams</i> . . . . .	94
Andrea Luca Rizzo, Kadir Dirik, I. Tonguc Uysal, Antonio Caracausi, Francesco Italiano, Mariagrazia Misseri, Galip Yuçe, Halim Mutlu, Ezgi Unal-Imer, Abidin Temel, Serdar Bayari, Nur Ozyurt <i>Chemical and isotope composition of fluids related to travertine formation in Western and Central Turkey: inferences on the role of tectonics in fluid circulation</i> . . . . .	96
Anna Twaróg, Henryk Sechman, Piotr Guzy, Adrianna Góra <i>Anomalous zones of light hydrocarbon recorded in the soil gas samples above Mszana Dolna tectonic window – Polish Outer Carpathians.</i> . . . . .	99
Xu Fanghao, Xu Guosheng <sup>†</sup> , Yuan Haifeng, Liang Jiaju, Liu Yong <i>Reservoir geochemical characteristics and fluid system of the Sinian Dengying and Cambrian Longwangmiao Formation in Sichuan Basin, China</i> . . . . .	103
Yingqin Wu, Yanhong Liu, Yongli Wang, Zuodong Wang, Tianzhu Lei, Yanqing Xia <i>The Effect of Maturation on Gas Carbon Isotope in Different Types of Hydrocarbon Source Rocks</i> . . . . .	105
Galip Yüçe, Uwe Ring, I.Tonguç Uysal, Francesco Italiano <i>Is Australia a stable or moving continent? Recent findings in Eastern and South-Central Australia</i> . . . . .	108
<b>6. Noble Gases Applications</b>	
Tadeusz A. Przylibski, Stanisław Żak, Elżbieta Domin, Agata Kowalska <i>Applying <sup>222</sup>Rn to <sup>226</sup>Ra activity concentration measurements in environmental water samples by using an Ultra Low Level Liquid Scintillation Spectrometer</i> . . . . .	113
Solecki A.T., Tchorz-Trzeciakiewicz D.E., Kowalczyk Ł. <i>Radon as a monitoring tool of atmospheric influx to landfill gas</i> . . . . .	115
Wang Xiaobo, Li Jian, Li Zhisheng, Xie Zengye, Wang Yifeng, Wang Zhihong, Cui Huiying, Ma Wei, Hao Aisheng, Qi Xuening <i>Geochemical characteristics and their differences of helium and argon in coal-derived gases and oil-typed gases, China</i> . . . . .	117
	211

## 7. Gases and Geo-hazards

Camarda Marco, Caracausi Antonio, Chiaraluce Lauro, De Gregorio Sofia, Favara Rocco <i>Two years of geochemical monitoring along the Alto Tiberina Fault (Italy): new inferences on fluids and seismicity in central Apennines</i> . . . . .	121
Ching-Chou Fu, Lou-Chuang Lee, Tsanyao Frank Yang, Peng-Kang Wang, <i>Cheng-Horng Lin, Vivek Walia, Cheng-Hong Chen, Arvind Kumar Radon and gamma rays anomalies in northern Taiwan and its tectonic Implications</i> . . . . .	123
J. Heinicke, T. Fischer, J. Vlček, C. Matyska <i>Increased fluid emission after a <math>M_L</math> 3.5 event in the earthquake swarm region of NW-Bohemia/ Vogtland</i> . . . . .	124
Francesco Italiano, Antonio Caracausi, Alessandra Nigrelli, Giovanni Martinelli, Sergio Bovini, Margherita Lemmi <i>Fluids Geochemistry and Tectonics: What we have Learned from the Last Central Italy Seismic Crisis</i> . . . . .	125
Horst Kämpf, Jan Schüssler, Karin Bräuer, Ulrich Koch, Mashal Alawi <i>Earthquake impact on iron isotope signatures recorded in mineral spring water</i> . . . . .	129
Martinelli G., Facca G.L., Genzano N., Gherardi F., Lisi M., Pierotti L., Tramutoli V. <i>Earthquake-related signals simultaneously detected in Central Italy by geochemical, hydrogeologic and satellite techniques in the period 2006-2016</i> . . . . .	132
Martinelli G., Ciolini R., Facca G.L., Fazio F., Gherardi F., Heinicke J., Pierotti L. <i>Earthquake-related signals recorded in Central Italy, Southern Italy and in Sicily by geochemical and hydrogeologic methods</i> . . . . .	134
Hardy Pfanz <sup>1</sup> , Galip Yüce <i>Mofettes as ancient gates to hell.</i> . . . . .	136
Hardy Pfanz, Olivier Ruiz, Laura Siegert, Annika Thomalla <i>Mofette bowls as deadly CO<sub>2</sub>-gas traps for animals – an example for a “recent” autochthonic thanatocoenosis</i> . . . . .	137
Pfanz H. <i>Geogenic CO<sub>2</sub>-degassing and its effects on environment and organisms.</i> . . . . .	138
Arndt Schimmelmann, Dương Nguyễn-Thuỳ, Hương Nguyễn-Văn, Nguyễn Thị Ánh Nguyễn, Minh Ngọc Schimmelmann <i>Thoron (<sup>220</sup>Rn) exhalation into room air of earthen dwellings in northern Vietnam: Recognition of health geohazard and strategy for remediation</i> . . . . .	139

## 8. Shale Gas and Tight Gas

Chunhui Cao, Mingjie Zhang, Li Du, Liwu Li <i>Gas Geochemistry Characteristics of Shale Gas in Changning-Weiyuan Area, Sichuan Basin, China</i> . . . . .	145
Ziqi Feng, Weilong Peng, Shipeng Huang <i>Geochemical characteristics of Longmaxi Formation shale gas in Weiyuan area that located the China's oldest gas field, Sichuan Basin.</i> . . . . .	148

Yuhong Liao, Yijun Zheng, Yunpeng Wang, Weiming Liu, Yongqiang Xiong, Ping'an Peng <i>Geochemical, Physical Properties and Shale Gas Exploration Prospects of the Longmaxi Shale in Nanchuan, Southeast Margin of the Sichuan Basin</i> .....	150
Yan Liu, Liwu Li, Jincai Tuo, Zhongping Li, Yingqin Wu, Hui Yang, Xianbin Wang <i>Factors affecting chemical composition analysis of gases released by crush methods from rocks</i> .....	153
Zepeng Sun, Yongli Wang, Zhifu Wei, Mingfeng Zhang, Gen Wang, Liang Xu <i>Characteristics and origin of desorption gas of the Permian Shanxi Formation shale in the Ordos Basin, China</i> .....	156
Yunpeng Wang, Lingling Liao, Chensheng Chen, Shuyong Shi, Shengfei Qin, Ziqi Feng, Jinxing Dai <i>Isotopic and Molecular Compositions of Shale Gas from the Silurian Longmaxi Shale of the Sichuan Basin: maturation or accumulation control?</i> .....	159
<b>9. Techniques of measurements</b>	
Bonczyk M., Chałupnik S., Smoliński A., Wysocka M., Howaniec N. <i>Testing device for radon migration experiments – the construction and preliminary results.</i> .....	165
Li Du, Xuan Fang <i>Comparative study on the gas released from rock samples by pyrolysis using mass spectrometry.</i> .....	166
Li Liwu, Cao Chunhui, Li Zhongping, Xing Lantian, Zhang Mingjie, Wang Xianbin <i>Gas chromatography combined mass spectrometry for the chemical composition of gases from rock samples</i> .....	169
Martinelli G., Dadomo A. <i>Natural and artificial constraints to detectability of anomalous Thermal Infrared Signals by satellite techniques</i> .....	171
Kazuya Miyakawa, Fumiaki Okumura <i>Preliminary research on the effects of microbial methane oxidation on drill-core head-space gas analysis</i> .....	173
Sauer, U., Streil, T., Borsdorf, H., Horak, G. <i>Depth oriented measurement of <sup>222</sup>Rn and CO<sub>2</sub> concentration and fluxes with a novel measuring device and a modular probe system</i> .....	177
T. Streil, V. Oeser <i>Radon Scout Home The Radon Recorder For Your Home</i> .....	180
Hajimu Tamura, Yoko Saito-Kokubu, Koji Umeda <i>Resolution of small neon isotope anomaly in helium rich gas samples from Kii peninsula, Japan by a NGX multi-collector noble gas mass spectrometer.</i> .....	181

## 10. Coal-derived Gases and Coalbed Methane

Jianping Chen, Yunyan Ni, Chunping Deng, Xulong Wang <i>Geochemical Characteristics and Sources of Natural Gas in the Southern Margin of Junggar Basin</i> .....	185
Deyu Gong, Jinxing Dai, Yanzhao Wei <i>Geochemical characteristics of natural gases related to Late Paleozoic coal measures in China</i> .....	187
Li Jian, Wang Xiaobo, Li Zhisheng, Xie Zengye, Wang Yifeng, Li Jin, Ma Chenghua, Cui Huiying, Qi Xuening <i>Geochemical characteristics of carbon dioxide and their differences in coal-derived and oil-type gases, China</i> .....	189
Liu Dan, Dai Jinxing, Liu Jiaqi, Li Jian, Feng Ziqi <i>Genetic mechanism of the carbon isotope reversal in over-mature coal-derived gas in Ordos Basin, China</i> .....	191
Yunyan Ni, Fengrong Liao, Deyu Gong, Jianping Chen, Dijia Zhang <i>Geochemical characteristics of the typical coal-derived early thermogenic gas with extremely low <math>\delta^{13}\text{C}</math> values from the Turpan-Hami Basin, China</i> .....	196
Weilong Peng, Guoyi Hu, Ziqi Feng, Shipeng Huang <i>Geochemical Characteristics of Light Hydrocarbons in the Natural Gas and Their Influencing Factors of the Kuqa Depression, NW China</i> .....	198
<b>11. CO<sub>2</sub> and Greenhouse Gases</b>	
J. Nęcki, M. Zimnoch, M. Gałkowski, Ł. Chmura, A. Jasek, M. Kotarba, K. Róžański, W. Wołkowicz <i>Bottom-up characterization of largest anthropogenic methane source in Europe: Upper Silesian Coal Basin, Southern Poland</i> .....	203

The organizers gratefully acknowledge the financial support of:



WROCLAW



Wrocławskie  
Centrum  
Akademickie



Uniwersytet  
Wrocławski



Politechnika Wroclawska



WYDZIAŁ NAUK O ZIEMI I KSZTAŁTOWANIA ŚRODOWISKA

Wydział Geoinżynierii,  
Górnictwa i Geologii



ISBN 978-83-946706-3-4